

**INVESTIGATING THE IMPACT OF  
POLYMICROBIAL INTERACTIONS ON  
MUCORALES PATHOGENICITY**

by

**Courtney Alice Kousser**

A thesis submitted to the University of Birmingham for the degree of DOCTOR  
OF PHILOSOPHY

Institute of Microbiology and Infection

School of Biosciences

College of Life and Environmental Sciences

University of Birmingham

July 2019

UNIVERSITY OF  
BIRMINGHAM

**University of Birmingham Research Archive**

**e-theses repository**

This unpublished thesis/dissertation is copyright of the author and/or third parties. The intellectual property rights of the author or third parties in respect of this work are as defined by The Copyright Designs and Patents Act 1988 or as modified by any successor legislation.

Any use made of information contained in this thesis/dissertation must be in accordance with that legislation and must be properly acknowledged. Further distribution or reproduction in any format is prohibited without the permission of the copyright holder.

## Abstract

Within the human body, microorganisms reside as part of a complex and varied ecosystem, where they rarely exist in isolation. Bacteria and fungi have co-evolved to develop elaborate and intricate relationships, utilising both physical and chemical communication mechanisms. Mucorales are filamentous fungi that are the causative agents of mucormycosis in immunocompromised individuals. Key to the pathogenesis is the ability to germinate and penetrate the surrounding tissues, leading to angioinvasion, vessel thrombosis, and tissue necrosis. It is currently unknown whether Mucorales participate in polymicrobial relationships, and if so, how this affects the pathogenesis. This project analyses the relationship between Mucorales and the microorganisms they may encounter. Here we show that *Pseudomonas aeruginosa* culture supernatants and live bacteria inhibit *Rhizopus microsporus* germination through the sequestration of iron. Therefore, treatment of *P. aeruginosa* in a patient could result in the release of this inhibition, leaving the patient more susceptible to an underlying fungal infection. However, *P. aeruginosa* responds to the presence of *R. microsporus* by enhancing siderophore production, which increases host mortality in a zebrafish co-infection model. This project highlights the complex competition between these organisms and the possible enhanced disease pathology when *R. microsporus* and *P. aeruginosa* meet in a host.

Happiness does not come from doing easy work  
but from the afterglow of satisfaction that comes  
after the achievement of a difficult task that  
demanded our best.

*Theodore Isaac Rubin*

## **Acknowledgements**

I am a firm believer that it takes a village to make a PhD, and it feels almost impossible to thank everyone who has helped me along the way. This was the hardest and most rewarding experience of my life, and I couldn't have done it without a strong support system. I truly believe I have emerged a stronger, more confident person, and I will always be grateful for this time in my life. Firstly, thank you to my supervisor, Rebecca Hall, who has provided immense support, both personally and professionally. Thank you for always being available for my endless questions, and for listening to me when I was panicking about research, careers, or life in general. Thank you to my PhD besties, Pau, Jes, Nick, Ria, Liam, and Emily. You will never know how grateful I am for your friendship and for always holding me up when I felt like crumbling. I am so lucky to have you guys, and I couldn't have done this without you. Thank you to Callum Clark, who contributed to this body of work, taught me how to supervise a student, and became a wonderful support system and friend. A huge thank you to the entire HAPI lab, whose friendship and expertise made this experience so much easier. Thank you for welcoming me immediately, encouraging me to no end, and helping me become a confident scientist and communicator. Thank you especially to Sarah Sherrington for her contributions to this work. A special thank you to Robin May for being a wonderful mentor and providing advice and support when I needed it. Thank you to my husband, Anton, who went above and beyond to support me during the past four years. Thank you very much to my examiners for taking the time to read this tome. Last, but certainly not least, thank you to the Darwin Trust of Edinburgh for funding my PhD.

## Table of Contents

List of Figures.....	viii
List of Tables.....	x
List of Equations.....	x
List of Abbreviations.....	xi
<b>Chapter 1 : GENERAL INTRODUCTION</b> .....	<b>1</b>
1.1 Fungi.....	2
1.1.2 Fungi: friend or foe?.....	2
1.1.3 Importance of studying pathogenic fungi. ....	4
1.2 Mucorales.....	5
1.2.1 Mucoralean lifecycle. ....	6
1.2.1.1 Asexual reproduction.....	6
1.2.1.2 Sexual reproduction.....	7
1.2.2 The cell wall. ....	8
1.2.3 Spore swelling and germination.....	10
1.2.4 Mucormycosis.....	13
1.2.5 Pathogenesis and infection.....	15
1.2.6 Iron dependency, uptake, and storage.....	17
1.2.7 Diagnosis.....	20
1.2.8 Treatment.....	21
1.2.8.1 Antifungals.....	22
1.2.8.2 Alternative strategies.....	24
1.3 Polymicrobial interactions.....	25
1.3.1 Mechanisms of intra- and inter-species interactions. ....	27
1.3.2 Competitive vs. cooperative relationships.....	28
1.3.3 Mucorales and <i>C. albicans</i> .....	29
1.3.4 Mucorales and bacteria.....	30
1.4 Aim of this study.....	33
<b>Chapter 2 : MATERIALS AND METHODS</b> .....	<b>34</b>
2.1 Strains and culture conditions.....	35
2.1.2 Maintaining and sub-culturing Mucorales.....	38
2.1.3 Harvesting sporangiospores.....	38
2.1.4 Creating frozen spore stocks.....	38
2.2 Elucidating the effect of supernatants on Mucorales.....	39

2.2.1 Exposing Mucorales to <i>Candida albicans</i> supernatant. ....	39
2.2.2 Exposing Mucorales to bacterial supernatants.....	39
2.2.3 Testing the effect of pH change and nutrient starvation on germination. ....	40
2.2.4 Exposure of pre-germinated <i>R. microsporus</i> spores to <i>P. aeruginosa</i> supernatant.....	40
2.2.5 Observing the effect of <i>P. aeruginosa</i> supernatant on <i>R. microsporus</i> antifungal susceptibility.....	41
2.3 Quantifying the effects of microbial secreted molecules on fungal germination. ....	41
2.3.1 Fungal quorum sensing molecules. ....	42
2.3.2 Bacterial quorum sensing molecules. ....	42
2.3.3 Bacterial toxins.....	43
2.4 Characterising the inhibitory compound. ....	43
2.4.1 Denaturation of proteins in <i>P. aeruginosa</i> supernatant. ....	43
2.4.2 Organic extraction of <i>P. aeruginosa</i> supernatant.....	44
2.5 Investigating the role of metal restriction on supernatant-dependent growth inhibition. ....	45
2.5.1 Addition of iron, zinc, copper, and manganese to <i>R. microsporus</i> spores following exposure to <i>P. aeruginosa</i> supernatant.....	45
2.5.2 Exposure of <i>R. microsporus var microsporus</i> , <i>R. microsporus var chinensis</i> , <i>R. delemar</i> , and <i>M. circinelloides</i> to <i>P. aeruginosa</i> supernatant +/- iron. ....	45
2.5.3 Exposure of <i>R. microsporus</i> to purified, exogenous bacterial siderophores. ....	46
2.5.3.1 Pyoverdine. ....	46
2.5.3.2 Enterobactin. ....	46
2.6 Quantification of bacterial virulence factor production.....	47
2.6.1 Pyocyanin secretion.....	47
2.6.2 Overall siderophore production. ....	48
2.6.3 Pyoverdine secretion. ....	48
2.7 Microscopy.....	48
2.7.1 Live-cell imaging. ....	49
2.7.2 Endpoint imaging. ....	49
2.7.3 Quantifying spore germination. ....	49
2.7.4 Spore swelling.....	49

2.7.5 Time to first germ tube. ....	50
2.7.6 Hyphal width. ....	51
2.8 Quantifying chitin. ....	51
2.8.1 Staining spores. ....	51
2.8.2 Measuring fluorescence. ....	52
2.9 Live co-cultures of <i>R. microsporus</i> and <i>P. aeruginosa</i> . ....	52
2.9.1 Determining colony forming units from bacterial absorbance. ....	52
2.9.2 Investigating the impact of live bacteria on <i>Rhizopus microsporus</i> germination. ....	52
2.9.3 Addition of enterobactin to live co-cultures. ....	53
2.9.4 Investigating the ability of live <i>P. aeruginosa</i> to decrease spore viability, in an iron-dependent manner. ....	53
2.10 Molecular biology ....	54
2.10.1 Gel Electrophoresis. ....	54
2.10.1.1 DNA Gel Electrophoresis. ....	54
2.10.1.2 Non-denaturing RNA Gel Electrophoresis. ....	55
2.10.2 Genomic DNA extraction from Mucorales. ....	55
2.10.3 Genomic DNA isolation of bacteria. ....	56
2.10.4 RNA extraction of Mucorales. ....	56
2.10.5 RNA extraction of bacteria. ....	57
2.10.6 Designing Primers. ....	59
2.10.7 Polymerase Chain Reaction (PCR). ....	60
2.10.8 Checking RNA for DNA contamination. ....	60
2.10.9 Removing DNA from contaminated RNA. ....	61
2.10.10 Quantitative Reverse Transcriptase PCR (qRT-PCR). ....	61
2.10.11 Creating fluorescent <i>P. aeruginosa</i> . ....	62
2.10.11.1 <i>E. coli</i> plasmid extraction. ....	62
2.10.11.2 Transformation of <i>P. aeruginosa</i> . ....	63
2.11 Zebrafish infections. ....	63
2.11.1 Ethics. ....	63
2.11.2 Maintenance. ....	63
2.11.3 Preparation of inoculum. ....	64
2.11.4 Hindbrain injections. ....	65
2.11.4.1 <i>R. microsporus</i> and <i>P. aeruginosa</i> hindbrain mono-injections. ....	65

2.11.4.2 R. microsporus hindbrain mono-injections with pyoverdine or enterobactin. ....	66
2.11.4.3 R. microsporus and P. aeruginosa hindbrain co-infections. ....	66
2.11.5 Yolk sac injections. ....	67
2.11.5.1 R. microsporus and P. aeruginosa yolk sac mono infections. ....	67
2.11.6 Swim bladder injections. ....	67
2.11.6.1 R. microsporus and P. aeruginosa swim bladder co-infections. ....	68
2.11.6.2 Spore viability following zebrafish infection. ....	68
2.11.7 Imaging of zebrafish. ....	69
2.11.8 Statistical analysis of zebrafish survival experiments. ....	69
2.12 Statistical analysis. ....	69
2.12.1 Arcsine transformations. ....	70

### **Chapter 3 : IMPACT OF POLYMICROBIAL INTERACTIONS ON MUCORALES** .....

3.1 Introduction .....	72
3.1.1 Organisms studied in this chapter. ....	72
3.1.1.1 Candida albicans. ....	72
3.1.1.2 Burkholderia cenocepacia. ....	74
3.1.1.3 Klebsiella pneumoniae. ....	75
3.1.1.4 Pseudomonas aeruginosa. ....	76
3.1.1.5 Staphylococcus aureus. ....	80
3.1.1.6 Escherichia coli. ....	81
3.2 Aim of this chapter. ....	82
3.3 Results .....	82
3.3.1 <i>Candida albicans</i> supernatant delays the germination of <i>Rhizopus microsporus</i> , <i>Lichtheimia corymbifera</i> , and <i>Cunninghamella bertholletiae</i> . ....	82
3.3.2 Farnesol delays the growth and germination of <i>R. microsporus</i> , <i>C. bertholletiae</i> , and <i>L. corymbifera</i> . ....	87
3.3.3 Bacterial supernatants significantly impact the growth of <i>R. microsporus</i> , <i>L. corymbifera</i> , and <i>C. bertholletiae</i> . ....	93
3.3.4 Growth promotion and phenotype alteration of <i>C. bertholletiae</i> by <i>P. aeruginosa</i> supernatant is likely caused by pH changes and nutrient depletion. ....	100
3.3.5 <i>P. aeruginosa</i> supernatant significantly inhibits the germination of <i>R. microsporus</i> , while pH changes and nutrient depletion have no impact. ....	104
3.3.6 <i>P. aeruginosa</i> supernatant halts the growth of pre-germinated <i>R. microsporus</i> spores. ....	106

3.3.7 Inhibition of <i>R. microsporus</i> growth by <i>P. aeruginosa</i> is not specific to lab-evolved strains.....	107
3.3.8 <i>P. aeruginosa</i> supernatant decreases <i>R. microsporus</i> swelling in early times points and reduces cell wall chitin. ....	108
3.3.9 Live <i>P. aeruginosa</i> strongly inhibits the germination of <i>R. microsporus</i> . ....	112
3.4 Discussion.....	114
3.4.1 Fungal-fungal interactions.....	114
3.4.2 Inhibition of <i>R. microsporus</i> germination by <i>P. aeruginosa</i> secreted factors. ....	115
3.4.3 Response variation between distantly related Mucorales following exposure to bacterial supernatants.....	116
<b>Chapter 4 : CHARACTERISATION OF <i>P. AERUGINOSA</i>-MEDIATED INHIBITION OF <i>R. MICROSPORUS</i>.....</b>	<b>118</b>
4.1 Introduction .....	119
4.1.1 Mucorales and <i>P. aeruginosa</i> in the human host.....	119
4.1.2 Mucorales and <i>Pseudomonas spp.</i> in the environment. ....	121
4.2 Aim of this chapter. ....	122
4.3 Results .....	123
4.3.1 Bacterial quorum sensing molecules (QSMs) do not inhibit <i>R. microsporus</i> growth.....	123
4.3.2 Pyocyanin does not impact <i>R. microsporus</i> growth. ....	123
4.3.3 Inhibitory substance secreted by <i>P. aeruginosa</i> is a hydrophilic, heat-stable non-protein. ....	126
4.3.4 Inhibition of growth is not impacted by removal of <i>R. microsporus</i> endosymbiont. ....	127
4.3.5 Inhibition of fungal growth is not due to zinc, copper, or manganese restriction. ....	129
4.3.6 Addition of exogenous iron rescues <i>R. microsporus</i> growth and germination. ....	131
4.3.7 The presence of <i>P. aeruginosa</i> supernatant induces an iron-starvation response in <i>R. microsporus</i> . ....	134
4.3.8 Iron-dependent inhibition of Mucorales by <i>P. aeruginosa</i> is not <i>R. microsporus</i> species-specific. ....	136
4.3.9 Siderophore-deficient <i>P. aeruginosa</i> strains lack the ability to suppress germination.....	138
4.3.10 Pyoverdine is sufficient to inhibit <i>R. microsporus</i> growth. ....	138

4.3.11 The presence of <i>R. microsporus</i> induces iron stress in <i>P. aeruginosa</i> and promotes bacterial siderophore production.....	141
4.3.12 The concentration of siderophores produced by bacteria correlates with inhibition of <i>R. microsporus</i> growth.....	144
4.3.13 The presence of <i>P. aeruginosa</i> supernatant impacts the antifungal susceptibility of <i>R. microsporus</i> . ....	147
4.4 Discussion.....	150
4.4.1 Inter-kingdom iron competition.....	150
4.4.2 Enterobactin protects <i>R. microsporus</i> from <i>P. aeruginosa</i> supernatant-induced growth inhibition. ....	152
4.4.3 Bacterial-induced susceptibility to antifungals.....	153
<b>Chapter 5 : DEVELOPMENT OF A ZEBRAFISH MODEL.....</b>	<b>155</b>
5.1 Introduction. ....	156
5.1.1 Advantages of the zebrafish model.....	156
5.1.2 Sites of infection.....	158
5.1.2.1 Hindbrain.....	158
5.1.2.2 Yolk sac.....	159
5.1.2.3 Swim bladder.....	159
5.1.3 Zebrafish as a model for mucormycosis. ....	160
5.1.4 Zebrafish as a model for <i>P. aeruginosa</i> infections. ....	161
5.1.5 Polymicrobial infections in zebrafish. ....	162
5.1.6 Limitations of the zebrafish model.....	162
5.2 Aim of this chapter. ....	163
5.3 Results .....	163
5.3.1 <i>R. microsporus</i> moderately reduces survival following hindbrain injection of healthy zebrafish embryos. ....	164
5.3.2 The <i>P. aeruginosa</i> siderophore, pyoverdine, reduces <i>R. microsporus</i> virulence in the hindbrain of healthy zebrafish. ....	166
5.3.3 The <i>E. coli</i> siderophore, enterobactin, does not impact <i>R. microsporus</i> virulence in the hindbrain. ....	166
5.3.4 <i>P. aeruginosa</i> PA14 inhibits <i>R. microsporus</i> growth via iron sequestration. ....	168
5.3.5 Zebrafish are resistant to swim bladder mono- and co-infections with <i>P. aeruginosa</i> and <i>R. microsporus</i> .....	169
5.3.6 <i>R. microsporus</i> is moderately pathogenic in healthy zebrafish embryos via yolk sac injections, while <i>P. aeruginosa</i> is highly virulent. ...	172

5.3.7 <i>P. aeruginosa</i> decreases viability in a dose-dependent manner following hindbrain injections of healthy zebrafish embryos.....	174
5.3.8 Co-infection with <i>P. aeruginosa</i> and <i>R. microsporus</i> enhances virulence in a zebrafish hindbrain co-infection model.....	175
5.4 Discussion.....	177
5.4.1 Choosing site of infection and validating model. ....	177
5.4.2 Impact of pyoverdine on <i>R. microsporus</i> virulence <i>in vivo</i> . ....	179
5.4.3 <i>In vivo</i> co-infection model. ....	179
<b>Chapter 6 : DISCUSSION AND CONCLUDING REMARKS</b> .....	181
6.1 Iron competition.....	183
6.1.1 Speculation regarding germination cessation as a defensive strategy. ....	184
6.2 Xenosiderophores. ....	186
6.3 General Mucoralean response to opportunistic pathogens. ....	189
6.3.1 Potential <i>R. microsporus</i> and <i>S. aureus</i> cooperation. ....	189
6.3.2 <i>R. microsporus</i> , QSMs, and toxins.....	190
6.4 Impact of polymicrobial interactions on the host.....	191
6.4.1 Comparing human and zebrafish iron-sequestering proteins.....	192
6.4.2 Enhancement of virulence in a co-infection model.....	193
6.4.3 Antifungal resistance.....	195
6.5 Clinical implications: patient management. ....	196
6.6 Future work. ....	197
6.6.1 Host-pathogen interactions. ....	197
6.6.2 Relationships with opportunistic bacteria. ....	199
6.7 Concluding remarks .....	202
List of References .....	204
Publication.....	236

## List of Figures

<b>Figure 1.1</b> Reproductive life cycles of Zygomycetes.....	8
<b>Figure 1.2</b> Cell wall of Mucorales.....	10
<b>Figure 1.3</b> Spore swelling and germination of Mucorales .....	13
<b>Figure 1.4</b> Iron acquisition mechanisms in Mucorales .....	19
<b>Figure 1.5</b> Sites of polymicrobial infections.....	27
<b>Figure 3.1</b> <i>Candida albicans</i> supernatant delays the germination of <i>Rhizopus</i> <i>microsporus</i> .....	84
<b>Figure 3.2</b> <i>Candida albicans</i> supernatant delays the germination of <i>Lichtheimia</i> <i>corymbifera</i> .....	85
<b>Figure 3.3</b> <i>Candida albicans</i> supernatant delays the germination of <i>Cunninghamella bertholletiae</i> .....	86
<b>Figure 3.4</b> Farnesol delays the growth and germination of <i>Rhizopus</i> <i>microsporus</i> .....	88
<b>Figure 3.5</b> Farnesol delays the germination of <i>Cunninghamella bertholletiae</i> .	90
<b>Figure 3.6</b> Farnesol delays the germination of <i>Lichtheimia corymbifera</i> .....	92
<b>Figure 3.7</b> Bacterial supernatants significantly impact the growth of <i>R.</i> <i>microsporus</i> .....	95
<b>Figure 3.8</b> Bacterial supernatants promote early overall germination of <i>L.</i> <i>corymbifera</i> and <i>C. bertholletiae</i> .....	97
<b>Figure 3.9</b> Bacterial supernatants do not promote initiation of <i>L. corymbifera</i> and <i>C. bertholletiae</i> germination on an individual spore level.....	99
<b>Figure 3.10</b> Exposure to bacterial supernatants decreases <i>L. corymbifera</i> and <i>C. bertholletiae</i> spore swelling.....	100
<b>Figure 3.11</b> Growth promotion and phenotype alteration of <i>C. bertholletiae</i> by <i>P. aeruginosa</i> supernatant is likely caused by pH changes and nutrient depletion.....	103
<b>Figure 3.12</b> <i>P. aeruginosa</i> supernatant significantly inhibits the germination of <i>R. microsporus</i> , while pH changes and nutrient depletion have no impact ....	105
<b>Figure 3.13</b> <i>P. aeruginosa</i> supernatant halts the growth of pre-germinated <i>R.</i> <i>microsporus</i> spores .....	107
<b>Figure 3.14</b> Inhibition of <i>R. microsporus</i> growth by <i>P. aeruginosa</i> is not specific to lab-evolved strains.....	108
<b>Figure 3.15</b> <i>P. aeruginosa</i> supernatant decreases <i>R. microsporus</i> spore swelling and chitin .....	111
<b>Figure 3.16</b> <i>P. aeruginosa</i> strongly inhibits the germination of <i>R. microsporus</i> .....	113
<b>Figure 4.1</b> Bacterial QSMs and pyocyanin do not inhibit <i>R. microsporus</i> growth. .....	125
<b>Figure 4.2</b> Inhibitory compound secreted by <i>P. aeruginosa</i> is a hydrophilic, heat-stable non-protein and is not endosymbiont-mediated.....	128
<b>Figure 4.3</b> Addition of zinc, copper, and manganese does not rescue <i>R.</i> <i>microsporus</i> growth when exposed to <i>P. aeruginosa</i> supernatant .....	130

<b>Figure 4.4</b> Growth of <i>R. microsporus</i> spores exposed to <i>P. aeruginosa</i> is rescued by addition of exogenous iron.....	133
<b>Figure 4.5</b> The presence of <i>P. aeruginosa</i> supernatant induces an iron-starvation response in <i>R. microsporus</i> .....	135
<b>Figure 4.6</b> Iron-dependent inhibition of Mucorales by <i>P. aeruginosa</i> is not <i>R. microsporus</i> species-specific.....	137
<b>Figure 4.7</b> <i>P. aeruginosa</i> -imposed iron restriction is largely mediated via pyoverdine.....	140
<b>Figure 4.8</b> The presence of <i>R. microsporus</i> induces iron stress in <i>P. aeruginosa</i> and promotes bacterial siderophore production .....	143
<b>Figure 4.9</b> Enterobactin does not inhibit <i>R. microsporus</i> growth and can enhance germination during exposure to <i>P. aeruginosa</i> supernatant. ....	146
<b>Figure 4.10</b> Release of iron stress identifies a potential role of bacterial supernatants in regulating antifungal resistance .....	149
<b>Figure 5.1</b> <i>R. microsporus</i> moderately reduces viability in healthy zebrafish embryos via hindbrain injection, in a dose dependent manner .....	165
<b>Figure 5.2</b> The <i>P. aeruginosa</i> siderophore, pyoverdine, reduces <i>R. microsporus</i> virulence in a zebrafish model of infection.....	167
<b>Figure 5.3</b> <i>P. aeruginosa</i> PA14 inhibits the germination of <i>R. microsporus</i> through iron sequestration.....	169
<b>Figure 5.4</b> Zebrafish are resistant to swim bladder infections with <i>P. aeruginosa</i> and <i>R. microsporus</i> .....	171
<b>Figure 5.5</b> <i>R. microsporus</i> is moderately pathogenic in healthy zebrafish embryos via yolk sac injections, while <i>P. aeruginosa</i> is highly virulent.....	173
<b>Figure 5.6</b> <i>P. aeruginosa</i> decreases viability in a dose-dependent manner following hindbrain injections of healthy zebrafish embryos.....	175
<b>Figure 5.7</b> Co-infection with <i>P. aeruginosa</i> and <i>R. microsporus</i> enhances virulence in a zebrafish hindbrain co-infection model .....	176
<b>Figure 6.1</b> Proposed clinical scenario where <i>R. microsporus</i> enhances <i>P. aeruginosa</i> virulence .....	195
<b>Figure 6.2</b> Hypothetical clinical model of <i>P. aeruginosa</i> and <i>R. microsporus</i> interaction.....	201

## List of Tables

<b>Table 1.1</b> Incidence and mortality rates of representative opportunistic invasive fungal infections .....	3
<b>Table 2.1</b> Strains used in this project .....	35
<b>Table 2.2</b> Primers used in this study .....	59
<b>Table 2.3</b> PCR conditions .....	60
<b>Table 2.4</b> Quantitative Reverse Transcriptase PCR conditions .....	62
<b>Table 6.1</b> Homology of nutritional-immunity related proteins in <i>Homo sapiens</i> and <i>Danio rerio</i> using the BLAST .....	193

## List of Equations

<b>Equation 1:</b> Calculating radius from the area of a sphere .....	50
<b>Equation 2:</b> Calculating the volume of a sphere .....	50
<b>Equation 3:</b> Calculating fluorescence intensity .....	52
<b>Equation 4:</b> Arcsine transformations for percentage data .....	70

## List of Abbreviations

<b>AIDS</b>	Acquired Immune Deficiency Syndrome
<b>ATCC</b>	American Type Culture Collection
<b>Atf</b>	Activating transcription factor
<b>AVC</b>	Apical Vesicle Crescent
<b><i>B. c.</i></b>	<i>Burkholderia cenocepacia</i>
<b>BDSF</b>	Cis-2-dodecenoic acid
<b>BG tests</b>	β-1,3-D-glucan tests
<b>C12 HSL</b>	N-(3-oxododecanoyl)-L-homoserine lactone
<b>C4 HSL</b>	N-butanoyl-L-homoserine lactone
<b>C6 HSL</b>	N-hexanoyl-DL-homoserine lactone
<b>C8 HSL</b>	N-octanoyl-L-homoserine lactone
<b>CaCl<sub>2</sub></b>	Calcium Chloride
<b>cAMP</b>	Cyclic adenosine monophosphate
<b>CF</b>	Cystic Fibrosis
<b>CFU</b>	Colony Forming Units
<b>CFW</b>	Calcofluor white
<b>COPD</b>	Chronic Obstructive Pulmonary Disorder
<b>CuSO<sub>4</sub></b>	Cupric sulphate
<b>DEFEAT Mucor</b>	Deferasirox–AmBisome Therapy for Mucormycosis
<b>DKA</b>	Diabetic ketoacidosis
<b>dH<sub>2</sub>O</b>	Deionized water
<b>DMSO</b>	Dimethyl sulfoxide
<b>DNA</b>	Deoxyribonucleic acid
<b>dpf</b>	Days post fertilisation
<b><i>E. c.</i></b>	<i>Escherichia coli</i>
<b>EDTA</b>	Ethylenediaminetetraacetic acid
<b>EGFR</b>	Epithelial growth factor receptor
<b>Fe<sup>2+</sup></b>	Ferrous Iron
<b>Fe<sup>3+</sup></b>	Ferric Iron

<b>FeCl<sub>3</sub></b>	Iron Chloride
<b>gDNA</b>	Genomic DNA
<b>GLASS</b>	Global Antimicrobial Resistance Surveillance System
<b>GRP78</b>	Glucose-Regulated Protein 78
<b>HIV</b>	Human Immunodeficiency Virus
<b>hpf</b>	Hours post fertilisation
<b>hpi</b>	Hours post infection
<b><i>K. p.</i></b>	<i>Klebsiella pneumoniae</i>
<b>KCl</b>	Potassium Chloride
<b>LB</b>	Lysogeny broth
<b>LPS</b>	Lipopolysaccharide
<b>MAPK</b>	Mitogen-activated protein kinase
<b>MgSO<sub>4</sub></b>	Magnesium Sulfate
<b>MgSO<sub>4</sub></b>	Manganese sulphate
<b>MOI</b>	Multiplicity of Infection
<b>NaCl</b>	Sodium Chloride
<b>NaOH</b>	Sodium hydroxide
<b>NC3Rs</b>	National Centre for Replacement, Refinement, and Reduction of Animals in Research
<b>NETs</b>	Neutrophil Extracellular Traps
<b>OD<sub>600</sub></b>	Optical Density (600 nm wavelength, absorbance)
<b><i>P.a.</i></b>	<i>Pseudomonas aeruginosa</i>
<b>PBS</b>	Phosphate Buffered Saline
<b>PCR</b>	Polymerase Chain Reaction
<b>PCR</b>	Polymerase Chain Reaction
<b>PKA</b>	Protein Kinase A
<b>PTU</b>	1-phenyl-2-thiourea
<b>PVP</b>	Polyvinylpyrrolidone
<b>qRT-PCR</b>	Quantitative Reverse Transcriptase PCR
<b>QSM(s)</b>	Quorum Sensing Molecule(s)
<b>RNA</b>	Ribonucleic acid

<b>ROS</b>	Reactive Oxygen Species
<b>ROUT method</b>	Robust regression and Outlier removal
<b>rpm</b>	Revolutions per minute
<b>S. a.</b>	<i>Staphylococcus aureus</i>
<b>SAB</b>	Sabouraud dextrose agar or broth
<b>SEM</b>	Standard error of mean
<b>T3SS</b>	Type 3 Secretion System
<b>T6SS</b>	Type 6 Secretion System
<b>TAE</b>	Tris-acetate-EDTA
<b>UV</b>	Ultraviolet
<b>WHO</b>	World Health Organisation
<b>YPD</b>	Yeast Extract Peptone Dextrose
<b>ZnCl<sub>2</sub></b>	Zinc chloride

## DECLARATION OF AUTHORSHIP

This is to confirm that Courtney Alice Kousser was first author and major contributor to the publication "*Pseudomonas aeruginosa* inhibits *Rhizopus microsporus* germination through sequestration of free environmental iron." This was published in *Scientific Reports* in April 2019, with Rebecca A Hall as the corresponding author.

Text from this publication has been included in the following thesis entitled "Investigating the impact of polymicrobial interactions on Mucorales pathogenicity," submitted to the University of Birmingham in July 2019. Parts of this publication have been included in Chapters 2, 3, 4, and 5, with further declarations included at the beginning of each chapter.

Signed:



Courtney Kousser



Rebecca A Hall (corresponding author)

# **Chapter 1 : GENERAL INTRODUCTION**

## 1.1 Fungi.

**1.1.2 Fungi: friend or foe?** Amongst the Kingdoms of Life, fungi represent a particularly vast, diverse group of organisms which range from single-celled microorganisms to enormous, multicellular structures spanning thousands of square metres (Smith, Bruhn and Anderson, 1992). There are up to an estimated 3.8 million species of fungi, though only around 120,000 of these are defined (Hawksworth and Lucking, 2017). Fungi are important in the production of staple foods, such as cheese and bread, and beverages, such as beer and wine (Deacon, 2006). They play direct roles in the production of important medicines, including steroids (Christy Hunter *et al.*, 2009), anti-cholesterol drugs (Endo, Kuroda and Tsujita, 1976), and antibiotics e.g. penicillin (Alexander Fleming, 1929). In the environment, fungi are important for carbon recycling during the decomposition of dead matter. They also form mutualistic relationships with plants, where they receive nutrients and, in turn, help the roots acquire water (Money, 2016a). Furthermore, the presence of mycorrhizal fungi is essential for proper ecosystem plant diversity (Van Der Heijden *et al.*, 1998). However, their saprophytic nature causes major economic loss through food spoilage. Approximately 25% of food produced is wasted due to microbial spoilage, globally (Fisher *et al.*, 2012).

In the human host, fungi are members of the microbiota, where *Candida spp.* are the most prevalent colonisers (Hallen-Adams and Suhr, 2017). While the presence of fungi can protect hosts against bacterial overgrowth and infection,

colonisation with *Candida albicans* can exacerbate diseases, such as ulcerative colitis and Crohn's disease (Balzola *et al.*, 2011).

Of the thousands of identified fungal species, only 300 are known to cause disease in humans (Taylor, Latham and Woolhouse, 2001). Fungal infections can range from mild superficial infections to life-threatening systemic diseases. More than 1 billion people suffer from fungal infections annually, with 1.6 million being fatal (Bongomin *et al.*, 2017). These infections are usually related to immunocompromising conditions, such as HIV/AIDS, cancer, corticosteroid therapy, and organ transplantation. The most common causative agents include *Candida*, *Aspergillus*, and *Cryptococcus* (Bongomin *et al.*, 2017). Annual incidence and mortality rates for opportunistic invasive fungal infections are found in Table 1.1 (Brown *et al.*, 2012).

**Table 1.1 Incidence and mortality rates of representative opportunistic invasive fungal infections.** (Brown *et al.*, 2012)

<b>Disease</b>	<b>Location</b>	<b>Life-threatening infections per year</b>	<b>Mortality rates (%)</b>
Aspergillosis	Worldwide	>200,000	30-95
Candidiasis	Worldwide	>400,000	46-75
Cryptococcosis	Worldwide	>1,000,000	20-70
Mucormycosis	Worldwide	>10,000	30-90
Pneumocystis	Worldwide	>400,000	20-80

Key to the successful control of fungal infections involves early diagnosis, and delayed treatment is associated with poor prognosis (Antinori *et al.*, 2009). However, diagnostic techniques are currently lacking, with culture-based methods being the gold standard of fungal diagnostics despite low sensitivities (Kozel and Wickes, 2014). A combination of antigen detection and polymerase chain reaction (PCR)-based diagnostics techniques have a higher sensitivity and specificity than culture-based methods, but their use is not yet widespread (Nguyen *et al.*, 2012). Due to difficulties in diagnosis, many fungal infections are not diagnosed until autopsy; for example, only 15% of aspergillosis cases are diagnosed ante-mortem (Denning, 2015).

**1.1.3 Importance of studying pathogenic fungi.** Antimicrobial resistance is a major health threat, with a recent widespread initiative to combat over-prescribing of antibiotics and to develop novel antimicrobial therapy. While public awareness regarding bacterial resistance to antimicrobials is rising, less focus has been on the problem of antifungal resistance and the development of novel antifungals (WHO, 2014). Mortality rates associated with fungal infections are rising, and more people die from fungal infections every year than from breast cancer and malaria (Brown *et al.*, 2012). Resistance has been documented for all three classes of antifungals: the echinocandins, polyenes, and azoles (Robbins, Caplan and Cowen, 2017). Over prescription of antifungals and the widespread use of azoles in agricultural have contributed to the development of antifungal resistance (Snelders *et al.*, 2009; Berger *et al.*, 2017). *Candida auris* is an emerging multi-drug resistant global outbreak pathogen that has gained recent

publicity (Lockhart *et al.*, 2017; Forsberg *et al.*, 2019), though many strains of *Lomentospora (Scedosporium) prolificans* and *Fusarium solani* are also resistant to most known antifungals (McCarthy *et al.*, 2018). There are currently no global surveillance programmes for antifungal resistance. However, the World Health Organisation (WHO) has recently made the addition of global antifungal surveillance programmes for *Candida* infections a priority within the Global Antimicrobial Resistance Surveillance System (GLASS) (WHO, 2018). Together, these highlight the growing issue of antifungal resistance and the need to develop novel antifungals.

Mucoralean fungi are resistant to many available antifungals, infections are rising in prevalence, and they are associated with high mortality rates (Roden *et al.*, 2005; Katragkou, Walsh and Roilides, 2014; Dannaoui, 2017). Little is known about the pathogenesis of mucormycosis in comparison to other invasive fungi, and almost nothing is known about the impact of other opportunistic pathogens on virulence. For these reasons, this study focuses on gaining an understanding of the impact of polymicrobial relationships on Mucorales.

## **1.2 Mucorales.**

Mucorales are ubiquitous, filamentous fungi that mainly reside as saprophytes on decaying organic matter and in the soil. These basal fungi are important causes of post-harvest food spoilage and contribute to economic loss due to crop wastage (Saito, Michailides and Xiao, 2016). They are also the causative agents

of fatal mucormycosis in immunocompromised individuals. Mucorales and Entomophthorales were previously grouped into a single phylum, Zygomycota, though they have been separated following molecular genotyping and Entomophthorales has risen to its own phylum (Humber, 2012). The Order Mucorales comprises a group of distinct potentially pathogenic fungi that are linked based on their morphology (broad, aseptate hyphae), rapid growth, and ability to form zygospores during sexual reproduction (Hoffmann *et al.*, 2013). *Rhizopus*, *Mucor*, and *Lichtheimia* are the most common etiological agents of mucormycosis, causing 70-80% of infections, with other genera including *Cunninghamella*, *Rhizomucor*, *Apophysomyces*, *Saksenaea*, *Cokeromyces*, *Actinomucor*, and *Syncephalastrum* being rare sources of infection (Roden *et al.*, 2005). The phylogenetic relationships between several species have been established following genome sequencing, indicating that Mucorales are an evolutionarily diverse group of fungi (Chibucos *et al.*, 2016).

### **1.2.1 Mucoralean lifecycle.**

**1.2.1.1 Asexual reproduction.** The Mucoralean lifecycle involves both sexual and asexual reproduction (Figure 1.1), though asexual spores are the main mode of dispersal (Richardson, 2009). Asexual reproduction begins under favourable conditions (i.e. moisture, temperature, and nutrients) when an aerial hypha, or sporangiophore, sprouts from the lateral mycelium. Nutrients, cytoplasm, and nuclei accumulate at the tip of the sporangiophore, forming a bulbous sporangium. Within the thin-walled sporangia, multinucleated spores form around the tip of the stalk, called the columella. The sporangium bursts, and spores are

released and passively dispersed through the air until they land on a suitable substrate. The spores will then undergo germination (Section 1.2.3), form sporangiophores, and the cycle continues (Deacon, 2006). This study involves the investigation of asexual spores.

**1.2.1.2 Sexual reproduction.** Mucorales have two distinct mating types, (+) and (-). Sexual reproduction (Figure 1.1) begins when two hyphae of complimentary mating types meet adjacently. The hyphae release pheromones (trisporic acid) which trigger hyphal branches (progametangia) to form and grow toward each other (Mesland, Huisman and Van Den Ende, 1974; Money, 2016a). Nutrients, cytoplasm, and nuclei migrate toward the ends and cause swelling. Septa form at the end of each branch, trapping nuclei at the tips and forming gametangia. These gametangia fuse, pairs of opposite nuclei fuse, and a multinucleated, diploid zygospore is formed (Deacon, 2006; Money, 2016a). Following a variable period of dormancy, meiosis occurs within the zygospore, and a new aerial promycelium grows. Sporangia are formed at the tip of the promycelium, and spores develop within. Spores are later released to continue the lifecycle (Deacon, 2006; Lee and Heitman, 2014).

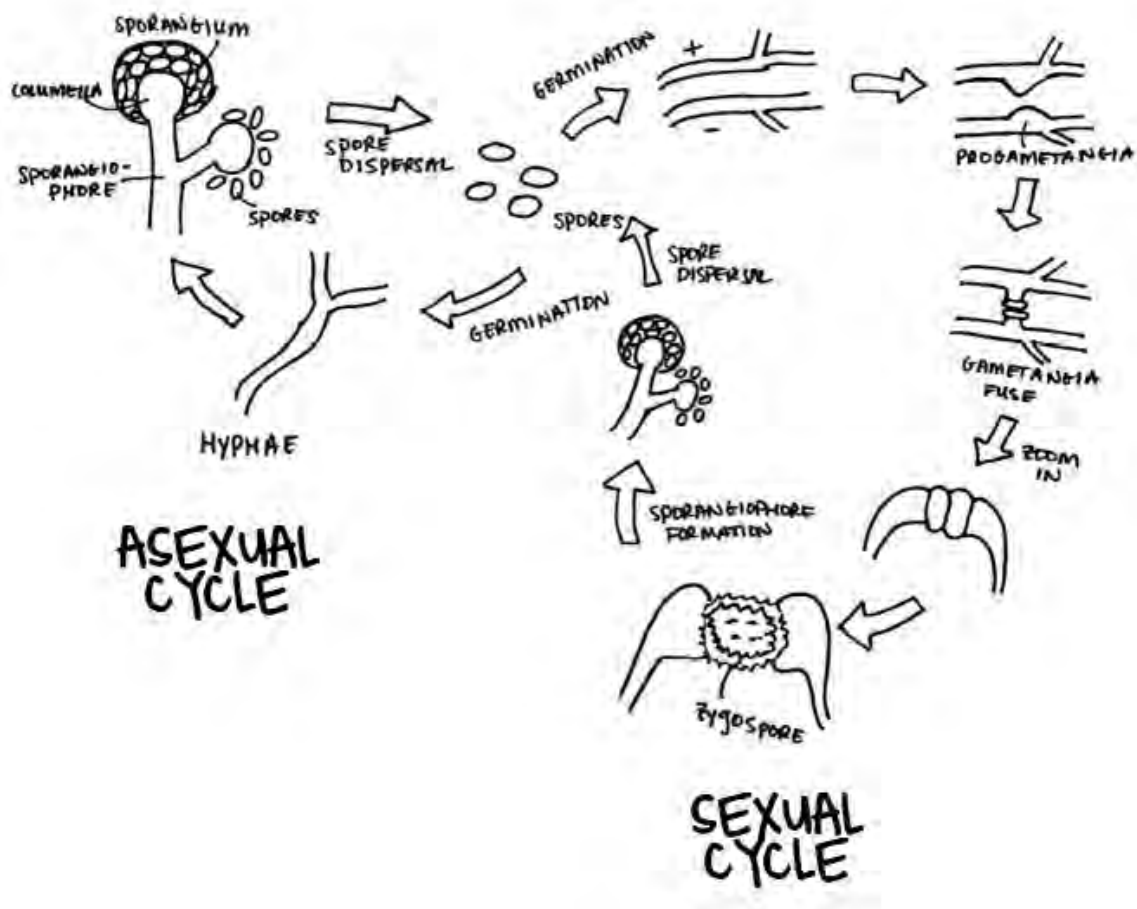


**Figure 1.1 Reproductive life cycles of Zygomycetes.** In the asexual cycle, spores germinate and form hyphae. Upon adequate conditions, sporangiophores form, with spore-filled sporangia on top. Spores are then dispersed, and cycle continues. Sexual reproduction begins with hyphae of opposite mating types meeting and hyphae (progametangia) branching toward each other. Swollen gametangia fuse and form a zygospore. After dormancy, a sporangiophore sprouts from the zygospore and the cycle continues. (Adapted from Deacon, 2006).

**1.2.2 The cell wall.** For most pathogenic fungi, the structure of the fungal cell wall is well-characterised. For example, in *Candida albicans* the cell wall is comprised of a chitin and  $\beta$ -glucan inner layer, with an outer layer containing

mannosylated glycoproteins (Shibata *et al.*, 2007; Wheeler *et al.*, 2008; Gow, Latge and Munro, 2017). In *Aspergillus spp.* conidia,  $\alpha$ -1,3-glucan, melanin, and hydrophobic proteins cover the inner chitin and  $\beta$ -1,3-glucan (Wessels, 1996; Paris *et al.*, 2003; Beauvais *et al.*, 2005; Gow, Latge and Munro, 2017). The outer cell wall of *A. fumigatus* hyphae is comprised of  $\alpha$ -1,3-glucan, galactomannan, galactosaminoglycan, and proteins, with the inner cell wall being chitin and  $\beta$ -1,3-glucan (Fontaine *et al.*, 2000; Gow, Latge and Munro, 2017).

The cell wall of Mucorales is less defined as compared to *C. albicans* and *Aspergillus spp.*, and the exact structure is not known (Figure 1.2). However, it is understood to be mainly comprised of chitosan (26-28%) and chitin (10-15%) (Compos-Takaki G.M, Dietrich and Beakes, 2014).  $\beta$ -glucan makes up a very small proportion of the Mucoralean cell wall, and mucormycosis is not easily diagnosed through  $\beta$ -glucan detection tests (Karageorgopoulos *et al.*, 2011). Mucorales secrete very small amounts of  $\beta$ -glucan in culture supernatants (Odabasi *et al.*, 2006), and this polysaccharide likely does not make up a major part of the cell wall, is not readily shed, and/or is only present in dormant spores. The un-germinated *Mucor circinelloides* spore has an outer melanin layer and an inner component containing chitin, chitosan, glucan, and mannan (Bartnicki-Garcia and Reyes, 1964; Bartnicki-Garcia, Nelson and Cota-Robles, 1968). The hyphal cell wall is made of chitin, chitosan, mucoran, and mucoric acid (Bartnicki-Garcia, Nelson and Cota-Robles, 1968). According to Bartnicki-Garcia *et al.* (1968), hyphae contain little  $\beta$ -glucan, which is probably be due to the decrease

in glucan synthase and *de novo* cell wall synthesis during the germination process, though the mechanism of restructuring is unknown.

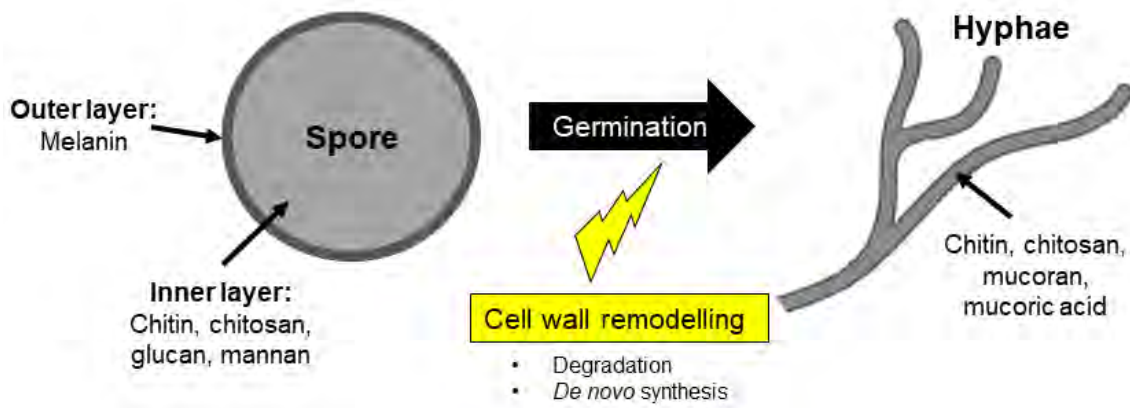


**Figure 1.2 Cell wall of Mucorales.** The cell wall structure of Mucorales is largely undefined. The components of the un-germinated spore and hyphal cell wall are distinct. Spores have an outer layer comprised of melanin and an inner layer with chitin, chitosan, glucan, and mannan. Hyphae contain chitin, chitosan, mucoran, and mucoric acid. (Adapted from Lecointe *et al.*, 2019).

**1.2.3 Spore swelling and germination.** Key to the pathogenesis of Mucorales is the ability of spores to transition from a dormant, resting state to metabolically active swelling spores and eventual germination (Figure 1.3). Fungal germination is a virulence determinant, which leads to angioinvasion, vessel thrombosis, tissue necrosis, and death (Ibrahim, Spellberg, *et al.*, 2005). Exposure to acidic pH, water, and nutrients (such as glucose and nitrogen) activates two pH-dependent aquaporins (RdAQP1 and RdAQP2) on the surface of *R. delemar* spores (Figure 1.3A) (Turgeman *et al.*, 2016). This induces an active isotropic

growth, where the spores swell approximately 3-fold, allowing the acquisition of water and necessary nutrients to begin germinating (Figure 1.3B) (Turgeman *et al.*, 2016). While dormant spores exhibit very little chitin, swelling enhances the surface chitin (Sephton-Clark *et al.*, 2018). Molecularly, swelling involves cell wall biogenesis, protein synthesis, sugar metabolism, and an increase in intracellular reactive oxygen species (ROS) (Sephton-Clark *et al.*, 2018).

Isotropic growth provides nutrients necessary for driving germination. Following this, the spores become polarised and germ tubes emerge at polarised regions prior to hyphal elongation (Figure 1.3C) (Money, 2016b). Mechanisms for germination are less defined in Mucorales than in other filamentous fungi, though *Rhizopus delemar* has been shown transcriptionally to enhance cytoskeleton regulation, cell wall remodelling, and stress response genes during germination (Sephton-Clark *et al.*, 2018). In *Aspergillus nidulans*, germination is triggered by available carbon sources, which activate RasA and initialise protein synthesis (Osherov and May, 2000). While *C. albicans* filamentation is regulated by the cyclic adenosine monophosphate (cAMP) / Protein Kinase A (PKA) and mitogen-activated protein kinase (MAPK) pathways (Stoldt *et al.*, 1997; Alonso Monge *et al.*, 2006), *A. fumigatus* germination is not PKA dependent (Osherov and May, 2000).

Rather than restructuring the cell wall for hyphal protrusion, *M. circinelloides* synthesises a new cell wall underneath the existing one during swelling before

the germ tube breaks through (Figure 1.3D and E) (Bartnicki-Garcia, Nelson and Cota-Robles, 1968). During filamentation, cell membrane synthesis, migration of the cytoplasm, and maintenance of hyphal turgor pressure also occur (Steinberg, 2007; Money, 2016b). Germination involves the delivery and accumulation of vesicles from the Golgi apparatus to the growing hyphal tip along microfilaments (Johnston, Prendergast and Singer, 1991). In most fungi, these vesicles form a dark body, known as the Spitzenkörper which facilitates hyphal elongation via the delivery of essential nucleic acids, F-actin, and other components of the cell wall that fuse to the growing tip (Howard and Aist, 1979; Bartnicki-Garcia *et al.*, 1995). Mucorales hyphae also utilise a vesicle-based delivery service, termed the apical vesicle crescent (AVC), which is essential for proper germination (Figure 1.3F) (Fisher and Roberson, 2016b). In contrast to the Spitzenkörper, the AVC has an unorganised structure and does not strongly control directional growth (Fisher and Roberson, 2016b). The exact contents of the AVC are unknown, and it is currently debated whether the AVC is a type of Spitzenkörper or if they are completely different structures (Fisher and Roberson, 2016a).

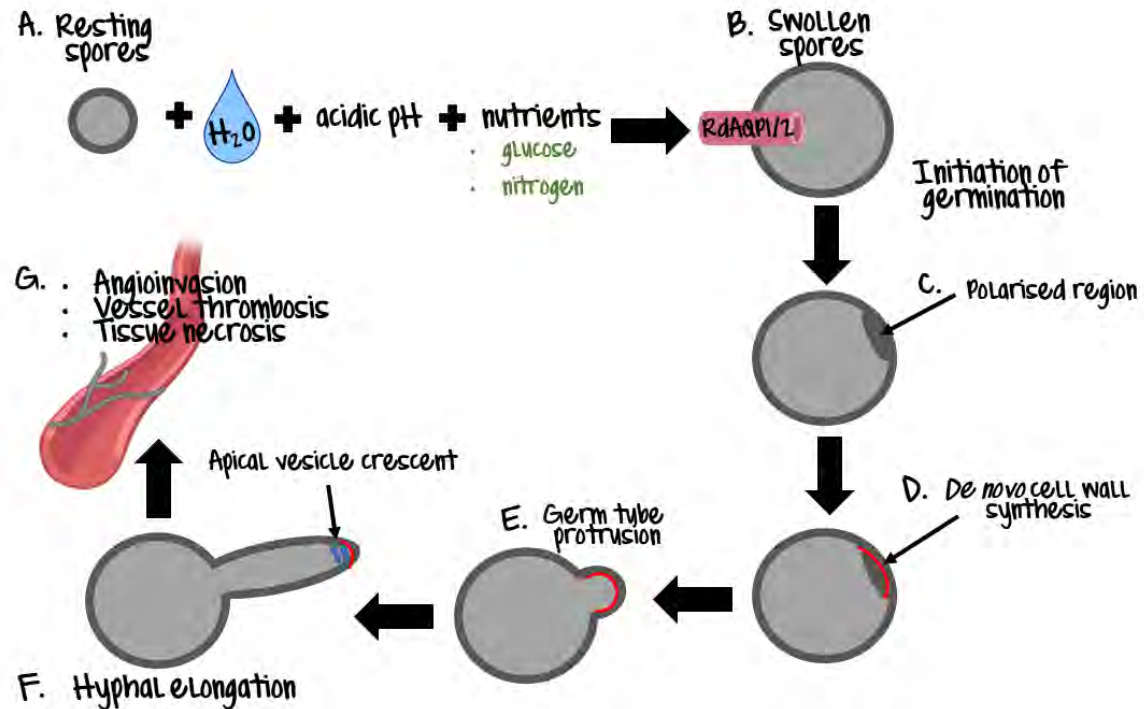


**Figure 1.3 Spore swelling and germination of Mucorales.** (A) When resting spores are exposed to water, acidic pH, and nutrients, the aquaporins RdAQP1 and RdAQP2 are activated. (B) These allow for the influx of water and nutrients necessary to drive germination, resulting in swollen spores. Swelling involves cell wall biogenesis and increased chitin. Germination is initiated through (C) polarisation and (D) *de novo* cell wall synthesis under existing cell wall. (E) Germ tube protrudes at polarised point. (F) Hyphal elongation is mediated by delivery of vesicles to the growing tip, called the apical vesicle crescent. Within a host, germination results in (G) angioinvasion, vessel thrombosis, and tissue necrosis. Created with Biorender ([www.biorender.com](http://www.biorender.com)).

**1.2.4 Mucormycosis.** Mucorales are the etiological agents of mucormycosis, a fatal infection occurring in immunocompromised patients. This includes individuals with cancer, neutropenia, chronic renal failure, and burn, blast, or traumatic wounds. Mucormycosis also occurs post-transplantation, post-

tuberculosis, and following corticosteroid therapy (Roden *et al.*, 2005; Prakash and Chakrabarti, 2019). The most common underlying condition is uncontrolled diabetes, which accounts for 38% of cases (Roden *et al.*, 2005). Different to other fungal infections, such as candidiasis and cryptococcosis, HIV/AIDS is not a major risk factor for mucormycosis, and co-infection with the virus is rare (Moreira *et al.*, 2016). This is likely because of the necessity of innate immune cells, rather than T-cells, to control Mucorales (Ibrahim *et al.*, 2012). Mucormycosis does occur in late-stage AIDS, in patients with median CD4<sup>+</sup> counts of 47, and it is usually associated with neutropenia or intravenous drug use (Moreira *et al.*, 2016).

The most frequent manifestations of Mucorales infections are rhinocerebral, cutaneous, and pulmonary mucormycosis (Jeong *et al.*, 2019). Mortality is exceptionally high, and mortality rates are 54% overall though outcome varies based on location of infection. Death occurs in 46% of rhinocerebral, 76% of pulmonary, and 96% of disseminated mucormycosis, where 13-23% of infections become disseminated (Roden *et al.*, 2005; Jeong *et al.*, 2019).

Mucormycosis is classically considered to be a rare disease. However, epidemiological studies have reported rising incidences of infection, and it is now considered the second most common invasive mould infection and the third most prevalent cause of angioinvasive fungal disease (Kennedy *et al.*, 2016; Trieu *et al.*, 2017; Prakash and Chakrabarti, 2019). A 10-year retrospective study in

France reported an elevated incidence of mucormycosis from 0.7 to 1.2 cases per million hospitalised persons, rising 7.3% each year (Bitar *et al.*, 2009). In the United States, approximately 0.12 per 10,000 patients are hospitalised with mucormycosis (Kontoyiannis *et al.*, 2016). This rise is likely due to enhanced awareness, improved diagnostic methods, and increases in diabetes and age-associated immunocompromising diseases. Global prevalence is estimated to be less than 10,000 cases per year (Bongomin *et al.*, 2017), but some regions are more prone to mucormycosis, with India and Pakistan seeing 140 cases of mucormycosis per million patients (Chakrabarti and Dhaliwal, 2013; Jabeen *et al.*, 2017).

**1.2.5 Pathogenesis and infection.** Spores enter the body through inhalation, exposure to mucosal surfaces, ingestion of contaminated food, or contamination of wounds. In a healthy individual, phagocytes engulf spores and inhibit germination, though resting spores are resistant to killing (Waldorf, Ruderman and Diamond, 1984). However, swollen spores are susceptible to killing by macrophages and neutrophils (Levitz *et al.*, 1986). More recently, swollen *Rhizopus microsporus* spores were shown to inhibit macrophage phagocytosis and survive within macrophages, which is dependent on the presence of the bacterial endosymbiont, *Ralsonia pickettii* (Itabangi *et al.*, 2019, preprint). Intracellular inhibition of spore swelling and germination through iron restriction maintains melanin on the cell wall, which inhibits phagosome maturation and prevents killing (Andrianaki *et al.*, 2018). Some virulent *M. circinelloides* strains can survive and germinate within macrophages *in vitro*. This process is

dependent on ROS response pathways and is regulated by the transcription factors Atf1 and Atf2 (activating transcription factor) (Pérez-Arques *et al.*, 2019).

Following infection, neutrophils exhibit delayed recruitment to infection sites, possibly due to the lack of neutrophil chemoattractants produced by resting spores. Once swollen, spores then produce chemotactic molecules (Waldorf and Diamond, 1985). Mucorales activate Toll-like receptor 2 on polymorphonuclear neutrophils and stimulate the immune system through the NF- $\kappa$ B pathway (Chamilos *et al.*, 2008). Despite this, neutrophils cannot kill resting spores, though they are able to damage and kill the hyphae of germinated *Rhizopus oryzae* through oxidative stress, defensins, and neutrophil extracellular traps (NETs) (Ibrahim *et al.* 2012; Diamond & Clark 1982). However, neutrophil damage to Mucoralean hyphae is still attenuated when compared with *A. fumigatus* (Chamilos *et al.*, 2008).

Immunodeficiency results in decreased lymphocyte numbers, insufficient chemotaxis, and/or depressed phagocytosis, and the immune system is unable to effectively control infection (Waldorf, Ruderman and Diamond, 1984). Adherence and invasion of epithelial cells is key for the pathogenesis of mucormycosis, and the initial adherence is mediated by the host's epithelial growth factor receptor (EGFR). Inhibition of EGFR signalling decreases virulence of *R. oryzae* in mouse models (Watkins *et al.*, 2018). Angioinvasion is a hallmark of mucormycosis, and attachment to endothelial cells is mediated by the binding

of the spore cell wall ligand CotH to glucose-regulated protein 78 (GRP78) on the surface of endothelial cells (Gebremariam *et al.*, 2014). Binding of CotH by GRP78 only occurs in germlings, rather than un-germinated spores (Liu *et al.*, 2010). Copies of *CotH* in the genome is associated with prevalence of infection, with the most common etiological agent, *R. delemar*, containing 6-7 copies of *CotH* and the rarer species, *C. bertholletiae*, only containing 1-2 copies (Baldin *et al.*, 2018). In diabetic patients, increased glucose, ketone bodies (such as  $\beta$ -hydroxy butyrate), and iron enhance the expression of GRP78 and *CotH*, which explains why diabetes is a major risk factor for mucormycosis (Liu *et al.*, 2010).

**1.2.6 Iron dependency, uptake, and storage.** While iron is essential for the pathogenesis of all microorganisms, Mucorales have a uniquely strong dependence on available iron. In comparison to *C. albicans* and *A. fumigatus*, the virulence of *R. oryzae* is highly regulated by iron availability (Abe *et al.*, 1990). Mucorales are unable to grow in human serum and supplementation with exogenous iron recovers germination, suggesting their inability to scavenge iron from host proteins (Artis *et al.*, 1982). Consistent with this, conditions where iron overload occurs, such as during blood transfusions or renal failure, are risk factors for mucormycosis (Ibrahim, Spellberg and Edwards, 2008). In patients with diabetic ketoacidosis (DKA), where blood pH is between 7.3-6.8, the hydrogen bonds connecting iron to transferrin are weakened, increasing the levels of free iron (Figure 1.4). The normal concentration of serum iron in healthy individuals is  $10^{-18}$  M ( $1 \times 10^{-13}$   $\mu\text{g/dl}$ ) (Bullen, Rogers and Griffiths, 1978). However, acidotic individuals have levels between 13  $\mu\text{g/dl}$  to 69  $\mu\text{g/dl}$ , and

exposure of *R. oryzae* to these conditions allows for germination (Artis *et al.*, 1982). Iron is also essential for spore survival, and extended periods of iron starvation induces apoptosis (Shirazi, Kontoyiannis and Ibrahim, 2015).

Most fungi produce hydroxamate siderophores; however, Mucorales produce a carboxylate siderophore called rhizoferrin, which has a much lower affinity for iron than the hydroxamates (Thieken and Winkelmann, 1992). Unlike many bacterial and fungal siderophores, rhizoferrin is unable to extract iron from host sequestering proteins and is therefore not currently believed to play a role in fungal pathogenicity (Ibrahim, Spellberg and Edwards, 2008).

The main route for Mucorales to acquire iron is via the high affinity iron permease, Ftr1 (Figure 1.4) (Fu *et al.*, 2004; Ibrahim *et al.*, 2010). *FTR1* is expressed in iron-deprived conditions and works in cooperation with ferric reductases on the cell wall. These reduce ferric to ferrous iron in preparation for intracellular transport. After being transported through the cell wall, a copper oxidase converts ferrous iron to ferric iron, before further transport into the cytoplasm (Stearman *et al.*, 1996). Iron is bound to ferritin for storage, and Mucorales are the only fungi which synthesise ferritin (Figure 1.4) (Matzanke, 1994; Ibrahim *et al.*, 2012). *FTR1* is necessary for virulence of *R. oryzae in vivo*, providing further evidence of the essentiality of iron for pathogenesis (Ibrahim *et al.*, 2010).

While rhizoferrin is ineffective in human infections, Mucorales utilise deferoxamine as a xenosiderophore. Deferoxamine is a siderophore produced by *Streptomyces pilosis* (Yamanaka *et al.*, 2005) and is an iron chelation drug for patients with risk of iron-overload (Windus *et al.*, 1987). Mucorales bind ferrioxamine (the iron rich form of deferoxamine) through Fob1 and Fob2 receptors that allow the spores to extract, reduce, and absorb the bound iron (Figure 1.4) (Liu *et al.*, 2015).

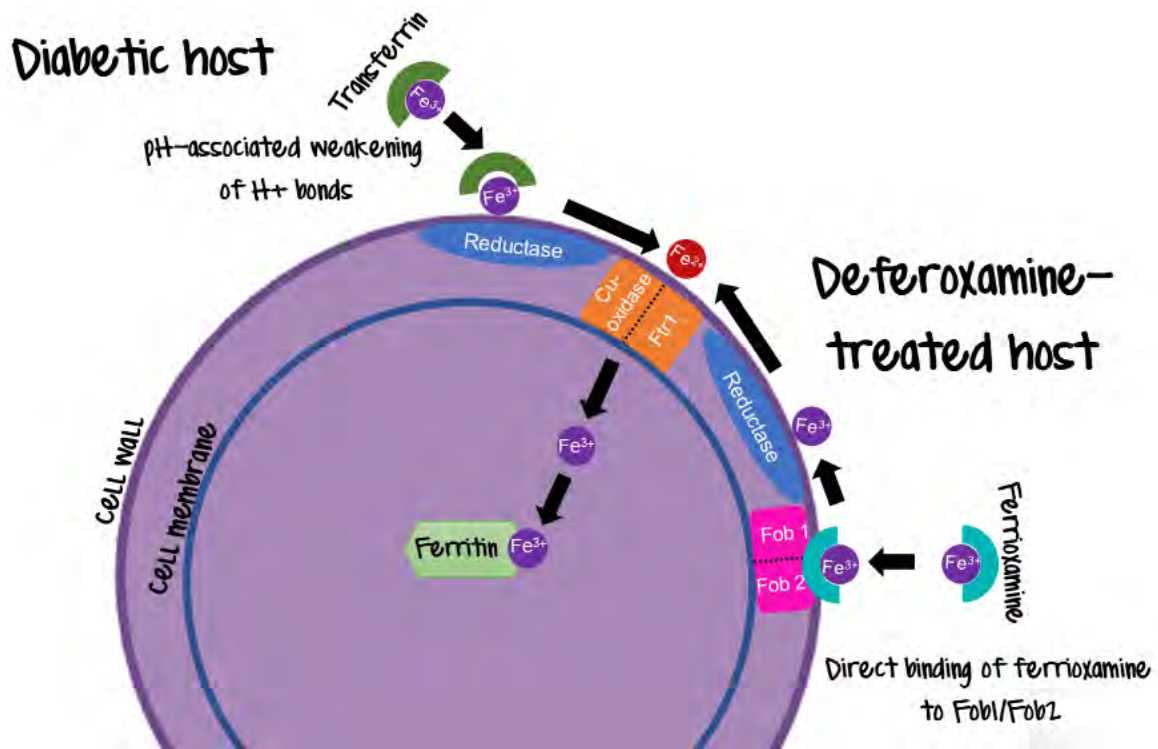


**Figure 1.4 Iron acquisition mechanisms in Mucorales.** In a diabetic host, DKA weakens hydrogen bonds, allowing for the scavenging of iron from transferrin. Ferric (Fe<sup>3+</sup>) iron is reduced to its ferrous (Fe<sup>2+</sup>) form via a reductase on the cell surface. Fe<sup>2+</sup> is then oxidised by a copper-oxidase and transferred into the cytoplasm via Ftr1. Iron is bound to ferritin for storage. Deferoxamine is a xenosiderophore, and ferrioxamine (the iron-rich form of deferoxamine) binds to Fob1/Fob2 on the spore surface. Reductive

uptake continues as previously described. (Adapted from Ibrahim, Spellberg and Edwards, 2008).

**1.2.7 Diagnosis.** While early diagnosis is essential for the effective treatment of mucormycosis, diagnostic methods are currently lacking. Clinical characteristics are generic and are often confused with other fungal infections, such as aspergillosis and fusariosis, or bacterial infections, like *P. aeruginosa* (Katragkou, Walsh and Roilides, 2014). Pulmonary infections manifest as a high fever, non-productive cough, chest pain, and difficulty breathing. Radiographical diagnosis is difficult, as chest images also provide non-specific results that are often confused with aspergillosis (Petrikkos *et al.*, 2012). The most common form of mucormycosis, rhinocerebral mucormycosis, presents as pain and blurred vision, and is usually identified by black, necrotic tissue on the face or hard palate (Petrikkos *et al.*, 2012). However, after infection has progressed to this extent, survival is unlikely.

Biopsy and histopathology are used as diagnostic techniques and can be accurate if performed by highly trained personnel familiar with distinguishing between aspergillosis and mucormycosis (Baldin *et al.*, 2018). Microscopically, Mucorales present as irregular, broad, aseptate hyphae (Frater, Hall and Procop, 2001), while *Aspergillus spp.* have thin, septate hyphae that are regularly branched at acute angles (Hope, Walsh and Denning, 2005).

There are currently no serological diagnosis tests used for mucormycosis. However, assays have been developed for the diagnosis of *C. albicans* and *Aspergillus spp.*, based on the detection of circulating  $\beta$ -1,3-D-glucan (BG tests) (Richardson and Page, 2018). However, these are generally ineffective for diagnosing mucormycosis as Mucorales contain very little cell wall glucans (Mélida *et al.*, 2015; Richardson and Page, 2018). However, this is a source of contention in the field, as there have been reports of positive BG tests in patients with confirmed mucormycosis (Angebault *et al.*, 2016), and  $\beta$ -glucan synthetase can be found in the genome (Ibrahim, Bowman, *et al.*, 2005).

Mycological culture remains the gold standard, even though Mucorales are poorly culturable from active, necrotic lesions. Sensitivity of culture is low, with only one-third of mucormycosis cases detected this way (Lackner, Caramalho and Lass-Flörl, 2014). Molecular diagnostic approaches are in its infancy, though there has been recent progress in developing a non-invasive PCR-based assay. Here, the antigen CotH could be accurately detected in the urine of infected mice, with a sensitivity of 90% and specificity of 100%. This was effective for all Mucorales tested and was negative for mice infected with *A. fumigatus* as a control (Baldin *et al.*, 2018). Therefore, future diagnostic methods will likely involve PCR identification for rapid, non-invasive, specific detection.

**1.2.8 Treatment.** Extensive necrosis makes this infection difficult to treat, with necrotic tissue preventing leukocytes and antifungals from reaching the infection

site (Ibrahim *et al.*, 2012). Effective therapy involves intensive antifungal treatment, surgical debridement, and reversal of underlying condition. Antifungal therapy alone is rarely effective and surgical debridement of the affected tissue is usually required. This leads to extensive, permanent disfiguration and high patient morbidity (Kontoyiannis and Lewis, 2011). Despite therapeutic interventions, mortality can reach 96% in disseminated mucormycosis even with rigorous antifungal administration (Katragkou, Walsh and Roilides, 2014). Treatment of mucormycosis is expensive, with each patient costing approximately \$112,000 in the United States (Kontoyiannis *et al.*, 2016).

**1.2.8.1 Antifungals.** Mucorales are inherently resistant to short-tail azoles, such as fluconazole and voriconazole. Azoles' main mode of action is through destabilisation of the cell membrane through the inhibition of ergosterol biosynthesis, as ergosterol is the major component of the fungal cell membrane (Hitchcock *et al.*, 2015). Azoles specifically act on the lanosterol 14 $\alpha$ -demethylase in the ergosterol biosynthesis pathway, and Mucoralean resistance to short-tailed azoles is due to an amino acid substitution in this enzyme (Caramalho *et al.*, 2017). However, mid- and long-tail azoles can be effective in mucormycosis, as isavuconazole and posaconazole are used as salvage therapies (van Burik *et al.*, 2006; Graves *et al.*, 2016).

Due to the limited efficacy of the azoles against Mucorales, the polyene amphotericin B is the first-line treatment for mucormycosis. Like the azoles,

amphotericin B disrupts the fungal cell membrane. However, instead of inhibiting biosynthesis, amphotericin B binds to ergosterol and creates pores in the cell membrane (Finkelstein and Holz, 1973). While mostly effective, some strains of Mucorales display resistance to amphotericin B, and high doses are necessary to impact fungal growth, often resulting in renal failure (Ibrahim, Spellberg and Edwards, 2008). Because of this, lipid formulations of amphotericin B (also known as AmBisome) are utilised to reduce nephrotoxicity, though damage still occurs in prolonged treatment with high doses (Personett *et al.*, 2019). For patients with haematological malignancies, amphotericin B treatment leads to 39% survival, while liposomal amphotericin increases survival rates to 62% (Gleissner *et al.*, 2004). Distribution of the antifungals into necrotic tissue is difficult, though utilisation of polymethylmethacrylate beads loaded with amphotericin B as a delivery system within a soft-tissue necrotic wound reduced fungal burden in a patient with cutaneous mucormycosis (Heller *et al.*, 2017). Mucorales exhibit high variability of antifungal susceptibility between species, with minimum inhibitory concentrations of amphotericin B for *Cunninghamella* being significantly higher than for *Rhizopus* and *Mucor*. Further, *R. oryzae* tends to be resistant to posaconazole, while *M. circinelloides* is generally susceptible (Katragkou, Walsh and Roilides, 2014).

Echinocandins alone are not effective against Mucorales. These drugs inhibit cell wall synthesis, and the lack of activity against Mucorales could be caused by an upregulation of chitin synthase in response to the induced cell wall stress, as found with *C. albicans* (Walker *et al.*, 2008). However, studies have found a

combination of amphotericin B and caspofungin to synergise against *R. delemar* (Reed *et al.*, 2008; Kazak *et al.*, 2013).

**1.2.8.2 Alternative strategies.** As iron is essential for the pathogenesis of mucormycosis, iron chelators have been explored as adjunct therapies. When administered alongside amphotericin B, deferasirox (also known as Exjade) synergises and improves survival of infected mice (Ibrahim *et al.*, 2007). Furthermore, deferasirox used as a salvage therapy following liposomal amphotericin B treatment in a patient with rhinocerebral mucormycosis led to complete recovery (Reed *et al.*, 2006). Because of this, a clinical trial known as the DEFEAT Mucor (Deferasirox–AmBisome Therapy for Mucormycosis) study was performed, but unfortunately more patients in the deferasirox treated arm died than in the control (Spellberg *et al.*, 2012).

Recently, anti-CotH antibodies have been shown to protect mice against mucormycosis and synergize with antifungals (Gebremariam *et al.*, 2019). This indicates a potential use for immunotherapy in treating human infection in the future.

Taken together, this highlights the necessity for novel therapeutic targets and investigation into unknown regulators of pathogenesis, including the impact of polymicrobial interactions on fungal virulence.

### 1.3 Polymicrobial interactions.

Microbiological research has historically been approached from a mono-pathogen perspective, and many clinical diseases were originally thought to be caused by a single etiological agent. However, in recent years there is an increase in the understanding that no organism lives in isolation, and that to fully understand the pathogenesis of an individual microbe, the influence of others must be recognised. Bacteria, fungi, and viruses have co-evolved to develop elaborate and intricate relationships, which are present in both healthy and diseased states. These relationships can strongly influence the pathogenesis of each organism, the progression of infection, and the overall patient prognosis. For example, while mono-infections with *C. albicans* or *S. aureus* in a murine model of peritonitis were not life-threatening, co-infection resulted in a 40% mortality rate, increased inflammation, and greater microbial burden (Peters and Noverra, 2013). Polymicrobial interactions can occur throughout the body (Figure 1.5) and can be more resistant to antimicrobial therapy, resulting in poorer host prognosis (Carlson, 1982; Harriott and Noverr, 2009).

As Mucorales are naturally environmental saprophytes, they have evolved alongside microbes within the soil, on decaying plants and animals, and while colonising plant roots. In a clinical setting, mucormycosis can occur in blast, burn, and traumatic wounds, where 70% of infections are polymicrobial (Akers *et al.*, 2014; Warkentien *et al.*, 2015). Furthermore, mucormycosis can emerge post-transplantation in patients with Cystic Fibrosis (CF) whose lung environment is usually polymicrobial even post-transplantation (Hunstad, Cohen and St. Geme,

1999; Brugière *et al.*, 2005; Rabin and Surette, 2012; Syed *et al.*, 2016). The impact of other microorganisms on Mucorales virulence is largely unknown, though polymicrobial interactions play a definitive role in the pathogenicity of other microbes (Peters *et al.*, 2012).

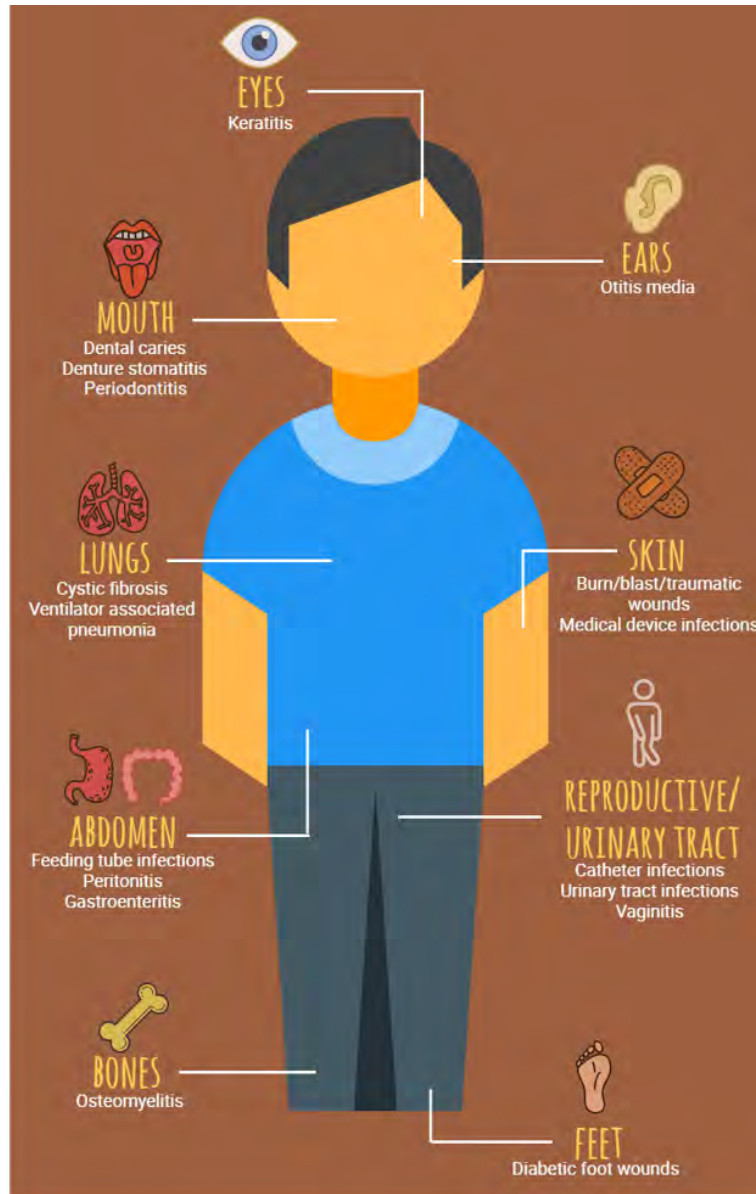


**Figure 1.5 Sites of polymicrobial infections.** Polymicrobial interactions can occur in various sites throughout the body and can impact overall disease outcome (This figure has been published in *Microbiology Today*, Kousser, Alam and Hall, 2019).

**1.3.1 Mechanisms of intra- and inter-species interactions.** Microorganisms can interact through a variety of different methods. The most well-studied mechanisms include physical cell-to-cell contact, such as biofilm formation or

attachment of bacteria to fungal hyphae (Hogan and Kolter, 2002; Harriott and Noverr, 2009; Schlecht *et al.*, 2015); and chemical interactions, where the production of toxins, secondary metabolites, or other molecules influences the growth and development of the other microbe (Holcombe *et al.*, 2010; Mowat *et al.*, 2010). Another method of interaction is through the alteration of host immune responses. For example, *C. albicans* can prime the immune system upon initial, sub-lethal exposure, and enhance immune response to secondary *P. aeruginosa* infection. This leads to more effective clearing of the bacterial burden (Quintin *et al.*, 2012; Mear *et al.*, 2014).

**1.3.2 Competitive vs. cooperative relationships.** Polymicrobial interactions can manifest in the form of cooperative or competitive relationships. Cooperative interactions result in the individual organisms working together to survive within a host. The result of cooperation can be additive, where the impact of each organism combines. Additive effects are usually found within multi-species biofilms, for example in periodontal disease, where a myriad of Gram-negative and Gram-positive bacteria and *C. albicans* form complex biofilms in the oral cavity (Kolenbrander, 2002). Some cooperative relationships can also be synergistic, where the relationships between microbes enhance their respective virulence. This results in effects greater than additive and can promote more aggressive infections. *C. albicans* and *S. aureus* have been found to work synergistically together, where co-infections lead to enhanced microbial burden of each organism in the vaginal epithelium (Pidwill *et al.*, 2018). The binding of *S. aureus* to *C. albicans* hyphae promotes deeper penetration of bacteria into the

host and can lead to systemic infection (Schlecht *et al.*, 2015). Furthermore, Group B *Streptococcus* promotes the survival of *E. coli* in a urinary tract infection, resulting in more aggressive, reoccurring infections (Kline *et al.*, 2012).

However, not all microbes work together. Some relationships are antagonistic, where they compete for resources and space. Organisms can either actively fight against their competition or they can make colonisation difficult by creating a hostile niche. Competition between organisms usually results in the death or inhibition of virulence of one or both organisms. *P. aeruginosa* is implicated in a variety of antagonistic relationships with both bacteria and fungi. For example, *P. aeruginosa* and *A. fumigatus* form a mutually antagonistic relationship within the CF lung (Reece *et al.*, 2018). In this case, *P. aeruginosa* induces apoptosis of *A. fumigatus*, while *A. fumigatus* can inhibit biofilm formation of *P. aeruginosa* (Shirazi *et al.*, 2016; Reece *et al.*, 2018). *P. aeruginosa* can also inhibit filamentation of *C. albicans*, while *C. albicans* can reduce the virulence of *P. aeruginosa* by suppressing virulence factor secretion (Hogan, Vik and Kolter, 2004; Lopez-Medina *et al.*, 2015). Bacteria can also compete against each other. For instance, there is an inverse association between individuals who test positive as carriers for *Streptococcus pneumoniae* and those who carry *S. aureus*, presumably due to competition (Regev-Yochay *et al.*, 2004; Chao *et al.*, 2015).

**1.3.3 Mucorales and *C. albicans*.** *C. albicans* is the most well-characterised and commonly implicated fungus participating in polymicrobial interactions. As it is

part of the microbiome and present in numerous niches, interactions between *C. albicans* and Mucorales likely occur. Because standard diagnostic techniques for identifying mucormycosis have a low sensitivity and the incidence of fungi is under-reported in general, there is limited data regarding co-isolation with other fungi. Therefore, it is not currently known whether *C. albicans* interacts with any Mucorales. However, both fungi are present in burn and post-traumatic wounds, diabetic-associated infections, and CF-associated lung transplantations (Kubak, 2012; Neto *et al.*, 2014; Mendoza *et al.*, 2015). Furthermore, *Candida glabrata* and *Rhizopus microsporus* were co-isolated in a case of peritonitis (Monecke *et al.*, 2006). It is possible to extrapolate the potential interaction between *R. microsporus* and *C. albicans* in this context, as *C. albicans* is also isolated in peritonitis and associated with high mortality rates (Cheng *et al.*, 2013). Interestingly, fungal chitosan extracted from *Rhizomucor miehei* and *Mucor racemosus* was shown to have anti-fungal properties on *C. albicans* and *C. glabrata*, which could indicate a potential contact-dependent interaction (Tajdini *et al.*, 2010). *C. albicans* inhibits other filamentous fungi via secreted factors (Semighini *et al.*, 2006; Semighini, Murray and Harris, 2008), therefore it is reasonable to hypothesize that *C. albicans* will have similar inhibitory effects on Mucorales.

**1.3.4 Mucorales and bacteria.** As immunocompromised individuals are at high risk for polymicrobial infections involving both opportunistic bacteria and fungi, it is likely that Mucorales come into contact with several bacterial species. For instance, *Rhizopus spp.* and *Klebsiella pneumoniae* have been co-isolated in

cases of pulmonary gangrene (Chougule *et al.*, 2015). Mucormycosis was also found in a patient with uncontrolled diabetes who originally suffered from *K. pneumoniae* infection and tuberculosis (Dogra *et al.*, 2015). Moreover, Dimaka *et al.* (2014) explain that chronic rhinocerebral mucormycosis may present as a co-infection with other organisms, and they specifically highlight *P. aeruginosa*. The majority of wound infections are polymicrobial (Akers *et al.*, 2014; Warkentien *et al.*, 2015) and 19% of mucormycosis cases are cutaneous (Roden *et al.*, 2005; Jeong *et al.*, 2019). *P. aeruginosa*, *S. aureus*, and *Escherichia coli* are the most commonly isolated bacterial species from chronic wounds (Gjødtsbøl *et al.*, 2006; Kalan *et al.*, 2016), and are therefore likely to interact with Mucorales spores. Furthermore, fungal chitosan extracted from *R. miehei* and *M. racemosus* is not only antimicrobial against *C. albicans*, but also against *P. aeruginosa* and *Escherichia coli* (Tajdini *et al.*, 2010). *Serratia marcescens* interacts with *R. oryzae* by binding to, migrating along, and killing the hyphae of *R. oryzae* (Hover *et al.*, 2016). This is most likely not a *S. marcescens*-specific phenomenon and it is probable that other bacteria are able to interact in a similar way.

Mucormycosis presents with non-specific symptoms and is commonly misdiagnosed as being caused by other infectious agents. Sometimes the presence of commensal bacteria or a bacterial infection will mask mucormycosis, a situation known as “Green Herring Syndrome” (Peixoto *et al.*, 2014). This delays diagnosis of mucormycosis and leads to poorer patient outlook and increased mortality. Examples of this occurring in mucormycosis patients with concurrent *E. coli* or *P. aeruginosa* infections have been reported, and *P.*

*aeruginosa* infection is one of the differential diagnoses for mucormycosis (Katragkou, Walsh and Roilides, 2014; Peixoto *et al.*, 2014).

Mucormycosis has been associated with the use of antibiotics, and it is suggested that treatment with broad spectrum antibiotics can lead to fungal infections (Ribes, Vanover-Sams and Baker, 2000). Early speculation regarding the emergence of mucormycosis was attributed to the growing widespread use of antibiotics (Baker, 1957). Furthermore, another early study found a 10-fold increase in aseptic fungal burn wound infections following the advent of topical antibiotics (Nash *et al.*, 1971). This could indicate that antibiotics kill inhibitory bacteria, removing pressures and allowing for secondary mucormycosis.

Increasing evidence suggests that most species of Mucorales harbour endosymbiotic bacteria, usually *Burkholderia* or *Ralstonia spp.*, that influence fungal reproduction and virulence (Mondo *et al.*, 2017; Itabangi *et al.*, 2019, preprint) though there has been conflicting results (Ibrahim *et al.*, 2008). In terms of plant pathogenesis, the endosymbionts *Burkholderia rhizoxinica* and *Burkholderia endofungorum* secrete rhizoxin, a chemical which causes rice seedling blight (Partida-Martinez *et al.*, 2007).

#### **1.4 Aim of this study.**

Mucormycosis is a debilitating infection with limited treatment options and a high mortality rate. While the presence of other microorganisms is known to impact the growth and development of fungi such as *Aspergillus spp.* and *C. albicans* (Kerr *et al.*, 1999; Hogan and Kolter, 2002; Hogan, Vik and Kolter, 2004; Ferreira *et al.*, 2015), little is known about the impact of polymicrobial interactions on Mucoralean pathogenesis. As bacteria and fungi rarely exist in isolation, the progression of mucormycosis is likely affected by these organisms. This study aims to investigate whether Mucorales are influenced by polymicrobial interactions, the mechanisms surrounding these relationships, and how the host could be affected.

## Chapter 2 : MATERIALS AND METHODS

Parts of this chapter have been previously published:

Kousser, C., Clark, C., Sherrington, S., Voelz, K. and Hall, R. (2019).  
*Pseudomonas aeruginosa* inhibits *Rhizopus microsporus* germination  
through sequestration of free environmental iron. *Scientific Reports*, 9.  
DOI 10.1038/s41598-019-42175-

## 2.1 Strains and culture conditions.

All media and chemicals were purchased from Sigma-Aldrich unless stated otherwise. For details of fungal and bacterial strains used, please see (Table 1). Mucorales were routinely sub-cultured ( $1 \times 10^4$  spores/ml, Section 2.1.2), maintained on Sabouraud 4% dextrose agar (SAB, Merck Millipore, Germany), and incubated for 10-14 days before use (25°C). *Candida albicans* was maintained on Yeast Extract Peptone Dextrose (YPD) with 2% agar. Bacteria were maintained on Lysogeny broth (LB) with 2% agar.

**Table 2.1 Strains used in this project.**

Strain	Characteristics	Source
<i>Rhizopus microsporus</i> 12.6652333	Clinical isolate, non-invasive	(Trzaska <i>et al.</i> , 2015) Queen Elizabeth Hospital
<i>Cunninghamella bertholletiae</i> 182	Clinical isolate, lungs	(Simitsopoulou <i>et al.</i> , 2010) University of Kentucky College of Medicine
<i>Lichtheimia corymbifera</i>	Clinical isolate, wound	(Trzaska <i>et al.</i> , 2015) Queen Elizabeth Hospital
<i>Candida albicans</i> SC5314	Wild type	(Meyers <i>et al.</i> , 1968)
<i>R. microsporus var. microsporus</i>	Clinical isolate	Westerdijk Fungal Biodiversity Institute

CBS 699.68		
<i>R. microsporus</i> var. <i>chinensis</i> CBS 631.82	Clinical isolate	Westerdijk Fungal Biodiversity Institute
<i>R. delemar</i> RA 99-880	Clinical isolate	Fungal Genetics Stock Centre
<i>Mucor circinelloides</i> NRRL3631	Clinical isolate	ARS Culture Collection (NRRL)
<i>Burkholderia</i> <i>cenocepacia</i> K56-2	Clinical isolate from Cystic Fibrosis	(Darling <i>et al.</i> , 1998)
<i>Klebsiella pneumoniae</i> ATCC43816R	Spontaneously rifampicin-resistant. Derived from clinical isolate ATCC43816	(Bakker-Woudenberg <i>et al.</i> , 1985)
<i>Staphylococcus aureus</i> USA300	Wild type	(Hawley <i>et al.</i> , 2013)
<i>Escherichia coli</i> MG1655	Wild type	(Stones <i>et al.</i> , 2017)
<i>Pseudomonas</i> <i>aeruginosa</i> PAO1 ATCC15692	Wild type	American Type Culture Collection (ATCC)
<i>P. aeruginosa</i> PAO1	Wild type	(Holloway, 1955; Ghysels <i>et al.</i> , 2004)
<i>P. aeruginosa</i> $\Delta$ pchEF	PAO1, deleted pyochelin	(Ghysels <i>et al.</i> , 2004)

<i>P. aeruginosa</i> $\Delta$ pvdD	PAO1, deleted pyoverdine	(Ghysels <i>et al.</i> , 2004)
<i>P. aeruginosa</i> $\Delta$ pchEF $\Delta$ pvdD	PAO1, deleted pyochelin and pyoverdine	(Ghysels <i>et al.</i> , 2004)
<i>P. aeruginosa</i> PA14	Wild type	(Rahme <i>et al.</i> , 1995)
<i>P. aeruginosa</i> :mCherry	PA14 with PME6032:mcherry plasmid	This study
<i>P. aeruginosa</i> CHA	Clinical isolate, Cystic Fibrosis	(Delic-Attree <i>et al.</i> , 1996) Centre Hospitalier Universitaire of Grenoble
<i>P. aeruginosa</i> MID	Clinical isolate, Cystic Fibrosis	(Scott and Pitt, 2004) Heartlands Hospital
<i>P. aeruginosa</i> LIV	Clinical isolate, Cystic Fibrosis	(Cheng <i>et al.</i> , 1996) Heartlands Hospital
<i>P. aeruginosa</i> blood	Clinical isolate, blood	Queen Elizabeth Hospital Birmingham
<i>P. aeruginosa</i> 985	Clinical isolate, burn wound	(Quick <i>et al.</i> , 2014)
<i>P. aeruginosa</i> 1008	Clinical isolate, burn wound	(Quick <i>et al.</i> , 2014)
<i>P. aeruginosa</i> 1009	Clinical isolate, burn wound	(Quick <i>et al.</i> , 2014)

**2.1.2 Maintaining and sub-culturing Mucorales.** Fungal spores were maintained on SAB agar (25°C) and routinely sub-cultured onto fresh SAB agar plates once per week to maintain active stocks. A 100 µl droplet of sterile phosphate buffered saline (PBS) was added to each new agar plate. A small sample of spores were scraped from a parent plate using a sterile pipette tip, added to the PBS, and spread using an L-shaped spreader. Every two months, the active spore stock was replaced with spores from a freezer stock, stored in CryoTubes (Fisher-Scientific, Pro-Lab Diagnostics Microbank Bacterial and Fungal Preservation System) at -80°C.

**2.1.3 Harvesting sporangiospores.** After at least 10 days of growth on SAB agar, plates containing fungi were flooded with 10 ml PBS. Hyphae were carefully broken to release spores by gently using an L-shaped spreader, and spores were collected into a 15 ml falcon tube. The spore solution was centrifuged (3000 rpm, 3 minutes), washed and resuspended in PBS. Spores were counted using a haemocytometer, adjusted to desired concentration, and kept on ice until needed to prevent swelling and metabolic activity.

**2.1.4 Creating frozen spore stocks.** After 10-14 days of growth, spores were harvested as above, centrifuged (3000 rpm, 3 minutes), and resuspended in 800 µl PBS. Concentrated spore stocks were added to CryoTubes (Fisher-Scientific, Pro-Lab Diagnostics Microbank Bacterial and Fungal Preservation System) in

duplicate and mixed well. One vial was stored in liquid nitrogen and the other in a -80°C freezer.

## **2.2 Elucidating the effect of supernatants on Mucorales.**

**2.2.1 Exposing Mucorales to *Candida albicans* supernatant.** YPD broth (5 ml) was inoculated with *C. albicans* and incubated for 24 hours (37°C, 200 rpm) in 50 ml falcon tubes. Cultures were centrifuged (4000 rpm, 4 minutes) and sterilised using 0.22 µm syringe filters. Sterile supernatants were stored at -80°C until required. *R. microsporus* (n=4), *L. corymbifera* (n=3), and *C. bertholletiae* (n=3) spores ( $1 \times 10^4$  spores/ml) were added to a well plate containing either 50% SAB and 50% YPD broth or 50% SAB and 50% supernatant. Fungal germination was monitored over 18 hours using live cell imaging (37°C with humidity), and the percent of spores germinated in each field of view was quantified (Section 2.7.3). Two-way Repeated Measures ANOVA with Tukey's multiple comparisons test was used on arcsine transformed data to analyse significance (Section 2.13.1).

**2.2.2 Exposing Mucorales to bacterial supernatants.** LB broth (10 ml) was inoculated with bacteria (*P. aeruginosa*, *B. cenocepacia*, *E. coli*, *K. pneumoniae*, or *S. aureus*) and incubated for 24 hours (37°C, 200 rpm) in 50 ml glass conical flasks until absorbance (OD<sub>600</sub>) reached at least 3.0. Cultures were separated into 10 ml aliquots and centrifuged (4500 rpm, 10 minutes) and the resulting supernatant was sterilised using 0.22 µm syringe filters. Sterile supernatants

were stored at  $-80^{\circ}\text{C}$  until required. Spores ( $1 \times 10^4$  spores/ml) were added to a well plate containing either 50% SAB and 50% LB, or 50% SAB and 50% supernatant. Fungal germination and growth were determined by endpoint analysis after 24 hours using absorbance ( $\text{OD}_{600}$ ) as a quantifier of growth (FLUOstar Omega plate reader) and/or percent of spore germination in each field of view was analysed following live cell imaging. Absorbance was analysed using Kruskal Wallis with Dunn's multiple comparisons test. For percent germination, Two-way Repeated Measures ANOVA with Tukey's multiple comparisons test was used on arcsine transformed data (Section 2.13.1) to analyse significance.

**2.2.3 Testing the effect of pH change and nutrient starvation on germination.** SAB broth (5 ml) was added to 5 ml of sterile supernatant and thoroughly mixed. The pH was measured using a bench-top pH meter (Mettler Toledo). Fresh SAB and LB were mixed 50:50, and the pH was adjusted to match the pH of the supernatant mixture using 5 M sodium hydroxide (NaOH) and filter sterilised. To model nutrient depletion, PBS and SAB were mixed 50:50 and pH was adjusted to match normal SAB/LB control. Two-way Repeated Measures ANOVA with Tukey's multiple comparisons test was used on arcsine transformed data (Section 2.13.1) to analyse significance ( $n=3$ ).

**2.2.4 Exposure of pre-germinated *R. microsporus* spores to *P. aeruginosa* supernatant.** Spores were harvested and added to 500  $\mu\text{l}$  of SAB broth at a concentration of  $1 \times 10^6$  spores/ml in triplicate in a 24 well plate. Spores were

incubated statically for 4 to 5 hours at 37°C until germlings emerged and then either 500 µl of sterile *P. aeruginosa* supernatant or 500 µl LB was added. The plate was incubated for 18 hours at 37°C, and the endpoint absorbance (OD<sub>600</sub>) of each well was measured (n=4, Mann-Whitney U test).

**2.2.5 Observing the effect of *P. aeruginosa* supernatant on *R. microsporus* antifungal susceptibility.** Stock solutions of amphotericin B, posaconazole, and fluconazole were prepared in dimethyl sulfoxide (DMSO, 5 mg/ml), aliquoted, and stored at -20°C. Stocks were diluted in 50:50 SAB:LB or 50:50 SAB:supernatant (64 µg/ml) and doubling dilutions were prepared in a 96-well plate to a final concentration of 0.0625 µg/ml for posaconazole and fluconazole and 0.00775 µg/ml for amphotericin B. *R. microsporus* spores (1 x 10<sup>4</sup> spores/ml) were added to each well and incubated for 24 hours at 37°C. Endpoint measurement of fungal growth was analysed via absorbance (OD<sub>600</sub>, n=3, Kruskal Wallis test with Dunn's multiple comparisons test).

### **2.3 Quantifying the effects of microbial secreted molecules on fungal germination.**

Resting Mucorales spores (1 x 10<sup>4</sup> spores/ml) were added to SAB broth with the addition of the below chemicals. Endpoint absorbance (OD<sub>600</sub>) readings were measured after 24 hours incubation at 37°C to determine overall fungal growth for all chemicals, except farnesol and dodecanol, which were imaged via time lapse microscopy.

**2.3.1 Fungal quorum sensing molecules.** Farnesol was prepared in 100% methanol to a final concentration of 200  $\mu\text{M}$  in SAB broth. This solution (200  $\mu\text{l}$ ) was added to 96 well plates in duplicate, *Rhizopus microsporus*, *Cunninghamella bertholletiae*, and *Lichtheimia corymbifera* spores ( $1 \times 10^4$  spores/ml) were added, and 2 positions per well were imaged via time lapse microscopy (37°C). Controls included SAB only and SAB + methanol, as solvent control. Two-way Repeated Measures ANOVA on arcsine-transformed data (Section 2.13.1) with Tukey's multiple comparisons test was used to analyse data (n=3).

**2.3.2 Bacterial quorum sensing molecules.** The quorum sensing molecule (QSM) mimic, dodecanol, was prepared in 100% methanol to a final concentration of 200  $\mu\text{M}$  in SAB broth. This (200  $\mu\text{l}$ ) was added to 96 well plates in duplicate, *R. microsporus*, *C. bertholletiae*, and *L. corymbifera* spores were added ( $1 \times 10^4$  spores/ml), and 2 positions per well were imaged via time lapse microscopy (37°C). Controls included SAB only and SAB + methanol. Two-way Repeated Measures ANOVA on arcsine-transformed data with Tukey's multiple comparisons test was used to analyse data (n=3).

Stock solutions of the *P. aeruginosa* QSMs N-butanoyl-L-homoserine lactone (C4 HSL), N-hexanoyl-DL-homoserine lactone (C6 HSL), N-octanoyl-L-homoserine lactone (C8 HSL), and N-(3-oxododecanoyl)-L-homoserine lactone (C12 HSL) were made in DMSO to a total concentration of 50 mM. Working concentrations

were 10, 50, 100, and 200  $\mu\text{M}$  diluted in 1 ml SAB broth. The diluted QSMs (200  $\mu\text{l}$ ) were added to 96 well plates in duplicate and *R. microsporius* spores were added ( $1 \times 10^4$  spores/ml). Controls included SAB only and SAB + DMSO, (n=3, Kruskal-Wallis test with Dunn's multiple comparisons test).

**2.3.3 Bacterial toxins.** Pyocyanin (ready-made solution; 5 mg/ml in DMSO) was diluted to 12.5, 25, and 50  $\mu\text{M}$  in SAB broth. Controls include SAB broth only and SAB + DMSO, (n=3, Kruskal-Wallis test with Dunn's multiple comparisons test).

## **2.4 Characterising the inhibitory compound.**

**2.4.1 Denaturation of proteins in *P. aeruginosa* supernatant.** To determine if the inhibitory substance is proteinaceous, *P. aeruginosa* supernatants were collected, filter sterilised, and a 1 ml sample was boiled at  $100^\circ\text{C}$  for 1 hour to denature proteins. To remove the effect of any heat-stable proteins, Proteinase K (20  $\mu\text{g}/\text{ml}$  stock, New England Biolabs) was added to 1 ml of supernatant at a concentration of 150  $\mu\text{g}/\text{ml}$  and incubated at  $37^\circ\text{C}$  for 2 hours. The Proteinase K was inactivated by heating at  $100^\circ\text{C}$  for 1 hour. Spores were added to 50% treated supernatants and 50% SAB at a total volume of 200  $\mu\text{l}/\text{well}$  in a 96 well plate. Controls included 50:50 SAB + LB, and 50:50 SAB + untreated supernatant. Well plates were incubated for 18 hours at  $37^\circ\text{C}$  and endpoint absorbance ( $\text{OD}_{600}$ ) was measured, (n=6, Kruskal-Wallis test with Dunn's multiple comparisons test).

**2.4.2 Organic extraction of *P. aeruginosa* supernatant.** To determine whether the inhibitory molecule is hydrophilic or hydrophobic, chloroform extractions were performed on *P. aeruginosa* supernatants. *P. aeruginosa* supernatant (40 ml) was collected, sterilised and placed in a glass extraction funnel with the addition of chloroform (50% volume). This was mixed thoroughly and allowed to settle into aqueous and organic phases. The organic phase was removed, and the process was repeated two more times. Sodium sulphate was added to the organic phase until any remaining water was removed, and dried using a rotary evaporator. The resulting powder was reconstituted in 1 ml DMSO and further resuspended with LB to a total volume of 40 ml. The aqueous phase was also placed on a rotary evaporator to remove any remaining chloroform. As a procedural control, this chloroform extraction was also performed on fresh LB, (n=5, Kruskal-Wallis test with Dunn's multiple comparisons test).

**2.4.3 Removal of *R. microsporus* endosymbiont.** To determine whether the resident bacterial endosymbiont is mediating *R. microsporus* inhibition, the endosymbiont was removed via antibiotic treatment. *R. microsporus* spores were harvested and sub-cultured for at least 10 generations onto SAB agar plates + 60 µg/ml ciprofloxacin to kill bacterial endosymbiont. Loss of endosymbiont was confirmed through SYTO9 staining and microscopy. Cured spores were exposed to *P. aeruginosa* supernatant as previously described for parent spores in Section 2.2.2 (n=3, Kruskal-Wallis test with Dunn's multiple comparisons test).

## **2.5 Investigating the role of metal restriction on supernatant-dependent growth inhibition.**

**2.5.1 Addition of iron, zinc, copper, and manganese to *R. microsporus* spores following exposure to *P. aeruginosa* supernatant.** To determine whether micronutrient depletion was inducing the germination defect, spores were exposed to ferric chloride (FeCl<sub>3</sub>), zinc chloride (ZnCl<sub>2</sub>), cupric sulphate (CuSO<sub>4</sub>), and manganese sulphate (MgSO<sub>4</sub>). Metal stocks (100 mM in dH<sub>2</sub>O) were diluted to 1, 10, 50, 100, 200, and 500 µM (2x concentrated) in *P. aeruginosa* supernatants (500 µl). The metals were allowed to associate with any chelating molecules for 15 minutes before the addition of an equal volume of SAB broth. Wells containing the SAB/supernatant mixture without metals were included as controls. *R. microsporus* spores (1 x 10<sup>4</sup> spores/ml) were added to each well and incubated for 24 hours. Absorbance (OD<sub>600</sub>) was used to measure fungal growth (n=3, Kruskal-Wallis test with Dunn's multiple comparisons test).

**2.5.2 Exposure of *R. microsporus var microsporus*, *R. microsporus var chinensis*, *R. delemar*, and *M. circinelloides* to *P. aeruginosa* supernatant +/- iron.** To determine if *P. aeruginosa* supernatant had the same effect on closely related Mucorales (Chibucos *et al.*, 2016), ferric chloride (100 mM stocks) was diluted to 100 µM (2x concentrated) in *P. aeruginosa* supernatants (500 µl). The metals were allowed to associate with any chelating molecules for 15 minutes before the addition of an equal volume of SAB broth. Wells containing the SAB/supernatant mixture without metals were included as controls. *R.*

*microsporus* spores ( $1 \times 10^4$  spores/ml) were added to each well and incubated for 24 hours. Absorbance ( $OD_{600}$ ) was used to measure fungal growth (n=3, Kruskal-Wallis test with Dunn's multiple comparisons test).

### **2.5.3 Exposure of *R. microsporus* to purified, exogenous bacterial siderophores.**

**2.5.3.1 Pyoverdine.** To determine whether the major siderophore produced by *P. aeruginosa*, pyoverdine, is capable of inhibiting *R. microsporus* growth, spores were exposed to exogenous pyoverdine. Pyoverdine (10 mg/ml in dH<sub>2</sub>O) was diluted to 15  $\mu$ M (17.4  $\mu$ g/ml) in SAB broth before the addition of spores ( $1 \times 10^4$  spores/ml) and subsequent incubation for 24 hours (37°C, n=6, Mann-Whitney U test).

**2.5.3.2 Enterobactin.** To determine if siderophore-mediated inhibition is a universal effect, *R. microsporus* spores were exposed to a high-affinity siderophore produced by *E. coli*, enterobactin (Carrano and Raymond, 1979). A stock solution of enterobactin was made in DMSO to a concentration of 50 mM. Working concentrations of 10, 50, and 100  $\mu$ M were made in SAB broth before the addition of spores ( $1 \times 10^4$  spores/ml) and subsequent incubation for 24 hours (37°C, n=3, Kruskal-Wallis with Dunn's multiple comparisons test).

To determine if enterobactin can enhance *R. microsporus* germination when exposed to *P. aeruginosa* supernatant, 50  $\mu$ M enterobactin was added to 50% *P.*

*aeruginosa* supernatant + 50% LB. *R. microsporus* ( $1 \times 10^4$  spores/ml) were incubated in solutions at 37°C for 24 hours before images were taken using a Zeiss AxioObserver inverted microscope (x20 magnification).

**2.5.4 Viability of spores exposed to *P. aeruginosa* supernatant.** Iron starvation has been shown to induce apoptosis in *Rhizopus oryzae* (Shirazi, Kontoyiannis and Ibrahim, 2015). To determine the impact of *P. aeruginosa* supernatant on *R. microsporus* viability, spores ( $1 \times 10^6$  spores/ml) were exposed to 100% *P. aeruginosa* supernatant for 96 hours (statically, 37°C). Every 24 hours, 100 spores were plated on SAB agar and incubated at 25°C for 24 hours. Following incubation, the number of viable spores were counted and compared to 0-hour control plates (n=3, Kruskal-Wallis test with Dunn's multiple comparisons test).

## **2.6 Quantification of bacterial virulence factor production.**

To determine the overall secretion of toxins and siderophores in this system, supernatants from either mono- or co-cultured *P. aeruginosa* PAO1 were analysed using the following methods:

**2.6.1 Pyocyanin secretion.** *P. aeruginosa* was grown in LB (24 hours, 37°C, 200 rpm), and supernatants were prepared by centrifugation (4500 rpm, 10 minutes) and sterilisation using a 0.22  $\mu\text{m}$  syringe filter. Absorbance (690 nm) was

measured using a FLUOstar Omega plate reader and compared to a pyocyanin standard curve.

**2.6.2 Overall siderophore production.** Siderophore concentration in bacterial supernatants or co-culture supernatants (Section 2.9.2) were quantified by using the SideroTec Assay Kit (Emergen Bio) according to the manufacturer recommendations (n=3, Mann-Whitney U test).

**2.6.3 Pyoverdine secretion.** *P. aeruginosa* and *R. microsporus* ( $1 \times 10^6$  spores/ml) were co-cultured in 1 ml RPMI-1640 (Thermo-Fisher) at multiplicity of infection (MOI) ratios of 1:1, 1:10, 1:50, and 1:100 in a 24 well plate (statically, 24 hours, 37°C). Plates were centrifuged (4000 rpm, 5 minutes) and 200 µl from each well was transferred to a 96 well plate in duplicate. Pyoverdine production was measured at 405 nm (Stintzi *et al.*, 1996). Absorbance of co-culture supernatant was compared to absorbance of supernatants from *P. aeruginosa* alone, with the same starting concentration of bacteria (n=4, Kruskal-Wallis test with Dunn's multiple comparisons test).

## **2.7 Microscopy.**

Mucoralean virulence is dependent on the ability to germinate and penetrate surrounding tissues (Ibrahim *et al.*, 2012). Microscopy was used to visualise the germination of spores following exposure to desired conditions.

**2.7.1 Live-cell imaging.** To observe fungal growth and germination over time, live-cell imaging was performed for 12-18 hours at 37°C with humidity using a Zeiss AxioObserver inverted microscope (20x magnification). Images were taken every 10 minutes to create a time-lapse movie, and spore germination was quantified as described in Section 2.7.3.

**2.7.2 Endpoint imaging.** Following 18-24 hours of spore exposure to experimental conditions, at least four images per condition were captured using a Zeiss AxioObserver inverted microscope (20x magnification). Images were analysed as described below.

**2.7.3 Quantifying spore germination.** For both live-cell imaging and endpoint microscopy, the percentage of germinated spores compared to total spores in each field of view was determined. Germination was defined as the point in which the germ tube reached the same size as the spore diameter. Fiji Image J software (Schindelin *et al.*, 2012) was used to count germinated spores. Data was analysed using a Two-way ANOVA performed on arcsine transformed data (Section 2.13.1).

**2.7.4 Spore swelling.** To compare the isotropic growth of Mucorales spores in the presence of microbial secreted factors, the area of resting versus swollen

spores were measured using Fiji Image J software (Schindelin *et al.*, 2012) following live-cell imaging. Spores were considered resting at the first time point imaged and maximum isotropic growth was measured for all non-germinated spores at the final time point before 50% of the spores in the field of view have germinated.

To convert spore area to volume, the radius was first calculated according to Equation 1 and the volume was calculated according to Equation 2:

Equation 1: Calculating radius from the area of a sphere

$$\text{radius} = \sqrt{\frac{\text{area}}{\pi}}$$

Equation 2: Calculating the volume of a sphere

$$\text{Volume} = \frac{4}{3}\pi r^3$$

Statistical significance was calculated using Kruskal Wallis with Dunn's multiple comparisons test.

**2.7.5 Time to first germ tube.** To determine whether the presence of microbial secreted factors impacts the initiation of germination on an individual, rather than population level, the time point (minutes) in which the first spore germinated was recorded following live-cell imaging (Kruskal Wallis with Dunn's multiple comparisons test).

**2.7.6 Hyphal width.** As a marker for nutrient starvation (Turgeman *et al.*, 2014), hyphal width of germinated spores was measured using Fiji Image J software (Schindelin *et al.*, 2012). One hour after the first germ tube protruded, the average width of each hyphae was measured at three different points for at least 100 hyphae per condition per experiment (n=3). (Kruskal Wallis with Dunn's multiple comparisons test).

## **2.8 Quantifying chitin.**

To determine if *P. aeruginosa* impacts *R. microsporus* cell wall chitin, spores were harvested (Section 2.1.3) and exposed to 15 ml of either 50:50 SAB:LB to promote swelling, or 50% *P. aeruginosa* supernatant for 4 hours (200rpm, 37°C). Resting spores were maintained in PBS on ice to prevent swelling.

**2.8.1 Staining spores.** Spores were washed three times with PBS and stained with 250 µg/ml calcofluor white (CFW) for 45 minutes (37°C, 200 rpm). Stained spores were washed three times with PBS (centrifuged at 3000 rpm, 3 minutes), wet mounted onto glass slides, and imaged on a Zeiss AxioObserver at 63x magnification. Four images per condition were captured. Relative fluorescence intensity was measured through image analysis of at least 50 spores per condition per experiment (Section 2.8.2).

**2.8.2 Measuring fluorescence.** The fluorescence intensity of CFW stained spores correlates to the chitin content of the fungal cell wall (Monheit, Cowan and Moore, 1984). Endpoint images were analysed using Fiji ImageJ software (Schindelin *et al.*, 2012). A circle was drawn around each spore, and the corrected total cell fluorescence (CTCF) was measured according to Equation 3:

Equation 3: Calculating fluorescence intensity

$$\text{CTCF} = \text{Integrated Density} - (\text{Cell area} \times \text{Mean fluorescence of background})$$

Data was analysed using Kruskal Wallis with Dunn's multiple comparisons test (n=4).

## **2.9 Live co-cultures of *R. microsporus* and *P. aeruginosa*.**

**2.9.1 Determining colony forming units from bacterial absorbance.** LB (5 ml) was inoculated with bacteria and incubated for at least 18 hours (37°C, 200 rpm). Bacteria were washed two times with PBS by centrifugation (8000 rpm, 2 minutes), and absorbance (OD<sub>600</sub>) was measured by spectrophotometer. Samples were diluted to an OD<sub>600</sub> of 0.01, 0.02, 0.04, and 0.05 and serially diluted to 10<sup>-4</sup>. Dilutions (10 µl of 10<sup>-2</sup>, 10<sup>-3</sup>, and 10<sup>-4</sup>) were plated onto LB agar, incubated for 18 hours (37°C) and colonies were counted to determine correlation between absorbance and colony forming units (CFUs).

**2.9.2 Investigating the impact of live bacteria on *Rhizopus microsporus* germination.** To determine whether there is any contact-dependent inhibition of

bacteria on *R. microsporus* germination, LB was inoculated with *P. aeruginosa*, *K. pneumoniae*, *B. cenocepacia*, *E. coli*, or *S. aureus* and incubated for 24 hours (37°C, 200 rpm). Bacteria were washed three times with PBS. *R. microsporus* spores ( $1 \times 10^4$  spores/ml) were added to 50% SAB, 50% LB in a 96-well plate. Bacteria were added to each well at a multiplicity of infection (MOI) ratio of 1:1, 1:10, 1:50, and 1:100 and incubated for 24 hours (static, 37°C). Wells were imaged using an inverted Zeiss AxioObserver microscope (20x magnification). The number of germinated spores per field of view were quantified for spores exposed to *P. aeruginosa* (n=4, Two-way ANOVA performed on arcsine transformed data).

**2.9.3 Addition of enterobactin to live co-cultures.** Enterobactin was added to live co-cultures of *R. microsporus* and *P. aeruginosa* (MOI 1:100) to determine whether the addition of enterobactin can aid fungal growth. Co-cultures were prepared as described above (Section 2.9.2). A 50 mM stock of enterobactin was prepared in DMSO. Enterobactin was diluted to 50  $\mu$ M in 50:50 SAB:LB before the addition of spores ( $1 \times 10^4$  spores/ml) and bacteria ( $1 \times 10^6$  CFUs/ml) and subsequent incubation for 24 hours (static, 37°C). Endpoint images were taken using a Zeiss AxioObserver inverted microscope (20x magnification) (n=3).

**2.9.4 Investigating the ability of live *P. aeruginosa* to decrease spore viability, in an iron-dependent manner.** *R. microsporus* ( $1 \times 10^4$  spores/ml) and *P. aeruginosa* ( $1 \times 10^6$  CFUs/ml) were added to 1 ml of 50:50 SAB:LB +/- 100  $\mu$ M

FeCl<sub>3</sub> in a 24 well plate and incubated for 24 hours (statically, 37°C). Following incubation, each well was mixed thoroughly, and 100 spores were spread onto SAB agar containing 100 µg/ml tetracycline. Agar plates were incubated for 24 hours (25°C) before the number of viable spores were counted and compared to 0 hour control plates (n=3, Two-way ANOVA with Sidak's multiple comparisons test).

## **2.10 Molecular biology**

**2.10.1 Gel Electrophoresis.** For visualisation of nucleic acids following RNA extraction, DNA extraction, plasmid isolation, or polymerase chain reaction (PCR), agarose gels (1%) were prepared in 1x TAE (Tris-acetate-EDTA) buffer with SYBER Safe DNA gel stain (2 µl per 40 ml agarose, Thermo-Fisher Scientific). A GeneRuler 1 kb Plus DNA Ladder (5 µl, Thermo-Fisher Scientific) was run alongside the samples. Electrophoresis was carried out at 75 volts for 35 minutes, and RNA or DNA were observed by ultraviolet (UV) trans-illumination on a Bio Rad ChemiDoc MP imaging system using Image Lab 4.1 software.

**2.10.1.1 DNA Gel Electrophoresis.** To visualise concentration and quality of DNA, 5 µl of PCR products, plasmid isolates, or extracted DNA were mixed with 1 µl gel loading dye (6x concentrated, New England Biolabs) before gel electrophoresis as described in Section 2.10.1.

**2.10.1.2 Non-denaturing RNA Gel Electrophoresis.** RNA quality was confirmed by separating the RNA via electrophoresis. RNA samples (5 µl) were mixed with 1 µl gel loading dye (6x concentrated, New England Biolabs) and heated at 70°C for 5 minutes to denature the RNA. Samples were centrifuged briefly and 5 µl was loaded onto the agarose gel and run as previously described (Section 2.10.1).

**2.10.2 Genomic DNA extraction from Mucorales.** *R. microsporus* spores were harvested, washed in PBS, and counted. Genomic DNA was extracted using a Qiagen DNeasy PowerSoil kit according to manufacturer instructions. Pelleted spores (at least  $1 \times 10^7$ ) were resuspended in Solution C1 (500 µl), transferred into 2 ml tubes containing 0.5 mm glass beads (Precellys, VWR, Product code VK05), and homogenised using a Precellys 24 tissue homogeniser (Berlin Instruments, 2 x 20 seconds, 6500 rpm, 2 cycles). Tubes were placed on ice between cycles and before centrifugation (10000 rpm, 30 seconds). Supernatant was removed and transferred to a new 2 ml collection tube. Following a series of washes using an MB spin column with the provided solutions as per manufacturer instructions, 100 µl of Solution C6 (elution buffer) was added directly to the membrane before centrifugation (10000 rpm, 30 seconds). DNA quality was confirmed through gel electrophoresis and imaging using UV trans-illumination (Section 2.10.1.1). Concentration of DNA was quantified by diluting 1:100 in dH<sub>2</sub>O and using a spectrophotometer, where an OD<sub>260</sub> of 1 equals 50 µg/ml of double stranded DNA. Purity was measured through absorbance wavelength ratios of 260/280 and 260/230.

**2.10.3 Genomic DNA isolation of bacteria.** Genomic DNA was extracted from *P. aeruginosa* cultures following incubation in LB (18 hours, 37°C, 200 rpm). A sample (200 µl) of the culture was heated (100°C, 10 minutes) to lyse the cells and denature DNases. This was centrifuged (13000 rpm, 30 seconds), the supernatant was collected, and stored at -20°C until needed.

**2.10.4 RNA extraction of Mucorales.** Extraction of fungal RNA involved modification of the Qiagen RNeasy Plus Mini kit manufacturer protocol. *R. microsporus* spores ( $2.5 \times 10^6$  spores/ml) were exposed to 50:50 SAB:LB or 50% *P. aeruginosa* supernatant, 50% SAB (10 ml total volume in 50 ml glass conical flasks). Flasks were incubated statically at 37°C for 7 hours. Spores were centrifuged (3000 rpm, 3 min), pellets were snap frozen in liquid nitrogen, and stored at -80°C. When ready to extract RNA, 1 ml of TRIzol (Invitrogen) was added to each sample and thawed on ice. Samples were transferred into 2 ml tubes containing 0.5 mm glass beads (Precellys, VWR), and homogenised using a Precellys 24 tissue homogeniser (Berlin Instruments, 2 x 20 seconds, 6500 rpm, 2 cycles). Tubes were placed on ice between cycles and before centrifuging at 13000 rpm, 4°C for 1 minute. Chloroform (200 µl) was added to each sample, vortexed thoroughly, and centrifuged at 13000 rpm, 4°C, for 15 minutes. The aqueous layer was collected and run through the gDNA (genomic DNA) eliminator column (10000 rpm, 1 minute). An equal volume of 100% ethanol was added to the resulting flow-through. This solution, including precipitates, was

transferred to the RNeasy column, and centrifuged for 30 seconds, 10000 rpm. The membrane was washed with RW1 buffer (350  $\mu$ l, 10000 rpm, 30 seconds) before the addition of RNase-Free DNase (Qiagen) directly to the membrane according to manufacturer recommendations. The column was incubated at room temperature for 20 minutes before washing once with RW1 buffer (350  $\mu$ l, 10000 rpm, 30 seconds), and twice with RPE buffer (10000 rpm for 30 seconds, followed by 2 minutes). RNA was eluted from the membrane by adding 50  $\mu$ l dH<sub>2</sub>O, incubating for 1 minute (room temperature), centrifuging for 1 minute (10000 rpm) and repeating with 30  $\mu$ l dH<sub>2</sub>O.

RNA quality was confirmed through gel electrophoresis and imaging of using UV trans-illumination (Section 2.10.1.2). The concentration was measured by diluting RNA 1:100 in dH<sub>2</sub>O and using a spectrophotometer, where an OD<sub>260</sub> of 1 equals 40  $\mu$ g/ml of double stranded RNA. Purity was measured through absorbance wavelength ratios of 260/280 and 260/230. RNA was stored at -80°C until required.

**2.10.5 RNA extraction of bacteria.** *P. aeruginosa* ( $1 \times 10^8$  CFUs/ml) was exposed to 50:50 SAB:LB (+/- 100  $\mu$ M FeCl<sub>3</sub>) or *R. microsporus* spores ( $1 \times 10^6$  spores/ml, +/- 100  $\mu$ M FeCl<sub>3</sub>). Flasks were incubated at 37°C and 50 rpm for 7 hours. Samples (1 ml) from each culture were centrifuged (8000 rpm, 3 minutes), snap frozen in liquid nitrogen, and stored at -80°C. The RNeasy Mini Plus Kit (Qiagen) protocol for purification of total RNA from bacteria was followed. Following

addition of 700  $\mu$ l of RLT buffer +  $\beta$ -mercaptoethanol (10  $\mu$ l  $\beta$ -mercaptoethanol per 1 ml RLT buffer) to each frozen sample, suspensions were transferred into 2 ml tubes containing 0.5 mm glass beads (Precellys, VWR), and homogenised using a Precellys 24 tissue homogeniser (Berlin Instruments, 2 x 20 seconds, 6500 rpm, 2 cycles). Tubes were placed on ice between cycles and before centrifuging at 13000 rpm for 1 minute. The supernatant was removed and run through the gDNA eliminator column (10000 rpm, 1 minute) before an equal volume of 70% ethanol was added. 700  $\mu$ l of mixture was transferred to RNeasy spin columns and centrifuged for 30 seconds, 10000 rpm. The membrane was washed with RW1 buffer (350  $\mu$ l, 10000 rpm, 30 seconds) before the addition of RNase-Free DNase (Qiagen) directly to the membrane according to manufacturer recommendations. The column was incubated at room temperature for 20 minutes before washing once with RW1 buffer (350  $\mu$ l, 10000 rpm, 30 seconds), and twice with RPE buffer (10000 rpm for 30 seconds, followed by 2 minutes). RNA was eluted from the membrane by adding 50  $\mu$ l dH<sub>2</sub>O, incubating for 1 minute (room temperature), centrifuging for 1 minute (10000 rpm) and repeating with 30  $\mu$ l dH<sub>2</sub>O.

RNA quality was confirmed through gel electrophoresis and imaging of gel using UV trans-illumination (Section 2.10.1.2). The concentration was measured by diluting RNA 1:100 in dH<sub>2</sub>O and using a spectrophotometer, where an OD<sub>260</sub> of 1 equals 40  $\mu$ g/ml of double stranded RNA. Purity was measured through absorbance wavelength ratios of 260/280 and 260/230. RNA was stored at -80°C until required.

**2.10.6 Designing Primers.** DNA sequences were obtained through the National Center for Biotechnology Information (NCBI) database. Primers were designed using the NCBI Primer-BLAST tool or used from previous studies (Table 2.2) and validated via PCR (Section 2.10.7).

**Table 2.2 Primers used in this study.**

<b>Name</b>	<b>Organism</b>	<b>Sequence</b>	<b>Source</b>
FTR1 forward	<i>R. microsporus</i>	GTG-GTG-TCT-CCT-TGG-GTG-TT	This study
FTR1 reverse	<i>R. microsporus</i>	CCA-CCA-CGG-TAG-ATG-AGG-A	This study
18s forward	<i>R. microsporus</i>	GGC-GAC-GGT-CCA-CTC-GAT-TT	This study
18s reverse	<i>R. microsporus</i>	TCA-CTA-CCT-CCC-CGT-GTC-GG	This study
rpoD forward	<i>P. aeruginosa</i>	GGG-CGA-AGA-AGG-AAA-TGG-TC	(Lopez-Medina <i>et al.</i> , 2015)
rpoD reverse	<i>P. aeruginosa</i>	CAG-GTG-GCG-TAG-GTG-GAG-AA	(Lopez-Medina <i>et al.</i> , 2015)
pchA forward	<i>P. aeruginosa</i>	CTG-CCT-GTA-CTG-GGA-ACA-GC	(Lopez-Medina <i>et al.</i> , 2015)
pchA reverse	<i>P. aeruginosa</i>	GCA-GAG-CAA-TTG-CCA-GTT-TT	(Lopez-Medina <i>et al.</i> , 2015)
pvdS forward	<i>P. aeruginosa</i>	ACC-GTA-CGA-TCC-TGG-TGA-AG	(Lopez-Medina <i>et al.</i> , 2015)
pvdS reverse	<i>P. aeruginosa</i>	TGA-ACG-ACG-AAG-TGA-TCT-GC	(Lopez-Medina <i>et al.</i> , 2015)

**2.10.7 Polymerase Chain Reaction (PCR).** To test primers and to check for DNA contamination of extracted fungal and bacterial RNA (Section 2.10.4 and 2.10.5), a PCR was performed. Master mixes were made using 125 µl MyTaq Red (Bioline), 1 µl forward primer (diluted 1:10), 1 µl reverse primer (diluted 1:10), 1 µl of DNA or 2 µl RNA, and dH<sub>2</sub>O for a total volume of 50 µl. PCR conditions are detailed in Table 2.3, using a Sensoquest Labcycler. PCR products were visualised following gel electrophoresis (Section 2.10.1).

**Table 2.3 PCR conditions.**

	<b>Step</b>	<b>Temperature (°C)</b>	<b>Time</b>	<b># passes</b>	<b>Other</b>
1	Initial denaturation	95	5 min	1	
2	Denaturation	95	30 sec	30	
3	Annealing	55	30 sec	30	
4	Initial extension	72	3 min	30	Repeat from step 2
5	Final Extension	72	10 min	1	
6	Hold	10	∞	n/a	

**2.10.8 Checking RNA for DNA contamination.** To confirm that RNA samples were free of any contaminating genomic DNA, a PCR amplifying 18s rRNA for *R. microsporus* and rpoD for *P. aeruginosa* was used. RNA spiked with genomic DNA was used as a PCR procedural control. See Table 2.2 for primers and Section 2.10.7 for PCR details.

**2.10.9 Removing DNA from contaminated RNA.** For RNA contaminated with genomic DNA, an RNA clean-up procedure was performed using an RNase-free DNase kit (Qiagen) and RNeasy Mini Plus kit (Qiagen). RNA (50  $\mu$ l), RDD buffer (10  $\mu$ l), DNase (2.5  $\mu$ l) and dH<sub>2</sub>O (37.5  $\mu$ l) were mixed thoroughly and incubated at room temperature for 15 minutes. 350  $\mu$ l of RLT buffer +  $\beta$ -mercaptoethanol (10  $\mu$ l  $\beta$ -mercaptoethanol per 1 ml RLT buffer) were added to each sample, transferred to the gDNA eliminator columns, and centrifuged (10000 rpm, 1 minute). 250  $\mu$ l of 100% ethanol was added to the flow-through and samples were transferred to the RNeasy spin columns. The protocol was continued according to manufacturer guidelines. RNA quality and concentration were measured via spectrophotometer and gel electrophoresis (Section 2.10.1.2). A PCR was used to determine whether any residual DNA remained in the samples (Section 2.10.7).

**2.10.10 Quantitative Reverse Transcriptase PCR (qRT-PCR).** A qRT-PCR was performed to determine the expression of iron-related genes in both *R. microsporus* and *P. aeruginosa*. An iTaq Universal SYBR Green One-Step Kit (Bio Rad) was used with 10 ng/ $\mu$ l RNA and a total reaction volume of 20  $\mu$ l. Reactions were prepared with 10  $\mu$ l iTaq universal SYBR green reaction mix (2x), 1  $\mu$ l iScript reverse transcriptase, 0.8  $\mu$ l forward primer, 0.8  $\mu$ l reverse primer, and both primers were diluted 1:10 in dH<sub>2</sub>O. Controls with no reverse transcriptase were included to ensure DNA was completely removed from RNA during the extraction process. Conditions for qRT-PCR are detailed in Table 2.4, using a Bio Rad CFX Connect Real Time System and Bio Rad CFX Manager 3.1 software.

qRT-PCR data for *FTR1* was analysed via  $2^{-\Delta\text{CT}}$  and presented as gene expression relative to *18S* mRNA. Significance was analysed using a Mann-Whitney U test (n=4). qRT-PCR for *pchA* and *pvdS* were analysed via  $2^{-\Delta\Delta\text{CT}}$  analysis, and presented as fold change compared to housekeeping gene (*rpoD*). Significance was analysed using a 2-way ANOVA with Tukey's multiple comparisons test.

**Table 2.4 Quantitative Reverse Transcriptase PCR conditions.**

	<b>Step</b>	<b>Temperature</b>	<b>Time</b>	<b># passes</b>	
1	cDNA synthesis (reverse transcription)	45	10 min	1	
2	Polymerase activation	95	2 min	1	
3	Denaturation	95	5 sec	39	
4	Annealing	59	30 sec	39	
5	Denaturation	95	10 sec	39	
6	Annealing/Extension	65	5 sec	39	Repeat from step 3
7	Dissociation gradient	65-95	30 sec	1	

### 2.10.11 Creating fluorescent *P. aeruginosa*.

**2.10.11.1 *E. coli* plasmid extraction.** A Qiagen Miniprep kit was used to purify mCherry (PME6032:mcherry) and GFP (PME6032:gfp) plasmids from overnight cultures (5 ml) of fluorescent *E. coli* DH5 $\alpha$  according to manufacturer guidelines. Integrity of DNA was confirmed through gel electrophoresis and stored at -20°C until needed.

**2.10.11.2 Transformation of *P. aeruginosa*.** *P. aeruginosa* PAO1 and PA14 were grown overnight in LB at 37°C and 200 rpm. Bacteria (2 x 1 ml) were made electrocompetent by washing twice in 300 mM sucrose (8000 rpm, 3 minutes). Plasmid DNA (5 µl) was added to the bacteria, with one sample of each strain acting as plasmid-negative control. Both positive and negative samples were placed into electrocuvettes and transformed via electroporation. Fresh LB was immediately added to cuvettes, mixed thoroughly, transferred to 1.5 ml Eppendorf tubes, and incubated for 1 hour (37°C, 200 rpm) to allow for recovery. Both plasmid-positive and plasmid-negative bacteria (neat and diluted 1:10) were streaked onto LB agar (+/- 100 µg/ml tetracycline) and grown overnight at 37°C. Positive colonies were re-streaked onto LB agar + 100 µg/ml tetracycline and again incubated overnight. Cultures (5 ml) were prepared in LB broth + 100 µg/ml tetracycline, incubated overnight (37°C, 200 rpm), and fluorescence was confirmed via microscopy.

## **2.11 Zebrafish infections.**

**2.11.1 Ethics.** Zebrafish care and experiments were performed under Home Office project license P51AB7F76 and personal license I5B923969 in accordance with the Animal Scientific Procedures Act 1986.

**2.11.2 Maintenance.** Adult wild type (AB) *Danio rerio* zebrafish were maintained at the University of Birmingham Aquatic Facility in recirculating tanks with 14

hours light/10 hours dark cycles at 28°C. Adult zebrafish naturally spawned overnight in groups of 11 fish (six females, five males). Embryos were transferred to E3 medium (5 mM NaCl, 0.17 mM KCl, 0.33 mM CaCl<sub>2</sub>, 0.33 mM MgSO<sub>4</sub>, pH 7) with 0.3 µg/ml methylene blue and 0.003% 1-phenyl-2-thiourea (PTU) for the first 24 hours post fertilisation (hpf) and maintained at 28°C. Sample sizes for injections were calculated via power analysis using an alpha value of 0.05, power of 80%, mean effect size of 4.2%, and standard deviation of 8%, based on preliminary data and standards accepted by the zebrafish infection community.

**2.11.3 Preparation of inoculum.** Mucorales hyphae are fragile and sporangiophores tend to clump, causing needles to readily clog during micro-injections. Because of this, *R. microsporus* spores were gently harvested for injections by slowly dropping 10 ml of PBS onto each plate of fungi and carefully swirling before collecting into falcon tubes, repeating plate wash with fresh PBS, and washing pellets once. After resuspending in PBS (5 ml), heavier clumps of spores were allowed to settle to the bottom of the falcon tube for approximately 1 minute and the upper 4 ml were removed and counted. If microscopic visualisation of *R. microsporus* spores was necessary, spores were stained as described in Section 2.8 before counting. *P. aeruginosa* PA14 (1 ml) from an overnight LB culture was washed twice in PBS via centrifugation (8000 rpm, 2 minutes), and absorbance (OD<sub>600</sub>) was measured.

*R. microsporus* spores or *P. aeruginosa* PA14 were resuspended in 25  $\mu$ l polyvinylpyrrolidone (PVP, 10% in PBS + 0.05% phenol red) to achieve desired infection dose. Specific infection doses varied between experiments and are explicitly stated below. Samples were kept on ice until needed to prevent spore swelling and bacterial growth.

**2.11.4 Hindbrain injections.** Hindbrain injections were performed as previously described (Voelz, Gratacap and Wheeler, 2015). At 24 hpf larvae were manually dechorionated and anaesthetised (160  $\mu$ g/ml Ethyl 3-aminobenzoate methanesulfonate salt [Tricaine]). Samples (2 nl) were injected into the hindbrain via the otic vesicle. Any fish that did not survive the injection process were removed. Following injections, survival was recorded every 24 hours until larvae were sacrificed at 5 dpf (96 hours post infection) through 10x overdose of Tricaine.

**2.11.4.1 *R. microsporus* and *P. aeruginosa* hindbrain mono-injections.**

Embryos were injected into the hindbrain with PVP only, PVP + *R. microsporus*, or PVP + *P. aeruginosa* PA14 to achieve a desired dose of 10, 50, or 100 spores/fish and 10, 50, 100, 500, or 1000 bacterial CFUs/fish. *P. aeruginosa* injections with 10000 bacterial CFUs/fish were completed separately, with separate controls. For *R. microsporus* experiments, data were pooled from two independent experiments with a total of 32, 40, 38, and 42 fish for control, 10, 50, and 100 spores, respectively. For *P. aeruginosa* experiments, data were pooled

from four independent experiments with a total of 70, 80, 80, 80, 79, and 79 fish for controls, 10, 50, 100, 500, and 1000 CFUs/fish. For *P. aeruginosa* with 10000 CFUs/fish, data were pooled from two independent experiments with 31 control and 35 treated fish.

**2.11.4.2 *R. microsporus* hindbrain mono-injections with pyoverdine or enterobactin.** Embryos were injected into the hindbrain with PVP + *R. microsporus* only, *R. microsporus* + 60  $\mu\text{M}$  (69.6  $\mu\text{g/ml}$ ) pyoverdine, or *R. microsporus* + 50  $\mu\text{M}$  (33.5  $\mu\text{g/ml}$ ) enterobactin, with a desired dose of 50 spores/fish. Control embryos were injected into the hindbrain with either PVP only, PVP + 60  $\mu\text{M}$  pyoverdine, PVP + DMSO, or PVP + 50  $\mu\text{M}$  enterobactin. For the pyoverdine experiment, data were pooled from four separate experiments with a total of 87, 80, 80, and 81 fish for control, pyoverdine only, spores only, and spores + pyoverdine, respectively. For the enterobactin experiment, data were pooled from two separate experiments with a total of 42, 44, 46, 43, and 50 fish for control, DMSO, enterobactin only, spores only, and spores + enterobactin, respectively.

**2.11.4.3 *R. microsporus* and *P. aeruginosa* hindbrain co-infections.** Embryos (24 hpf) were injected into the hindbrain with PVP only, *R. microsporus* only (100 spores), *P. aeruginosa* PA14 only (10000 CFUs), or *R. microsporus* + *P. aeruginosa*. Data were pooled from three separate experiments with 51, 61, 60, and 61 fish per condition, respectively.

**2.11.5 Yolk sac injections.** At 48 hpf, zebrafish embryos were anaesthetised (160 µg/ml Tricaine). Samples (2 nl) were injected into the dorsal end of the yolk sac to avoid circulation. Any fish that did not survive the injection process were removed. Following injections, survival was recorded every 24 hours until larvae were sacrificed at 5 dpf (72 hours post infection) through 10x overdose of Tricaine.

**2.11.5.1 *R. microsporus* and *P. aeruginosa* yolk sac mono infections.**

Embryos were injected into the yolk sac with PVP only, PVP + *R. microsporus*, or PVP + *P. aeruginosa* PA14 to achieve a desired dose of 10, 50, or 100 spores/fish and 10, 50, 100, 500, or 1000 bacterial CFUs/fish. For *R. microsporus* experiments, data were pooled from two independent experiments with a total of 26, 34, 35, and 34 fish for control, 10, 50, and 100 spores, respectively. For *P. aeruginosa* experiments, data were pooled from two independent experiments with a total of 35, 40, 40, 35, 40, and 40 fish for controls, 10, 50, 100, 500, and 1000 CFUs/fish.

**2.11.6 Swim bladder injections.** Swim bladder injections were performed as previously described (Gratacap, Bergeron and Wheeler, 2014). Zebrafish larvae (96 hpf) were anaesthetised (160 µg/ml Tricaine) and samples (4 nl) were injected into the swim bladders. Any fish that did not survive the injection process were

removed. Following injections, survival was recorded after 24 hours, after which larvae were sacrificed through 10x overdose of Tricaine.

#### **2.11.6.1 *R. microsporius* and *P. aeruginosa* swim bladder co-infections.**

Based on the literature, mono-infections with *P. aeruginosa* and *R. microsporius* were unlikely to reduce viability at low concentrations (Voelz, Gratacap and Wheeler, 2015; Bergeron *et al.*, 2017). Therefore, instead of performing mono-injections to determine concentration curve, co-infections were attempted first with high concentrations. Zebrafish larvae (96 hpf) were injected into the swim bladder with PVP only, *R. microsporius* only (100 spores), *P. aeruginosa* PA14 only (10000 CFUs), or *R. microsporius* + *P. aeruginosa*. Data were pooled from two separate experiments with 40, 40, 42 and 42 fish per condition, respectively.

#### **2.11.6.2 Spore viability following zebrafish infection.**

Zebrafish (4 dpf) were injected into the swim bladder with 4 nl of *R. microsporius* spores (50) or *R. microsporius* + *P. aeruginosa* (MOI 1:100). To quantify *R. microsporius* survival at 0 hours and 24 hours, at each timepoint 3 larvae per condition were euthanised with 1600 µg/ml Tricaine and placed into 1.5 ml Eppendorf tubes. E3 media was replaced with 200 µl Trypsin EDTA (0.25%) and fish were homogenised with a motorised pestle until dissociation was complete. PBS (800 µl) was added, mixed thoroughly, and 500 µl was plated onto SAB agar + antibiotic cocktail (60 µg/ml tetracycline, 30 µg/ml gentamycin, 30 µg/ml chloramphenicol). Plates were incubated at 25°C overnight before CFUs were counted. After counting CFUs,

one plate was statistically recognised as an outlier using the ROUT method (Robust regression and Outlier removal) and was removed. Data was pooled from 3 individual experiments with 3 fish per experiment, tested for normality using the D'Agostino & Pearson omnibus normality test, and analysed for significance using a T-test (n=9).

**2.11.7 Imaging of zebrafish.** Following hindbrain or swim bladder injections, 5 fish per condition were anaesthetised with Tricaine and positioned in 6 well plates containing 5 ml of low-gelling temperature agarose (1% in 1x E3 + 160 µg/ml Tricaine). For real time microscopy, images were taken every 10 minutes for 16 hours using a Zeiss AxioObserver inverted microscope (28°C, 10x magnification).

**2.11.8 Statistical analysis of zebrafish survival experiments.** Survival data was inputted and analysed using Graphpad Prism 6 software. A Kaplan-Meyer curve was created and statistical significance between curves were calculated by using a Mantel-Cox log-rank test with the Bonferroni method for multiple comparisons.

## **2.12 Statistical analysis.**

In most cases, experiments were performed with at least two technical and two biological replicates. Microsoft Excel 2016 and GraphPad Prism 6 were used to record and analyse data. Statistical tests used are indicated in individual sections.

All analyses were performed on non-normalised raw data or arcsine transformed data where appropriate. A p-value of  $p < 0.05$  was considered statistically significant. Statistical significance is indicated by \* =  $p < 0.05$ , \*\* =  $p < 0.01$ , and \*\*\* =  $p < 0.001$ .

**2.12.1 Arcsine transformations.** As data with percentages are non-normal and on a fixed scale, proportions were transformed using arcsine transformations to stabilise the variance and normalise the data (Sokal and Rohlf, 1995). Transformations were performed on Microsoft Excel 2016 using Equation 4:

Equation 4: Arcsine transformations for percentage data

$$=\text{DEGREES}(\text{ASIN}(\text{SQRT}(xx)))$$

Parametric statistical tests were performed on arcsine transformed data, as they are considered normal following transformation.

# Chapter 3 : IMPACT OF POLYMICROBIAL INTERACTIONS ON MUCORALES

Parts of this chapter have been previously published:

Kousser, C., Clark, C., Sherrington, S., Voelz, K. and Hall, R. (2019).  
*Pseudomonas aeruginosa* inhibits *Rhizopus microsporus* germination  
through sequestration of free environmental iron. *Scientific Reports*, 9.  
DOI 10.1038/s41598-019-42175-0

### 3.1 Introduction

While the presence and influence of polymicrobial communities are becoming increasingly acknowledged, research into the dynamics of these interactions is still incomplete, and focus tends to remain on a few key organisms. There is a distinct lack of understanding about polymicrobial interactions involving fungi, though the gap in knowledge is slowly being addressed. The majority of fungal polymicrobial research has focused on the more common invasive fungi, such as *Candida albicans* and *Aspergillus spp.* However, there is not much known about relationships involving Mucorales. To thoroughly understand the pathogenesis, it is important to consider the impact of surrounding microorganisms on the virulence of Mucorales.

Mucormycetes are most commonly associated with pulmonary, rhinocerebral, or cutaneous infections, which are known to host a plethora of bacteria and fungi (Torres-Narbona *et al.*, 2007). *Candida albicans*, *Burkholderia cenocepacia*, *Klebsiella pneumoniae*, and *Pseudomonas aeruginosa* were studied in this chapter initially as they are commonly associated with polymicrobial infections and are isolated in similar niches as Mucorales. *Staphylococcus aureus* and *Escherichia coli* were added to later experiments due to their prevalence in polymicrobial research.

#### 3.1.1 Organisms studied in this chapter.

**3.1.1.1 *Candida albicans.*** *C. albicans* is a polymorphic fungus that can grow as

yeast, pseudohyphae, true hyphae and chlamydospores (Kabir, Hussain and Ahmad, 2012). *C. albicans* is routinely isolated from the skin, oral, vaginal and gastrointestinal tracts. Approximately 70% of the human population is naturally colonised with *C. albicans*, with over 80% of women testing positive for *C. albicans* genital-flora (Vermitsky *et al.*, 2008; Mayer, Wilson and Hube, 2013), *C. albicans* can cause superficial mucosal infections including oral and genital thrush, or life-threatening systemic candidiasis in severely immunocompromised individuals (Kabir, Hussain and Ahmad, 2012). The ability of *C. albicans* to switch morphology is critical to its virulence, with yeast- or hyphal-locked strains displaying a significant reduction of virulence in animal models (Murad *et al.*, 2001). During colonisation and dissemination, *C. albicans* mainly resides as yeast, but many host and environmental factors induce a morphological switch to the invasive hyphae form. These triggers include alkaline pH, increased temperature, presence of serum, change in concentration of quorum sensing molecules (QSMs), and the presence of other microorganisms (Brown *et al.*, 1999). This ability to switch between morphologies is key to the virulence of *C. albicans* and factors that alter this mechanism can strongly impact pathogenesis.

*C. albicans* is known to participate in many different polymicrobial relationships, and is the most commonly studied fungus in polymicrobial research, along with *Aspergillus spp.* *C. albicans* produces the QSM, farnesol, which prevents morphological switch and biofilm formation (Hornby *et al.*, 2001; Ramage *et al.*, 2002). This molecule also affects viability and biofilm formation in bacterial and fungal species. For example, the presence of farnesol decreases the ability of *S.*

*aureus* and *Streptococcus mutans* to form biofilms; for the former, farnesol also weakens the cell membrane integrity and enhances the efficacy of antimicrobials (Koo *et al.*, 2003; Jabra-Rizk *et al.*, 2006). This molecule has also been shown to increase the susceptibility of *Burkholderia pseudomallei* and *Acinetobacter baumannii* to antibiotics, which indicates a potential therapeutic application (Kostoulas *et al.*, 2015; Castelo-Branco *et al.*, 2016). Farnesol also affects other fungal pathogens, and inhibits the growth of *Cryptococcus neoformans* (Cordeiro *et al.*, 2012) and induces apoptosis in *Aspergillus nidulans* (Semighini *et al.*, 2006), *Aspergillus flavus* (Wang *et al.*, 2014), and *Fusarium graminearum* (Semighini, Murray and Harris, 2008). *C. albicans* has been identified in many polymicrobial diseases such as CF, ventilator-associated pneumonia, oral infections, trauma-associated wounds, peritonitis, and burn wounds (Tsang and Samaranayake, 2000; Peleg, Hogan and Mylonakis, 2010; Mallick and Bennett, 2013; Rapisarda *et al.*, 2015).

**3.1.1.2 *Burkholderia cenocepacia*.** *B. cenocepacia* is a Gram-negative opportunistic pathogen and member of the *Burkholderia cepacia* complex, a group of 22 environmental bacteria that can cause potentially fatal complications in CF lungs. *Burkholderia spp.* are typically resistant to multiple classes of antibiotics, such as polymyxins,  $\beta$ -lactams, fluoroquinolones, tetracyclines, and trimethoprim (Rhodes and Schweizer, 2016). This resistance is due to the production of modified lipopolysaccharides, decreased membrane permeability, over-expression of efflux pumps, production of  $\beta$ -lactamases, and drug target modification (Loutet and Valvano, 2011; Rhodes and Schweizer, 2016). *B.*

*cenoepecia* is particularly harmful and typically leads to high mortality in infected CF patients (Jones *et al.*, 2004).

*B. cenoepecia* is isolated in the CF lung alongside other fungi, bacteria, and viruses such as *Aspergillus spp.*, *C. albicans*, *Haemophilus influenzae*, *S. aureus*, *P. aeruginosa*, and respiratory syncytial virus (Rogers *et al.*, 2003; Etherington *et al.*, 2014). *B. cenoepecia* has been found to work synergistically with *Aspergillus niger*, and co-cultures increase biomass and phosphate solubilisation (Braz and Nahas, 2012). Conversely, a QSM produced by *B. cenoepecia*, Cis-2-dodecenoic acid (BDSF), inhibits filamentation, biofilm formation, and attachment of *C. albicans* (Boon *et al.*, 2008; Zhang *et al.*, 2011; Tian *et al.*, 2013). This indicates that *B. cenoepecia* can participate in diverse polymicrobial relationships with fungi.

**3.1.1.3 *Klebsiella pneumoniae*.** *K. pneumoniae* is a Gram-negative commensal of the gastrointestinal system and nasopharynx, and becomes an opportunistic pathogen following host immune suppression (Heitman and Brasher, 1971; Struve and Krogfelt, 2004). This bacterium is a major nosocomial pathogen, causing urinary tract infections, ventilator-associated pneumonia, diarrhoea, wound infections, bacteraemia, and septicaemia (Balestrino *et al.*, 2005). Many strains of multi-drug-resistant carbapenemase- and  $\beta$ -lactamase-producing *K. pneumoniae* have emerged, making these infections particularly difficult to treat (Podschun and Ullmann, 1998; Patel *et al.*, 2008). The prevalence of antibiotic-resistant *K. pneumoniae* is dramatically increasing, with incidences of

carbapenem-resistant isolates rising from 2.4% to 52% in 10 years (Datta *et al.*, 2012).

The main virulence factor of *K. pneumoniae* is its thick, acidic polysaccharide capsule (Podschun and Ullmann, 1998). *K. pneumoniae* is able to avoid phagocytosis by utilising this capsular protection and activating phosphoinositide 3-kinase to inhibit phagosome maturation (Cano *et al.*, 2014). Virulence is also mediated through siderophores, adhesins, lipopolysaccharide, and urease (Rosen *et al.*, 2016).

*K. pneumoniae* is frequently found within polymicrobial environments, as it is a member of the gut microbiome and is commonly isolated in urinary tract infections (Garcia de la Torre *et al.*, 1985; Behzadi *et al.*, 2010; Lin *et al.*, 2012). Catheter-associated urinary tract infections are usually caused by multi-species biofilms. (Frank *et al.*, 2009). Moreover, *K. pneumoniae* has been co-isolated with *C. albicans*, *E. coli*, *Staphylococcus epidermidis*, and *Enterococcus faecium* in patients with abdominal peritonitis (Hwang *et al.*, 2014).

**3.1.1.4 *Pseudomonas aeruginosa*.** *P. aeruginosa* is a Gram-negative, motile, opportunistic pathogen that is found in soil and as a member of the human skin flora (Hogan and Kolter, 2002). This bacterium can cause potentially fatal infections in immunocompromised individuals, and in catheters, ventilators, burns, traumatic wounds, or the CF lung (Gonzalez *et al.*, 2016). Overall mortality

rates for *P. aeruginosa* infections reach around 60% for hospitalised patients (Kang *et al.*, 2003). This infection is particularly prevalent in CF, where it infects 64% of adult CF patients and increases the risk of mortality (Parad *et al.*, 1999; Crull *et al.*, 2016). The WHO has recently prioritised *P. aeruginosa* as one of the top three pathogens requiring focus for antibiotic development, highlighting the importance of this bacterium on a global scale (WHO, 2017).

The pathogenesis of *P. aeruginosa* involves direct contact and adherence with the epithelium. Secretion systems play a major role in host infection, especially Type II, III, and VI. The Type II secretion system is not contact-dependent and involves the extracellular release of toxins such as elastase, phospholipase C, exotoxin A, and phosphatases (Kipnis, Sawa and Wiener-Kronish, 2006). The Type III secretion system (T3SS) is activated after binding to host cells, where a needle-like appendage injects several specific effector proteins into host cells, leading to cell death and bacterial dissemination (Yahr, Goranson and Frank, 1996). The Type VI secretion system (T6SS) is another contact-dependent delivery system, with machinery that resembles bacteriophages (Cascales and Cambillau, 2012). Similar to the T3SS, the T6SS facilitates virulence and injects prey cells with toxins (Mougous *et al.*, 2006). This system has been found to act against other bacteria (Hood *et al.*, 2010), and the *Serratia marcescens* T6SS can kill *C. albicans* (Trunk *et al.*, 2018).

The most commonly implicated extracellular chemicals involved in polymicrobial relationships include QSMs, phenazines, and siderophores. *P. aeruginosa* secretes several QSMs, which are mechanisms for communication between cells, both intra- and inter-species (Nealson and Hastings, 1979; Waters and Bassler, 2005). This density-dependent mechanism allows bacteria to sense other organisms and coordinate appropriate responses as a population. This includes the secretion of virulence factors, swarming, bioluminescence, apoptosis, and the induction of biofilm formation (Kipnis, Sawa and Wiener-Kronish, 2006). They have been found to depress host immune response and inhibit the growth of other organisms (Telford *et al.*, 1998). 3-oxo-C12 homoserine lactone (C12 HSL) is the major QSM, and inhibits filamentation of *C. albicans* and sporulation of *A. fumigatus* (Hogan, Vik and Kolter, 2004; Mowat *et al.*, 2010).

The phenazine pyocyanin is a blue-pigmented toxin that causes deleterious effects on both the host and neighbouring microorganisms. Pyocyanin damages host cells by enhancing intracellular ROS and decreasing catalase and superoxide dismutase (Muller, 2002; Rada *et al.*, 2011). The toxin also depresses the host immune response by disrupting lysosome formation and inducing apoptosis in neutrophils, promoting *P. aeruginosa* survival (Allen *et al.*, 2005; Prince *et al.*, 2013). Pyocyanin can exacerbate infections during CF, and this phenazine can reach concentrations of 130  $\mu\text{M}$  in sputum (Wilson *et al.*, 1988). Concentrations of pyocyanin can be up to 8  $\mu\text{M}$  in infected wounds, and the presence of burn wound exudate increases the production of pyocyanin, thus perpetuating the cellular damage in these patients (Gonzalez *et al.*, 2016; Hall *et*

*al.*, 2016). Phenazines can also negatively impact other microorganisms, for instance pyocyanin and 1-hydroxy-phenazine can inhibit the growth of *C. albicans* and *A. fumigatus* (Kerr *et al.*, 1999; Morales *et al.*, 2013). Phenazine-1-carboxylic acid has been explored as a potential biocontrol agent to inhibit germination of *Botrytis cinerea*, the causative agent of grey mould in soft fruits (Simionato *et al.*, 2017).

*P. aeruginosa* also produces potent siderophores, which are important secreted virulence factors. Siderophores are low molecular weight chelators that specifically bind iron (Braud, Hoegy, *et al.*, 2009). *P. aeruginosa* produces pyoverdine and pyochelin, which have affinity constants for iron of  $10^{36} \text{ M}^{-1}$  and  $10^5 \text{ M}^{-1}$ , respectively (Cox and Graham, 1979; Albrecht-Gary *et al.*, 1994). Pyoverdine is the major siderophore produced by *P. aeruginosa*, as it has the highest affinity for iron and can acquire iron from host transferrin (Xiao and Kisaalita, 1997). Pyoverdine is essential for *P. aeruginosa* virulence, and deletion of pyoverdine synthesis reduces pathogenicity *in vivo* (Meyer *et al.*, 1996). Though the major role for pyoverdine is iron acquisition, it also participates in cellular communication, regulates biofilm formation, and mediates the secretion of virulence factors, such as exotoxin A, endoproteases, and pyoverdine itself (Lamont *et al.*, 2002; Cézard, Farvacques and Sonnet, 2015). Pyoverdine chelates ferric iron, binds to the *P. aeruginosa* ferripyoverdine outer membrane transport receptor FpvA and enters the bacterial periplasm (Poole *et al.*, 1993). Iron is dissociated from pyoverdine through a reductive process (Schalk, Abdallah and Pattus, 2002) involving the FpvCDEF ABC-transporter and enters

the cytoplasm via FpvDE transporter. The apo-siderophore (iron-free) is recycled after iron removal and secreted again through the PvdRT-OmpQ efflux pump (Brillet *et al.*, 2012; Cézard, Farvacques and Sonnet, 2015).

**3.1.1.5 *Staphylococcus aureus*.** *S. aureus* is a common commensal of the skin and nasal cavities, with 20-30% of individuals being chronically colonised (Kluytmans, Van Belkum and Verbrugh, 1997). A person's own colonising strains are generally the cause of infection, though transmission of commensal bacteria between healthy and susceptible individuals is also a common route of infection (von Eiff *et al.*, 2001). This opportunistic pathogen is a major cause of antimicrobial resistant community- and hospital- associated infections, causing over 50,000 deaths per year and costing billions of dollars annually in the United States (Goetghebeur *et al.*, 2007; Lee *et al.*, 2013). *S. aureus* attaches to the surface of host cells and medical devices where they readily form persistent, difficult to eradicate biofilms (Foster and Höök, 1998). These bacteria can survive and hide within host cells, and are associated with capsule formation and small colony variants that promote recurrent infections (Kahl *et al.*, 1998; Tzianabos, Wang and Lee, 2001). Host damage occurs through the secretion of degrading enzymes (proteases, lipases, and elastases), toxins (such as  $\alpha$ -toxin, leukocidins, delta-hemolysin, and enterotoxins) and superantigens that can lead to further dissemination, chronic wounds, and diseases such as toxic shock syndrome or food poisoning (as reviewed in McCormick, Yarwood and Schlievert, 2002; Otto, 2014). *S. aureus* has been implicated in polymicrobial relationships with *C.*

*albicans* (Schlecht *et al.*, 2015; Kong *et al.*, 2016) and *A. fumigatus* (Granillo *et al.*, 2015).

**3.1.1.6 *Escherichia coli*.** *E. coli* is an abundant member of the intestinal flora of mammals, and generally lives as a harmless commensal. However, when a host becomes immunocompromised, intestinal barriers are breached, or the bacterium is transported to other body sites, severe gastroenteritis, urinary tract infections, wound infections, meningitis, or bloodstream infections can occur. Virulence factors vary based on *E. coli* pathovar, though all pathogenesis includes adherence to the host mucosa by utilising fimbriae or other adhesins, multiplication and biofilm formation, and toxin production. Examples of toxins include haemoglobin-binding protease, urease, Shiga-toxin, heat-labile and -stable enterotoxins, and cytolethal distending toxin (as reviewed in Kaper, Nataro and Mobley, 2004). The pro-inflammatory compound located on the surface of *E. coli* cell wall, lipopolysaccharide (LPS), can cause septic shock by binding to Toll-like receptor 4 and inducing an acute inflammatory response (Tapping *et al.*, 2000).

As *E. coli* is such a prominent member of the microbiome, it forms diverse relationships with fungi. For instance, *E. coli* can enhance the pathogenicity of *C. albicans* in a rat bladder model (Levison and Pitsakis, 1987) but can also kill *C. albicans* through secretion of a soluble antifungal substance (Cabral *et al.*, 2018). It is possible that these relationships vary based on location, where they compete

for resources as commensals in the highly populated gut, but they work together in a sparse urinary tract infection scenario. Furthermore, *E. coli* produces a protein that was found to have anti-*Aspergillus* activity (Yadav *et al.*, 2005), while LPS produced by *E. coli* enhances the production of gliotoxin in *A. fumigatus* (Svahn *et al.*, 2014).

### **3.2 Aim of this chapter.**

Although Mucoralean fungi are ubiquitous in the environment and come into contact with countless species of fungi and bacteria, their interaction with other organisms is currently uncharacterised. While it is likely that they have evolved specific mechanisms to communicate with and respond to neighbouring microorganisms, it is unknown whether these relationships impact Mucoralean pathogenesis. As virulence of these filamentous fungi is dependent on germination, this chapter aims to understand the impact of candidate bacteria and fungi on the germination and overall growth of representative Mucoralean species.

### **3.3 Results**

#### **3.3.1 *Candida albicans* supernatant delays the germination of *Rhizopus microsporus*, *Lichtheimia corymbifera*, and *Cunninghamella bertholletiae*.**

To begin investigating the role of opportunistic microorganisms in influencing the pathogenesis of Mucorales, we exposed *Lichtheimia corymbifera* (low virulence, 35% mortality), *Rhizopus microsporus* (moderate virulence, 47% mortality), and

*Cunninghamella bertholletiae* (high virulence, 77% mortality) to supernatants from opportunistic pathogens (Jeong *et al.*, 2019).

To understand whether *C. albicans* impacts the growth of Mucorales, spores ( $1 \times 10^4$  spores/ml) were exposed to 50% *C. albicans* supernatant. Live-cell imaging was used to visualise spore swelling and germination over time. The addition of 50% *C. albicans* supernatant induced moderate delays in *R. microsporus* (Figure 3.1), *L. corymbifera* (Figure 3.2) and *C. bertholletiae* (Figure 3.3) germination. *R. microsporus* germination was decreased by 47.26% (+/- 15.48%) after exposure to the supernatant for 8 hours (Figure 3.1B), and germination remained lower than the control throughout the time course of the experiment. For *L. corymbifera*, germination was delayed by 39.54% (+/- 15.65%) at 6 hours (Figure 3.2B). *C. albicans* supernatant decreased *C. bertholletiae* germination by 64.04% (+/- 24.13%,  $p = 0.0029$ ) after 5 hours (Figure 3.3B).

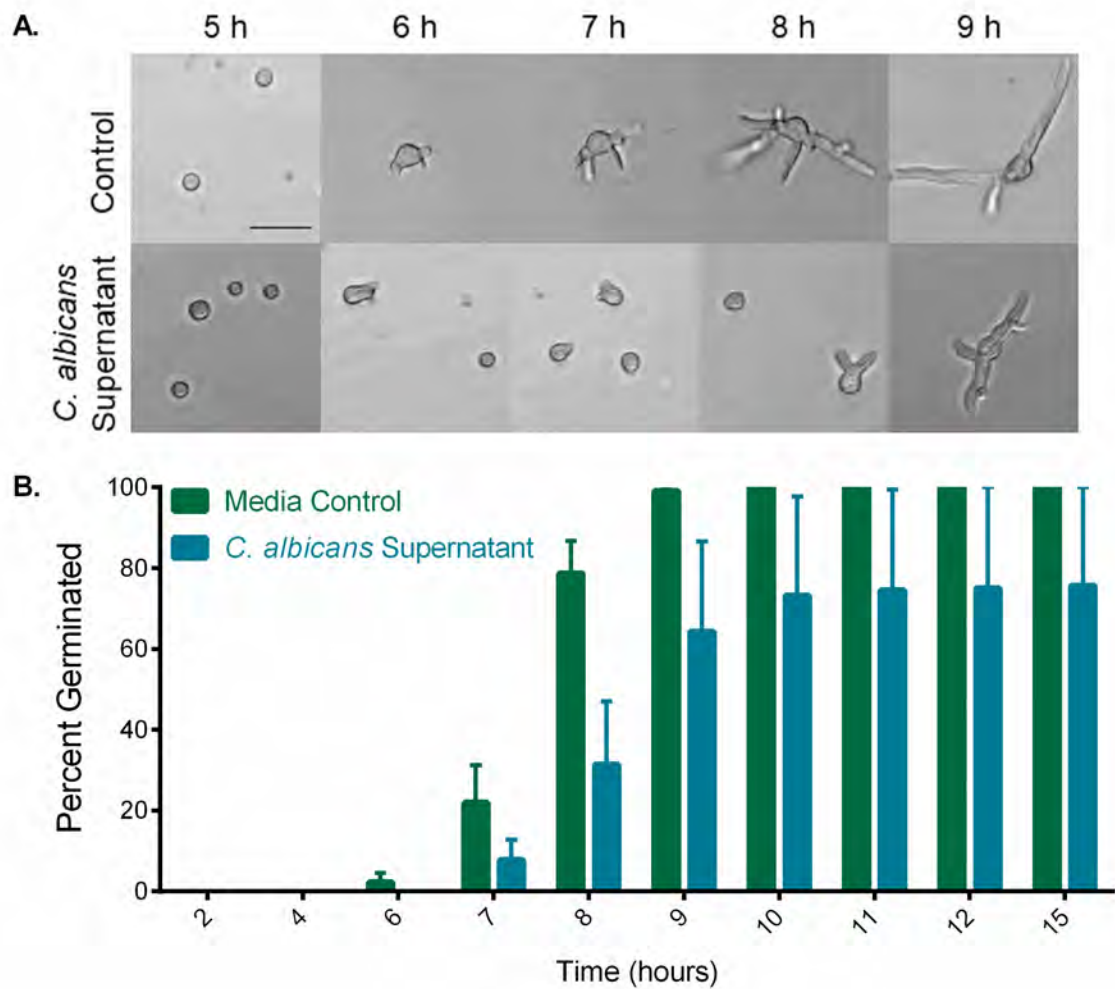


**Figure 3.1** *Candida albicans* supernatant delays the germination of *Rhizopus microsporus*. *R. microsporus* spores were exposed to sterile supernatants from overnight cultures of *C. albicans* and **(A)** representative images were taken. Scale bar = 50  $\mu$ m. **(B)** Percent of spores germinated over 15 hours was calculated (n=3). Two-way Repeated Measures ANOVA on arcsine-transformed data was used to determine significance with Tukey's multiple comparisons test ( $\alpha = 0.05$ ). Data represent mean and standard error of mean (SEM).

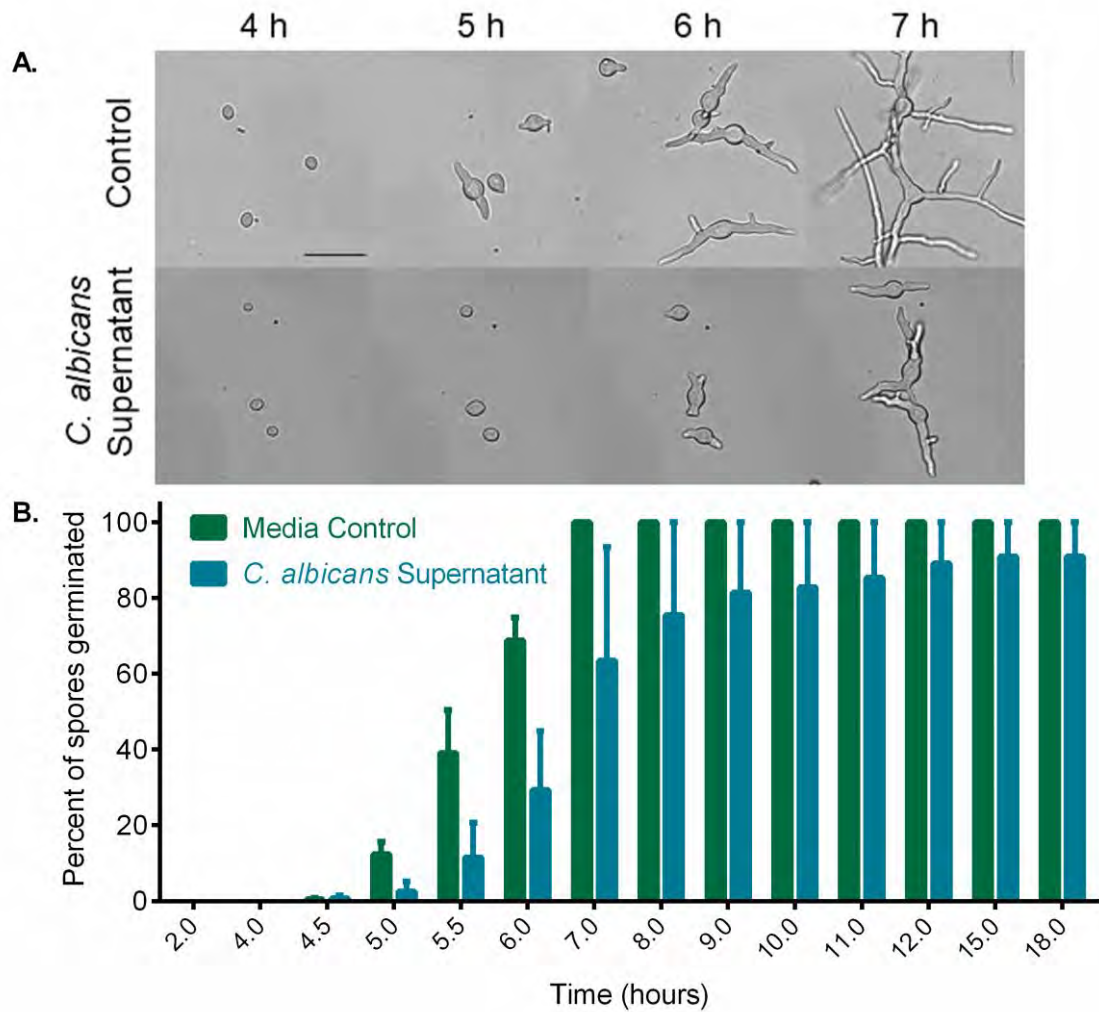


**Figure 3.2** *Candida albicans* supernatant delays the germination of *Lichtheimia corymbifera*. *L. corymbifera* spores were exposed to sterile supernatants from overnight cultures of *C. albicans* and **(A)** representative images were taken. Scale bar = 50  $\mu$ m. **(B)** Percent of spores germinated over 18 hours was calculated (n=3). Two-way Repeated Measures ANOVA on arcsine-transformed data was used to determine significance with Tukey's multiple comparisons test ( $\alpha = 0.05$ ). Data represent mean and SEM.

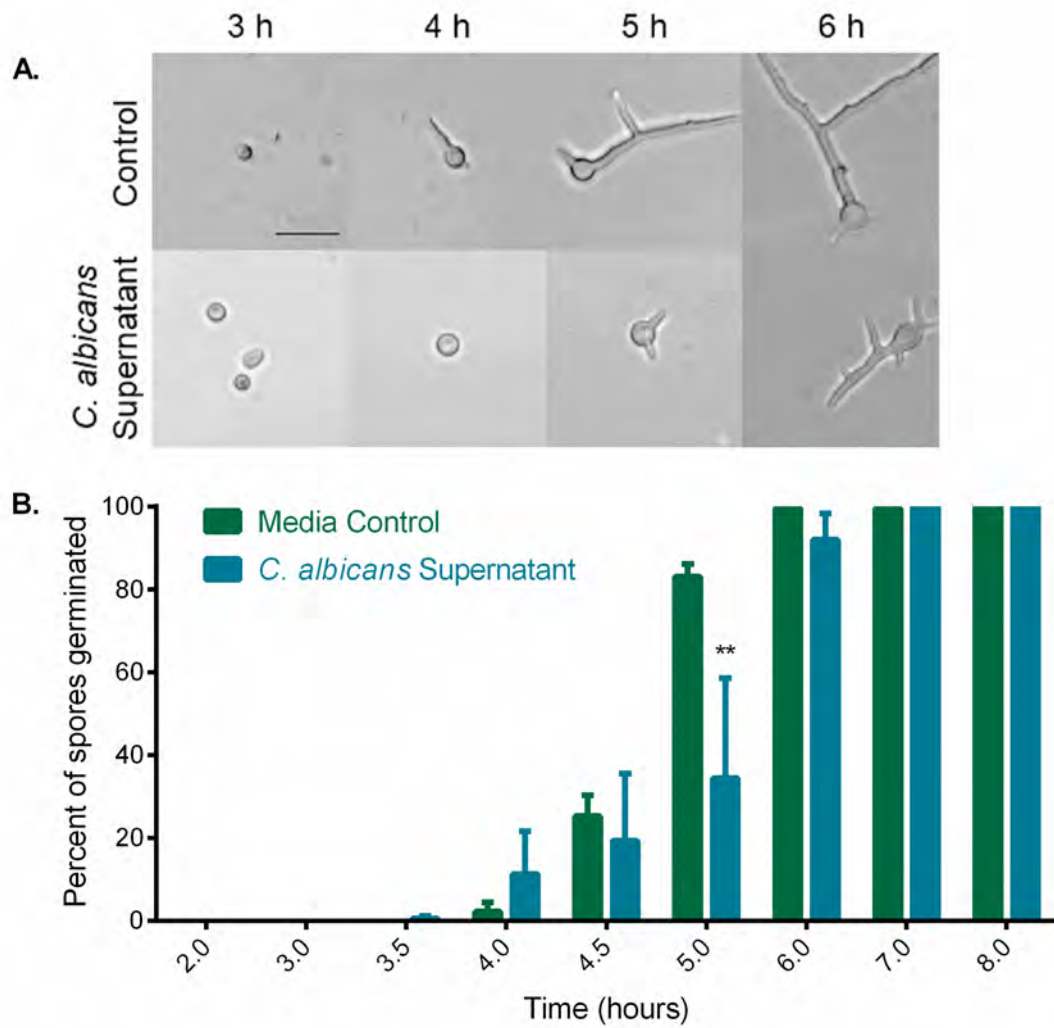


**Figure 3.3** *Candida albicans* supernatant delays the germination of *Cunninghamella bertholletiae*. *L. corymbifera* spores were exposed to sterile supernatants from overnight cultures of *C. albicans* and **(A)** representative images were taken. Scale bar = 50  $\mu$ m. **(B)** Percent of spores germinated over 8 hours was calculated (n=3). Two-way Repeated Measures ANOVA on arcsine-transformed data was used to determine significance with Tukey's multiple comparisons test ( $\alpha = 0.05$ ). Data represent mean and SEM.

**3.3.2 Farnesol delays the growth and germination of *R. microsporus*, *C. bertholletiae*, and *L. corymbifera*.** *R. microsporus*, *C. bertholletiae*, and *L. corymbifera* spores were exposed to commercially purified farnesol and imaged for 18 hours via live cell microscopy (Figures 3.4, 3.5, and 3.6). Addition of exogenous farnesol to *R. microsporus* spores resulted in a mild delay in germination, with farnesol-treated spores taking 10 hours for over 90% of the population to germinate, while solvent control spores reached 100% germination within 9 hours (Figure 3.4A and B). To determine whether the presence of farnesol delays the initiation of germination, the time when the first spore began producing a germ tube was measured (Figure 3.4C). Farnesol slightly delayed the time to first germ tube formation, with methanol control spores initialising germination after 6.97 hours (+/- 0.23) and farnesol-exposed spores after 8.14 hours (+/- 0.04). Spores exposed to farnesol swelled more than control spores before germination was initiated (Figure 3.4D), suggesting that spores are still metabolically active even though germination was delayed. Therefore, farnesol imposes a mild stress on *R. microsporus*, which results in a slight delay in the onset of germination.

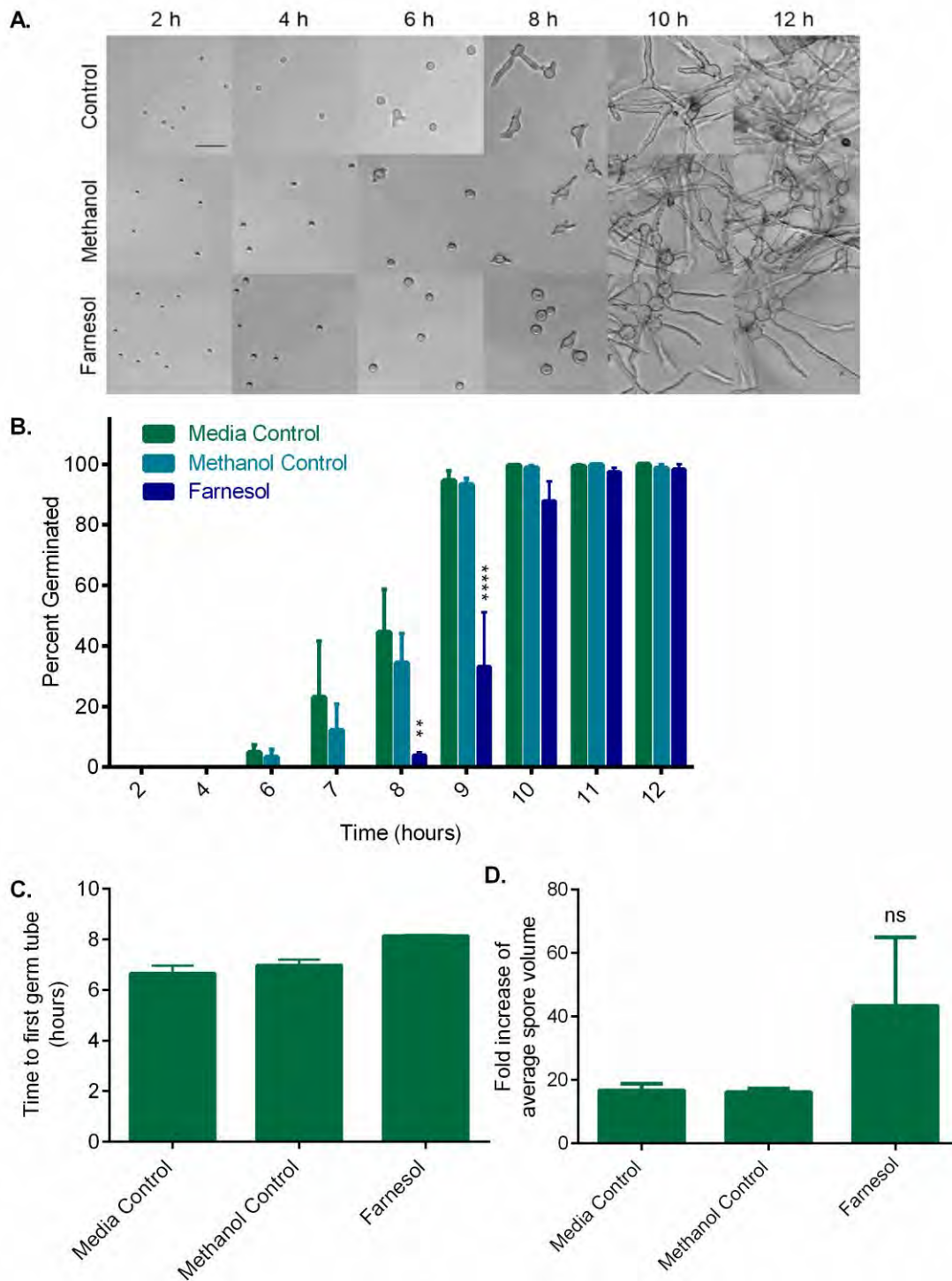


**Figure 3.4 Farnesol delays the growth and germination of *Rhizopus microsporus*.** *R. microsporus* spores were exposed to 200  $\mu$ M farnesol and **(A)** representative images were collected. Scale bar = 50  $\mu$ m. **(B)** Percent of *R. microsporus* spores germinated

over time, **(C)** time to first germ tube emergence, and **(D)** fold increase of spore volume after exposure to farnesol was calculated (n=3). For percent germination, Two-way Repeated Measures ANOVA on arcsine-transformed data with Tukey's multiple comparisons test ( $\alpha = 0.05$ ) was used, comparing farnesol to methanol control. For time to first germ tube emergence and spore swelling, Kruskal Wallis with Dunn's multiple comparisons test was used. Data represent mean and SEM. \* =  $p < 0.05$ , \*\* =  $p < 0.01$ , \*\*\*\* =  $p < 0.0001$ .

Farnesol also delayed the germination of *C. bertholletiae* (Figure 3.5A). Here, 1.59% (+/- 1.59%,  $p < 0.0001$ ) of spores germinated after 4 hours, while 55.01% (+/- 4.77%) of solvent control germinated (Figure 3.5B). However, germination reached 93.03% (+/- 6.34%) after 6 hours. While there was an overall delay in germination, the time to first germ tube formation was not impacted by the presence of farnesol (Figure 3.5C).

*L. corymbifera* had the least significant delay in growth (Figure 3.6A), and 53.47% (+/- 18.70%,  $p = 0.0341$ ) of farnesol-exposed spores still germinated at 6 hours. After 9 hours, 93.40% (+/- 4.57%) of spores germinated (Figure 3.6B), and the time to first germ tube formation was not impacted after treatment with farnesol (Figure 3.6C),

In all, this data suggests that *C. albicans* induces a modest effect on the germination of the representative Mucoralean species, *R. microsporus*, *C. bertholletiae* and *L. corymbifera*.

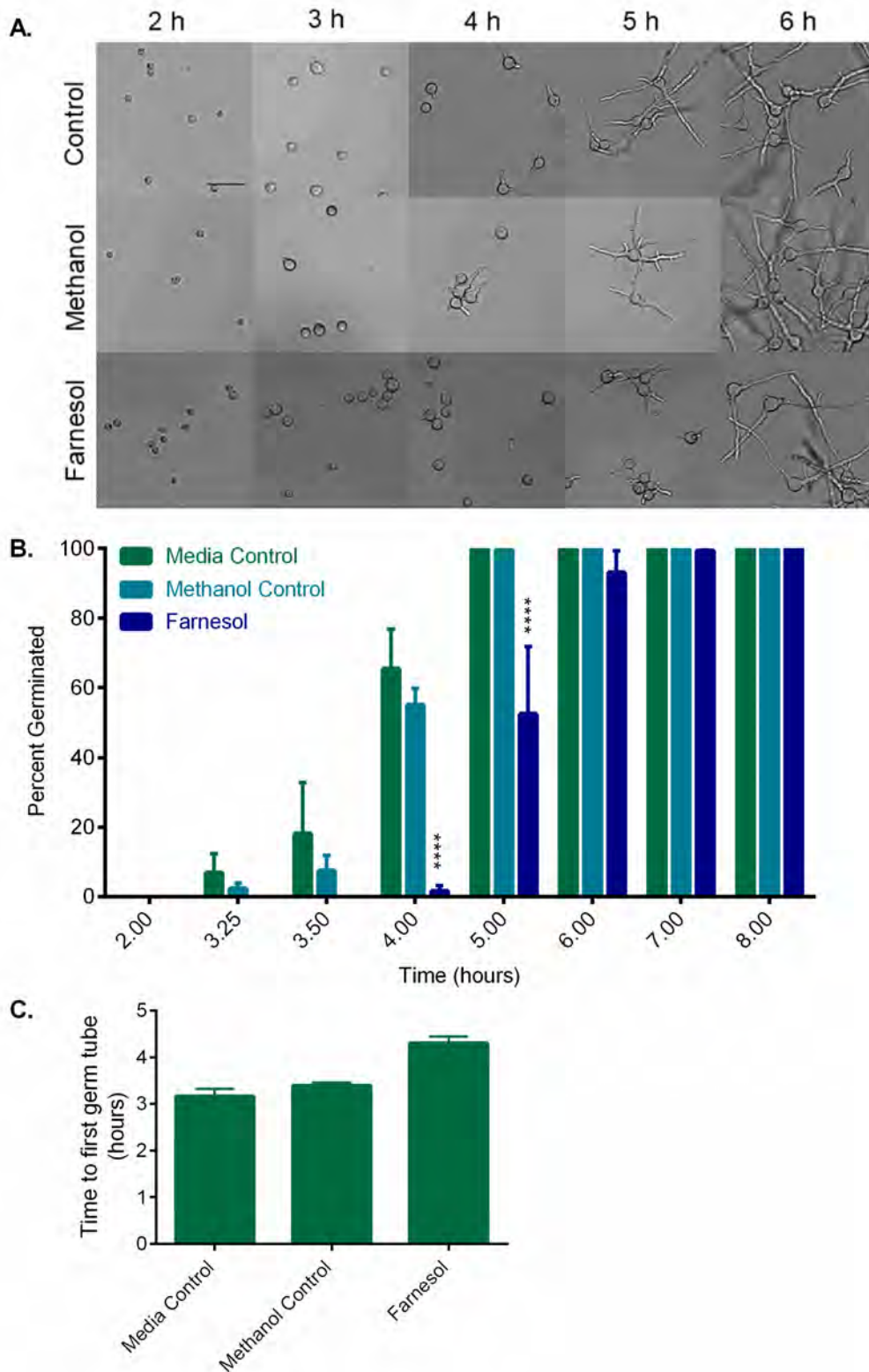


**Figure 3.5** Farnesol delays the germination of *Cunninghamella bertholletiae*. *C. bertholletiae* spores were exposed to 200  $\mu$ M farnesol and **(A)** representative images

were collected. Scale bar = 50  $\mu\text{m}$ . **(B)** Percent of *C. bertholletiae* spores germinated over time and **(C)** time to first germ tube emergence after exposure to farnesol were calculated (n=3). For percent germination, Two-way Repeated Measures ANOVA on arcsine-transformed data with Tukey's multiple comparisons test ( $\alpha = 0.05$ ) was used, comparing farnesol to methanol control. For time to first germ tube emergence, Kruskal Wallis with Dunn's multiple comparisons test was used. Data represent mean and SEM. \* =  $p < 0.05$ , \*\* =  $p < 0.01$ , \*\*\*\* =  $p < 0.0001$ .

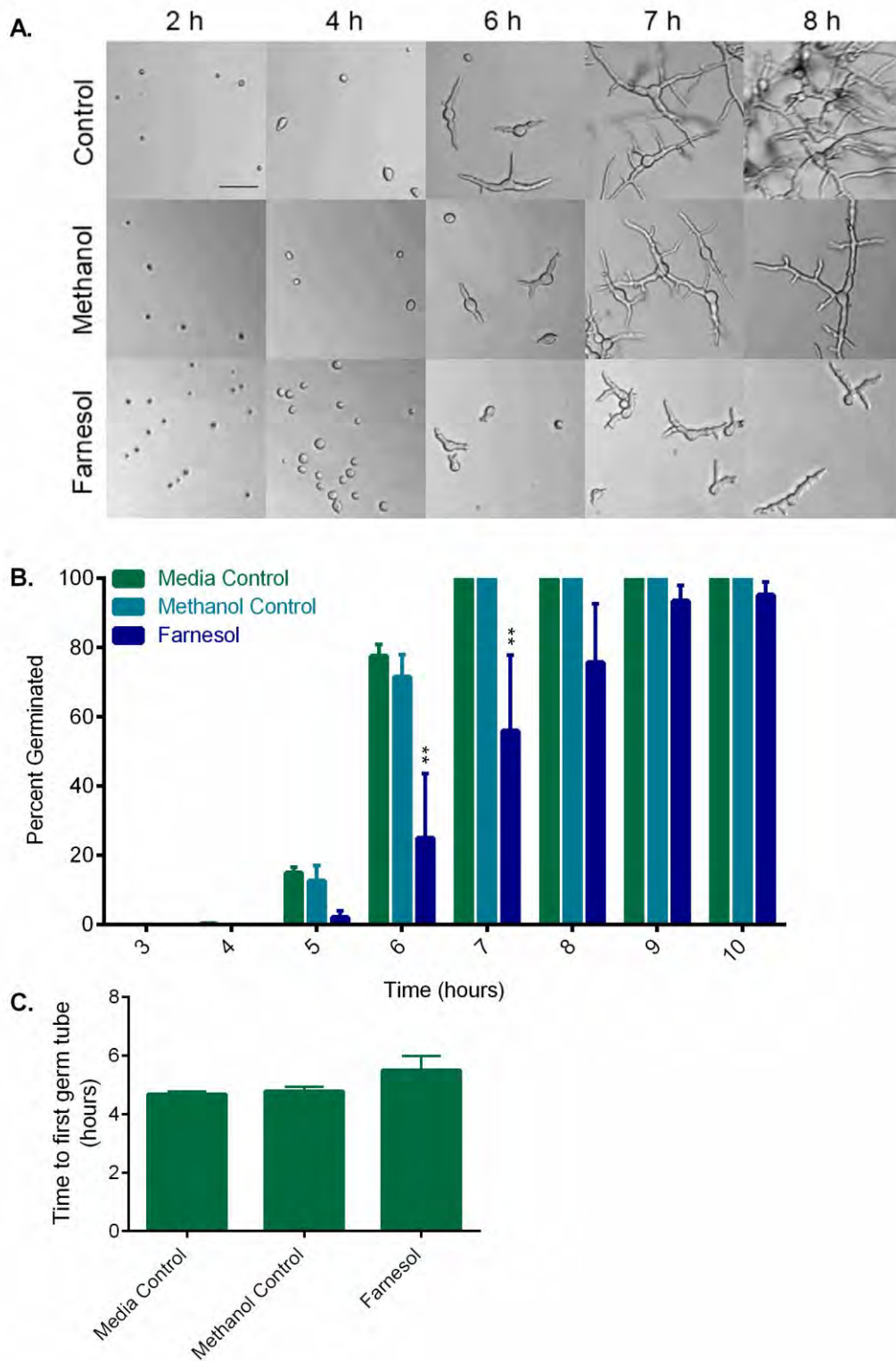


**Figure 3.6** Farnesol delays the germination of *Lichtheimia corymbifera*. *L. corymbifera* spores were exposed to 200  $\mu$ M farnesol and **(A)** representative images

were collected. Scale bar = 50  $\mu\text{m}$ . **(B)** Percent of *L. corymbifera* spores germinated over time and **(C)** time to first germ tube emergence after exposure to farnesol were calculated (n=3). For percent germination, Two-way Repeated Measures ANOVA on arcsine-transformed data with Tukey's multiple comparisons test ( $\alpha = 0.05$ ) was used, comparing farnesol to methanol control. For time to first germ tube emergence, Kruskal Wallis with Dunn's multiple comparisons test was used. Data represent mean and SEM. \* =  $p < 0.05$ , \*\* =  $p < 0.01$ , \*\*\*\* =  $p < 0.0001$ .

**3.3.3 Bacterial supernatants significantly impact the growth of *R. microsporus*, *L. corymbifera*, and *C. bertholletiae*.** To determine whether the presence of *P. aeruginosa*, *K. pneumoniae*, and *B. cenocepacia* would impact the pathogenicity of Mucorales, *R. microsporus*, *L. corymbifera*, and *C. bertholletiae* were exposed to 50% supernatants from overnight cultures of these bacteria. Live cell imaging was used to monitor spore swelling and germination (Figure 3.7A and 3.8A).

While *B. cenocepacia* supernatant had a very mild impact on *R. microsporus*, *K. pneumoniae* delayed germination by 2 hours (Figure 3.7B). Germination eventually reached 100%. On the other hand, the presence of *P. aeruginosa* supernatant resulted in almost total inhibition of *R. microsporus* germination, with only 6.7% (+/- 3.8,  $p < 0.0001$ ) of spores germinating after 18 hours.

The time in which the first spore produced a germ tube was also recorded (Figure 3.7C). Controls began germinating at 6.72 hours (+/- 0.073). While *K. pneumoniae* delayed the first germ tube protrusion by 2.31 hours (+/- 0.083), *P. aeruginosa* supernatant significantly delayed the onset of hyphal formation, with the first spore germinating at 13.13 hours (+/- 0.99,  $p = 0.0288$ ). This indicates that *P. aeruginosa* secretes a substance that inhibits the cue for *R. microsporus* to begin producing hyphae.

To determine the impact of bacterial supernatants on spore swelling, the average volume of spores immediately before germ tube protrusion was measured and compared to the earliest imaged timepoint (Figure 3.7D). The fold increase of *R. microsporus* spore volume after exposure to *P. aeruginosa* supernatant increased by 21.17-fold (+/- 7.07), while control spores increased 13.36-fold (+/- 0.43), indicating that the spores continue to swell without germinating. The fold-increase upon treatment with *K. pneumoniae* (9.57-fold +/- 1.34) and *B. cenocepacia* 6.06-fold (+/- 0.43) supernatants is lower than controls, suggesting that full swelling is not necessary for germination. In all, this indicates that spores can swell without producing hyphae or germinate without reaching maximum isotropic growth.

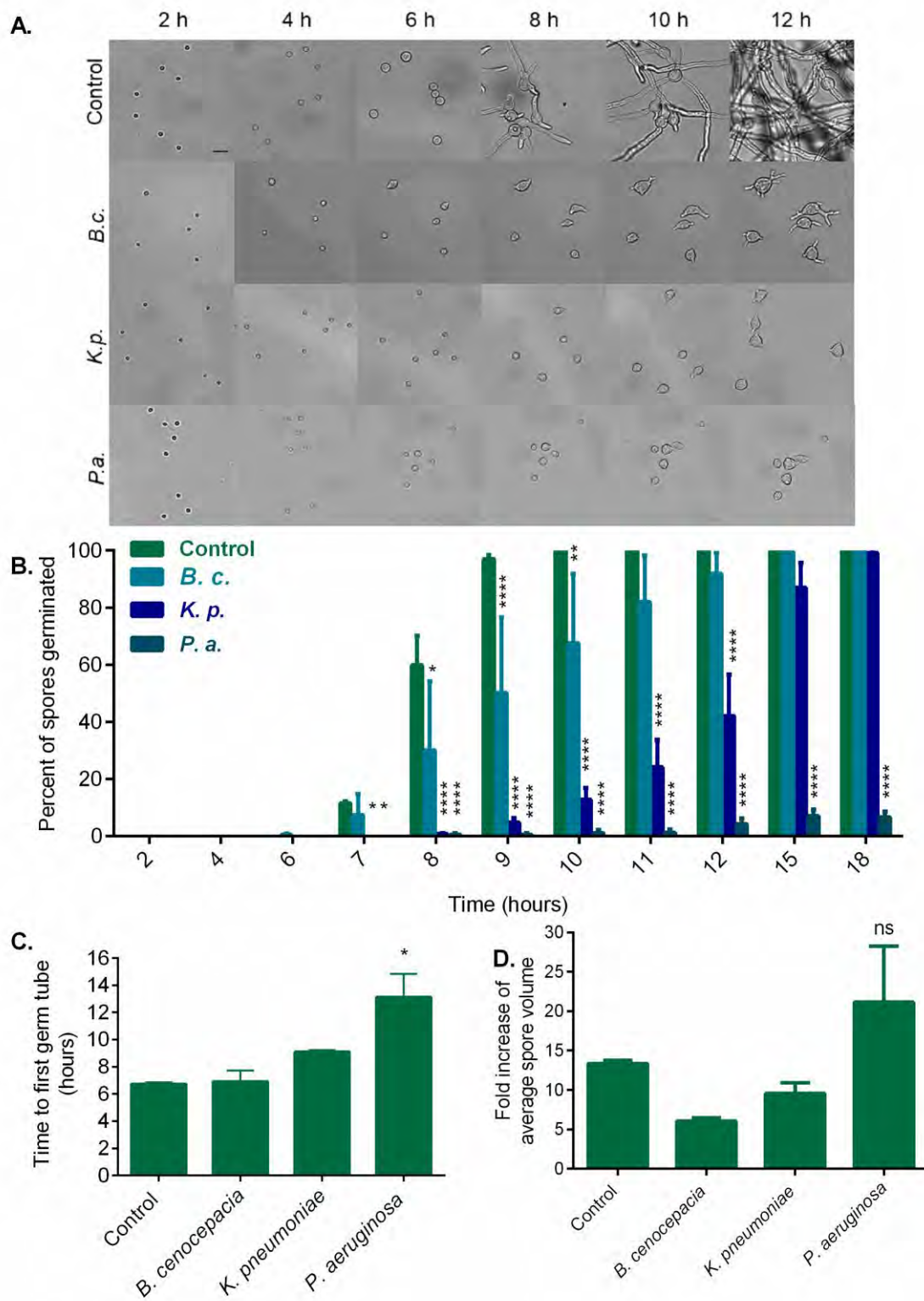


**Figure 3.7 Bacterial supernatants significantly impact the growth of *R. microsporus*.** *R. microsporus* spores were exposed to 50% *P. aeruginosa* (*P.a.*), *K.*

*pneumoniae* (*K.p.*) or *B. cenocepacia* (*B.c.*) supernatants and **(A)** representative images were taken. Scale bar = 20  $\mu\text{m}$  **(B)** Percent of spores germinated over time was calculated (n=4). **(C)** Time to first germ tube emergence (n=3) and **(D)** fold increase of the average spore volume was measured after exposure to 50% supernatants (n=3). For percent germination, Two-way Repeated Measures ANOVA on arcsine-transformed data with Tukey's multiple comparisons test ( $\alpha = 0.05$ ) was used. For time to first germ tube emergence and spore swelling, Kruskal Wallis with Dunn's multiple comparisons test was used. Data represent mean and SEM. \* =  $p < 0.05$ , \*\* =  $p < 0.01$ , \*\*\*\* =  $p < 0.0001$ .

Exposure to *B. cenocepacia*, *K. pneumoniae*, and *P. aeruginosa* supernatants induced a surprising response from *L. corymbifera* and *C. bertholletiae*. Instead of inhibiting germination, as seen with *R. microsporus*, all three supernatants promoted early germination and led to the production of thin, misshapen hyphae (Figures 3.8A and 3.8B). Germination of *L. corymbifera* spores increased by 34.92% (+/- 11.40%) with *B. cenocepacia* supernatant, 58.04% (+/- 7.56%) with *K. pneumoniae*, and 49.07% (+/- 6.06%) with *P. aeruginosa*, as compared to the control at 5 hours (Figure 3.8B). *C. bertholletiae* filamentation increased by 69.83% (+/- 12.88%,  $p = 0.0004$ ) with *B. cenocepacia*, 75.80% (+/- 4.88%,  $p < 0.0001$ ) with *K. pneumoniae*, and 54.68% (+/- 20.99%,  $p = 0.0039$ ) with *P. aeruginosa* at 4 hours (Figure 3.8C).

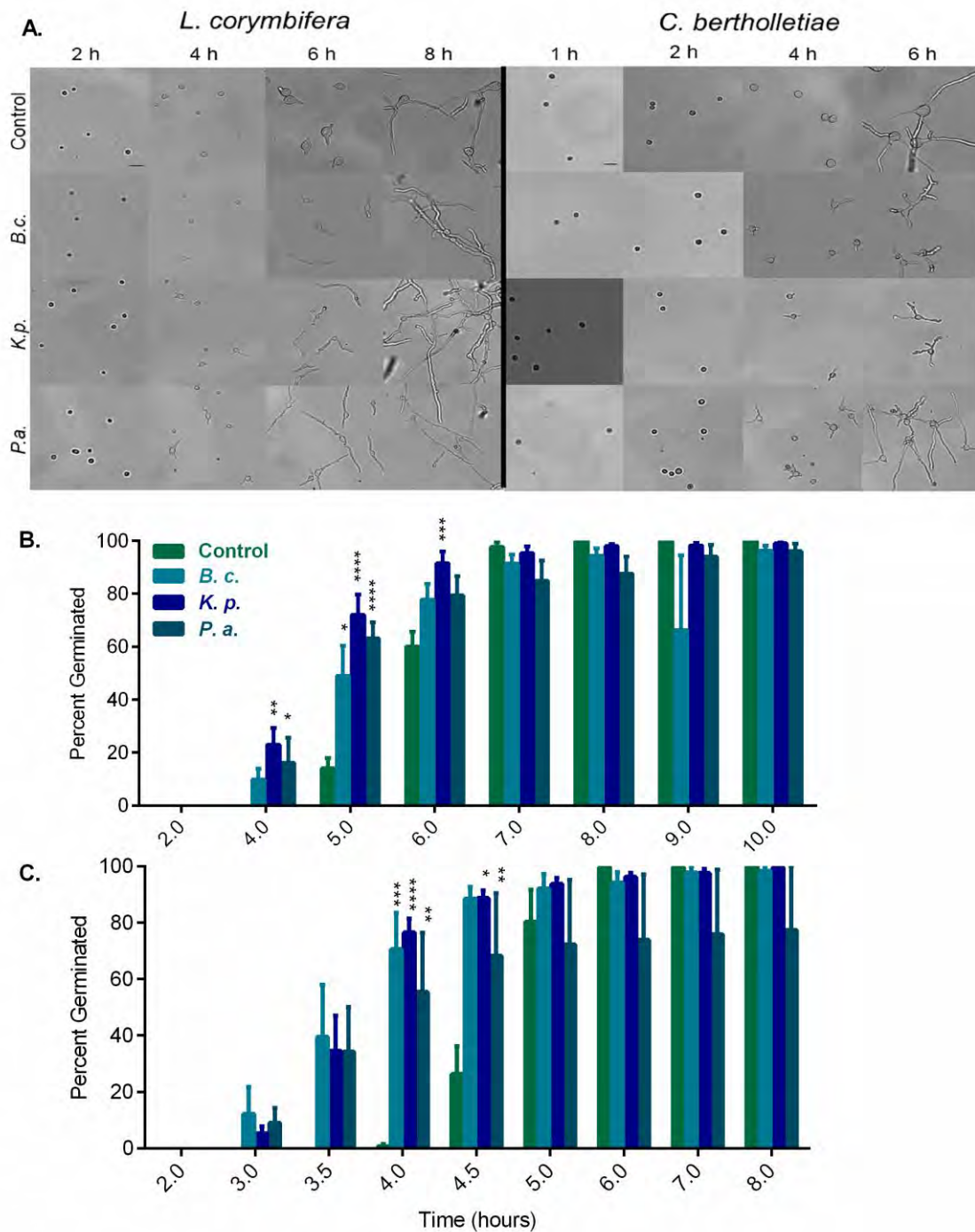


**Figure 3.8** Bacterial supernatants promote early overall germination of *L. corymbifera* and *C. bertholletiae*. Spores were exposed to 50% *P. aeruginosa* (*P.a.*), *K. pneumoniae* (*K.p.*) or *B. cenocepacia* (*B.c.*) supernatants and **(A)** representative images were taken. Scale bar = 20  $\mu$ m. Percent of **(B)** *L. corymbifera* and **(C)** *C.*

*bertholletiae* spores germinated over time was calculated (n=4). Two-way Repeated Measures ANOVA on arcsine-transformed data with Tukey's multiple comparisons test was used ( $\alpha = 0.05$ ). Data represent mean and SEM. \* =  $p < 0.05$ , \*\* =  $p < 0.01$ , \*\*\* =  $p < 0.001$ .

The time to first germ tube emergence was calculated (Figure 3.9). While early filamentation of *L. corymbifera* was promoted overall when exposed to all three supernatants, only *K. pneumoniae* significantly decreased the time to first germ tube emergence (3.75 hours  $\pm$  0.024,  $p = 0.0485$ ) as compared to control (5.03 hours  $\pm$  0.16) (Figure 3.9A). For *C. bertholletiae*, there was no significant difference between control spores (4.42 hours  $\pm$  0.024) and *B. cenocypacia* (3.52 hours  $\pm$  0.10), *K. pneumoniae* (3.31 hours  $\pm$  0.20), or *P. aeruginosa* (4.76 hours  $\pm$  1.497) supernatants (Figure 3.9C). This suggests that while overall germination is promoted, the initiation of germination of individual spores is not always significantly impacted.

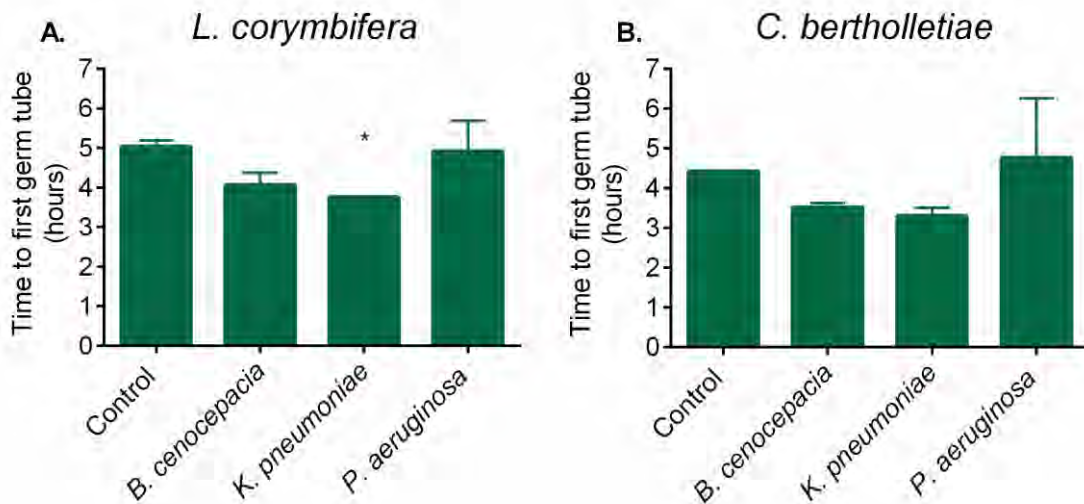


**Figure 3.9 Bacterial supernatants do not promote initiation of *L. corymbifera* and *C. bertholletiae* germination on an individual spore level. (A) *L. corymbifera* and (B) *C. bertholletiae* spores were exposed to 50% *P. aeruginosa*, *K. pneumoniae* or *B. cenocepacia* supernatants and time to first germ tube emergence was measured (n=3). Kruskal Wallis with Dunn's multiple comparisons test was used ( $\alpha = 0.05$ ). Data represent mean and SEM. \* =  $p < 0.05$ .**

To determine whether spore swelling was also impacted by the presence of the supernatants, the average spore volume was measured, comparing the initial time point to the final time point before 50% germination (Figure 3.10). The volume of *L. corymbifera* control spores increased by 10.41-fold (+/- 2.23), while spores exposed to *B. cenocepacia*, *K. pneumoniae*, and *P. aeruginosa* supernatants swelled by 3.94 (+/- 0.86), 3.56 (+/- 0.49), and 2.80 (+/- 0.46,  $p = 0.0293$ ) fold, respectively (Figure 3.10A). *C. bertholletiae* control spores increased by 7.05-fold (+/- 0.64), and treatment with *B. cenocepacia*, *K. pneumoniae*, and *P. aeruginosa* supernatants resulted in 1.93 (+/- 0.49), 1.75 (+/-

0.042), and 1.74 (+/- 0.13) fold increase. Therefore, the presence of the bacterial supernatants decreased spore swelling.

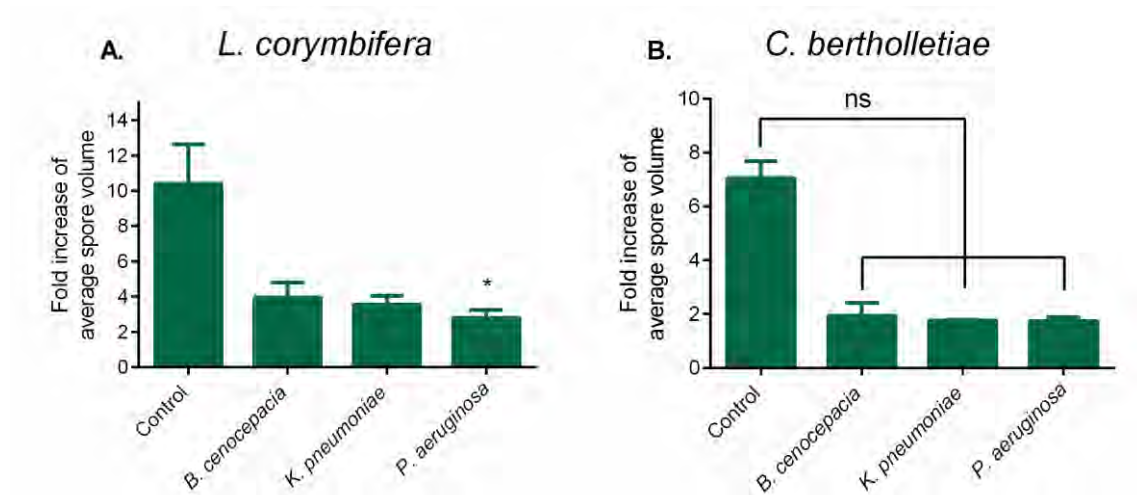


**Figure 3.10 Exposure to bacterial supernatants decreases *L. corymbifera* and *C. bertholletiae* spore swelling.** (A) *L. corymbifera* and (B) *C. bertholletiae* spores were exposed to 50% *P. aeruginosa*, *K. pneumoniae*, or *B. cenocepacia* supernatants. The fold increase of the average spore volume was measured after exposure to 50% supernatants (n=3). Kruskal Wallis with Dunn's multiple comparisons test was used ( $\alpha = 0.05$ ). Data represent mean and SEM. \* =  $p < 0.05$ .

**3.3.4 Growth promotion and phenotype alteration of *C. bertholletiae* by *P. aeruginosa* supernatant is likely caused by pH changes and nutrient depletion.** Addition of *B. cenocepacia*, *K. pneumoniae*, and *P. aeruginosa* supernatants to SAB broth resulted in mild alkalinisation of the media (average pH of 7.33 vs. 6.45). As fungal germination is dependent on environmental pH and nutrient availability (Buffo, Herman and Soll, 1984; Singh *et al.*, 2016), we

assessed whether the addition of the supernatants were influencing germination through modulation of these parameters. *C. bertholletiae* was used as a fungus that germinated early in response to supernatants, and *R. microsporus* was included as its germination was highly inhibited. Only *P. aeruginosa* supernatant was used in these experiments, as it produced the strongest, most consistent results.

Exposure of *C. bertholletiae* spores to 7.3 pH SAB/LB induced a similar phenotype as the addition of *P. aeruginosa* supernatant, producing deformed, thin, fragile hyphae (Figure 3.11A) and promoting early germination (Figure 3.11B). Filamentation of *C. bertholletiae* was rapidly enhanced with 7.3 pH SAB/LB, increasing germination by 59.13% (+/- 5.15%,  $p = 0.0005$ ) compared to control after only 4 hours. This was similar to the effect of *P. aeruginosa* supernatant, which increased germination by 38.89% (+/- 12.44%,  $p = 0.0391$ ) at 4 hours compared to control.

To elucidate the role of macronutrient restriction, SAB broth was diluted with 50% PBS to mimic the nutrient limitation imposed by the addition of 50% supernatant. As with the adjusted pH, nutrient dilution induced early germination, statistically similar to *P. aeruginosa* supernatants at all measured time points (Figure 3.11B). At 4 hours, germination was increased by 59.26% (+/- 1.63%,  $p = 0.0007$ ) with the addition of PBS compared to control.

Hyphal width is an indicator of nutrient status and decreased width suggests starvation (Turgeman *et al.*, 2014). While the width of control hyphae was 5.30  $\mu\text{m}$  ( $\pm$  0.15) 1-hour post germination, *C. bertholletiae* exposed to *P. aeruginosa* supernatant had a decreased hyphal width to 2.82  $\mu\text{m}$  ( $\pm$  0.15,  $p = 0.0383$ , Figure 3.11C). This was similar to the hyphal width in the nutrient starved condition, which was 2.79  $\mu\text{m}$  ( $\pm$  0.14,  $p = 0.0277$ ). This indicates that the unusual hyphal growth in response to supernatants (Figure 3.11A) is likely due to nutrient limitation. However, using PBS to dilute the media could also indicate osmotic stress due to the high levels of salt in PBS.

Taken together these results indicate that the early germination of *C. bertholletiae* induced by the presence of bacterial supernatants is likely caused by modulation of pH and nutrients, rather than production of hyphae-promoting molecules.

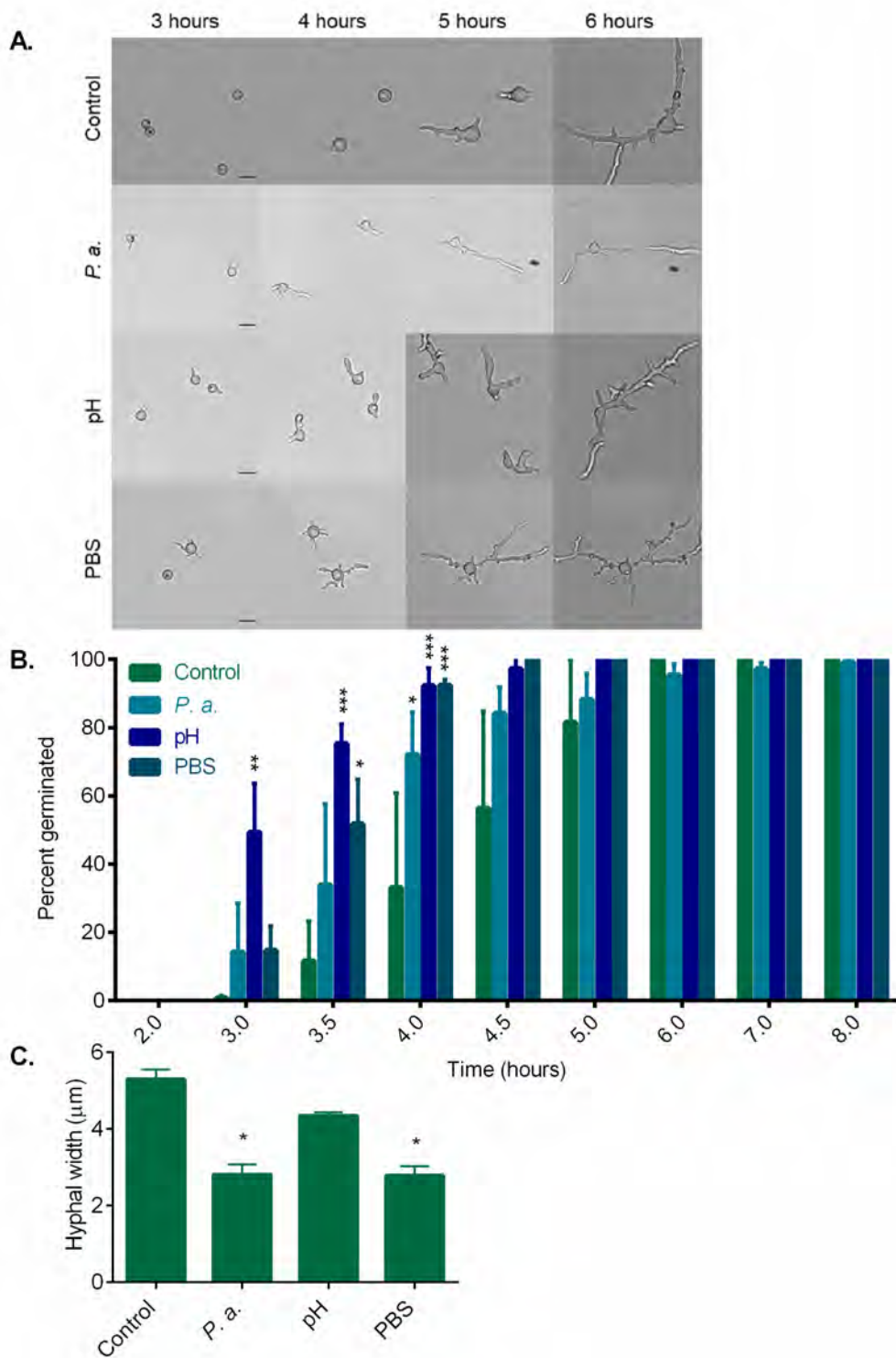


**Figure 3.11** Growth promotion and phenotype alteration of *C. bertholletiae* by *P. aeruginosa* supernatant is likely caused by pH changes and nutrient depletion. To determine if alteration of pH or nutrient depletion caused the promotion of fungal

germination, *C. bertholletiae* spores were exposed to 50% *P. aeruginosa* supernatant (*P. a.*), SAB/LB pH 7.3 (pH), and 50% PBS to mock nutrient starvation conditions and **(A)** representative images were taken. Scale bar = 20  $\mu$ m. **(B)** The percent of spores germinated over time were calculated (n=3). **(C)** Average width of *C. bertholletiae* hyphae was measured (n=3). For percent germination, Two-way Repeated Measures ANOVA on arcsine-transformed data was used to determine significance with Tukey's multiple comparisons test. For hyphal width, Kruskal Wallis with Dunn's multiple comparisons test was used ( $\alpha = 0.05$ ). Data represent mean and SEM. \* =  $p < 0.05$ , \*\* =  $p < 0.01$ , \*\*\* =  $p < 0.001$ , \*\*\*\* =  $p < 0.0001$ .

**3.3.5 *P. aeruginosa* supernatant significantly inhibits the germination of *R. microsporus*, while pH changes and nutrient depletion have no impact.** In contrast to *C. bertholletiae*, adjusting to pH 7.33 did not affect *R. microsporus* phenotype or germination (Figure 3.12A). While the supernatant inhibited germination by 95.19% (+/- 2.49%,  $p < 0.0001$ ) after 15 hours, the spores were still able to germinate normally with both 7.33 pH SAB/LB and 50% PBS (Figure 3.12B). There was no significant difference between control conditions, as *R. microsporus* reached 99.21% (+/- 0.399%), 97.67% (+/- 1.79%), and 88.76% (+/- 10.01%) germination with control, pH 7.33, and 50% PBS, respectively, after 9 hours. This indicates that pH alteration and nutrient starvation in isolation do not impact *R. microsporus* growth. While there could be a combination effect, it is likely that *P. aeruginosa* secretes a molecule(s) that can inhibit *R. microsporus* germination independent of pH changes or macro-nutrient limitation.

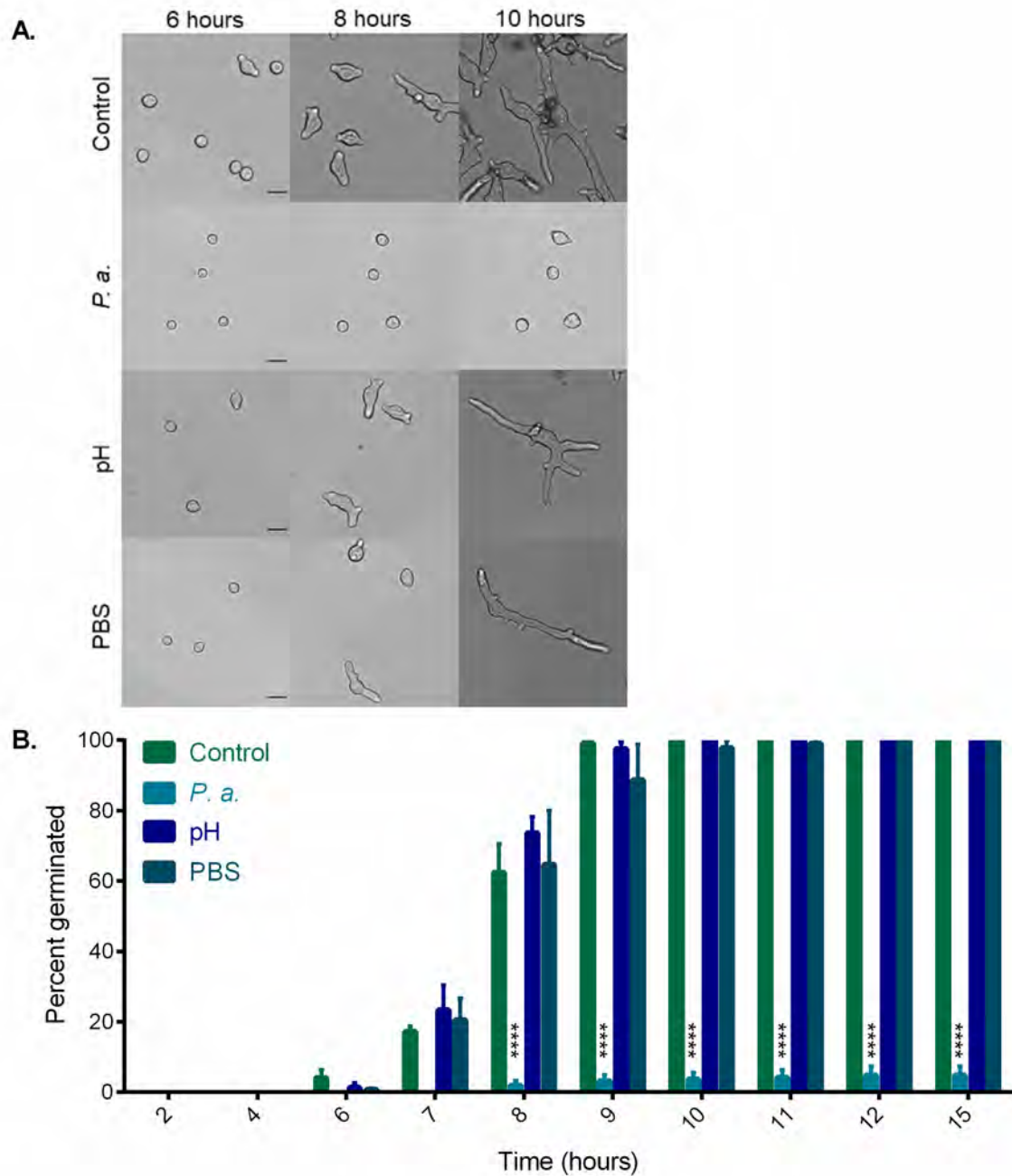


**Figure 3.12** *P. aeruginosa* supernatant significantly inhibits the germination of *R. microsporus*, while pH changes and nutrient depletion have no impact. To determine if alteration of pH or nutrient depletion caused the inhibition of fungal germination, *R. microsporus* spores were exposed to 50% *P. aeruginosa* supernatant (*P. a.*), SAB/LB pH 7.3 (pH), and 50% PBS (PBS) to mock nutrient starvation conditions

and **(A)** representative images were taken. Scale bar = 20  $\mu\text{m}$ . **(B)** The percent of spores germinated over time were calculated (n=3). Two-way Repeated Measures ANOVA on arcsine-transformed data was used to determine significance with Tukey's multiple comparisons test ( $\alpha = 0.05$ ). Data represent mean and SEM. \* =  $p < 0.05$ , \*\* =  $p < 0.01$ , \*\*\* =  $p < 0.001$ , \*\*\*\* =  $p < 0.0001$ .

**3.3.6 *P. aeruginosa* supernatant halts the growth of pre-germinated *R. microsporus* spores.** To deduce whether *P. aeruginosa* supernatants can inhibit fungal growth after germination has begun, spores were pre-germinated, and then incubated with 50% supernatant. After 24 hours, fungal growth was reduced by 81.4% (+/- 5.252,  $p = 0.0286$ ) in the presence of the supernatant as compared to the media control (Figure 3.13). Therefore, *P. aeruginosa* supernatant is able to halt further germination and growth of *R. microsporus*.

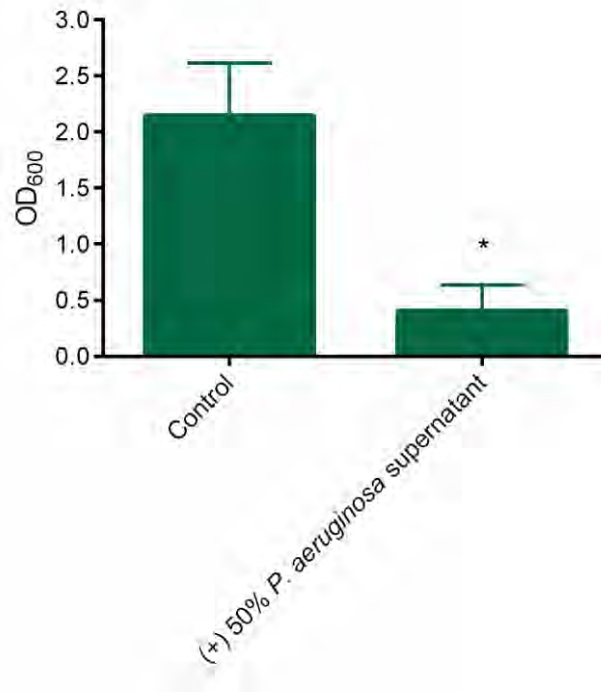


**Figure 3.13** *P. aeruginosa* supernatant halts the growth of pre-germinated *R. microsporus* spores. To determine whether the supernatant also inhibits the continuation of growth after germination is initiated, spores were incubated in SAB broth for 4-5 hours until germlings emerged, and subsequently exposed to 50% *P. aeruginosa* supernatant for 18 hours (n=4). Growth was measured using absorbance (OD<sub>600</sub>). A Mann-Whitney U test was used to determine significance. Data represent mean and SEM. \* =  $p < 0.05$ .

**3.3.7 Inhibition of *R. microsporus* growth by *P. aeruginosa* is not specific to lab-evolved strains.** To determine whether the inhibitory molecule(s) is produced by other *P. aeruginosa* strains, we tested the ability of supernatants from a series of *P. aeruginosa* isolates to inhibit spore germination. *R. microsporus* germination was inhibited in the presence of supernatants from all

*P. aeruginosa* clinical isolates (Figure 3.14), suggesting that the production of this inhibitory molecule is a general trait of *P. aeruginosa* and is not limited to laboratory-evolved strains.

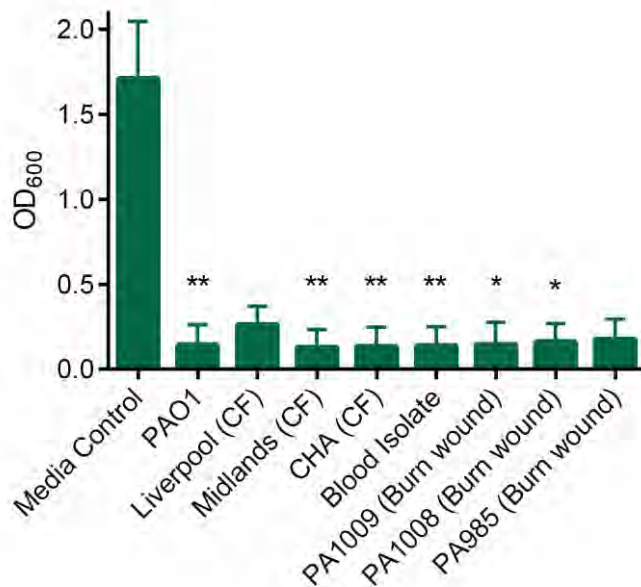


**Figure 3.14 Inhibition of *R. microsporus* growth by *P. aeruginosa* is not specific to lab-evolved strains.** To test whether the inhibition of fungal growth by *P. aeruginosa* is a lab strain-specific phenomenon, *R. microsporus* spores were exposed to supernatants from *P. aeruginosa* clinical isolates for 24 hours (n=6). Fungal growth was determined through absorbance (OD<sub>600</sub>). Data was analysed by a Kruskal-Wallis test with Dunn's multiple comparisons test ( $\alpha = 0.05$ ). CF = Cystic Fibrosis isolate. Data represent mean and SEM. \* =  $p < 0.05$ , \*\* =  $p < 0.01$ .

**3.3.8 *P. aeruginosa* supernatant decreases *R. microsporus* swelling in early times points and reduces cell wall chitin.** *R. microsporus* spores began germinating in control media after about 6 hours (Figure 3.7C). Figure 3.7D

determined that *P. aeruginosa* supernatant does not decrease spore swelling when the volume was measured immediately before the initiation of germination or at the end of the experiment if no spores germinated. However, decreased swelling in earlier time points could limit nutrient acquisition and reduce germination. Therefore, spore swelling after 4 hours exposure to 50% *P. aeruginosa* supernatant was compared to spores suspended in PBS on ice to reduce metabolic activity or suspended in 50:50 SAB/LB to induce swelling for 4 hours (Figure 3.15). The majority of PBS-incubated spores (80.54%) were between 10 and 15  $\mu\text{m}^2$ , while 65.79% of SAB/LB-incubated spores were greater than 20  $\mu\text{m}^2$ . Upon exposure to *P. aeruginosa* supernatant, *R. microsporus* spores continued to swell, but overall area was reduced, with only 29.76% of spores being greater than 20  $\mu\text{m}^2$  and 53.17% of spores being between 10 and 15  $\mu\text{m}^2$  (Figure 3.15A). This indicates that the presence of *P. aeruginosa* supernatant reduces swelling at early time points (4 hours). Reduction in isotropic could decrease nutrient uptake and influence germination.

Resting spores contain low levels of chitin, and this is increased during spore swelling and germination (Sephton-Clark *et al.*, 2018). Chitin can be anti-inflammatory (Wagener *et al.*, 2014), and decreased levels of this polysaccharide could influence the host immune response to *R. microsporus* by increasing inflammation. Because the presence of *P. aeruginosa* supernatant reduces spore swelling (Figure 3.15A), total chitin levels were measured. *R. microsporus* spores were exposed to 50% *P. aeruginosa* supernatant, PBS, or 50:50 SAB/LB for 4 hours, stained with 250  $\mu\text{g}/\text{ml}$  calcofluor white (CFW), and microscopic images

were taken (Figure 3.15B). Fluorescence was manually measured for 200 spores in each condition, relative to area. Relative fluorescence of SAB/LB-incubated spores was increased, compared to PBS-incubated ( $p = 0.0513$ , Figure 3.15C). The average relative fluorescence of spores exposed to *P. aeruginosa* supernatant was also increased as compared to PBS-incubated spores, but this was less significantly different ( $p = 0.3033$ ). This indicates that the decreased spore swelling after exposure to *P. aeruginosa* supernatant likely decreases total chitin content, which could influence the host immune response during co-infection.

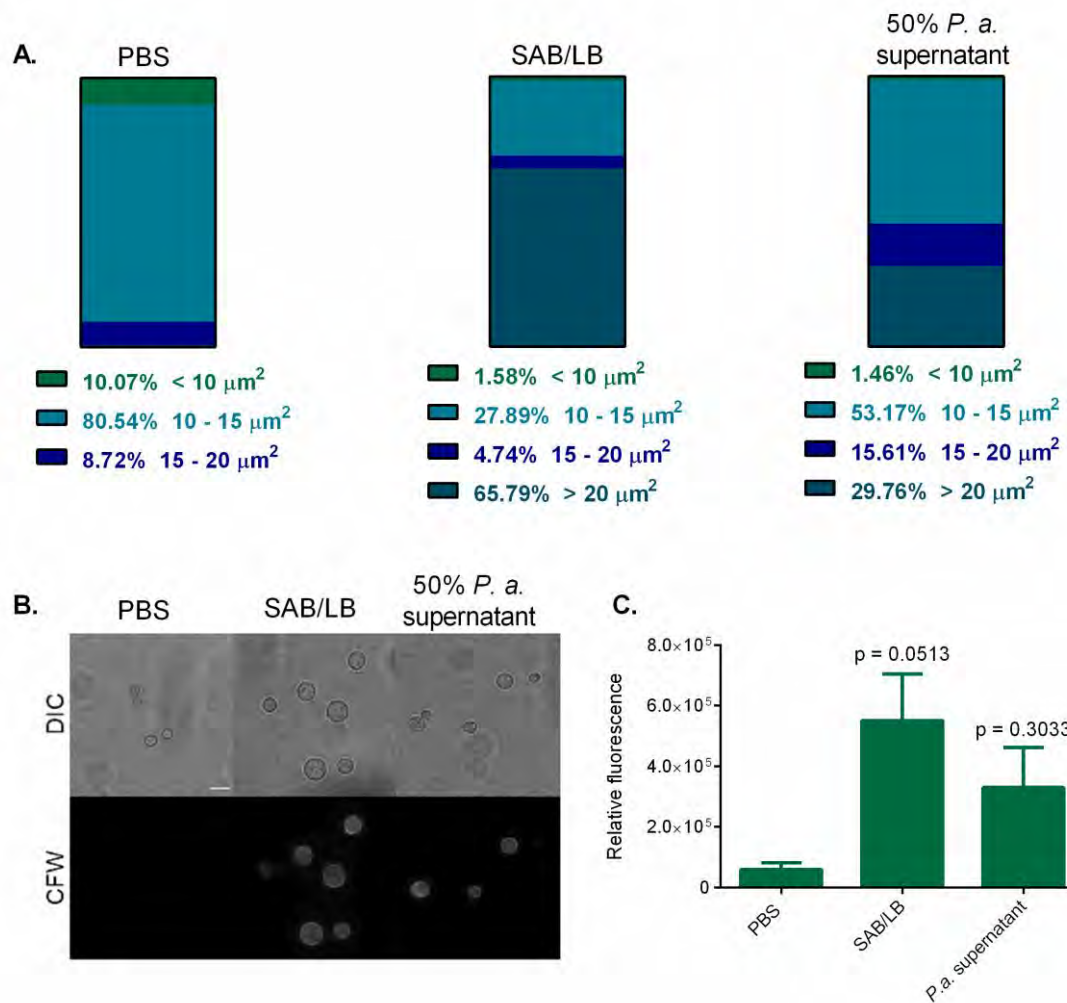


**Figure 3.15** *P. aeruginosa* supernatant decreases *R. microsporus* spore swelling and chitin. *R. microsporus* spores were exposed to 50% *P. aeruginosa* supernatant, PBS, or 50:50 SAB/LB for 4 hours before images were taken microscopically. (A) The average spore area under each condition was measured and grouped into size categories (< 10  $\mu\text{m}^2$ , 10-15  $\mu\text{m}^2$ , 15-20  $\mu\text{m}^2$ , and > 20  $\mu\text{m}^2$ ). Spores were stained with calcofluor white (CFW) and (B) representative images are shown. Scale bar = 25  $\mu\text{m}$ . (C) The fluorescence of spores under each condition was measured, relative to area. Data was analysed by a Kruskal-Wallis test with Dunn's multiple comparisons test ( $\alpha = 0.05$ ). Data represent mean and SEM.

**3.3.9 Live *P. aeruginosa* strongly inhibits the germination of *R. microsporus*.** *R. microsporus* spores were co-cultured with live *P. aeruginosa*, *K. pneumoniae*, *B. cenocepacia*, *S. aureus*, and *E. coli* to further observe cross-kingdom interactions (Figure 3.16A). Co-culture of *R. microsporus* with *P. aeruginosa* at MOIs of 1:50 and 1:100 for 24 hours resulted in 56.80% (+/- 8.269,  $p = 0.0023$ ) and 92% (+/- 2.784,  $p < 0.001$ ) inhibition of fungal germination, respectively (Figure 3.16B, quantified by Callum Clark). *K. pneumoniae* completely inhibited the germination of *R. microsporus* spores at all MOIs tested, and this observation is being investigated by other laboratory members. Conversely, co-culturing *R. microsporus* with *S. aureus*, *E. coli*, and *B. cenocepacia* did not affect fungal growth at any of the MOIs tested. Taken together, the results obtained from live co-cultures between *R. microsporus* and *P. aeruginosa* indicate that these two microbes undergo a competitive relationship resulting in reduced fungal germination.

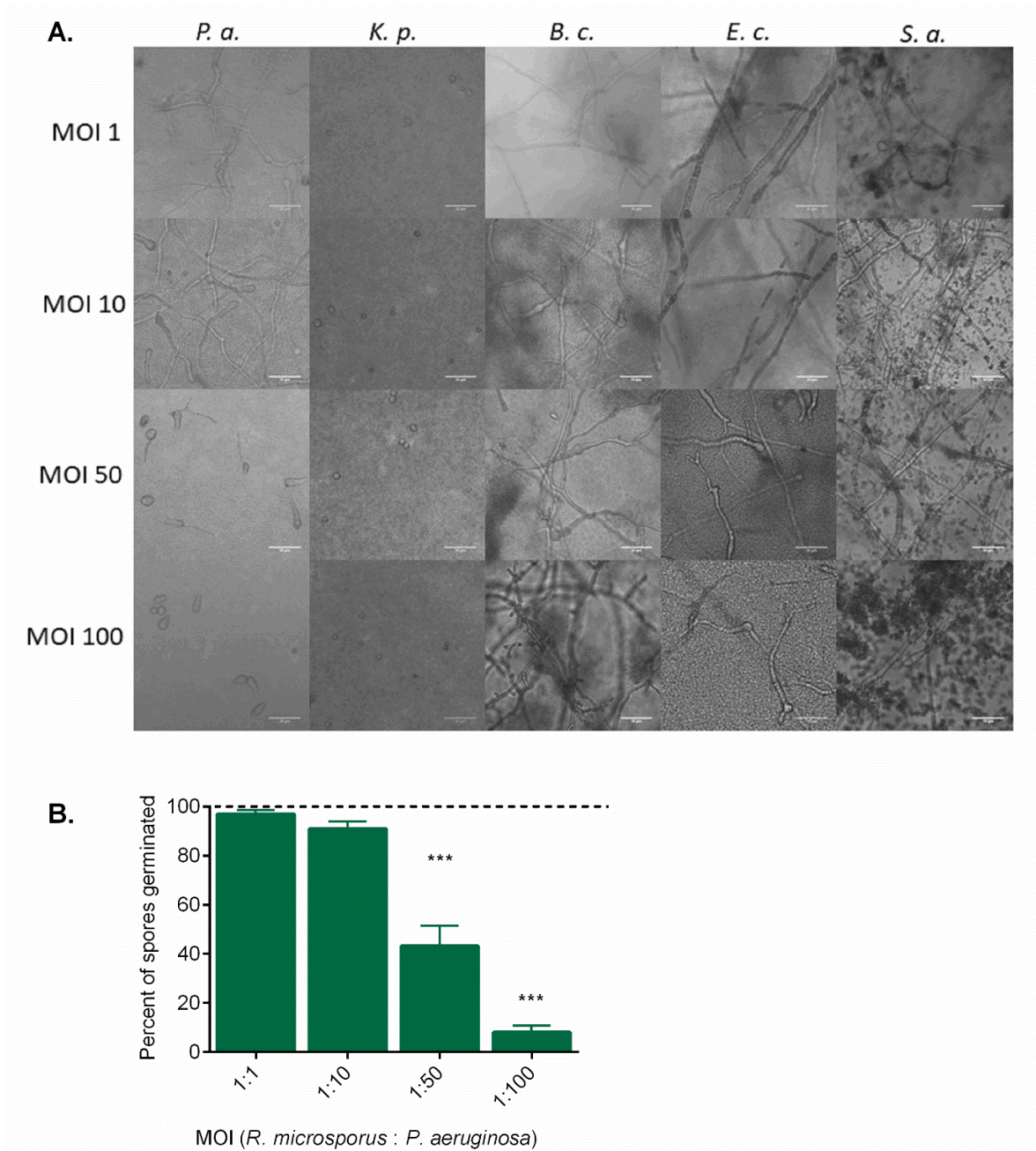


**Figure 3.16** *P. aeruginosa* strongly inhibits the germination of *R. microsporus*. *R. microsporus* spores were incubated with live *P. aeruginosa* (*P. a.*), *K. pneumoniae* (*K. p.*), *B. cenocepacia* (*B. c.*), *S. aureus* (*S. a.*), and *E. coli* (*E. c.*) at increasing multiplicities of infection (MOI) for 24 hours **(A)** Representative images after 24 hours exposure (37°C, static). Scale bars depict 50 µm. **(B)** Percent of spores germinated after 24 hours exposure to *P. aeruginosa*. Dotted line represents spore-only control. One-way ANOVA

performed on arcsine transformed data (n=6,  $\alpha = 0.05$ ). \*\*\* =  $p < 0.001$ . Data represent mean and SEM. (Kousser *et al.*, 2019).

### 3.4 Discussion.

This chapter highlights the ability of polymicrobial interactions to modulate the germination of Mucorales, which is a key virulence determinate (Ibrahim *et al.*, 2012). Here it was demonstrated that Mucorales have a varying, species-specific response to opportunistic bacteria and fungi.

**3.4.1 Fungal-fungal interactions.** *C. albicans* has been previously shown to modulate the growth and virulence of invasive fungi such as *Cryptococcus neoformans* (Cordeiro *et al.*, 2012), *Aspergillus nidulans* (Semighini *et al.*, 2006), *Aspergillus flavus* (Wang *et al.*, 2014), *Penicillium expansum* (P. Liu *et al.*, 2010), and *Fusarium graminearum* (Semighini, Murray and Harris, 2008) through the secretion of farnesol. However, *C. albicans* supernatant and isolated farnesol have limited effects on Mucorales germination.

Farnesol is an autoinhibitory molecule that prevents the morphological switch in *C. albicans* from disseminating or commensal yeast to invasive hyphae by acting on the cyclic adenosine monophosphate (cAMP) pathway (Hall *et al.*, 2011). As farnesol does not completely inhibit spore germination, it is possible that filamentation is regulated through a different pathway in Mucorales, though the exact pathway is unknown. During hyphal growth, *Rhizopus delemar* upregulates

stress response genes (Sephton-Clark *et al.*, 2018). *A. nidulans* responds to farnesol by enhancing the production of stress response proteins, including antioxidant enzymes and the MAPK regulated dehydrin-like protein (Wartenberg *et al.*, 2012). Therefore, perhaps *R. microsporus*, *C. bertholletiae*, and *L. corymbifera* overcome the farnesol-dependent inhibition by enhancing their stress response mechanisms.

**3.4.2 Inhibition of *R. microsporus* germination by *P. aeruginosa* secreted factors.** While *B. cenocepacia*, *K. pneumoniae*, and *P. aeruginosa* supernatants all significantly inhibited the growth of *R. microsporus*, *P. aeruginosa* had the most drastic, long-lasting effect. This is similar to observations in plant disease, where *Pseudomonas fluorescens* inhibits apple rot caused by *Mucor piriformis* through secreted molecules (Wallace, Hirkala and Nelson, 2018). *P. aeruginosa* is known to participate in polymicrobial interactions with fungi, frequently acting antagonistically and competing against other organisms. The result of these interactions usually ends in inhibition or death of the other organism (Hogan and Kolter, 2002; Hogan, Vik and Kolter, 2004; Mowat *et al.*, 2010; Filkins *et al.*, 2015). Because of this dramatic, long-lasting inhibition that is not confounded by pH changes or nutrient depletion, the interaction between *R. microsporus* and *P. aeruginosa* was chosen to study more in-depth.

Diagnosis of mucormycosis usually occurs once disease has already progressed, and a successful treatment would halt hyphal growth following the initiation of

germination. It has been shown previously that cessation of actively germinating Mucorales spores is possible through the addition of acetic acid (Trzaska *et al.*, 2015). Here we found that supernatants from *P. aeruginosa* can inhibit further growth of pre-germinated *R. microsporus* spores. This indicates that *P. aeruginosa* secreted factors also inhibit hyphal extension and could impact existing infections. This is contrary to work investigating the relationship between *Rhizopus stolonifer* and *Enterobacter cloacae*, where addition of *E. cloacae* to resting spores inhibited germination, but bacteria had a reduced effect on pre-germinated *R. stolonifer* (Wisniewski, Wilson and Hershberger, 1989).

Consistent with results from sterile supernatants, exposure to live *P. aeruginosa* inhibits *R. microsporus* growth more effectively than other tested bacteria, with the exception of *K. pneumoniae*. This bacterium can interact with *C. albicans* in a contact-dependent manner, where *P. aeruginosa* binds to fungi hyphae, forms a biofilm, and kills via the secretion of cytolytic phospholipase C (Gibson, Sood and Hogan, 2009). Therefore, it is possible that the presence of the bacteria also reduces viability of *R. microsporus*, and fungal survival during co-cultures will be explored in Chapter 4.

**3.4.3 Response variation between distantly related Mucorales following exposure to bacterial supernatants.** Bacterial supernatants promoted the early germination of *C. bertholletiae* and *L. corymbifera*. While germination occurred earlier than controls, hyphae were thin, fragile, and deformed. Previous studies

have found that nutrient starvation can lead to decreased hyphal width (Turgeman *et al.*, 2014) and that susceptibility to pH varied based on species (Singh *et al.*, 2016). Our observations that an increase of the media's pH impacts the growth of *C. bertholletiae* is consistent with previously published results that this species, along with *L. corymbifera*, is more sensitive to alkaline pH than *Rhizopus spp.* (Singh *et al.*, 2016). It is possible that secreted molecules from these bacteria or live bacteria could impact growth of *C. bertholletiae* and *L. corymbifera*, but these effects may be masked by the pH response. Aquaporins that actively regulate spore swelling are pH dependent. This factor could be responsible for the lower fold-increase of *C. bertholletiae* and *L. corymbifera* spores prior to germination (Turgeman *et al.*, 2016). Therefore, perhaps the media alkalisation modulated the pH-dependent aquaporins on the spore surface, limiting the swelling and nutrient acquisition of *C. bertholletiae* and *L. corymbifera*. This may have led to the malformed hyphae and decreased hyphal width, which is a characteristic of nutrient deprived spores (Turgeman *et al.*, 2014).

In all, this chapter has shown that opportunistic pathogens can impact the germination and growth of Mucorales, though there is inter-species variation. The next chapter will focus on the interaction between *R. microsporus* and *P. aeruginosa* to characterise the inhibitory molecule(s) and determine the causative agent.

# **Chapter 4 : CHARACTERISATION OF *P. AERUGINOSA*-MEDIATED INHIBITION OF *R. MICROSPORUS***

The majority of this chapter has been previously published:

Kousser, C., Clark, C., Sherrington, S., Voelz, K. and Hall, R. (2019). *Pseudomonas aeruginosa* inhibits *Rhizopus microsporus* germination through sequestration of free environmental iron. *Scientific Reports*, 9. DOI 10.1038/s41598-019-42175-0

Parts of this chapter were undertaken by MSci student, Callum Clark, who worked under my supervision; and Sarah Sherrington, a technician in Rebecca Hall's laboratory:

- Figures 4.3B, 4.8A, and 4.8B by Callum Clark
- Figure 4.7A by Sarah Sherrington

## 4.1 Introduction

In the previous chapter, we established that *Pseudomonas aeruginosa* inhibits the growth of *Rhizopus microsporus* through secreted factors. As there is a general lack of understanding regarding the pathogenesis of mucormycosis, dissecting the relationship between these organisms is important in the context of patient management and could provide insight into novel treatment options.

**4.1.1 Mucorales and *P. aeruginosa* in the human host.** Investigating the interaction between Mucorales and *P. aeruginosa* is medically relevant, as these organisms have been co-isolated from the rhinocerebral cavity and gastrointestinal system (Akhrass *et al.*, 2011; Martinello *et al.*, 2012), are routinely found in the same niches (Crull *et al.*, 2016; Kabulski and MacVane, 2018; Jeong *et al.*, 2019), and infect patients with similar underlying conditions (Atreja and Kalra, 2015). They are particularly likely to interact in traumatic and burn wounds, where bacteria such as *P. aeruginosa* are isolated in cutaneous mucormycosis (Lelievre *et al.*, 2014). As 75% of chronic wounds test positive for *P. aeruginosa*, it is very likely that Mucorales spores from the environment come into contact with this bacteria (De Oliveira *et al.*, 2017). However, the inhibitory action of *P. aeruginosa* on *R. microsporus* could reduce reporting of the fungus, and co-habitation of these organisms is likely higher than described.

Diabetes is the most common underlying disease leading to mucormycosis (Roden *et al.*, 2005). Diabetic patients, especially those with poorly controlled

diabetes, are at risk for developing infections with both *P. aeruginosa* and Mucorales. *P. aeruginosa* causes infections in chronic foot ulcers, Fournier's gangrene, and malignant otitis externa in diabetic individuals (Atreja and Kalra, 2015). Mucorales have also been documented in cases of diabetic foot wounds, Fournier's gangrene, and necrotising malignant otitis externa (Tuzcu *et al.*, 2006; Kumar *et al.*, 2011; Mandal *et al.*, 2013).

Pulmonary infection is one of the most prevalent manifestations of mucormycosis, and this can occur following lung transplantations in CF patients (Kabulski and MacVane, 2018). As *P. aeruginosa* commonly infects the lungs of adults with CF, even following transplantation (Suhling *et al.*, 2013), it is likely that they meet in this niche as well (Oliver *et al.*, 2000). Specific case reports have described co-isolation of *P. aeruginosa* and Mucorales. For example, one study presented an individual with rhinocerebral and palatal mucormycosis whose cultures also grew *P. aeruginosa* (Akhrass *et al.*, 2011). Another example involves a patient successfully treated for *Salmonella typhimurium* infection who developed gastrointestinal mucormycosis with multi-drug resistant *P. aeruginosa* also isolated following fungal diagnosis (Martinello *et al.*, 2012).

It is possible that the inhibitory nature of *P. aeruginosa* can mask the presence of Mucorales, and mucormycosis could emerge following antibiotic treatment. For instance, a person who originally tested positive for only *P. aeruginosa* sinus infection developed rhinocerebral mucormycosis following ciprofloxacin

treatment, though this could also be evidence for original misdiagnosis (Dimaka *et al.*, 2014). Furthermore, 94% of fungal peritonitis is associated with recent antibiotic therapy, usually for treatment of bacterial peritonitis. In these cases, *P. aeruginosa* is one of the most common causes of bacterial peritonitis, and non-*Candida* fungi such as *Aspergillus spp.*, *Cryptococcus spp.*, and Mucorales make up 10% of fungal infections (Cho and Struijk, 2017).

**4.1.2 Mucorales and *Pseudomonas spp.* in the environment.** As Mucorales are natural colonisers of soil and plants, human infections usually arise from exposure to environmental spores, especially following traumatic wounds. (Mousavi *et al.*, 2018). It is likely that Mucorales evolved relationships with bacteria in environmental niches, and that these relationships carry over into human infection. Studies investigating the interaction between Mucorales and *Pseudomonas spp.* in the agricultural sector provide insight into the relationship they may have within a medical setting.

Not only is mucormycosis a devastating infection in humans, but Mucorales are major causes of food spoilage. These fungi infect post-harvest fruits and vegetables such as peaches, apples, pears, sweet potatoes, strawberries, and grapes (Zahavi *et al.*, 2000; Northover and Zhou, 2002; Holmes and Stange, 2007; Zhang *et al.*, 2007; López *et al.*, 2015). There have been several studies investigating the potential use of bacterial biocontrol agents in reducing Mucoralean fruit rot, with *Pseudomonas spp.* being particularly effective. For

instance, *P. syringae* reduces *Rhizopus* rot caused by *R. stolonifer* more effectively than other bacteria, such as *Enterobacter cloacae* (Wilson, Franklin and Pusey, 1987; Zhou, Northover and Schneider, 1999; Northover and Zhou, 2002). The effectiveness of *Pseudomonas spp.* against mould infections of fruit is highlighted with the commercial biocontrol agent BioSave®. This product is effective against *Mucor* rot and *Rhizopus* rot of fruits, and the main active ingredient is *P. syringae* (Droby *et al.*, 2016).

Although our focus is investigating polymicrobial interactions in a medical setting, clues regarding their relationship can be drawn from these environmental examples. These cases highlight the antagonistic relationship between Mucorales and *Pseudomonas* and the potential medical implications.

## **4.2 Aim of this chapter.**

While *P. aeruginosa* and *R. microsporus* are likely to meet within the environment and the human host, the interaction has not been well defined. This chapter aims to systematically characterise the inhibitory compound produced by *P. aeruginosa* and dissect the mechanism mediating this interaction. We will also begin investigating the clinical repercussions of *P. aeruginosa* secreted molecules on *R. microsporus*.

## 4.3 Results

**4.3.1 Bacterial quorum sensing molecules (QSMs) do not inhibit *R. microsporus* growth.** The major *P. aeruginosa* QSM, C12 HSL, inhibits *C. albicans* filamentation (Hogan, Vik and Kolter, 2004). This antagonism is not specific to C12 HSL, as dodecanol, a 12-carbon molecule that is structurally similar to C12 HSL (Figures 4.1A and 4.1B), can also inhibit *C. albicans* filamentation (Hogan, Vik and Kolter, 2004). Therefore, we first tested the ability of dodecanol to inhibit the germination of *R. microsporus*. Dodecanol (200  $\mu$ M) slightly delayed the germination of *R. microsporus* by 16.66% (+/- 0.57%) at 9 hours, but 97.39% (+/- 1.29%) of the spores germinated by 10 hours as compared to solvent control (Figure 4.1C).

As dodecanol is not a physiological QSM, we tested the ability of the major *P. aeruginosa* QSMs to inhibit *R. microsporus* growth. Exposure of *R. microsporus* spores to N-butanoyl-L-homoserine lactone (C4 HSL), N-hexanoyl-DL-homoserine lactone (C6 HSL), and N-octanoyl-L-homoserine lactone (C8 HSL), did not affect fungal growth (Figures 4.1D, 4.1E, and 4.1F). At high concentrations (200  $\mu$ M) C12 HSL resulted in 42.1% (+/- 0.1518%) reduction in growth (Figure 4.1G). Therefore, secreted bacterial QSMs appear to not be the major regulators of *R. microsporus* growth under these conditions.

**4.3.2 Pyocyanin does not impact *R. microsporus* growth.** Addition of purified pyocyanin resulted in 31.4% (+/- 0.1434) inhibition of *R. microsporus* growth at

concentrations above 100  $\mu\text{M}$  (Figure 4.1H). To deduce whether these pyocyanin concentrations were physiologically relevant, the concentration of pyocyanin in the *P. aeruginosa* supernatants was quantified through absorbance measurement (690 nm) and compared to a standard curve of pre-defined pyocyanin concentrations. Growth of *P. aeruginosa* in LB media at 200 rpm, 37°C did not result in the secretion of detectable levels of pyocyanin (performed by Callum Clark). Therefore, the inhibition of *R. microsporus* growth in the *P. aeruginosa* supernatant was not due to pyocyanin.

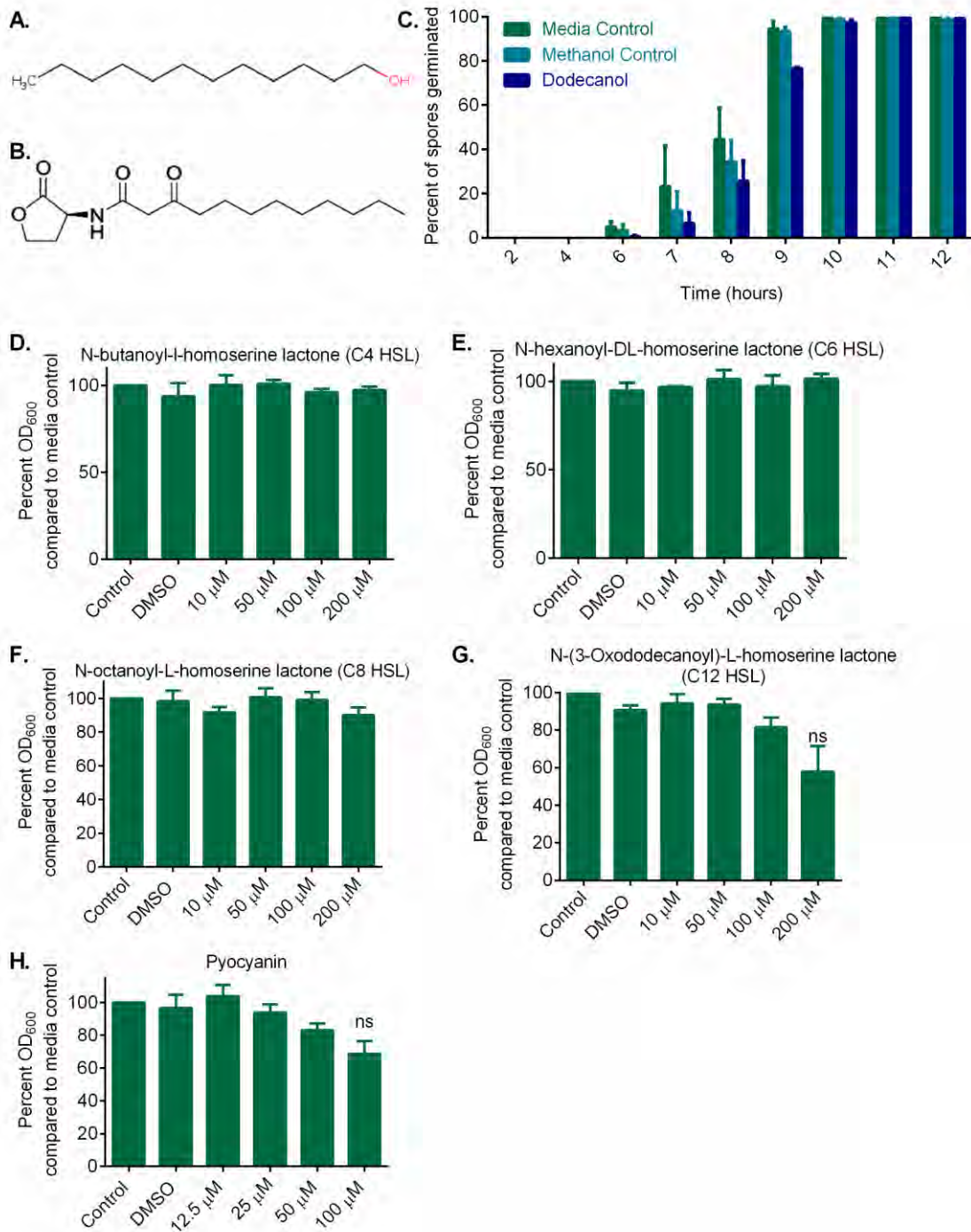


**Figure 4.1** Bacterial QSMs and pyocyanin do not inhibit *R. microsporus* growth.

The chemical structures of **(A)** dodecanol and **(B)** C12 HSL are shown to demonstrate their structural similarities. *R. microsporus* spores were exposed to 200 μM dodecanol and **(C)** the percent of spores germinated over time were calculated. *R. microsporus*

spores were incubated with increasing concentrations of **(D)** C4 HSL, **(E)** C6 HSL, **(F)** C8 HSL, **(G)** C12 HSL, and **(H)** pyocyanin. Fungal growth was quantified by absorbance ( $OD_{600}$ ) and normalised to media control (n=3). For percent germination, Two-way Repeated Measures ANOVA on arcsine-transformed data with Tukey's multiple comparisons test was used ( $\alpha = 0.05$ ). For all other data, Kruskal Wallis with Dunn's multiple comparisons test was used on non-normalised raw data ( $\alpha = 0.05$ ). Data represent mean and SEM.

**4.3.3 Inhibitory substance secreted by *P. aeruginosa* is a hydrophilic, heat-stable non-protein.** To determine whether the secreted factor responsible for inhibiting spore germination is proteinaceous, *P. aeruginosa* supernatants were boiled or treated with Proteinase K to degrade any secreted proteins. Supernatants that were boiled or treated with Proteinase K inhibited *R. microsporus* growth (by 97.62%, +/- 1.558,  $p = 0.0355$  and 99.03%, +/- 1.634,  $p = 0.0140$ , respectively) (Figure 4.2A), suggesting that a secreted heat-stable molecule mediates the observed inhibition of *R. microsporus* germination.

To determine whether the secreted factor is a lipophilic molecule, chloroform extractions were performed on *P. aeruginosa* supernatants to separate the hydrophilic and hydrophobic compounds. The organic phase of the supernatant did not significantly inhibit spore germination (18% inhibition, +/- 3.058), while the aqueous phase maintained its inhibitory action (95.1% inhibition, +/- 0.9559,  $p = 0.0079$ , Figure 4.2B). Therefore, a secreted, heat-stable, water-soluble molecule(s) inhibits the growth of *R. microsporus*.

**4.3.4 Inhibition of growth is not impacted by removal of *R. microsporus* endosymbiont.** The isolate of *R. microsporus* used in this study has been confirmed to contain the endosymbiont *Ralstonia pickettii* (Itabangi *et al.*, 2019, preprint). To determine whether the interaction between *P. aeruginosa* and *R. microsporus* was modulated by the endosymbiont, we used *R. microsporus* spores that had been treated with 60 µg/ml Ciprofloxacin to remove endosymbiont. Cured and parent spores were exposed to *P. aeruginosa* supernatant for 24 hours before measuring fungal growth. *P. aeruginosa* supernatant inhibited endosymbiont positive spores by 88.51% (+/- 7.69%) and negative spores by 87.95% (+/- 4.38%) (Figure 4.2C). As treated and un-treated spores were both inhibited by the presence of the supernatant, it is unlikely that the response was mediated by *R. pickettii*.

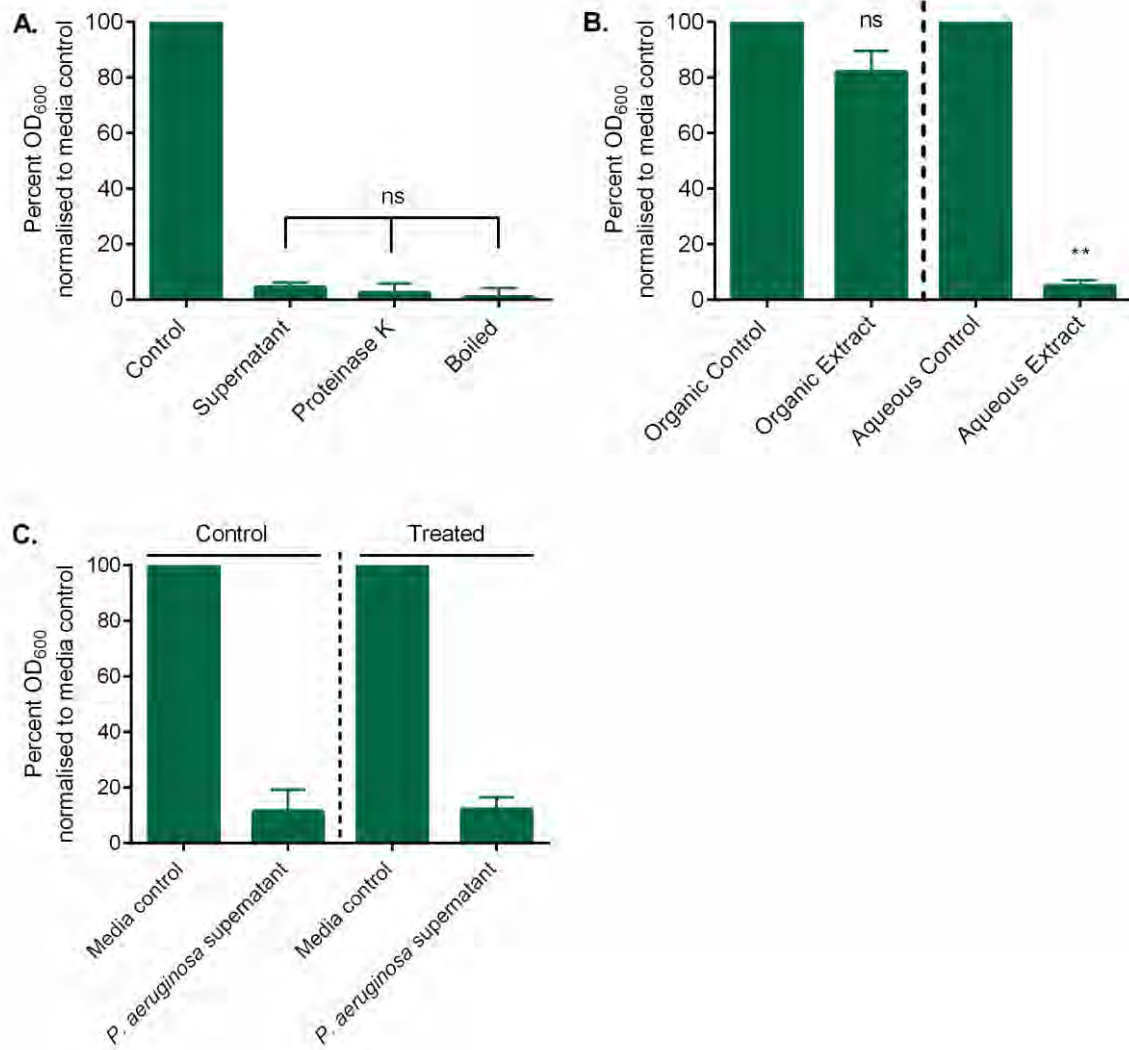


**Figure 4.2** Inhibitory compound secreted by *P. aeruginosa* is a hydrophilic, heat-stable non-protein and is not endosymbiont-mediated. **(A)** *P. aeruginosa* supernatant was treated with 150 µg/ml Proteinase K or boiled (100°C for 1 hour) to determine whether the inhibitory factor is a heat stable protein (n=6). **(B)** Chloroform extractions were performed to separate aqueous and organic molecules (n=5). **(C)** *R. microsporus* spores were treated with ciprofloxacin to remove the endosymbiont. Spores were exposed to 50% *P. aeruginosa* supernatant for 24 hours, fungal growth was quantified via absorbance (OD<sub>600</sub>) and normalised to media control (n=3). All data was

analysed by a Kruskal-Wallis test with Dunn's multiple comparisons test ( $\alpha = 0.05$ ). Data represent mean and SEM. \*\* =  $p < 0.01$ .

**4.3.5 Inhibition of fungal growth is not due to zinc, copper, or manganese restriction.** Metal micronutrients are essential for microbial growth and pathogenicity, and iron, zinc, copper, and manganese are the most important trace metals for the growth of fungi. While bacterial siderophores are primarily considered to be iron-binding molecules, they can also non-specifically sequester other important micronutrients, and in these cases could be considered metallophores (Braud, Hoegy, *et al.*, 2009). While these metals are essential for fungal growth, supplementation with zinc, copper or manganese did not rescue *R. microsporus* growth following exposure to *P. aeruginosa* supernatant (Figure 4.3). Therefore, the inhibition of fungal growth is via a different mechanism.

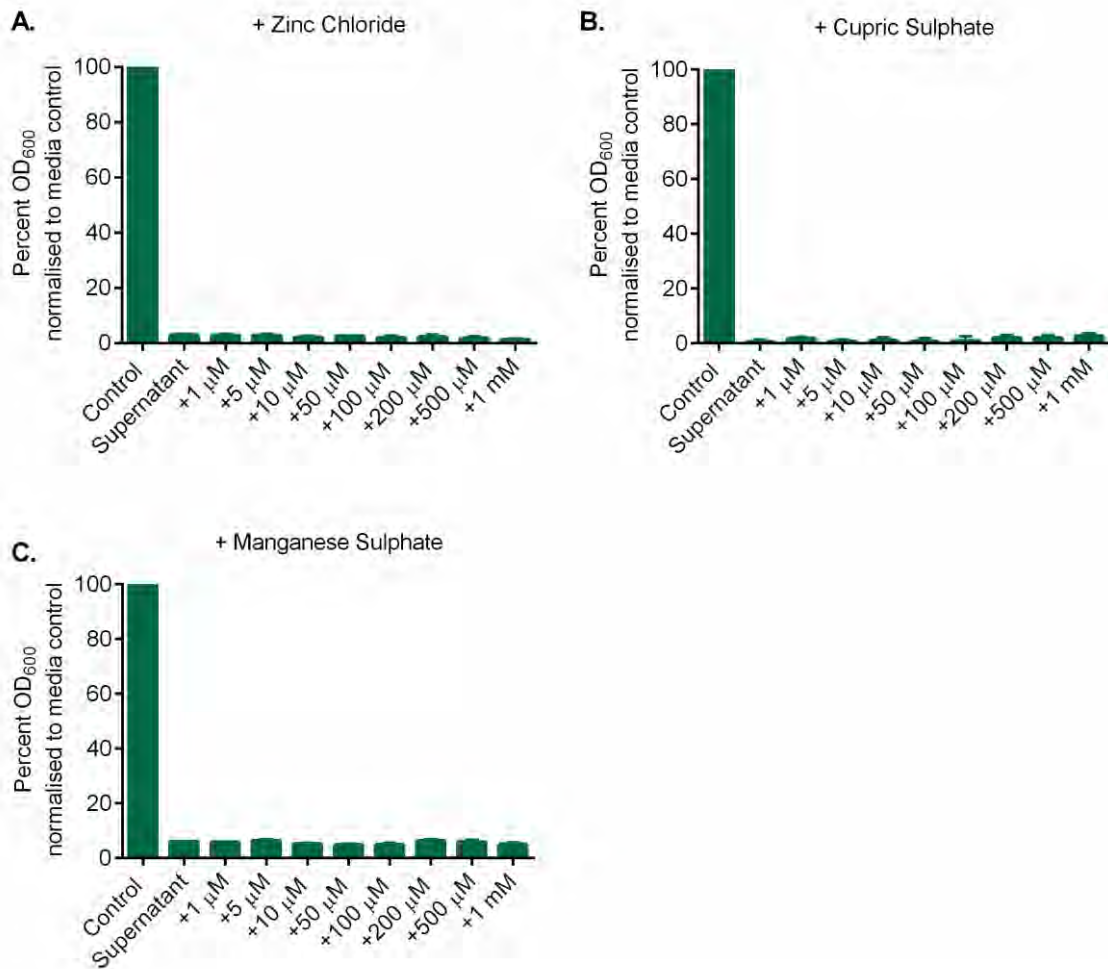


**Figure 4.3** Addition of zinc, copper, and manganese does not rescue *R. microsporus* growth when exposed to *P. aeruginosa* supernatant. *R. microsporus* spores were exposed to 50% *P. aeruginosa* supernatant and spiked with increasing concentrations of (A) zinc chloride, (B) cupric sulphate, and (C) manganese sulphate for 24 hours statically at 37°C. Fungal growth was measured through absorbance (OD<sub>600</sub>) and normalised to media control (n=3, Kruskal-Wallis with Dunn's multiple comparisons test,  $\alpha = 0.05$ ). Data represent mean and SEM.

**4.3.6 Addition of exogenous iron rescues *R. microsporus* growth and germination.** Mucorales are very sensitive to iron depletion, and deletion of their high affinity permease, *FTR1*, or co-injection with a chelator inhibits virulence *in vivo* (Ibrahim *et al.*, 2007, 2010). Supplementing *P. aeruginosa* supernatants with iron was able to partially restore fungal growth, resulting in 46.2% *R. microsporus* growth at concentrations above 200  $\mu\text{M}$  (+/- 6.660, Fig. 4.4A and C) and an insignificant difference as compared to the control.

To confirm that the inhibition of spore germination observed in the co-cultures was also attributed to iron restriction, co-cultures of *R. microsporus* and *P. aeruginosa* were spiked with iron. Germination of *R. microsporus* was recovered at concentrations above 100  $\mu\text{M}$  (41.9% +/- 12.46) (Figure 4.4B), confirming that in both scenarios, iron sequestration appears to be the major contributing factor in the inhibition of *R. microsporus* growth.

Iron starvation has been shown to induce apoptosis in *R. oryzae* after prolonged deprivation (Shirazi, Kontoyiannis and Ibrahim, 2015). Therefore, if spores are undergoing iron starvation when exposed to *P. aeruginosa* supernatant, prolonged exposure should decrease survival. To isolate the effects of the supernatant, we used 100% *P. aeruginosa* supernatant to monitor spore survival over time. In this condition, the viability of spores was reduced by 82.40% (+/- 13.44) after 24 hours, and no viable spores were recovered after 120 hours ( $p =$

0.0490, Figure 4.4D). This indicates that iron starvation induced by *P. aeruginosa* supernatant can have a strong impact on the survival of *R. microsporus*.

While the addition of iron increased the growth of *R. microsporus*, the rescue is not complete. To understand whether spore death during co-culture could account for the remaining un-germinated spores, *R. microsporus* was exposed to live *P. aeruginosa* with and without 100  $\mu\text{M}$   $\text{FeCl}_3$  for 24 hours before colony forming units (CFUs) were plated and counted (Figure 4.4E). The presence of *P. aeruginosa* decreased spore viability by 61.5% ( $p = 0.0581$ ). When iron was added to co-cultures, 56.37% ( $p = 0.1478$ ) of spores survived, compared to 0-hour control. While addition of iron increased viability by 17.87% compared to *P. aeruginosa* alone, there were still 43.63% of spores that were killed, despite iron treatment. Because of this, we believe that much of the remaining inhibition of germination following addition of  $\text{FeCl}_3$  in live co-cultures (Figure 4.3B) is likely due to bacteria-induced spore death independent of iron.

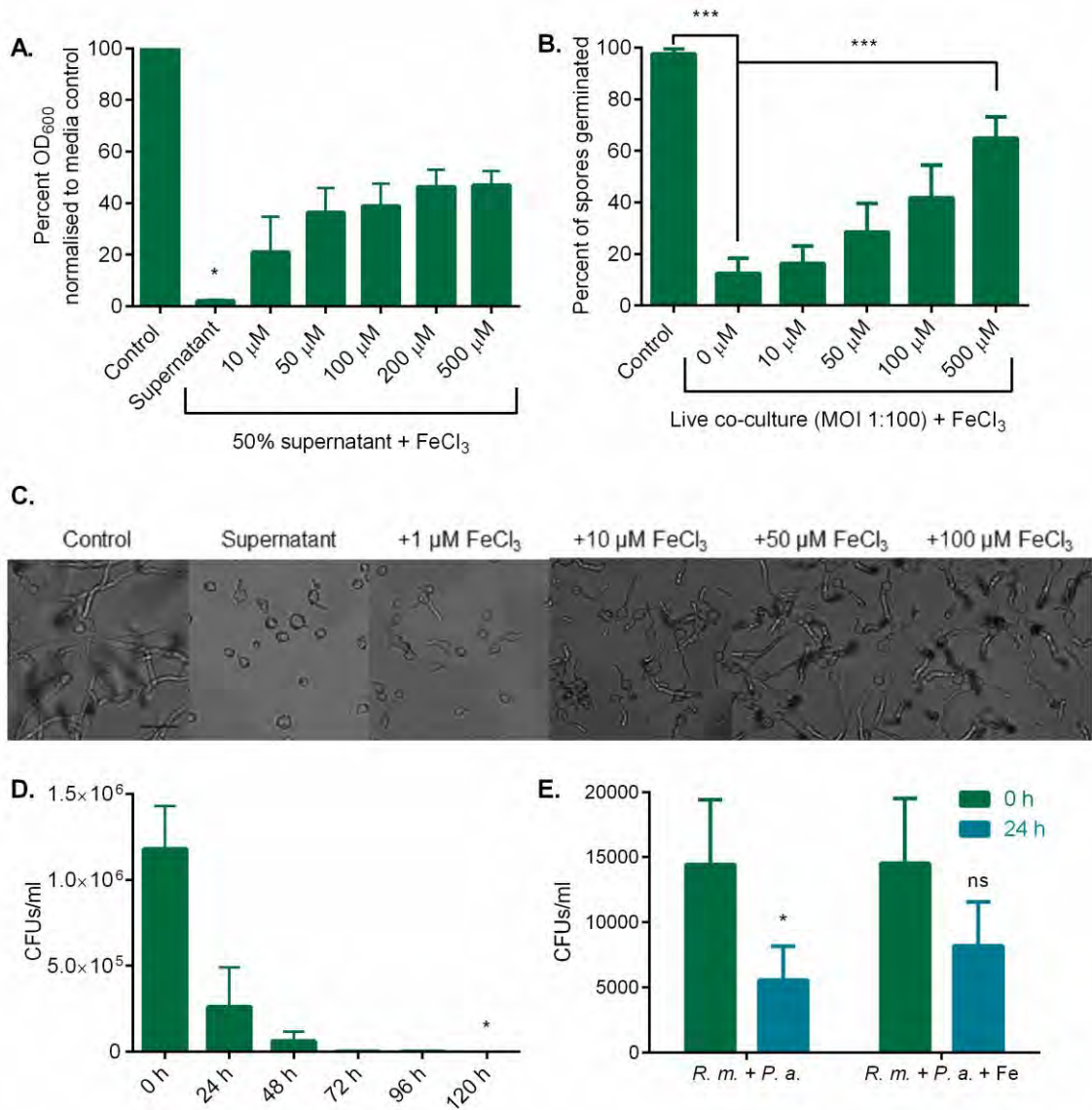


**Figure 4.4 Growth of *R. microsporus* spores exposed to *P. aeruginosa* is rescued by addition of exogenous iron.** *R. microsporus* spores were exposed to 50% *P. aeruginosa* supernatant and **(A)** spiked with increasing concentrations of ferric chloride for 24 hours. Fungal growth was measured through absorbance (OD<sub>600</sub>) and normalised to media control (n=3). **(B)** The ability of iron to rescue *R. microsporus* germination was confirmed in a live co-culture setting, where the addition of exogenous iron increased the percent of spores germinated after 24 hours in a dose-dependent manner. This was quantified by Callum Clark (n=8). As the addition of iron in 50% supernatant increased

overall growth, **(C)** representative images were collected at 9 hours to confirm ability to rescue germination. Scale bar depicts 50  $\mu\text{m}$ . **(D)** Spore viability in response to 100% *P. aeruginosa* supernatant over time was quantified by counting colony forming units (CFUs) every 24 hours for 120 hours (n=3). **(E)** To understand whether co-cultures decreased fungal viability, *R. microsporus* was exposed to live *P. aeruginosa* +/- 100  $\mu\text{M}$   $\text{FeCl}_3$  for 24 hours and colony forming units were counted. All data was analysed by a Kruskal-Wallis test with Dunn's multiple comparisons test on raw data. Data represent mean and SEM ( $\alpha = 0.05$ ). \* =  $p < 0.05$ , \*\*\* =  $p < 0.001$ .

**4.3.7 The presence of *P. aeruginosa* supernatant induces an iron-starvation response in *R. microsporus*.** Iron starvation has previously been shown to up-regulate the high affinity iron permease, *FTR1*, in *Rhizopus oryzae* (Shirazi, Kontoyiannis and Ibrahim, 2015). Therefore, to confirm that *R. microsporus* is undergoing iron starvation in the presence of *P. aeruginosa* supernatants, the expression levels of *FTR1* were determined by qRT-PCR. *FTR1* was highly upregulated (10-fold increase,  $p = 0.0286$ ) when exposed to 50% *P. aeruginosa* supernatant for 7 hours, as compared to the control (Fig. 4.5C). This further validates that *R. microsporus* is experiencing iron restriction mediated by *P. aeruginosa* supernatant.

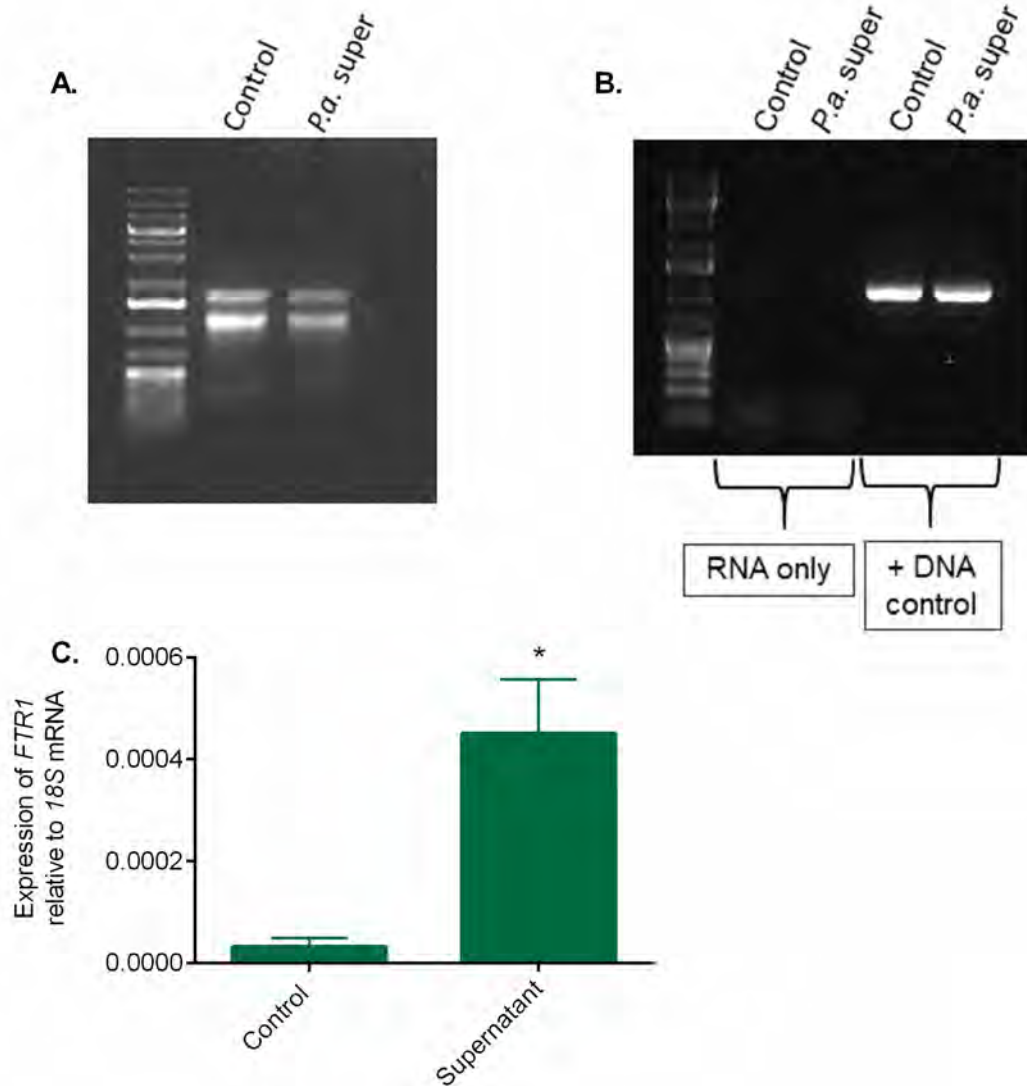


**Figure 4.5** The presence of *P. aeruginosa* supernatant induces an iron-starvation response in *R. microsporus*. *R. microsporus* was exposed to 50% *P. aeruginosa* supernatant for 7 hours. Following this, fungal RNA was extracted, quality was confirmed via **(A)** gel electrophoresis, and removal of genomic DNA was confirmed via **(B)** PCR and gel electrophoresis. **(C)** The expression of the high-affinity iron permease *FTR1* was quantified by qRT-PCR relative to 18S mRNA (n=4, Mann-Whitney U test). Data represent mean and SEM ( $\alpha = 0.05$ ). \* =  $p < 0.05$ .

**4.3.8 Iron-dependent inhibition of Mucorales by *P. aeruginosa* is not *R. microsporus* species-specific.** To delineate whether bacteria-associated iron restriction inhibits the growth of closely related Mucorales, we tested the ability of *P. aeruginosa* supernatant to inhibit the growth of *R. microsporus* var. *microsporus*, *R. microsporus* var. *chinensis*, *R. delemar*, and *M. circinelloides* (Figure 4.6). The growth of all isolates was significantly reduced in the presence of *P. aeruginosa* supernatant [83.85% (+/- 15.23), 98.26% (+/- 1.977), 99.01% (+/- 0.8695), and 84.29% (+/- 10.78), respectively], and was significantly rescued by the addition of 100  $\mu$ M of iron [64.36% (+/- 4.450), 41.30% (+/- 10.48), 55.14% (+/- 10.01), and 87.54% (+/- 6.219), respectively]. This confirms that the bacteria-associated inhibition of growth is not an artefact of our *R. microsporus* clinical isolate but is instead a general trait of closely-related Mucorales.

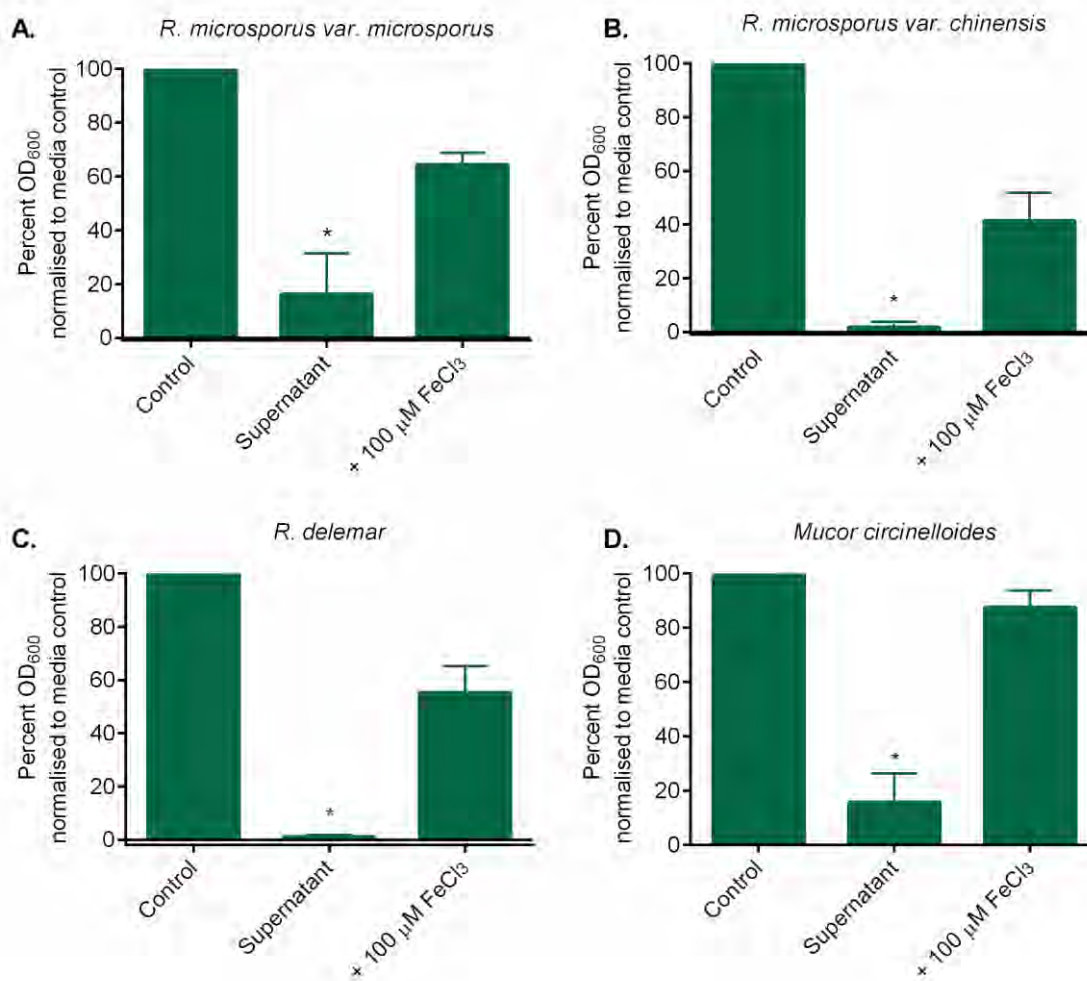


**Figure 4.6 Iron-dependent inhibition of Mucorales by *P. aeruginosa* is not *R. microsporus* species-specific.** Most experiments in this chapter were performed using an *R. microsporus* clinical isolate. To ensure the inhibitory effect of *P. aeruginosa* is not limited to this isolate, (A) *R. microsporus var. microsporus*, (B) *R. microsporus var. chinensis*, (C) *R. delemar*, and (D) *Mucor circinelloides* were exposed to 50% *P. aeruginosa* supernatant with and without the addition of 100 µM FeCl<sub>3</sub>. Fungal growth was determined at 24 hours by measuring absorbance (OD<sub>600</sub>) and normalising to control (n=3). All data was analysed by a Kruskal-Wallis test with Dunn's multiple comparisons test ( $\alpha = 0.05$ ). Data represent mean and SEM. \* = p < 0.05 (Kousser *et al.*, 2019).

**4.3.9 Siderophore-deficient *P. aeruginosa* strains lack the ability to suppress germination.** Pyoverdine and pyochelin are the two predominate siderophores produced by *P. aeruginosa*, with pyoverdine exhibiting the highest affinity for iron and being essential for virulence (Meyer *et al.*, 1996; Braud, Hannauer, *et al.*, 2009; Braud, Hoegy, *et al.*, 2009). To identify the role of these siderophores in this interaction, fungal growth was quantified in the presence of the supernatants from *P. aeruginosa* strains deficient in either siderophore alone or in combination. Growth of *R. microsporus* was inhibited when incubated with culture supernatants from *P. aeruginosa* strains defective in pyochelin biosynthesis ( $\Delta pchEF$ ), with growth being rescued by exogenous iron (Figure 4.7A), suggesting that this siderophore plays a minor role in sequestering iron in these experiments. However, *R. microsporus* germinated in the presence of bacterial supernatants from *P. aeruginosa* mutants defective in pyoverdine biosynthesis ( $\Delta pvdD$ ) or in pyoverdine and pyochelin biosynthesis ( $\Delta pchEF\Delta pvdD$ ) (Figure 4.7A), confirming that, under the tested conditions, *P. aeruginosa*-imposed iron restriction is largely mediated by the secretion of pyoverdine.

**4.3.10 Pyoverdine is sufficient to inhibit *R. microsporus* growth.** To confirm that pyoverdine alone can inhibit *R. microsporus* growth, spores were exposed to exogenous pyoverdine. To ensure a relevant concentration of pyoverdine was added, we measured the siderophores present in *P. aeruginosa* supernatant. These supernatants (100%) contained 58.9  $\mu\text{g/ml}$  ( $\pm 1.194$ ) siderophores, making the concentration of siderophores in this assay 29.45  $\mu\text{g/ml}$ , as 50%

supernatant was typically used. Therefore, *R. microsporus* spores were grown in the presence of 15  $\mu\text{M}$  (17.4  $\mu\text{g/ml}$ ) and 30  $\mu\text{M}$  (34.8  $\mu\text{g/ml}$ ) purified pyoverdine to resemble siderophore concentrations in the supernatants. Incubation of fungal spores with pyoverdine significantly reduced growth (73.8%,  $\pm$  5.503,  $p = 0.0022$ , Figure 4.7B). Therefore, pyoverdine alone is adequate to inhibit *R. microsporus* growth and germination.

Previously, we found that the germination of *C. bertholletiae* was promoted in the presence of *P. aeruginosa* supernatant, likely due to pH and nutrient changes. To determine whether *C. bertholletiae* was sensitive to the presence of pyoverdine, we exposed *C. bertholletiae* to 30  $\mu\text{M}$  (34.8  $\mu\text{g/ml}$ ) and 60  $\mu\text{M}$  (69.6  $\mu\text{g/ml}$ ) of exogenous pyoverdine and compared representative images to *R. microsporus* (Figure 4.7C). The addition of pyoverdine to *C. bertholletiae* did not impact germination or growth after 6 hours, while *R. microsporus* was strongly inhibited. This indicates that either *C. bertholletiae* is less dependent on iron than *Rhizopus spp.*, can use pyoverdine as a xenosiderophore, or that *C. bertholletiae* is more effective at acquiring iron.

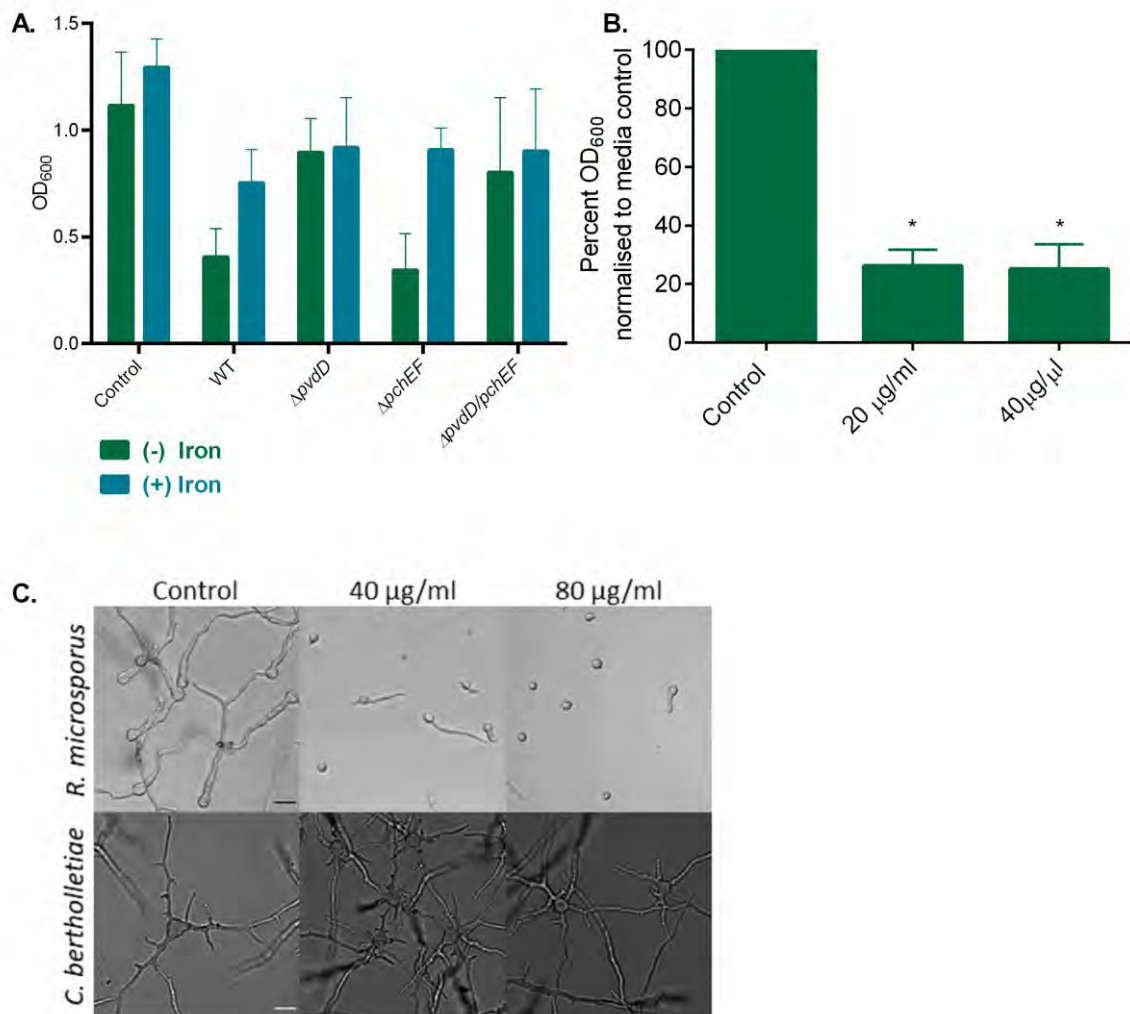


**Figure 4.7** *P. aeruginosa*-imposed iron restriction is largely mediated via pyoverdine. **(A)** *R. microsporus* was grown in supernatants from wild type *P. aeruginosa*, strains defective in siderophore biosynthesis, or control media +/- iron. Fungal growth was determined via absorbance ( $OD_{600}$ ) after 24 hours ( $n = 3$ ). This was performed by Sarah Sherrington. **(B)** *R. microsporus* spores were incubated in SAB with 20  $\mu\text{g/ml}$  and 40  $\mu\text{g/ml}$  pyoverdine. Fungal growth was measured through absorbance ( $OD_{600}$ ) and normalised to media control ( $n = 6$ ). The effect of pyoverdine on *R. microsporus* germination was compared to *C. bertholletiae*. Spores were exposed to 40 and 80  $\mu\text{g/ml}$  pyoverdine and **(C)** representative images are shown after 6 hours. Scale

bar = 25  $\mu\text{m}$ . Data was analysed by a Kruskal-Wallis test with Dunn's multiple comparisons test ( $\alpha = 0.05$ ). Data represent mean and SEM. \* =  $p < 0.05$ .

**4.3.11 The presence of *R. microsporus* induces iron stress in *P. aeruginosa* and promotes bacterial siderophore production.** The presence of fungi has been shown to modulate the expression of bacterial virulence factors (Lopez-Medina *et al.*, 2015). To determine whether *R. microsporus* can interfere with *P. aeruginosa* siderophore production, the concentration of siderophores after 24 hours mono- and co-culture was quantified using a SideroTec Assay kit (Figure 4.8A). Surprisingly, the concentration of siderophores in mono-cultures in SAB/LB was 11-fold lower than in LB (4.99  $\mu\text{g/ml}$ ,  $\pm$  5.834, vs 58.9  $\mu\text{g/ml}$  ( $\pm$  1.194)) suggesting that growth in SAB/LB reduces siderophore production. However, in co-cultures, siderophore concentration was increased 10-fold, to levels similar to LB supernatant (53.25  $\mu\text{g/ml}$ , ( $\pm$  0.4335) compared to 58.9  $\mu\text{g/ml}$  ( $\pm$  1.194)) indicative of iron stress. This increase in siderophore concentration was not observed in co-cultures containing siderophore deficient *P. aeruginosa* (Fig 4.8B), confirming that the increase in siderophore concentration is likely due to increased bacterial rather than fungal siderophore biosynthesis.

Pyoverdine is a fluorescent molecule with an excitation at 405 nm (Meyer and Abdallah, 1978; Cox and Adams, 1985). Calculating absorbance at this wavelength has been used to measure pyoverdine in a solution (Dao *et al.*, 1990;

Visca *et al.*, 1992). As the SideroTec kit (Figure 4.8A and 4.8B) measures total iron binding compounds within a solution, we wanted to determine whether pyoverdine specifically was increased in the presence of *R. microsporus*. Therefore, we measured the absorbance (OD<sub>405</sub>) of supernatants after 24 hours mono- and co-culture at MOIs 1:50 and 1:100 *R. microsporus*:*P. aeruginosa* (Figure 4.8C). Co-incubation with *R. microsporus* increased the absorbance by approximately 1.7-fold as compared to bacteria only. This suggests that *P. aeruginosa* responds to the presence of *R. microsporus* by enhancing the secretion of pyoverdine.

To further confirm that the presence of *R. microsporus* increases the production of bacterial siderophores, we measured the expression of key genes involved in pyoverdine and pyochelin biosynthesis (Figure 4.8F). Following exposure to *R. microsporus* for 7 hours, *P. aeruginosa* upregulated the expression of *pvdS* and *pchA*. However, this regulation was lost in the presence of exogenous iron (Figure 4.8F). These results confirm that during co-culture, the two organisms compete for iron, resulting in the upregulation of bacterial siderophore biosynthesis and *P. aeruginosa* outcompeting *R. microsporus* for iron and inhibiting fungal growth.

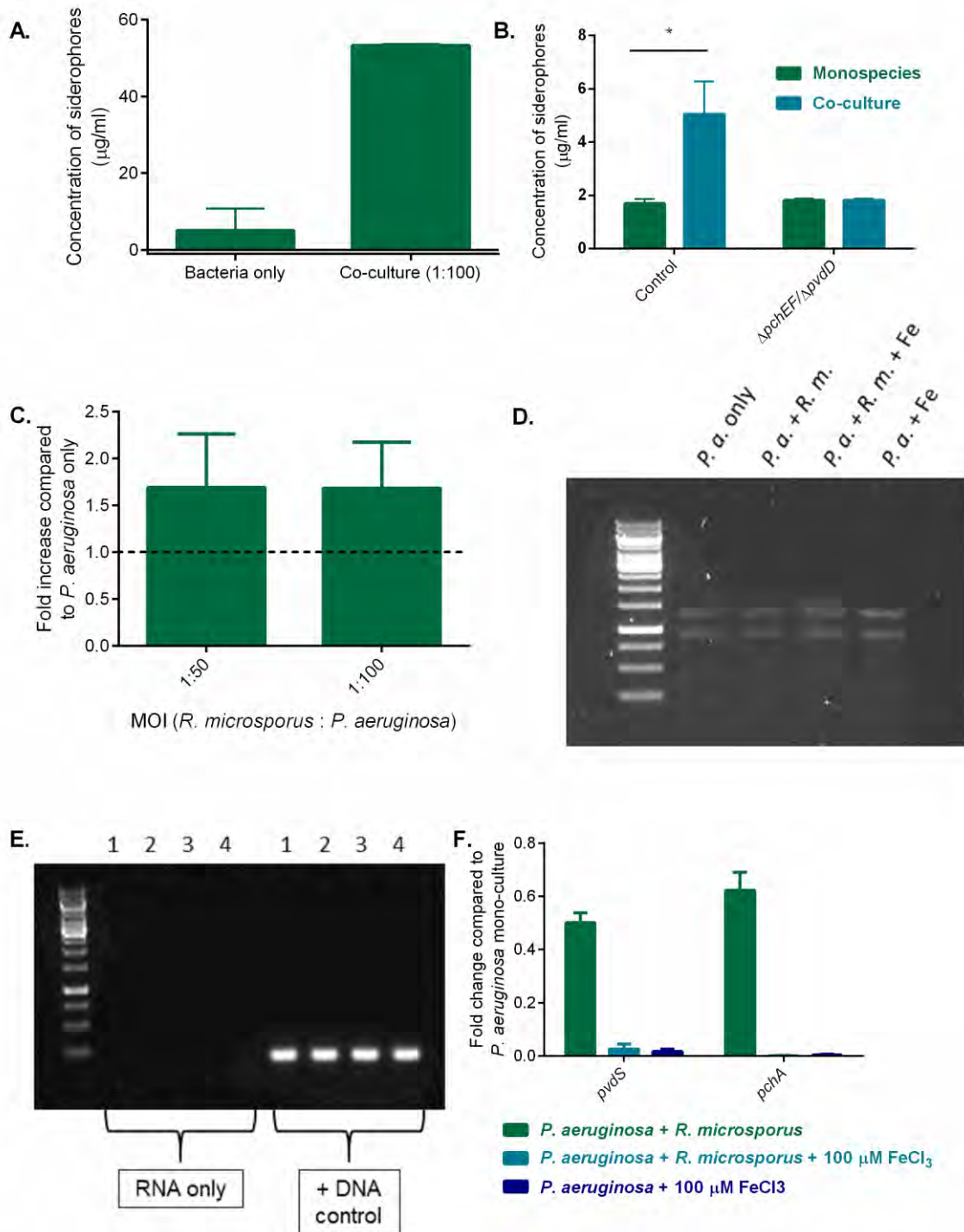


**Figure 4.8** The presence of *R. microsporus* induces iron stress in *P. aeruginosa* and promotes bacterial siderophore production. **(A)** Siderophore production following mono- and co-culture was measured by using the Siderotec Assay (EmerginBio) (n = 3, Mann-Whitney U test). This was performed by Callum Clark. **(B)**

Siderophore production of *P. aeruginosa* strains defective in siderophore biosynthesis was measured by using the Siderotec Assay (EmerginBio) following mono- and co-culture (n = 3, Mann-Whitney U test, ( $\alpha = 0.05$ ). This was performed by Callum Clark. **(C)** Fold increase of co-culture supernatant absorbance (OD<sub>405</sub>) compared to *P. aeruginosa* mono-culture supernatant absorbance is presented (n=4). Following co-culture, *P. aeruginosa* RNA was extracted, and quality was confirmed through **(D)** gel electrophoresis (*P. a.* = *P. aeruginosa*, *R. m.* = *R. microsporus*, and Fe = iron). Removal of genomic DNA was confirmed through **(E)** PCR and gel electrophoresis (1 = *P. aeruginosa* only, 2 = *R. microsporus* + *P. aeruginosa*, 3 = *R. microsporus* + *P. aeruginosa* + Fe, and 4 = *P. aeruginosa* + Fe). **(F)** The expression levels of PvdS and PchA were quantified by qRT-PCR relative to RpoD and normalised to *P. a.* grown in isolation. Data represent mean and SEM. \* =  $p < 0.05$ .

**4.3.12 The concentration of siderophores produced by bacteria correlates with inhibition of *R. microsporus* growth.** *P. aeruginosa* inhibits *R. microsporus* growth through siderophore-mediated iron sequestration. However, *E. coli*, *B. cenocepacia*, and *S. aureus* did not inhibit *R. microsporus* in live co-culture (Figure 3.16). This was surprising as these bacteria all produce siderophores (O'Brien, I, Cox and Gibson, 1970; Courcol *et al.*, 1991; Darling *et al.*, 1998). To investigate whether these bacteria can inhibit *R. microsporus* through secreted factors, spores were exposed to *E. coli*, *B. cenocepacia*, *K. pneumoniae*, and *S. aureus* sterile supernatants to determine their ability to inhibit *R. microsporus* growth as compared to *P. aeruginosa*. *P. aeruginosa* was the only supernatant able to significantly inhibit growth (Figure 4.9A). We then measured the amount of siderophores produced after 24 hours growth in LB, to

determine whether this lack of inhibition was associated with insufficient production of iron binding molecules. There was a negative correlation between fungal growth and siderophore production across different bacterial species ( $p = 0.0029$ , Figure 4.9B), suggesting that siderophore-mediated iron restriction may be a common mechanism of bacteria to compete with *R. microsporus*. However, the presence of supernatants from *E. coli* had no effect on fungal growth. This was unexpected, as *E. coli* produces enterobactin, a siderophore with a high affinity ( $10^{52} \text{ M}^{-1}$ ) for iron (Carrano and Raymond, 1979). In agreement with this, exogenous enterobactin did not inhibit *R. microsporus* growth (91%,  $\pm 6.170$ , Figure 4.9C), suggesting that *R. microsporus* is resistant to enterobactin-mediated iron sequestration.

Exogenous enterobactin was added to *R. microsporus/P. aeruginosa* co-cultures to determine if this would provide an advantage to the fungus. However, the presence of enterobactin exacerbated the inhibition of fungal growth (Figure 4.9D), presumably because *P. aeruginosa* can also utilise enterobactin as a xenosiderophore (Meyer and Abdallah, 1978). Because of this, we instead added enterobactin to sterile bacterial supernatants. *R. microsporus* displayed increased germination in *P. aeruginosa* supernatants supplemented with enterobactin, although fungal growth was not fully restored (Figure 4.9E), likely due to pyoverdine and pyochelin binding the majority of the free iron. Taken together, this indicates that *R. microsporus* may use enterobactin as a xenosiderophore, though further investigation is needed to confirm this hypothesis.

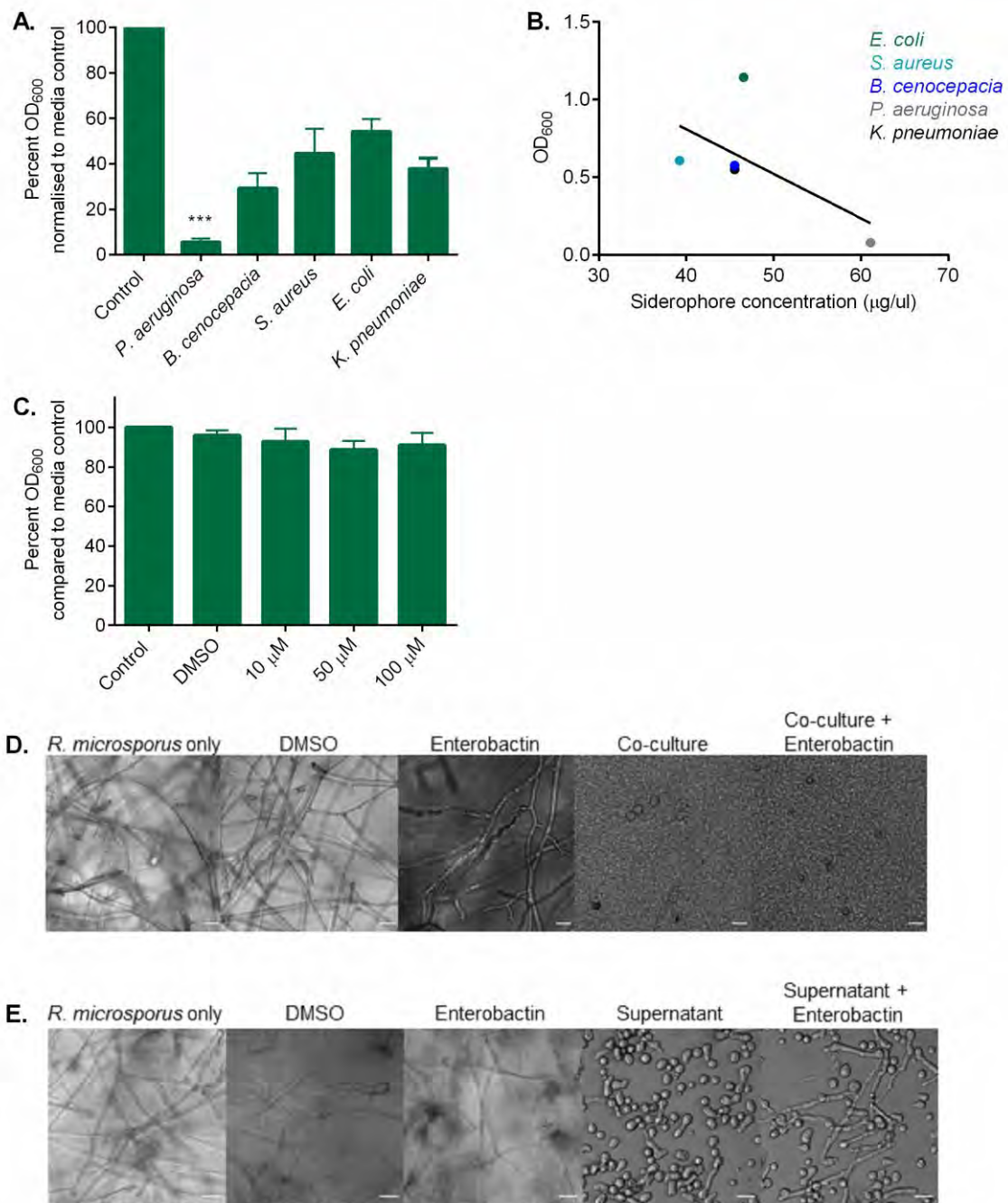


**Figure 4.9** Enterobactin does not inhibit *R. microsporus* growth and can enhance germination during exposure to *P. aeruginosa* supernatant. **(A)** Fungal growth following exposure to *P. aeruginosa*, *B. cenocepacia*, *S. aureus*, and *E. coli* supernatants was determined by absorbance (OD<sub>600</sub>) and normalised to control. (n=6). **(B)** The concentration of siderophores produced by bacteria was determined by using the

Siderotec Assay (EmerginBio) and the correlation between total siderophore production and fungal growth was determined by performing a linear regression with Pearson correlation (n=3). **(C)** *R. microsporus* spores were exposed to varying concentrations of purified enterobactin (n=3). Fungal growth was determined by absorbance (OD<sub>600</sub>) and normalised to control. **(D)** Enterobactin (50 µM) was added to co-cultures of *R. microsporus* and *P. aeruginosa* (MOI 1:100). **(E)** Enterobactin was added to 50:50 SAB:supernatant and incubated with *R. microsporus* spores. All data was analysed by a Kruskal-Wallis test with Dunn's multiple comparisons test unless indicated otherwise ( $\alpha = 0.05$ ). Scale bars = 20 µm. Data represent mean and SEM. \*\*\* =  $p < 0.001$  (Kousser *et al.*, 2019).

**4.3.13 The presence of *P. aeruginosa* supernatant impacts the antifungal susceptibility of *R. microsporus*.** To test the impact of polymicrobial interactions on antifungal resistance we used media with a higher iron concentration to prepare *P. aeruginosa* supernatants, to overcome iron-dependent restriction and enable the quantification of fungal growth.

*R. microsporus* spores were exposed to 50% *P. aeruginosa* supernatant with varying concentrations of fluconazole, posaconazole, and amphotericin B for 24 hours, 37 °C. Fungal growth was determined by measuring absorbance (OD<sub>600</sub>). Resistance to fluconazole was not impacted by the presence of *P. aeruginosa* supernatant (Figure 4.10A). Our isolate of *R. microsporus* is resistant to posaconazole and growth of control spores was not impacted by the presence of this antifungal (Figure 4.10B). However, the addition of 50% supernatant

increased susceptibility to posaconazole and fungal growth was decreased with the addition of 0.25 µg/ml posaconazole ( $p < 0.0001$ , Figure 4.10B). This effect was even more striking with amphotericin B. While growth of control spores was inhibited with 0.5 µg/ml amphotericin B, upon the addition of the supernatant, fungal growth was completely inhibited with only 0.0155 µg/ml amphotericin B ( $p < 0.0001$  Figure 4.10C). Therefore, exposure to *P. aeruginosa* supernatant enhances antifungal efficacy independent of iron restriction.

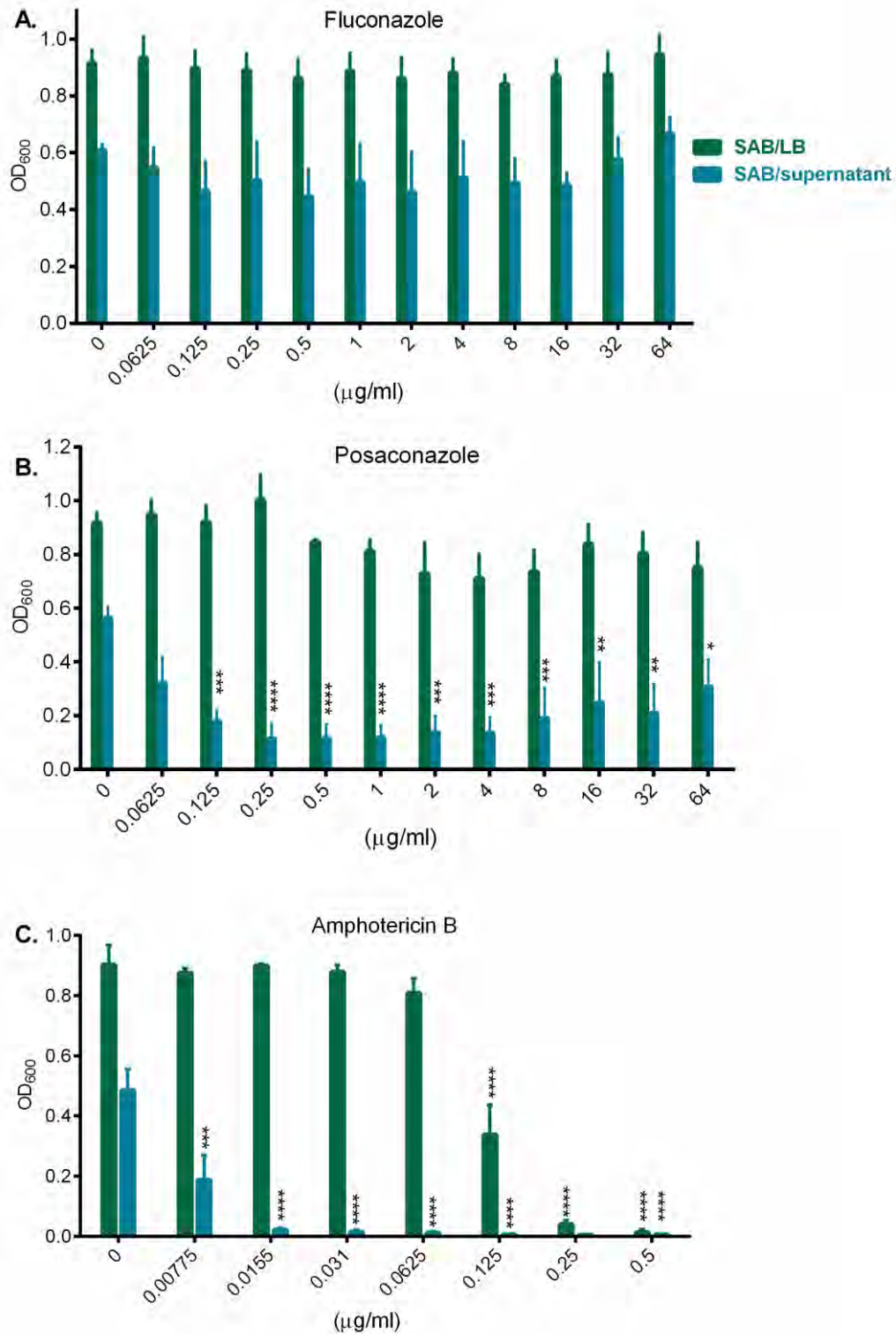


Figure 4.10 Release of iron stress identifies a potential role of bacterial supernatants in regulating antifungal resistance. *R. microsporius* spores were

exposed to 50% *P. aeruginosa* supernatants and various concentrations of **(A)** fluconazole, **(B)** posaconazole, and **(C)** amphotericin B for 24 hours, 37 °C. Fungal growth was measured through absorbance (OD<sub>600</sub>) Data was analysed using a 2-way ANOVA with Sidak's multiple comparisons test ( $\alpha = 0.05$ ), comparing each concentration to 0 µg/ml (n=3). \* =  $p < 0.05$ , \*\* =  $p < 0.01$ , \*\*\* =  $p < 0.001$ , \*\*\*\* =  $p < 0.0001$ .

## 4.4 Discussion.

Following the initial observation that *P. aeruginosa* supernatant strongly inhibited the germination and growth of *R. microsporus*, this chapter aimed to increase overall understanding of this interaction. The goals were to characterise the inhibitory molecule produced by *P. aeruginosa*, identify the major mediators in this interaction, define the mechanism by which they inhibit fungal growth, and begin understanding the impact this relationship could have on clinical outcome.

**4.4.1 Inter-kingdom iron competition.** As iron availability is known to be a key limiting factor in *Rhizopus* virulence (Ibrahim *et al.*, 2010), and *P. aeruginosa* secretes high affinity siderophores that are hydrophilic small molecules, we hypothesised that supernatant-induced iron depletion in the media is the inhibitory source. Addition of exogenous iron confirmed this theory as it enhanced fungal germination and overall growth in co-cultures and 50% supernatant. While the rescue is not complete, in co-cultures we believe the remaining inhibition is due to decreased fungal viability, and this is being investigated by other members of the group. For the remaining inhibition of supernatant-exposed spores, it is

possible that other aqueous pigments, such as pyorubrin and/or pyomelanin are also present and affecting fungal growth. While there is no evidence found in the literature that shows these pigments mediate polymicrobial interactions, both molecules modulate redox homeostasis (Hunter and Newman, 2010; Hosseinidoust, Tufenkji and van de Ven, 2013).

*P. aeruginosa* secretes several iron binding molecules, with pyoverdine being the major siderophore with a high affinity for iron. We found that exogenous pyoverdine, at concentrations comparable to those secreted by *P. aeruginosa* in our culture conditions, was sufficient to inhibit the growth of *R. microsporus*. This was comparable to levels seen after exposure to the bacterial supernatant. In addition, supernatants from *P. aeruginosa* mutants unable to synthesise the major siderophores were less potent, confirming a role for pyoverdine and pyochelin in controlling fungal growth. This iron-dependent inhibition of growth is also seen between *P. aeruginosa* and *A. fumigatus* and *P. aeruginosa* and *C. albicans*. For instance, *P. aeruginosa* decreases biofilm production of *A. fumigatus* through the production of pyoverdine (Sass *et al.*, 2018). Furthermore, the *P. aeruginosa* Pf4 bacteriophage inhibits *C. albicans* and *A. fumigatus* via iron-mediated mechanisms (Penner *et al.*, 2016; Nazik *et al.*, 2017). Taken together, this indicates that *P. aeruginosa* utilises iron restriction as a general mechanism for competing with fungi.

The presence of fungi has been shown to modulate the expression of siderophore biosynthetic genes in *P. aeruginosa*. For instance, *C. albicans* was described as down-regulating the production of pyoverdine and pyochelin through secreted proteins (Lopez-Medina *et al.*, 2015). Conversely, our study has found the production of pyoverdine to be increased in response to *P. aeruginosa* co-cultured with *R. microsporus*. This is consistent with a previous study that found a decrease in *C. albicans* metabolism was linked to the enhanced production of pyoverdine in mixed species biofilms (Purschke *et al.*, 2012). This highlights the dynamic response of *P. aeruginosa* to fungi, which is likely dependent on the individual microenvironment. The fact that the presence of *R. microsporus* enhances the production of siderophores in our system makes the interaction between the two organisms more dangerous for an infected host. Pyoverdine mediates the production of other virulence factors, such as exotoxin A and endoproteases, and increased pyoverdine can enhance overall bacterial virulence (Lamont *et al.*, 2002). Furthermore, if this interaction occurs in a burn wound environment, the siderophore production will be even more increased, as *P. aeruginosa* upregulates the biosynthesis of pyoverdine when exposed to burn wound exudate (Gonzalez *et al.*, 2016).

**4.4.2 Enterobactin protects *R. microsporus* from *P. aeruginosa* supernatant-induced growth inhibition.** Despite having an affinity for iron higher than pyoverdine, the presence of live *E. coli*, sterile supernatant, and exogenous enterobactin did not significantly impact fungal growth. From this work, it is hypothesised that *R. microsporus* may be able to utilise enterobactin

as a xenosiderophore, though further investigation is needed to confirm. Mucorales are known to utilise certain bacterial siderophores as sources of iron within the host, such as deferoxamine to promote its growth and virulence (Boelaert *et al.*, 1993). Unlike deferoxamine, and potentially enterobactin, *R. microsporus* cannot scavenge iron from pyoverdine, which suggests that molecules with similar structures may have the potential to be used to control mucormycosis. While utilising pyoverdine itself would be problematic due to its ability to enhance *P. aeruginosa* virulence (Lamont *et al.*, 2002), this siderophore could provide a starting point for the development of novel iron chelators. Given that pyoverdine has also been shown to limit the growth of other invasive fungi, such as *A. fumigatus* (Penner *et al.*, 2016; Sass *et al.*, 2018), molecules based on pyoverdine may have wide implications for the treatment of a range of invasive fungal diseases. For further speculation regarding enterobactin as a potential xenosiderophore, please see Chapter 6.

**4.4.3 Bacterial-induced susceptibility to antifungals.** Preliminary results from this study found that the presence of *P. aeruginosa* supernatant increases fungal susceptibility to both amphotericin B and posaconazole. This is opposite to findings in the literature during mixed species biofilms with *C. albicans* and *Staphylococcus epidermidis*, where bacteria produce extracellular polymers that block fluconazole penetration of the biofilm and enhance antifungal resistance (Adam, Baillie and Douglas, 2002). Treatment with liposomal or deoxycholate amphotericin B can be toxic and lead to harmful side effects, such as renal failure (Falci, Da Rosa and Pasqualotto, 2015). Therefore, the ability of *P. aeruginosa*

secreted factors to increase the susceptibility to amphotericin B has important clinical implications. Ideally, isolating and synthesising the sensitising compound could provide a novel adjunct therapy alongside antifungals and increase treatment efficacy. Further studies should determine if mean fungicidal concentration of these drugs are altered by *P. aeruginosa* supernatant, if this result continues with live bacteria, and if the response to the supernatant is general for different stressors.

Taken together, these results agree with the current understanding of Mucoralean pathogenesis where iron availability is considered essential. Here we highlight the ability of surrounding bacteria to control iron availability and the dynamic, specialised relationships between fungi and different bacterial species. To continue investigating the impact of the interaction between *R. microsporus* and *P. aeruginosa* on pathogenicity, the next chapter will focus on developing an *in vivo* zebrafish model for co-infection.

## Chapter 5 : DEVELOPMENT OF A ZEBRAFISH MODEL

Parts of this chapter have been previously published:

Kousser, C., Clark, C., Sherrington, S., Voelz, K. and Hall, R. (2019).  
*Pseudomonas aeruginosa* inhibits *Rhizopus microsporus* germination  
through sequestration of free environmental iron. *Scientific Reports*, 9.  
DOI 10.1038/s41598-019-42175-0

## 5.1 Introduction.

In the previous chapter we identified *P. aeruginosa* as inhibiting *R. microsporus* growth through the sequestration of iron. This was confirmed following exposure to both supernatants and live bacteria. While this provides information about how these organisms interact in isolation, additional factors inside a host can alter phenotypes. To understand the impact of co-infection on the host and determine whether *in vitro* results are physiologically relevant, a zebrafish model was developed.

**5.1.1 Advantages of the zebrafish model.** Mouse and rat models have been the gold standard of research into infectious diseases for decades. However, one limitation of mammalian models is the inability to observe cellular function during disease in a living host. While these models are important for gaining insight into infections of an animal that is physiologically similar to humans, zebrafish bridge the gap between invertebrates and mammals. There are many advantages to using zebrafish over other models, and in many cases zebrafish and mammalian models can be used simultaneously to provide a well-rounded understanding in disease pathogenesis, whilst abiding to the National Centre for Replacement, Refinement, and Reduction of Animals in Research's (NC3Rs) policy on reducing, refining and replacing the need for ethically protected animals in scientific research.

Zebrafish are mostly transparent for the first 2 to 3 weeks of life, though they do produce some pigmented spots. Chemical treatment can prevent the formation of any pigmented cells (Rosowski *et al.*, 2018). Methods for genetic modification of zebrafish embryos are established, and numerous specialised zebrafish lines are available, for example larvae with fluorescent or depleted immune cells (Harvie *et al.*, 2013). Their transparency and genetic tractability provide a unique opportunity to microscopically observe the progression of infection and interaction between pathogens and host immune cells.

Furthermore, their small size, high fecundity, and rapid development make them an economical and relatively quick method to obtain large quantities of data in a short period of time. A single breeding pair can produce hundreds of offspring per week, and embryos can be injected as early as 24 hours post fertilisation (hpf). They are also able to be anaesthetised and immobilised for long periods of time embedded within diffusible agarose, allowing for long-term live cell imaging.

The full zebrafish genome was published in 2013 and displayed extensive homology to humans, where it was shown that 70% of human genes have a zebrafish orthologue. The zebrafish immune system is surprisingly similar to humans, with the largest family of these orthologous genes relating to immunity (Howe *et al.*, 2013). Like humans, zebrafish contain both an innate and adaptive immune system. The innate immune system develops first, with macrophages present at 24 hpf and neutrophils developing around 36 hpf (Herbomel, Thisse

and Thisse, 1999). The adaptive branch does not develop until between 4- and 6-weeks post fertilisation (Willett *et al.*, 1999). Zebrafish respond to invading pathogens through the activation of the complement system and subsequent production of cytokines, chemokines, and interferons (Stein *et al.*, 2007; Bussmann and Raz, 2015). Zebrafish express Toll-like receptors on the surface of macrophages to recognise pathogen associated molecular patterns (Jault, Pichon and Chluba, 2004) and embryos utilise primitive macrophages and neutrophils to engulf and kill pathogens (Herbomel, Thisse and Thisse, 1999; Willett *et al.*, 1999). Because of these similarities, zebrafish are ideal models for studying the interaction between pathogens and the host's immune system.

**5.1.2 Sites of infection.** Although zebrafish do not contain the same organs as humans, specific sites have been used to model human infections. This study has focused on three injection sites, the hindbrain, yolk sac, and swim bladder.

**5.1.2.1 Hindbrain.** Models for fungal infections such as *Cryptococcus neoformans* (Davis *et al.*, 2016) and *Mucor circinelloides* (Voelz, Gratacap and Wheeler, 2015) have been developed in the hindbrain as proxies for cerebral and disseminated infections, respectively. The hindbrain has also been used to model *Streptococcus pneumoniae* meningitis, with high mortality occurring after injection with only 300 bacteria (Jim *et al.*, 2016). Other bacterial infections established in the zebrafish hindbrain include *P. aeruginosa* (Rocker *et al.*, 2015), *Mycobacterium marinum* (Davis *et al.*, 2002), *Bdellovibrio bacteriovorus*, and

*Shigella flexneri* (Willis *et al.*, 2016). This site allows for the longest monitoring of infection, as the hindbrain develops after 24 hpf and fish must be euthanised before 5 dpf without extended Home Office licensing (Kimmel *et al.*, 1995; HomeOffice, 2017). While primitive macrophages are observed from 24 hpf, neutrophils do not develop until 32-48 hpf (Herbomel, Thisse and Thisse, 1999; Fehr *et al.*, 2016). This could leave hindbrain-injected embryos more vulnerable to deadly infection.

**5.1.2.2 Yolk sac.** The yolk sac is the food source for embryos until they can begin free eating around 4-5 dpf, and it is the place of primitive macrophage differentiation (Herbomel, Thisse and Thisse, 1999). This injection site has been used to model cancers such as melanoma, prostate, breast, colon, and pancreatic (Haldi *et al.*, 2006; Teng *et al.*, 2013; Hill *et al.*, 2018). Limited infection studies have utilised the yolk sac. However, recently, injections into the yolk sac have been used to model tissue infections of *C. albicans* and to observe dissemination from the tissue into the blood stream (Seman *et al.*, 2018). Yolk sac injections are generally performed after 48 hpf, when the yolk membrane is less fragile (Stones 2017, personal communication). The yolk sac is highly vascularised (Isogai, Horiguchi and Weinstein, 2001), and easy spread to the blood stream can be a drawback to using this site if isolated infection is desired.

**5.1.2.3 Swim bladder.** Because the swim bladder is the only organ exposed to air, is lined with epithelial cells, and is transcriptionally similar to human lungs

(Zheng *et al.*, 2011), it has been utilised to model pulmonary and mucosal infections. For example, swim bladder models have been established for intracellular *Chlamydia* infections of the epithelia (Fehr *et al.*, 2016), *C. albicans* mucosal infections (Gratacap, Rawls and Wheeler, 2013), and *M. circinelloides* pulmonary infections (Voelz, Gratacap and Wheeler, 2015). The swim bladder develops after approximately 4 dpf, leaving only 24 hours for infection observation with standard Home Office licencing (Kimmel *et al.*, 1995; HomeOffice, 2017). Furthermore, some lymphocytes can be found from 4 dpf, though full adaptive immunity takes several weeks (Meijer and Spaink, 2011). However, the presence of adaptive immune cells could limit the ability to isolate the innate immune system in this model.

**5.1.3 Zebrafish as a model for mucormycosis.** Zebrafish models have been invaluable in understanding the interaction between Mucorales and the innate immune system. Much like humans, larval models have demonstrated site-dependent variability in virulence, where *M. circinelloides* moderately decreases viability in the hindbrain of healthy fish and is not deadly in the swim bladder (Voelz, Gratacap and Wheeler, 2015). For immunocompromised fish, hindbrain and swim bladder injections led to higher mortality (Voelz, Gratacap and Wheeler, 2015). Macrophages are more vital than neutrophils, and the depletion of macrophages increases mortality (Voelz, Gratacap and Wheeler, 2015). Early infection results in rapid recruitment of macrophages, where they engulf spores and control germination. However, there is a marked lack of oxidative burst and the host is unable to kill *M. circinelloides*. Utilisation of this transparent model

displayed the formation of latent granulomas within the fish, suggesting the possibility of later reemerging infections (Inglesfield *et al.*, 2018).

An adult zebrafish model further assessed the impact of *M. circinelloides* on immune response in a host with a full immune system. Intraperitoneal injection of *M. circinelloides* caused high recruitment of both macrophages and neutrophils and the induction of macrophage apoptosis, further confirming the importance of the innate immune system in mucormycosis (López-Muñoz *et al.*, 2018). While most of the studies involving zebrafish have investigated *M. circinelloides*, the impact of the *R. microsporus* endosymbiont has recently been explored. There, removal of the bacterial endosymbiont, *R. pickettii*, reduced overall virulence of fungal hindbrain infections (Itabangi *et al.*, 2019, preprint), contrary to evidence from murine or fly models (Ibrahim *et al.*, 2008).

**5.1.4 Zebrafish as a model for *P. aeruginosa* infections.** Infections with *P. aeruginosa* have highlighted the importance of both neutrophils and macrophages for immunity against *P. aeruginosa* infections (Brannon *et al.*, 2009). Neutrophils are especially important, and fish with only macrophages were more susceptible to killing by *P. aeruginosa* (Clatworthy *et al.*, 2009). Furthermore, this model has increased the understanding of *P. aeruginosa* virulence factors, demonstrating an interaction between the bacterial T3SS and host phagocytes during infection (Brannon *et al.*, 2009). *P. aeruginosa* is a common pathogen complicating CF and mutations in the zebrafish CF

transmembrane conductance regulator enhances susceptibility to infection and increases microbial burden of *P. aeruginosa* (Brannon *et al.*, 2009).

**5.1.5 Polymicrobial infections in zebrafish.** Most studies involving zebrafish infections have focused on mono-infections of pathogens, with polymicrobial models slowly emerging. Co-infections in the zebrafish swim bladder have provided insight into the interaction between *C. albicans* and *P. aeruginosa*. *P. aeruginosa* enhanced *C. albicans* virulence (Bergeron *et al.*, 2017), which is opposite to *in vitro* work that demonstrated *P. aeruginosa* inhibiting *C. albicans* growth (Hogan and Kolter, 2002; Hogan, Vik and Kolter, 2004; Morales *et al.*, 2013).

The impact of primary viral infection on bacterial pathogenesis has also been addressed in the zebrafish. Initial injection of sublethal Sindbis virus enhances *Shigella* survival and proliferation, leading to increased bacterial-induced mortality (Boucontet *et al.*, 2018).

**5.1.6 Limitations of the zebrafish model.** Besides the obvious anatomical differences between fish and human physiology, there are other limitations that should be considered. Firstly, fish antibodies are not widely available commercially, making immunological techniques such as Western Blotting or ELISA difficult. Also, without extended Home Office licencing, fish must be sacrificed after 5 dpf. This can limit experiments involving swim bladder injections,

for instance, where the organ only develops after 3-4 dpf. Furthermore, the cross-talk between the innate and adaptive immune systems cannot be investigated using the larval model, as the adaptive immune system does not develop until 4-6 weeks post fertilisation (Willett *et al.*, 1999). Transparent mutant adult zebrafish, known as “caspers” are available and could overcome this problem (White *et al.*, 2008). While the ability to isolate the innate immune system *in vivo* is generally an advantage, this is a limitation when attempting to carry results forward to compare to two-branched immune systems.

In all, the zebrafish is a powerful model for investigating host-pathogen interactions and provides an important mediator between cell culture and mammalian models.

## **5.2 Aim of this chapter.**

The previous two chapters demonstrated the ability of *P. aeruginosa* to out-compete *R. microsporius* for environmental iron *in vitro*, inhibiting fungal germination and growth. This chapter aims to develop a zebrafish model for co-infection between *R. microsporius* and *P. aeruginosa* to understand the impact of this relationship on overall virulence and determine whether *in vitro* and *in vivo* results are consistent.

## **5.3 Results**

**5.3.1 *R. microsporus* moderately reduces survival following hindbrain injection of healthy zebrafish embryos.** To confirm the hindbrain as an effective model for studying *R. microsporus* infections, zebrafish embryos were injected with 10, 50, and 100 spores into the hindbrain through the otic vesicle (Figure 5.1A). *R. microsporus* decreased the viability of the larvae in a dose-dependent manner, with 69% of fish surviving at 96 hpi after injection with 100 spores (Figure 5.1B). The ability of spores to germinate was confirmed through live cell microscopy, where fungal hyphae protruded through the heads of fish who were unsuccessful at controlling growth (Figure 5.1C)

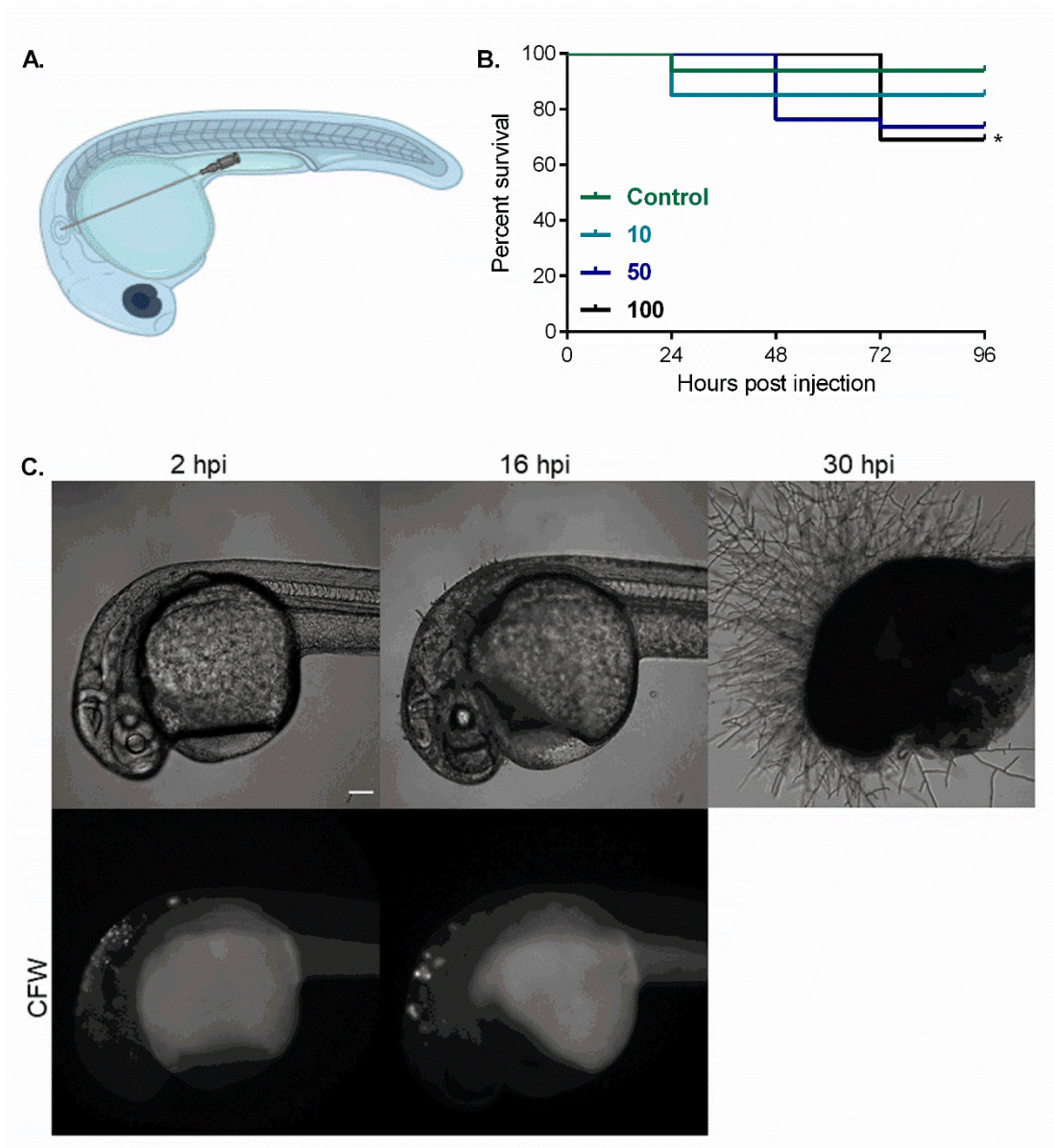


**Figure 5.1** *R. microsporius* moderately reduces viability in healthy zebrafish embryos via hindbrain injection, in a dose dependent manner. *R. microsporius* spores (10, 50, and 100) were injected into the hindbrain of zebrafish embryos at 24 hpf. **(A)** Illustration depicting 24 hpf embryo with hollow needle demonstrating injection site through otic vesicle into hindbrain. Image was created with BioRender. **(B)** Survival of larvae was quantified every 24 hours for 4 days. Shown are data pooled from two separate experiments with a total of 32, 40, 38, and 42 fish for control, 10, 50, and 100 spores. Data analysed with Mantel-Cox log-rank test with Bonferroni correction for

multiple comparisons, compared to control ( $\alpha = 0.05$ ). **(C)** Representative images of zebrafish larvae at 2, 16, and 30 hours post infection (hpi). Lower panel depicts calcofluor white (CFW) stained spores. Scale bar = 100  $\mu\text{m}$ . \* =  $p < 0.05$ .

**5.3.2 The *P. aeruginosa* siderophore, pyoverdine, reduces *R. microsporus* virulence in the hindbrain of healthy zebrafish.** Pyoverdine was found to be the main mechanism controlling fungal growth upon interaction with *P. aeruginosa in vitro*. Co-injection of *R. microsporus* with pyoverdine (60  $\mu\text{M}$ ) in the hindbrain (Figure 5.2A) resulted in significant increase in fish survival when compared to spores alone (Figure 5.2B) with 89% (+/- 6.377) of fish surviving across a 96-hr time course. This demonstrated that the presence of pyoverdine is sufficient to reduce host damage caused by *R. microsporus* infection.

**5.3.3 The *E. coli* siderophore, enterobactin, does not impact *R. microsporus* virulence in the hindbrain.** Enterobactin did not impact *R. microsporus* growth *in vitro*, and fish were infected with *R. microsporus* in the presence of enterobactin to determine if results were reproducible *in vivo*. Unlike pyoverdine, the addition of enterobactin did not increase the survival of the larvae compared to fish infected with *R. microsporus* alone (Figure 5.2C). This suggests that enterobactin is unable to sequester iron from *R. microsporus*, and the ability of pyoverdine to enhance host survival is not a general phenomenon.

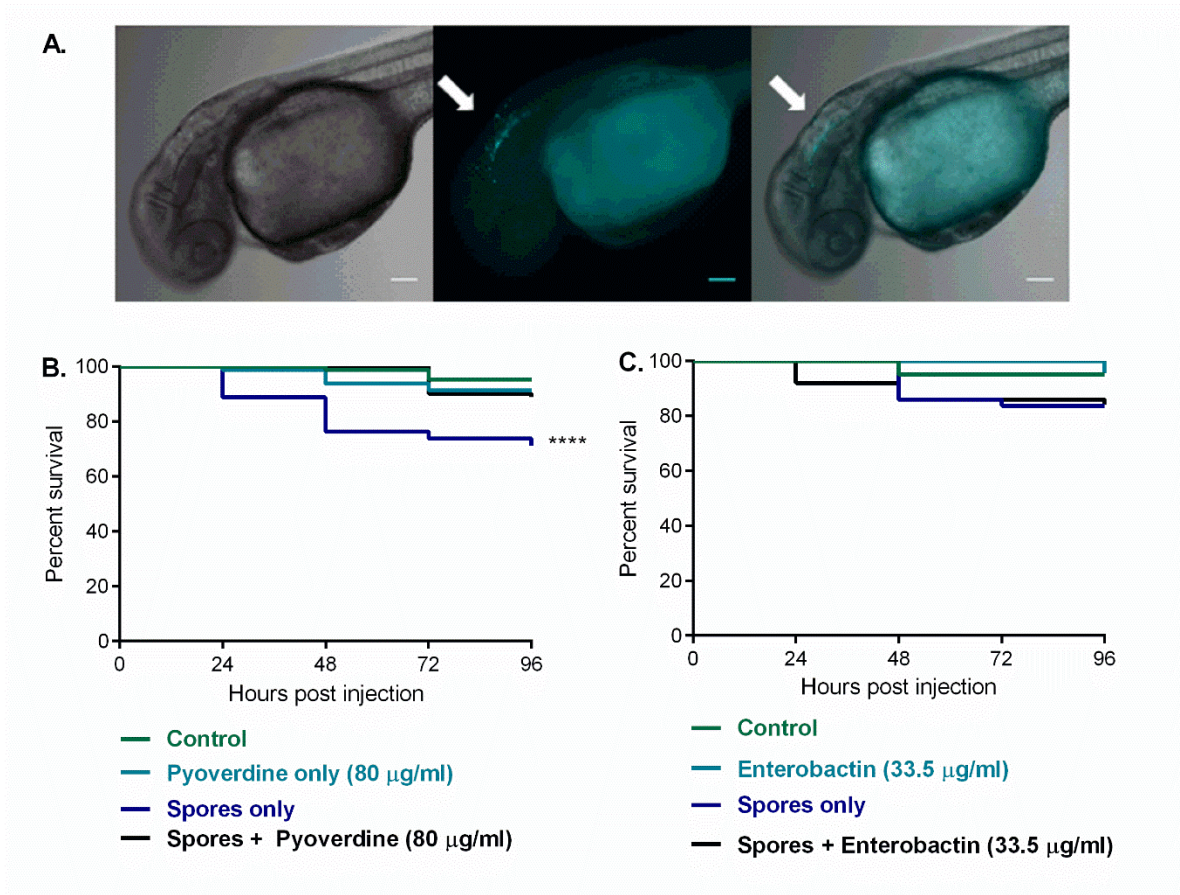


**Figure 5.2** The *P. aeruginosa* siderophore, pyoverdine, reduces *R. microsporus* virulence in a zebrafish model of infection. **(A)** Representative images of zebrafish larvae at 0 hpi. White arrows indicate *R. microsporus* spores (Calcofluor White stain, cyan pseudo-coloured) located within hindbrain compartment. Scale bars = 100  $\mu\text{m}$ . **(B)** Zebrafish were injected in the hindbrain with 50 spores +/- 60  $\mu\text{M}$  pyoverdine and fish survival was quantified over time. Shown are data pooled from four separate experiments with a total of 87, 80, 80, and 81 fish for control, pyoverdine only, spores only, and spores + pyoverdine, respectively. **(C)** Zebrafish larvae were injected in the hindbrain with 50 spores +/- 50  $\mu\text{M}$  enterobactin. Data shown is pooled from two independent experiments with a total of 42, 44, 46, 43, and 50 fish for control, DMSO, enterobactin only, spores only, and spores + enterobactin, respectively. Data analysed with Mantel-Cox log-rank

test with a Bonferroni test for multiple comparisons, compared to control ( $\alpha = 0.05$ ). \*\*\*\*  
=  $p < 0.0001$ . (Kousser *et al.*, 2019).

**5.3.4 *P. aeruginosa* PA14 inhibits *R. microsporus* growth via iron sequestration.** *In vitro* experiments used *P. aeruginosa* PAO1, but the following zebrafish experiments have used *P. aeruginosa* PA14. To utilise for future *in vivo* microscopy, fluorescently tagged strains were developed. Several attempts to transform *P. aeruginosa* PAO1 with the plasmid PME6032 to generate a cytoplasmic mCherry-expressing strain were unsuccessful. However, PME6032 was successfully transformed into *P. aeruginosa* PA14.

To check the ability of *P. aeruginosa* PA14 to inhibit *R. microsporus* growth, *R. microsporus* was exposed to 50% PA14 or PAO1 supernatants for 24 hours (Figure 5.3). PA14 reduced *R. microsporus* growth by 96.23% (+/- 0.58%,  $p = 0.0171$ ) (Figure 5.3A). This is comparable to PAO1 supernatant, which reduced *R. microsporus* growth by 94.40% (+/- 1.415%,  $p = 0.0159$ ). Rescue of fungal growth with the addition of 50  $\mu\text{M}$   $\text{FeCl}_3$  after exposure to PA14 supernatant was also confirmed (Figure 5.3B). Therefore, *P. aeruginosa* PA14 also inhibits the growth of *R. microsporus* through iron restriction, and PA14 was used in the following experiments.

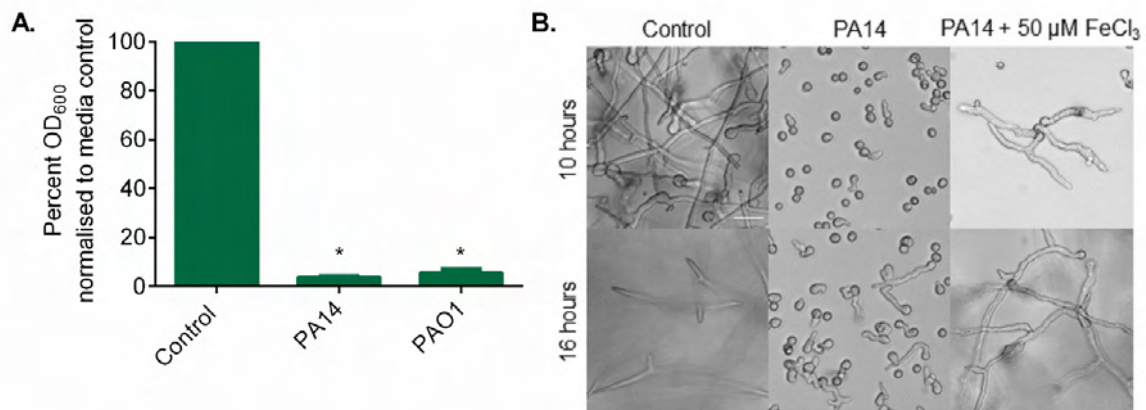


**Figure 5.3** *P. aeruginosa* PA14 inhibits the germination of *R. microsporius* through iron sequestration. **(A)** Spores were exposed to 50% supernatants from *P. aeruginosa* PA14 and PAO1 for 24 hours before fungal growth was measured by absorbance (OD<sub>600</sub>). To determine whether this inhibition is iron-dependent, *R. microsporius* spores were exposed to PA14 supernatant +/- 50 µM FeCl<sub>3</sub> and germination was visualised through live cell imaging (n=4). **(B)** Representative images of Control (SAB/LB only), 50% PA14 supernatant, and 50% PA14 supernatant + iron at 10 and 16 hours are shown. Scale bar = 25 µm. Data represents mean and SEM. Kruskal Wallis with Dunn's multiple comparisons test was used on non-normalised raw data ( $\alpha = 0.05$ ). \* =  $p < 0.05$ .

**5.3.5 Zebrafish are resistant to swim bladder mono- and co-infections with *P. aeruginosa* and *R. microsporius*.** Zebrafish larvae were injected with 100 *R. microsporius* spores and 10,000 *P. aeruginosa* cells. Consistent with the literature, *R. microsporius* did not decrease the viability of healthy fish, with 100% of larvae surviving after *R. microsporius* only injection (Figure 5.4A). Similarly, *P. aeruginosa* did not significantly reduce fish viability, with 92.50% of fish surviving mono-infection. This is consistent with previous studies that show a low virulence

of *P. aeruginosa* in healthy fish after swim bladder injection (Bergeron *et al.*, 2017). There was no difference in zebrafish survival between *P. aeruginosa* mono- and co-infection, with 92.86% of fish surviving after co-infection (Figure 5.4B).

To determine whether the fungi remained viable during the infection, *R. microsporus*, *P. aeruginosa*, and co-infection with an MOI of 1:100 (fungi:bacteria) were injected into the swim bladder of 4 dpf zebrafish. After 24 hours post infection (hpi), larvae were euthanised, homogenised, and the lysate was plated onto SAB agar + antibiotics. Viable *R. microsporus* spores were counted and compared to 0 hpi control. For *R. microsporus* mono-injection, 93.39% (+/- 20.70%) of spores survived, and 112.30% (+/- 23.19%) of co-injected spores survived (Figure 5.4C). Therefore, zebrafish swim bladder co-infection with *R. microsporus* and *P. aeruginosa* did not impact spore viability.

Due to the of the lack of pathogenicity of both *P. aeruginosa* and *R. microsporus* in the swim bladder, other injection sites were explored.

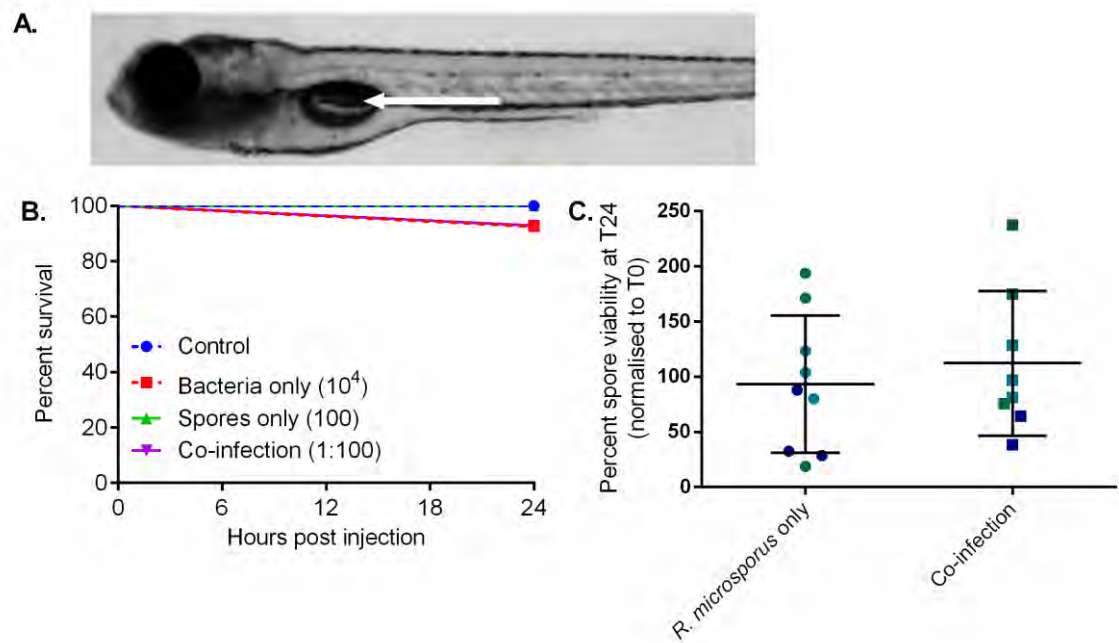


**Figure 5.4 Zebrafish are resistant to swim bladder infections with *P. aeruginosa* and *R. microsporus*.** (A) Image of 4 dpf zebrafish larvae, white arrow pointing toward swim bladder. (B) Zebrafish larvae (4 dpf) were injected into the swim bladder with injection buffer only, *R. microsporus* spores (100), *P. aeruginosa* PA14 cells (10,000) and co-injected. Survival was quantified after 24 hpi. Data presented is pooled from two independent experiments with 40, 42, 40, and 42 fish for control, spores only, bacteria only, and co-infection. Data analysed with Mantel-Cox log-rank test with a Bonferroni test for multiple comparisons. (C) To determine if the presence of *P. aeruginosa* enhances the killing of *R. microsporus* by host immune cells, 50 spores and 5,000 bacteria were injected into the swim bladder and zebrafish were homogenised in triplicate at 0 hpi and 24 hpi and plated on SAB agar + 60  $\mu\text{g/ml}$  tetracycline, 30  $\mu\text{g/ml}$  gentamycin, and 30  $\mu\text{g/ml}$  chloramphenicol to determine fungal viability. Colours correspond to points belonging to the same biological replicates. One outlier was determined using the Robust regression and Outlier removal (ROUT) method and removed. Data analysed using a Mann-Whitney U test ( $\alpha = 0.05$ ).

**5.3.6 *R. microsporus* is moderately pathogenic in healthy zebrafish embryos via yolk sac injections, while *P. aeruginosa* is highly virulent.**

Injection into the dorsal end of the yolk sac of 2 dpf zebrafish larvae (Figure 5.5A) with 10, 50, 100, 500, and 1000 *P. aeruginosa* cells resulted in a highly virulent infection (Figure 5.5B). After 72 hours, only 15% of fish survived the lowest dose of bacteria (10 cells), with 100% mortality after 24 hours injection with 1000 cells. This suggests that the bacteria are likely entering the blood stream, killing the fish. Injection into the yolk sac of *R. microsporus* spores mildly reduced viability. Survival following injection with 10, 50, and 100 spores is decreased in a dose-dependent manner, with the highest injection dose leading to 41.18% mortality 72 hpi.

To observe whether the inoculum was disseminating from original injection site, live cell microscopy was utilised. Representative images (Figure 5.5D) depict stained *R. microsporus* spores migrating from the injection site after 5 hours, suggesting that organisms injected into the yolk sac easily disseminate.

While these results indicate that the yolk sac could be an adequate model for mucormycosis, the high lethality associated with bacterial injection makes co-infection impractical at this site. Therefore, the hindbrain injection model was explored as a potential site for co-infection.

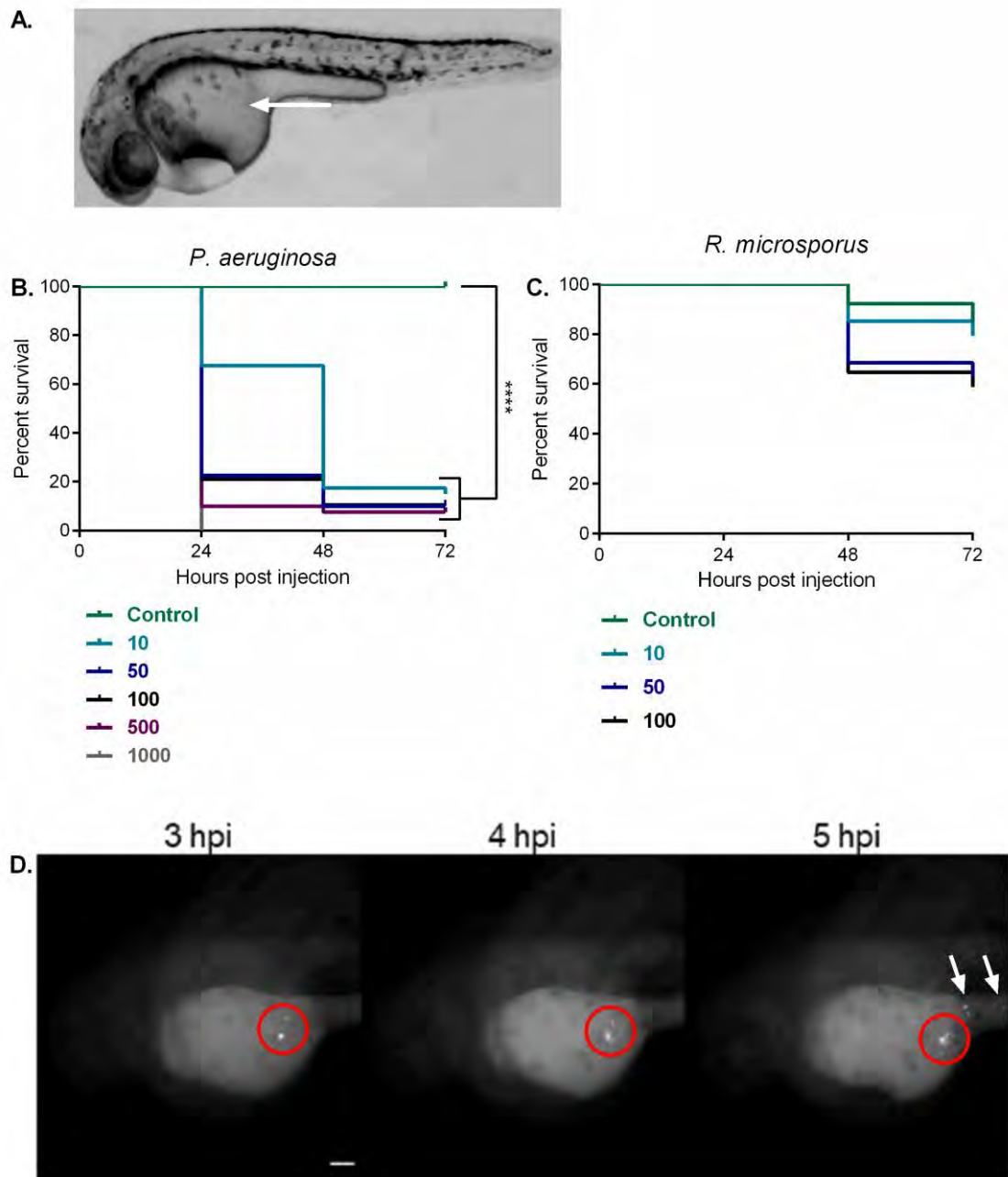


**Figure 5.5** *R. microsporus* is moderately pathogenic in healthy zebrafish embryos via yolk sac injections, while *P. aeruginosa* is highly virulent. (A) Image of 2 dpf zebrafish embryo, white arrow pointing towards injection site of yolk sac. Zebrafish were injected with a range of (B) *P. aeruginosa* or (C) *R. microsporus* cells in the yolk sac at 2 dpf and the survival of the fish monitored. Data presented is pooled from two independent experiments with 35, 40, 40, 35, 40, and 40 fish for the control, 10, 50, 100, 500, and 1000 cells, respectively.

500, and 1000 bacteria per fish, and 26, 34, 35, and 34 fish for control, 10, 50, and 100 spores per fish. **(D)** To observe dissemination, spores were stained with 250 µg/ml calcofluor white (CFW) before live cell microscopy was utilised to observe spore dissemination. Representative images are presented. Red circles highlight original site of injection. White arrows point to disseminated spores. Survival data was analysed with Mantel-Cox log-rank test with a Bonferroni test for multiple comparisons ( $\alpha = 0.05$ ). \*\*\*\* =  $p < 0.0001$ .

**5.3.7 *P. aeruginosa* decreases viability in a dose-dependent manner following hindbrain injections of healthy zebrafish embryos.** Before establishing a co-infection model, zebrafish survival following bacterial mono-infections was established. Zebrafish were injected in the hindbrain with 10, 50, 100, 500, and 1000 *P. aeruginosa* bacteria (Figure 5.6A). A moderately virulent infection was established following injection with 10, 50, 100, 500, and 1000 bacteria, and viability decreased in a dose-dependent manner. After injection with 1000 bacteria, 67.09% of fish survived at 96 hpi.

It was hypothesised that *P. aeruginosa* would decrease fungal virulence *in vivo*. Mono-injections with *R. microsporus* (Figure 5.1) indicated that a high dose of spores (100 spores) would be required to reduce zebrafish viability to an extent where changes could be observed. *In vitro* results suggested that an MOI of 1:100 (*R. microsporus* : *P. aeruginosa*) would be required to inhibit *R. microsporus* germination (Figure 3.16). Therefore, 10,000 bacteria would need to be injected

into the hindbrain during co-infections. This infection was highly virulent, with only 2.8% of fish surviving after 24 hours (Figure 5.6B).

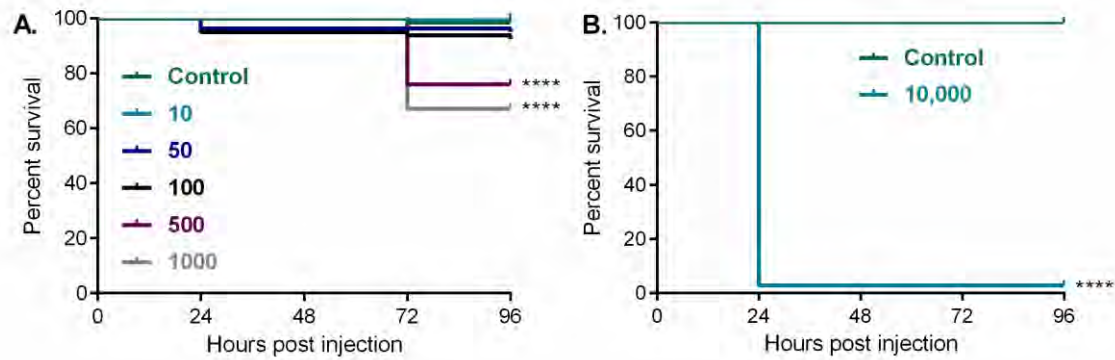


**Figure 5.6** *P. aeruginosa* decreases viability in a dose-dependent manner following hindbrain injections of healthy zebrafish embryos. To determine the impact of *P. aeruginosa* mono infection, PA14 was injected into the hindbrain with 10, 50, 100, 500, and 1000 CFUs/fish (A) Survival was monitored over time. Data shown is pooled from four separate experiments with 70, 80, 80, 80, 79, and 79 fish for control, 10, 50, 100, 500, and 1000 bacteria. (B) To reach adequate bacterial load for future co-infection experiments, 10,000 *P. aeruginosa* cells were injected into the hindbrain and survival was quantified over time. Data presented is pooled from two separate experiments with 31 control fish and 35 fish injected with 10,000 bacteria. Data analysed with Mantel-Cox log-rank test with a Bonferroni test for multiple comparisons ( $\alpha = 0.05$ ). \*\*\*\* =  $p < 0.0001$ .

**5.3.8 Co-infection with *P. aeruginosa* and *R. microsporus* enhances virulence in a zebrafish hindbrain co-infection model.** To determine the effect of co-infection *in vivo*, 100 *R. microsporus* and 10,000 *P. aeruginosa* were injected into the hindbrain (Figure 5.7). Spores alone showed limited virulence, with 86.89% of fish surviving after 96 hours. *P. aeruginosa* was also less virulent

than in previous experiments, though 76.67% of fish were still killed after 96 hpi. Surprisingly, co-injection resulted in a more highly virulent infection, and 100% of fish were killed at 96 hpi. Upon microscopic examination, the fish did not appear to die from fungal outgrowth, though further investigation would be needed to confirm this observation. This suggests that co-infection with *R. microsporius* and *P. aeruginosa* enhances bacterial virulence *in vivo*.

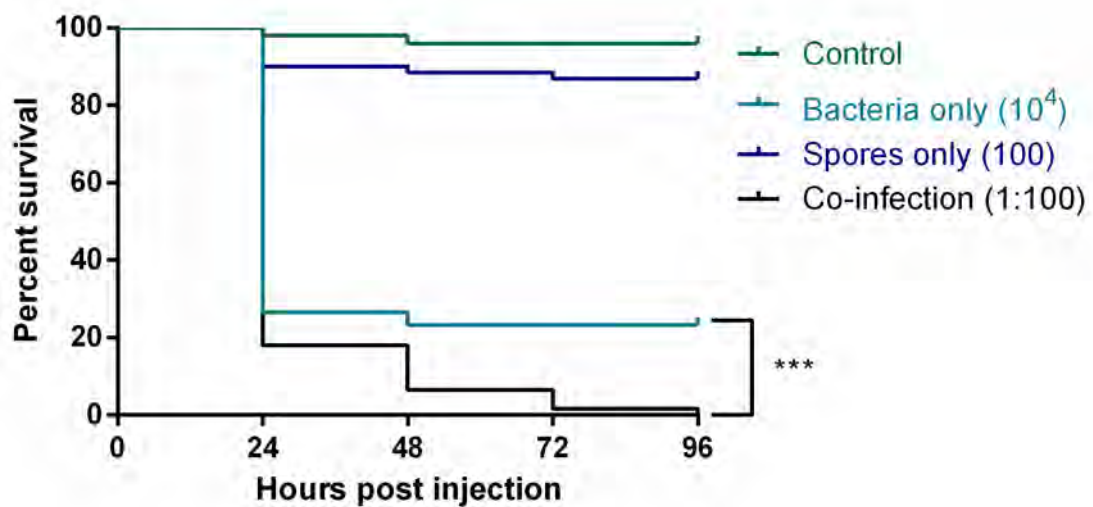


**Figure 5.7 Co-infection with *P. aeruginosa* and *R. microsporius* enhances virulence in a zebrafish hindbrain co-infection model.** *R. microsporius* spores (100) and *P. aeruginosa* PA14 (10,000) were injected into the hindbrain of zebrafish embryos at 24 hpi. Survival was monitored over time. Data presented is pooled from three independent experiments with 51, 60, 61, and 61 fish from control, bacteria only, spores only, and co-infection respectively. Data analysed with Mantel-Cox log-rank test with a Bonferroni test for multiple comparisons ( $\alpha = 0.05$ ). \*\*\* =  $p < 0.001$ .

## 5.4 Discussion.

### 5.4.1 Choosing site of infection and validating model.

This chapter began developing an *in vivo* zebrafish infection model to test the impact of the interaction between *R. microsporus* and *P. aeruginosa* on a host. The first goal was to analyse different injection sites to determine the optimal model for co-infection. Here we confirmed the site-dependent variability of Mucorales infection seen in previous zebrafish studies. As found with *M. circinelloides* (Voelz, Gratacap and Wheeler, 2015), injection into the swim bladder with *R. microsporus* did not result in overt infection. Likewise, *P. aeruginosa* did not cause significant mortality following swim bladder infection, which is also consistent with the literature (Bergeron *et al.*, 2017). While the time-course of this study is limited by Home Office licencing regulations (restricted to 5 dpf), longer incubation with *P. aeruginosa* or Mucorales has not demonstrated increased mortality in healthy fish (Voelz, Gratacap and Wheeler, 2015; Bergeron *et al.*, 2017). However, collaborators are currently exploring the impact of *R. microsporus* and *P. aeruginosa* swim bladder co-infections during extended time-course experiments.

The hindbrain compartment is the most commonly used site for fungal injections in the zebrafish, with established models for candidiasis, aspergillosis, cryptococcosis, and mucormycosis (Chao *et al.*, 2010; Knox *et al.*, 2014; Tenor *et al.*, 2015; Voelz, Gratacap and Wheeler, 2015). We identified this as the best location for co-infection with *R. microsporus* and *P. aeruginosa*, due to the dose-

dependent decrease in viability when exposed to either organism and the ability to monitor infections for longer time periods before Home Office licencing requires experiment termination. Injection with low (10), moderate (50), and high (100) doses of *R. microsporus* spores provided comparable results to *M. circinelloides* hindbrain infections (Voelz, Gratacap and Wheeler, 2015), confirming our technique. Mono-injection with *P. aeruginosa* into the hindbrain led to a dose-dependent decrease in viability. However, mortality was lower than seen in previous studies, likely due to strain and procedure differences (Rocker *et al.*, 2015; McCarthy *et al.*, 2017). Zebrafish do not develop neutrophils until 32 to 48 hpf, and this could account for the extensive mortality with the highest dose of bacteria (Lieschke *et al.*, 2001).

While variable, injection with *R. microsporus* at all sites did not lead to considerable death. As most fungal infections occur in immunocompromised hosts, it was not surprising that limited mortality was observed with the immunocompetent fish used in this study. Depressing zebrafish immune system through corticosteroid treatment or depletion of macrophages leads to higher mortality following *M. circinelloides* and *A. fumigatus* infections (Knox *et al.*, 2014; Voelz, Gratacap and Wheeler, 2015). Therefore, co-injection with *P. aeruginosa* and *R. microsporus* could better establish infection in immunocompromised zebrafish larvae. However, high *P. aeruginosa* virulence in an immunocompromised host may be a limiting factor in these experiments.

Furthermore, as diabetes is an important risk factor for mucormycosis, a diabetic zebrafish model could enhance baseline *R. microsporus* virulence. While most diabetic models use adult fish, a transgenic line has been developed which leads to insulin resistance and hyperglycaemia in larvae through disruption of the insulin receptors (Yin *et al.*, 2015). Models for diabetic DKA in zebrafish are lacking, though treatment with streptozotocin, which has been used to model DKA in mammals (Lam *et al.*, 2005), or ketones, such as  $\beta$ -hydroxybutyrate, could be promising.

**5.4.2 Impact of pyoverdine on *R. microsporus* virulence *in vivo*.** Through utilisation of the zebrafish hindbrain injection model, we confirmed the ability of pyoverdine to limit *R. microsporus* virulence. This is similar to murine experiments, where treatment with the iron chelator deferasirox decreased the virulence of *R. oryzae* and enhanced mouse survival (Ibrahim *et al.*, 2007). However, there have been reported cases of deferasirox-induced liver toxicity (Braga *et al.*, 2017). Furthermore, as adjunct treatment of deferasirox with amphotericin B failed clinical trials (Spellberg *et al.*, 2012), there is a need for novel iron chelators to treat mucormycosis.

**5.4.3 *In vivo* co-infection model.** Based on *in vitro* observations that *P. aeruginosa* decreases *R. microsporus* germination, we hypothesised that co-infection in the zebrafish would decrease fungal virulence. Instead, we observed a higher mortality following co-infection, presumably due to *P. aeruginosa*

infection. This is opposite to zebrafish studies involving *P. aeruginosa* and *C. albicans* where fungal virulence is enhanced *in vivo* (Bergeron *et al.*, 2017), and demonstrates the versatility of this bacterium when interacting with fungi. Injecting fish with mutant bacteria unable to secrete pyoverdine or pyochelin would help determine whether a fungal-induced increase in these virulence factors enhances mortality. Furthermore, co-injections of *R. microsporus* with another bacterial species could indicate whether this is a general phenomenon of opportunistic pathogens in the presence of *R. microsporus*, or if this is specific to *P. aeruginosa*.

In all, this work provides a unique insight into the potential implications of co-infection on the host and confirms the importance of studying polymicrobial interactions *in vivo*

## **Chapter 6 : DISCUSSION AND CONCLUDING REMARKS**

Just as humans live in diverse communities and are rarely alone, no microorganism lives in isolation. Because of this, dynamic relationships have emerged where microbes have developed specific reactions to the presence of certain pathogens. For instance, *C. albicans* is inhibited or killed when it comes into contact with *P. aeruginosa* (Hogan and Kolter, 2002; Hogan, Vik and Kolter, 2004), *Acinetobacter baumannii* (Peleg *et al.*, 2008), or *E. coli* (Cabral *et al.*, 2018). However, when *C. albicans* meets *S. aureus* (Schlecht *et al.*, 2015) or *S. epidermidis* (Pammi *et al.*, 2013), the microbes synergise, leading to increased bacterial dissemination and more aggressive infections.

Here we have identified the opportunistic Gram-negative bacterium, *P. aeruginosa*, as a novel factor that impacts *R. microsporus* pathogenicity. This interaction was found to be predominantly mediated by iron competition. While iron is already known to be a limiting factor in *Rhizopus spp.* infection, pyoverdine is a unique chelator that *R. microsporus* cannot utilise as an iron source. Further, this work gives insight into the complex battle between *R. microsporus* and *P. aeruginosa* when they meet in the environment or human host. With this information, clinicians could better predict disease outcome and understand risks associated with co-habitation of these particular organisms. In all, this study identified pyoverdine-mediated iron modulation as a novel mechanism by which *R. microsporus* interacts with other microorganisms and reinforced the importance of iron in the pathogenesis of these fungi.

## 6.1 Iron competition

Iron is essential in all lifeforms for biological processes such as oxygen transport, DNA synthesis, detoxification, cell growth/division, and electron transport to properly function (Abbaspour, Hurrell and Kelishadi, 2014). Iron is generally a limiting factor during infection, and as such the host has developed mechanisms for sequestering iron and other trace minerals from microbes, termed nutritional immunity (Hood and Skaar, 2012). This leads to only  $10^{-24}$  M unbound iron within the human body (Miethke and Marahiel, 2007). Along with pressures from the host, microorganisms must compete with other pathogens that are also fighting to scavenge iron from host iron-binding proteins. Many pathogenic bacteria and fungi have developed effective mechanisms for stealing iron from transferrin, including high affinity siderophores and haem oxygenases (Haas, 2014). Our study has shown that during the battle between *P. aeruginosa* and *R. microsporus*, *P. aeruginosa* siderophores are more efficient at chelating iron than *R. microsporus*. Here, the fungus is not able to scavenge iron from *P. aeruginosa* siderophores, as it can from other bacterial siderophores (Boelaert *et al.*, 1993). This results in the significant inhibition of *R. microsporus* germination *in vitro* and a pyoverdine-mediated reduction in fungal virulence *in vivo*.

Supplementation with zinc, manganese, and copper alone did not rescue fungal growth, even though these are also chelated by pyoverdine and pyochelin (Braud, Hannauer, *et al.*, 2009; Braud, Hoegy, *et al.*, 2009). However, further

investigation into the competition between Mucorales and opportunistic pathogens for these metals would be interesting. Zinc is essential for nucleotide synthesis and germination of Mucorales (Foster and Waksman, 1939; Wegener and Romano, 1963). Restriction of this metal inhibits *C. albicans* virulence by decreasing growth (Lulloff, Hahn and Sohnle, 2004) and induces Goliath cell formation (Malavia *et al.*, 2017), though *C. albicans* has developed scavenging mechanisms to compete with host zinc sequestration (Citiulo *et al.*, 2012). Zinc starvation also increases oxidative stress in *Cryptococcus gattii* (Schneider *et al.*, 2012) and the production of stress-associated proteins in *Paracoccidioides brasiliensis* (Parente *et al.*, 2013). Therefore, zinc competition between *R. microsporus* and *P. aeruginosa* could manifest in different parameters than germination inhibition. Limitation of manganese could also impact *R. microsporus* growth, as manganese is necessary for proper cell wall development of *A. niger* (Kisser, Kubicek and Rohr, 1980) and filamentation of *C. albicans* (Asleson *et al.*, 2000). Furthermore, the iron permease, *FTR1*, is coupled to a copper oxygenase during reductive iron uptake (Stearman *et al.*, 1996; Ibrahim *et al.*, 2010). Therefore, copper restriction could reduce iron uptake, and perhaps combined supplementation of copper with iron would further enhance *R. microsporus* growth. Nevertheless, iron competition, specifically via the siderophore pyoverdine, was implicated as the major source of *R. microsporus* growth inhibition in this study.

### **6.1.1 Speculation regarding germination cessation as a defensive strategy.**

Remaining un-germinated could be a defence mechanism employed by *R.*

*microsporus* to protect itself against competitors. As dormant fungal spores can survive extreme conditions (Dunn *et al.*, 2006), it could be a better strategy to wait until conditions are more favourable. Along these lines, perhaps iron availability acts as a cue to determine whether the desired nutrients are available to thrive. Maybe Mucorales aren't necessarily inefficient at obtaining iron, but decide that without available iron, the conditions will not be adequate to germinate and obtain other nutrients. This sensor could also act to warn Mucorales that other organisms are present. Perhaps *Rhizopus spp.* are the most prolific causes of mucormycosis because of this ability to more effectively recognise suitable conditions for hyphal growth. However, as iron starvation decreases spore survival over time (Shirazi, Kontoyiannis and Ibrahim, 2015 and this study), this mechanism could be a temporary defensive strategy in early timepoints, or other conditions in these experiments could decrease spore viability.

Mucorales are protected against host killing when they remain as spores, but their hyphae are vulnerable to neutrophil damage via NETs (Diamond *et al.*, 1978). Being aseptate means that hyphal injury is particularly dangerous for the fungus, as it is unable to wall off the affected area (Deacon, 2006). Remaining ungerminated within macrophages reduces killing and allows for intracellular persistence (Andrianaki *et al.*, 2018). Mucorales are thought to form granulomas within the host (Inglesfield *et al.*, 2018), which is hypothesised to act as a reservoir for the emergence of latent infections. This could be a similar defence strategy in response to competing pathogens. Perhaps the aggressiveness and efficiency of *P. aeruginosa*'s attack prompts the active decision to halt

germination and protect itself. However, this is not entirely successful, as live *P. aeruginosa* and prolonged exposure to supernatants decreases viability.

## 6.2 Xenosiderophores.

To overcome nutritional immunity and compete against other microorganisms, some pathogens have developed mechanisms for scavenging iron from siderophores produced by other bacteria and fungi. For example, *Neisseria gonorrhoeae* does not produce its own siderophores, but instead utilises enterobactin and salmochelin which are both produced by *E. coli*, *Salmonella spp.*, and *Klebsiella spp.*, along with host transferrin and lactoferrin (Strange, Zola and Cornelissen, 2011). Many fungi such as *C. albicans* (Heymann *et al.*, 2002), *C. glabrata* (Nevitt and Thiele, 2011), and *C. neoformans* (Tangen *et al.*, 2007) utilise hydroxamate siderophores produced by bacteria and other fungi. *P. aeruginosa* can utilise several siderophores from both bacteria and fungi such as deferoxamine (from *Streptomyces spp.*), ferrichrome (from *Aspergillus spp.* and *Penicillium spp.*), and Schizokinen (from *Bacillus megaterium*) all via the same FoxB transporter (Cuív *et al.*, 2007). *P. aeruginosa* can also use enterobactin (Ghysels *et al.*, 2005), aerobactin (from *E. coli*), and rhizobactin (from *Rhizobium meliloti*) (Cuív, Clarke and O'Connell, 2006) to obtain iron. Therefore, xenosiderophore usage is present throughout bacterial and fungal kingdoms and is an example of the evolved arms-race against competing community members.

Mucorales are no exception to this phenomenon and can utilise deferoxamine as a xenosiderophore. Deferoxamine was clinically used as an iron chelator in patients experiencing iron overload, usually in hereditary hemochromatosis, beta-thalassemia, or following blood transfusions (Mobarra *et al.*, 2016). However, these people became uniquely susceptible to mucormycosis (Boelaert *et al.*, 1993), despite Mucorales' dependency on available iron (Artis *et al.*, 1982). Under these conditions, mucormycosis was induced by ferrioxamine (iron-rich deferoxamine) binding to Fob1/Fob2 receptors on the cell surface (Liu *et al.*, 2015). This project suggests enterobactin, produced by *E. coli*, as a potential novel xenosiderophore for *R. microsporus*. While the *P. aeruginosa* siderophore pyoverdine strongly inhibited *R. microsporus* growth, addition of isolated enterobactin did not have any effect. This was surprising as enterobactin has a higher affinity ( $10^{52} \text{ M}^{-1}$ ) for iron than pyoverdine ( $10^{36} \text{ M}^{-1}$ ) (Carrano and Raymond, 1979). This is in contrast to *in vitro* studies involving *E. coli* with *C. albicans* and *Aspergillus spp.* In these cases, hydrophilic secreted molecules from *E. coli* kills *C. albicans* (Cabral *et al.*, 2018), and live co-cultures lead to inhibition of *A. fumigatus* and *A. flavus* growth (Yadav *et al.*, 2005). Furthermore, while pyoverdine reduces *R. microsporus* virulence in a zebrafish hindbrain injection model, enterobactin did not have an impact. Investigating the expression of Fob1/Fob2 when *R. microsporus* is exposed to exogenous enterobactin, *E. coli* supernatants, and live *E. coli* could provide evidence, though if it is a xenosiderophore, enterobactin uptake could be mediated by a different receptor to deferoxamine.

The fact that other bacteria and fungi can form synergistic relationships, such as *S. aureus* and *C. albicans* (Schlecht *et al.*, 2015), suggests that *E. coli* and *R. microsporus* might also work together to enhance pathology in a host. Clinically, concurrent *E. coli* infections and mucormycosis have been reported. Examples include diabetic individuals with infections at a surgical site following bowel resection (Patel *et al.*, 2010) and following drainage of an abdominal cellulitis abscess (Nain *et al.*, 2015). Another case occurred in a patient with non-Hodgkin's lymphoma who developed pulmonary mucormycosis with positive *E. coli* cultures following allogenic stem cell transplantation (Peixoto *et al.*, 2014). Finally, a person with chronic obstructive pulmonary disorder (COPD) developed *E. coli* sepsis, and mucormycosis was confirmed upon autopsy (Alhassan and Thirumala, 2015). In all cases found, *E. coli* was diagnosed first, and the patient ultimately expired. Therefore, xenosiderophore-mediated cooperation between Mucorales and *E. coli* may have serious clinical implications. Future studies could involve investigating co-infections *in vivo*.

While iron availability is a limiting factor in mucormycosis, Mucorales are not very efficient at acquiring iron. Perhaps they have ineffective siderophores with a low affinity for iron (Thieken and Winkelmann, 1992) because they have developed mechanisms to utilise siderophores from bacteria they commonly meet. Biosynthesis and secretion of siderophores is a metabolically costly behaviour (Griffin, West and Buckling, 2004). Utilising chelators from other organisms could be more cost-effective and still provide the necessary nutrients to fuel growth.

Ultimately, the ability of pyoverdine to inhibit *R. microsporus* growth while enterobactin induces no effect indicates that Mucorales participate in dynamic, species-specific relationships that have evolved into varying responses to different bacteria.

### **6.3 General Mucoralean response to opportunistic pathogens.**

This study has shown a variation in the response of *R. microsporus* to different pathogens. We have shown that *R. microsporus* is inhibited by the presence of *P. aeruginosa* and *K. pneumoniae*, while *S. aureus*, *E. coli*, and *B. cenocepacia* do not impact germination. This suggests evolved species-specific mechanisms for polymicrobial interactions and evidence for further investigation into these relationships.

**6.3.1 Potential *R. microsporus* and *S. aureus* cooperation.** *S. aureus* acts synergistically with *C. albicans*, and binding of *S. aureus* to fungal hyphae promotes deeper penetration of the bacterium into tissues (Schlecht *et al.*, 2015). Here, co-culture of *R. microsporus* and *S. aureus* resulted in bacterial attachment to germinating hyphae. Given that co-infections between *S. aureus* and Mucorales have been reported (Stasiak *et al.*, 2009), it is possible that this relationship could promote bacterial dissemination. Further experiments could investigate the impact of *S. aureus* co-infection with *R. microsporus in vivo* to determine if they synergise inside the host. *S. aureus* commonly colonises the

nasal cavity (Kluytmans, Van Belkum and Verbrugh, 1997) and mucormycosis most commonly presents in the sinuses (Roden *et al.*, 2005). Clinical correlation studies between rhinocerebral mucormycosis and colonisation of *S. aureus* would be interesting to understand if these carriers are more likely to die from the fungal infection.

**6.3.2 *R. microsporus*, QSMs, and toxins.** Investigating the source of inhibition within *P. aeruginosa* supernatant revealed bacterial QSMs and the toxin pyocyanin do not regulate *R. microsporus* germination. C12 HSL inhibits *C. albicans* filamentation by inhibiting the cAMP pathway (Hall *et al.*, 2011), and the lack of total inhibition when exposed to QSMs indicates a different pathway regulating *R. microsporus* germination. While C12 HSL inhibits *Aspergillus spp.*, the mode of action of is unknown (Briard *et al.*, 2019). Germination of *A. fumigatus* is not regulated by the PKA-dependent cAMP pathway, and is instead thought to be mediated by ras/MAPK signalling (Osherov and May, 2000). Therefore, it is possible that C12 HSL could act on this pathway in *A. fumigatus*. As *C. albicans* filamentation is also regulated by MAPK signalling (Monge *et al.*, 2006), it would be worth investigating whether cAMP or ras/MAPK signalling are involved in Mucoralean polymicrobial interactions. Farnesol, the QSM produced by *C. albicans*, delays germination but does not completely inhibit. Because farnesol autoinhibition is also regulated by cAMP (Davis-Hanna *et al.*, 2008), it is possible that live cell imaging of spores exposed to *P. aeruginosa* QSMs could reveal delayed germination, which is eventually overcome before endpoint measurement. As QSMs act as an inter- and intra-species communication

mechanism, the ability of *R. microsporus* to overcome high concentrations of QSMs could indicate an evolutionary defence. It would be interesting to see if this is a general trait of Mucorales, and if not, whether this correlates with rate of clinical infections.

*R. microsporus* is also resistant to pyocyanin. This is surprising, as *C. albicans*, *C. tropicalis*, *C. neoformans*, *A. fumigatus*, and *A. niger* are all sensitive to pyocyanin (Abdul-hussein and Atia, 2016), and phenazines are known to modulate redox homeostasis (Briard *et al.*, 2015; Hall *et al.*, 2016). The accumulation of intracellular ROS occurs during *R. delemar* hyphal growth (Sephton-Clark *et al.*, 2018). This indicates that ROS generation is a natural part of Mucoralean germination, and perhaps this explains why *R. microsporus* is resistant to pyocyanin. Further work could investigate ROS production in *R. microsporus* during pyocyanin exposure to understand the impact on oxidative stress in Mucorales.

Taken together, this study has demonstrated the ability of *R. microsporus* to participate in polymicrobial interactions with other opportunistic pathogens, and these relationships are variable, dynamic, and specialised.

#### **6.4 Impact of polymicrobial interactions on the host.**

Polymicrobial interactions can have a devastating impact on the progression of infectious diseases in a host. For instance, co-infection with *P. aeruginosa* and *A. fumigatus* in CF is associated with a more severe outcome and poorer

management of disease (Reece *et al.*, 2017). Furthermore, the presence of fungi within a polymicrobial chronic wound promotes stable, cross-kingdom biofilms and are associated with slower healing and necrosis (Kalan *et al.*, 2016). Therefore, understanding the impact of co-infection with *R. microsporus* and *P. aeruginosa* on host response and outcome was important to understand the clinical relevance of this interaction.

#### **6.4.1 Comparing human and zebrafish iron-sequestering proteins.**

Nutritional immunity is a host defence used to restrict essential metal nutrients from pathogens to prevent their successful growth (Weinberg, 1975). This is a common phenomenon amongst vertebrates, where metals are tightly sequestered in the serum and within tissues bound to specific proteins (Hennigar and McClung, 2016). Using the Basic Alignment Search Tool (BLAST), *Danio rerio* and *Homo sapiens* were found to contain homologous proteins related to nutritional immunity, making the zebrafish a valid model to study the relationship between *R. microsporus* and *P. aeruginosa in vivo* (Table 6.1, Altschul *et al.*, 1990). These proteins included the iron-transporter transferrin, the oxygen/carbon dioxide transporter haemoglobin, the phagosome associated metal transporter NRAMP1 (natural resistance associated macrophage protein 1), and the iron storage protein ferritin (Hood and Skaar, 2012). These similarities suggest that both organisms utilise similar mechanisms to restrict iron from microorganisms. As this study determined that the interaction between *R. microsporus* and *P. aeruginosa* was mediated by iron competition, zebrafish were a valid model for co-infection with *R. microsporus* and *P. aeruginosa*.

**Table 6.1 Homology of nutritional-immunity related proteins in *Homo sapiens* and *Danio rerio* using the BLAST. (Altschul *et al.*, 1990)**

Name	Percent Similarity
Transferrin	42%
Haemoglobin alpha subunit	54%
NRAMP1	70%
Ferritin	79%

**6.4.2 Enhancement of virulence in a co-infection model.** Co-infection in a zebrafish hindbrain injection model revealed enhanced larval mortality when both species were present. Lack of evident fungal growth and limited mortality from the injection with spores alone indicated that the increased death during co-infection was likely attributed to bacterial pathogenicity. This agrees with *in vitro* co-culture data which demonstrated an increased expression of pyoverdine and pyochelin biosynthetic genes and enhanced siderophores in supernatants. Pyoverdine is important for pathogenicity of *P. aeruginosa* (Meyer *et al.*, 1996) and can modulate virulence by regulating the production of toxins such as exotoxin A and endoproteases (Lamont *et al.*, 2002). Therefore, it is possible that the presence of *R. microsporus* in the zebrafish increases the virulence factor production of *P. aeruginosa* and enhances host mortality. Clinically, the presence of *C. albicans* can increase risk of *P. aeruginosa* infection (Azoulay *et al.*, 2006). We predict this could be similar when *R. microsporus* is present. In these scenarios, increased *P. aeruginosa* virulence would be a by-product of microbial competition.

As *P. aeruginosa* inhibits *R. microsporus* germination *in vitro*, we speculate that the presence of both microbes within a wound, for example, could mask fungal presence and enhance *P. aeruginosa* pathogenicity (Figure 6.1). This is opposite to zebrafish co-infections with *P. aeruginosa* and *C. albicans*, where *P. aeruginosa* enhances fungal germination and virulence *in vivo* (Bergeron *et al.*, 2017). In a murine model, *C. albicans* decreases the virulence and bacterial burden of *P. aeruginosa* by reducing the biosynthesis of pyoverdine and pyochelin (Lopez-Medina *et al.*, 2015).

Together, our results and evidence from the literature indicate a dynamic relationship between *P. aeruginosa* and different fungal species, where *P. aeruginosa* forms cooperative or competitive relationships depending on the situation and the fungus involved. Furthermore, it highlights the importance of siderophores in infection scenarios and the enhanced aggressiveness of polymicrobial infections.

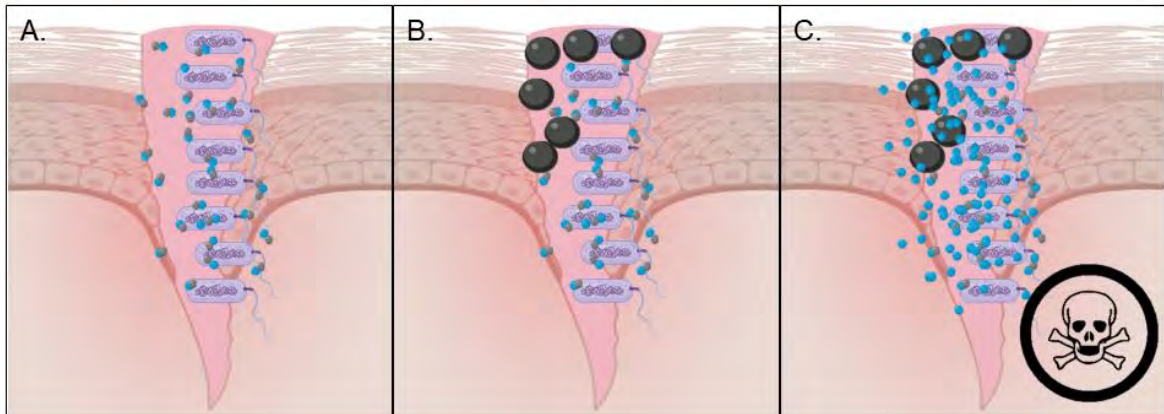


**Figure 6.1 Proposed clinical scenario where *R. microsporus* enhances *P. aeruginosa* virulence. (A)** A wound becomes infected with *P. aeruginosa*. *P. aeruginosa* secretes a plethora of molecules, including pyoverdine (blue spheres). Pyoverdine binds any available iron (grey spheres) in the area. **(B)** If *R. microsporus* spores (large spheres) enter the wound from the environment, there is no iron available, and the spores do not germinate. **(C)** However, the presence of *R. microsporus* enhances *P. aeruginosa* pyoverdine production which leads to enhanced virulence factor production and poorer patient prognosis. Not to scale.

**6.4.3 Antifungal resistance.** Interestingly, exposure to *P. aeruginosa* supernatant cultured under iron replete conditions increased *R. microsporus* sensitivity to amphotericin B and posaconazole, which are first-line and salvage therapies, respectively, for mucormycosis (Spellberg and Ibrahim, 2010). Susceptibility to amphotericin B varies between species and strains (Vitale *et al.*, 2012), and the resulting high concentrations and prolonged treatment can lead to nephrotoxicity (Fanos and Cataldi, 2000). In our study, the growth of *R. microsporus* was inhibited upon exposure to very low concentrations of amphotericin B (0.0155  $\mu\text{g/ml}$ ) when treated with *P. aeruginosa* supernatant.

Furthermore, treatment with supernatants induced posaconazole susceptibility, even though this strain was initially resistant to posaconazole. Amphotericin B creates pores in the fungal cell membrane after binding to ergosterol (Finkelstein and Holz, 1973) and posaconazole inhibits ergosterol synthesis (Hof, 2006). Therefore, it is possible that compounds present in the *P. aeruginosa* supernatant weaken the cell membrane themselves, enhance antifungal binding to membrane targets, or increase the drug activity after binding. Furthermore, recent studies have suggested that oxidative stress induced by amphotericin B attributes to the fungicidal activity in *A. fumigatus* (Shekhova, Kniemeyer and Brakhage, 2017). Perhaps the supernatant increases *R. microsporus* sensitivity to ROS. Identifying the factor(s) within the supernatant that enhances antifungal sensitivity could lead to novel adjunct therapies, reducing the dosage of amphotericin B or posaconazole needed to control infection. It is unclear as to whether the supernatant is inducing sensitivity to general stressors or specifically to antifungals, and this needs further experimentation.

Altogether, preliminary data indicates that patient management and host outcome could be impacted by co-infection with *R. microsporus* and *P. aeruginosa*.

## **6.5 Clinical implications: patient management.**

Beyond the previously discussed implications of this research, we propose a hypothetical clinical model (Figure 6.2). In our theorised model, a patient has a wound that becomes infected with *P. aeruginosa*. As the bacteria multiply, they secrete various metabolites, toxins, and molecules, including pyoverdine (Figure

6.2A). If this were a burn wound, pyoverdine production would be even greater, as biosynthesis is enhanced when exposed to burn wound exudate (Gonzalez *et al.*, 2018). Pyoverdine binds any available iron within the area, and if *R. microsporus* spores come into contact with the wound, germination would be inhibited due to lack of iron (Figure 6.2B). However, if the wound is treated with antibiotics and the *P. aeruginosa* is successfully removed, the spores no longer have the bacterial pressure (Figure 6.2C). This could lead to fungal germination and an aggressive secondary infection (Figure 6.2D). There is an example in the literature of the opposite occurring, where antifungal treatment of a *C. albicans* infection led to a *P. aeruginosa* infection (Nseir *et al.*, 2007). This is evidence that the pressures of microbial competition can control infection, and release of these pressures can result in secondary infection.

## 6.6 Future work.

**6.6.1 Host-pathogen interactions.** The zebrafish infection model is a powerful system for investigating host response to infections and could be utilised more extensively to examine *P. aeruginosa* and *R. microsporus* co-infections. Future experiments could measure changes in macrophage/neutrophil recruitment to the infection site in mono- versus co-infections. It would also be prudent to develop a technique for determining whether *R. microsporus* germinates within the zebrafish hindbrain during co-infection. Confocal microscopy has been used to determine *in vivo* filamentation of *C. albicans* (Brothers, Newman and Wheeler, 2011). However, acquiring fluorescent Mucoralean spores is difficult due to lack of genetic manipulability, though techniques are improving for *M. circinelloides*

and *R. delemar* with the development of CRISPR-Cas9 systems (Nagy *et al.*, 2017; Binder *et al.*, 2018; Vellanki *et al.*, 2018; Bruni *et al.*, 2019). Determining changes in genes associated with germination could be a promising avenue. Transcriptional regulation of genes associated with hyphal growth have been studied and provide promising targets to molecularly identify germination, such as actin and delta-9 desaturase expression (Sephton-Clark *et al.*, 2018).

As most mucormycosis occurs in immunocompromised individuals, co-infections following corticosteroid treatment of the fish could be a better model for understanding the impact on a host. Glucocorticoid treatment reduces pro-inflammatory transcriptional changes and neutrophil migration in zebrafish (Chatzopoulou *et al.*, 2016). *M. circinelloides* mounts a more aggressive infection following dexamethasone treatment (Voelz, Gratacap and Wheeler, 2015), and *R. microsporus* is likely similar. It would also be interesting to investigate how the use of antibiotics or antifungals impacts co-infection outcome, and previous studies have demonstrated the ability of antibiotics added to the water to reduce bacterial burden in zebrafish (Fehr *et al.*, 2015). Ideally, development of mammalian co-infection models would occur following zebrafish characterisation.

The fungal cell wall is the first point of contact with the host immune system and cell wall components can modulate host response (Wang, Aisen and Casadevall, 1995; Jawhara *et al.*, 2012; Wagener *et al.*, 2014). The presence of cell wall chitin in early timepoints following exposure to *P. aeruginosa* supernatant was

investigated in this study, where we found a decrease in total chitin which was likely associated to decreased spore swelling. Examining the impact of *P. aeruginosa* on  $\beta$ -glucan, melanin, and chitosan could give further clues into how this relationship affects the interaction between *R. microsporus* and the host.

Further experiments investigating host-pathogen interactions could include *in vitro* phagocytosis assays with co-culture or supernatant-treated spores to observe changes in macrophage or neutrophil ability to engulf spores. As treatment with *P. aeruginosa* supernatants is predicted to alter cell membrane sensitivity to antifungals, perhaps spores would be more sensitive to intracellular killing by phagocytic cells. Furthermore, looking at changes in cytokine expression *in vitro* and comparing this to *in vivo* expression in the zebrafish model could further indicate alterations in host inflammatory response during co-infection.

**6.6.2 Relationships with opportunistic bacteria.** While this study focused on the impact of *P. aeruginosa* on *R. microsporus* virulence, future work could further investigate the response of *P. aeruginosa* to the fungus, looking at any changes in growth and viability, and the expression of other virulence factors beyond pyoverdine and pyochelin, such as exotoxin A, pyocyanin, proteases, as well as the expression of contact-dependent secretion systems like T3SS and T6SS.

While we hypothesise a cooperative relationship between *R. microsporus* and *S. aureus* and/or *E. coli*, further investigation into these relationships are warranted. Time-lapse microscopy would help observe whether the presence of the bacteria impacts the speed of *R. microsporus* germination, and histological studies of mammalian models could indicate changes in bacterial or fungal tissue penetration. Zebrafish models could be used to observe bacterial dissemination during co-infection. Furthermore, as concurrent aspergillosis and mucormycosis have been described in the literature (Gupta *et al.*, 2014; Pouvaret *et al.*, 2019), investigating the interaction between these invasive fungal pathogens would be an interesting, clinically relevant avenue. As Mucorales are ubiquitous environmental organisms, there are countless organisms that would warrant investigation into polymicrobial relationships. Through increased awareness of Mucorales and of the potential for polymicrobial interactions to exacerbate disease, perhaps data regarding co-isolations will increase and clinically relevant targets of Mucoralean polymicrobial research will become clearer.

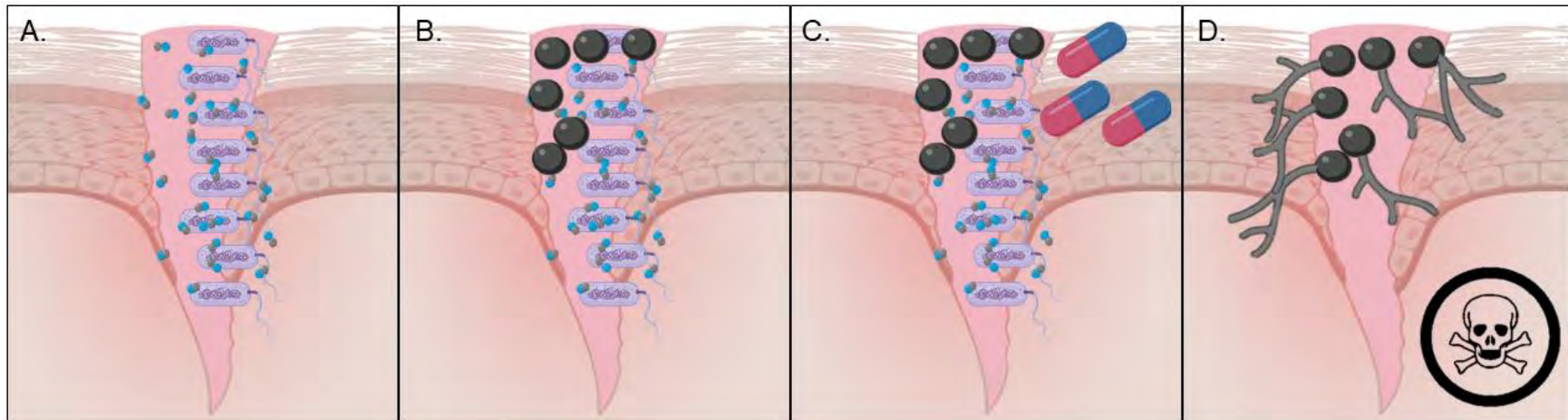


**Figure 6.2 Hypothetical clinical model of *P. aeruginosa* and *R. microsporus* interaction.** In this scenario, **(A)** A wound becomes infected with *P. aeruginosa*. *P. aeruginosa* secretes a plethora of molecules, including pyoverdine (blue spheres). Pyoverdine binds any available iron (grey spheres) in the area. **(B)** If *R. microsporus* spores (large spheres) enter the wound from the environment, there is no iron available, and the spores do not germinate. **(C)** Antibiotic treatment would remove *P. aeruginosa* **(D)** With the iron-dependent pressure removed, *R. microsporus* could germinate, penetrate surrounding tissues, and lead to aggressive infection. Not to scale.

## 6.7 Concluding remarks

Mucormycosis is a devastating infection with an unacceptably high mortality rate and a lack of effective treatment options. Here we have identified a novel mechanism for iron starvation, and further confirmed Mucorales' dependency on environmental iron for full virulence. Through this, our work has identified a potential starting point for the development of new chelation therapies. We have also demonstrated the importance of studying the interactions between microorganisms, and how these relationships can impact pathogenicity. While Mucorales might be lying dormant within a niche, it could still have strong effects on the virulence of other organisms who might sense it and respond aggressively. Further, treatment of an overt *P. aeruginosa* infection might release siderophore-mediated growth inhibition and leave a patient vulnerable to secondary fungal infection.

We live in a world filled with microorganisms that are forming their own community structures, complete with competitive and cooperative relationships. As human communities can impact those surrounding them, microbial relationships strongly influence the health of their hosts. When these quiet relationships become overt, humans can suffer. While the acknowledgement of the impact of polymicrobial interactions is growing, increasing the awareness of these relationships in the medical field is paramount to gaining a holistic understanding of infectious disease.

The world is not in your books and maps,  
it's out there

*Gandalf*

*The Lord of the Rings*

*J. R. R. Tolkien*

## List of References

Abbaspour, N., Hurrell, R. and Kelishadi, R. (2014) 'Review on iron and its importance for human health', *Journal of Research in Medical Sciences*, pp. 164–174. doi: 23914218.

Abdul-hussein, Z. R. and Atia, S. S. (2016) 'Antimicrobial effect of pyocyanin extracted from *Pseudomonas aeruginosa*', *Eur J Exp Bio*, 6, p. 6.

Abe, F. *et al.* (1990) 'Effects of iron and desferrioxamine on *Rhizopus* infection', *Mycopathologia*, 100(2), pp. 87–91.

Adam, B., Baillie, G. S. and Douglas, L. J. (2002) 'Mixed species biofilms of *Candida albicans* and *Staphylococcus epidermidis*', *Journal of Medical Microbiology*, 51(4), pp. 344–349. doi: 10.1099/0022-1317-51-4-344.

Akers, K. S. *et al.* (2014) 'Biofilms and persistent wound infections in United States military trauma patients: A case-control analysis', *BMC Infectious Diseases*, 14(1). doi: 10.1186/1471-2334-14-190.

Akhrass, F. Al *et al.* (2011) 'Palatal mucormycosis in patients with hematologic malignancy and stem cell transplantation', *Medical Mycology*, 49(4), pp. 400–405. doi: 10.3109/13693786.2010.533391.

Albrecht-Gary, A. M. *et al.* (1994) 'Bacterial iron transport: Coordination properties of pyoverdinin PaA, a peptidic siderophore of *Pseudomonas aeruginosa*', *Inorganic Chemistry*, 33(26), pp. 6391–6402. doi: 10.1021/ic00104a059.

Alexander Fleming (1929) 'On the antibacterial action of cultures of a *Penicillium*, with special reference to their use in the isolation of *B. influenzae*', *British Journal of Experimental Pathology*, 10(3), pp. 226–236.

Alhassan, S. and Thirumala, R. (2015) 'An unusual case of disseminated mucormycosis', *CHEST*. Elsevier, 148(4), p. 86A. doi: 10.1378/chest.2275578.

Allen, L. *et al.* (2005) 'Pyocyanin production by *Pseudomonas aeruginosa* induces neutrophil apoptosis and impairs neutrophil-mediated host defenses *in vivo*', *The Journal of Immunology*, 174, pp. 3643–3649. doi: 10.4049/jimmunol.174.6.3643.

Alonso Monge, R. *et al.* (2006) 'The MAP kinase signal transduction network in *Candida albicans*', *Microbiology*, 152(Pt 4), pp. 905–912. doi: 10.1099/mic.0.28616-0.

Altschul, S. F. *et al.* (1990) 'Basic local alignment search tool', *Journal of Molecular Biology*, 215(3), pp. 403–410. doi: 10.1016/S0022-2836(05)80360-2.

Andrianaki, A. M. *et al.* (2018) 'Iron restriction inside macrophages regulates pulmonary host defense against *Rhizopus* species', *Nature Communications*, 9, p. 3333. doi: 10.1038/s41467-018-05820-2.

Angebault, C. *et al.* (2016) 'Prospective evaluation of serum  $\beta$ -glucan testing in

patients with probable or proven fungal diseases', *Open Forum Infectious Diseases*, 3(3), p. ofw128. doi: 10.1093/ofid/ofw128.

Antinori, S. *et al.* (2009) 'Trends in the postmortem diagnosis of opportunistic invasive fungal infections in patients with AIDS: A retrospective study of 1,630 autopsies performed between 1984 and 2002', *American Journal of Clinical Pathology*, 132(2), pp. 221–227. doi: 10.1309/AJCPRAAE8LZ7DTNE.

Artis, W. M. *et al.* (1982) 'A mechanism of susceptibility to mucormycosis in diabetic ketoacidosis: Transferrin and iron availability', *Diabetes*, 31(12), pp. 1109–1114. doi: 10.2337/diabetes.31.12.1109.

Asleson, C. M. *et al.* (2000) 'Filamentous growth of *Saccharomyces cerevisiae* is regulated by manganese.', *Fungal genetics and Biology*, 30(2), pp. 155–62. doi: 10.1006/fgbi.2000.1214.

Atreja, A. and Kalra, S. (2015) 'Infections in diabetes', *Journal of the Pakistan Medical Association*, 65(9), pp. 1028–1030.

Azoulay, E. *et al.* (2006) '*Candida* colonization of the respiratory tract and subsequent *Pseudomonas* ventilator-associated pneumonia', *Chest*, 129(1), pp. 110–117. doi: 10.1378/chest.129.1.110.

Baker, R. (1957) 'Mucormycosis; a new disease?', *J Am Med Assoc*, 163(10), pp. 805–808.

Bakker-Woudenberg, I. A. J. M. *et al.* (1985) 'Relevance of serum protein binding of cefoxitin and cefazolin to their activities against *Klebsiella pneumoniae* pneumonia in rats', *Antimicrobial Agents and Chemotherapy*, 28(5), pp. 654–659. doi: 10.1128/AAC.28.5.654.

Baldin, C. *et al.* (2018) 'PCR-based approach targeting Mucorales-specific gene family for diagnosis of mucormycosis', *Journal of Clinical Microbiology*, 56(10), pp. e00746-18. doi: 10.1128/jcm.00746-18.

Balestrino, D. *et al.* (2005) 'Characterization of type 2 quorum sensing in *Klebsiella pneumoniae* and relationship with biofilm formation', *Society*, 187(8), pp. 2870–2880. doi: 10.1128/JB.187.8.2870.

Balzola, F. *et al.* (2011) 'The role of *Candida* in inflammatory bowel disease. Estimation of transmission of *C. albicans* fungi in gastrointestinal tract based on genetic affinity between strains', *Inflammatory Bowel Disease Monitor*, 16(10), pp. CR451-7.

Bartnicki-Garcia, S. *et al.* (1995) 'Evidence that Spitzenkörper behavior determines the shape of a fungal hypha: A test of the hyphoid model', *Experimental Mycology*, 19(2), pp. 153–159. doi: 10.1006/emyc.1995.1017.

Bartnicki-Garcia, S., Nelson, N. and Cota-Robles, E. (1968) 'Electron microscopy of spore germination and cell wall formation in *Mucor rouxii*', *Archiv für Mikrobiologie*, 63(3), pp. 242–255. doi: 10.1007/BF00412841.

Bartnicki-Garcia, S. and Reyes, E. (1964) 'Chemistry of spore wall differentiation in *Mucor rouxii*', *Archives of Biochemistry and Biophysics*, 108(1), pp. 125–133.

doi: 10.1016/0003-9861(64)90363-7.

Beauvais, A. *et al.* (2005) 'Two  $\alpha(1-3)$  glucan synthases with different functions in *Aspergillus fumigatus*', *Applied and Environmental Microbiology*, 71(3), pp. 1531–1538. doi: 10.1128/AEM.71.3.1531-1538.2005.

Behzadi, P. *et al.* (2010) 'A survey on urinary tract infections associated with the three most common uropathogenic bacteria.', *Maedica*, 5(2), pp. 111–115.

Berger, S. *et al.* (2017) 'Azole resistance in *Aspergillus fumigatus*: A consequence of antifungal use in agriculture?', *Frontiers in Microbiology*, 8, p. 1024. doi: 10.3389/fmicb.2017.01024.

Bergeron, A. C. *et al.* (2017) '*Candida albicans* and *Pseudomonas aeruginosa* interact to enhance virulence of mucosal infection in transparent zebrafish', *Infection and Immunity*, 85(11). doi: 10.1128/IAI.00475-17.

Binder, U. *et al.* (2018) 'Generation of a *Mucor circinelloides* reporter strain—A promising new tool to study antifungal drug efficacy and mucormycosis', *Genes*, 9(12), p. 613. doi: 10.3390/genes9120613.

Bitar, D. *et al.* (2009) 'Increasing incidence of zygomycosis (mucormycosis), France, 1997-2006', *Emerging Infectious Diseases*, 15(9), pp. 1395–1401. doi: 10.3201/eid1509.090334.

Boelaert, J. R. *et al.* (1993) 'Mucormycosis during deferoxamine therapy is a siderophore-mediated infection: *In vitro* and *in vivo* animal studies', *Journal of Clinical Investigation*, 91(5), pp. 1979–1986. doi: 10.1172/JCI116419.

Bongomin, F. *et al.* (2017) 'Global and multi-national prevalence of fungal diseases—Estimate precision', *Journal of Fungi*, 3(4), p. 57. doi: 10.3390/jof3040057.

Boon, C. *et al.* (2008) 'A novel DSF-like signal from *Burkholderia cenocepacia* interferes with *Candida albicans* morphological transition', *ISME Journal*, 2(1), pp. 27–36. doi: 10.1038/ismej.2007.76.

Boucontet, L. *et al.* (2018) 'A model of superinfection of virus-infected zebrafish larvae: Increased susceptibility to bacteria associated with neutrophil death', *Frontiers in Immunology*, 9, p. 1084. doi: 10.3389/fimmu.2018.01084.

Braga, C. *et al.* (2017) 'Deferasirox associated with liver failure and death in a sickle cell anemia patient homozygous for the -1774delG polymorphism in the *Abcc2* gene', *Clinical Case Reports*, 5(8), pp. 1218–1221. doi: 10.1002/ccr3.1040.

Brannon, M. K. *et al.* (2009) '*Pseudomonas aeruginosa* type III secretion system interacts with phagocytes to modulate systemic infection of zebrafish embryos', *Cellular Microbiology*, 11(5), pp. 755–768. doi: 10.1111/j.1462-5822.2009.01288.x.

Braud, A., Hoegy, F., *et al.* (2009) 'New insights into the metal specificity of the *Pseudomonas aeruginosa* pyoverdine-iron uptake pathway', *Environmental Microbiology*, 11(5), pp. 1079–1091. doi: 10.1111/j.1462-2920.2008.01838.x.

- Braud, A., Hannauer, M., *et al.* (2009) 'The *Pseudomonas aeruginosa* pyochelin-iron uptake pathway and its metal specificity', *Journal of Bacteriology*, 191(11), pp. 3517–3525. doi: 10.1128/JB.00010-09.
- Braz, R. R. and Nahas, E. (2012) 'Synergistic action of both *Aspergillus niger* and *Burkholderia cepacea* in co-culture increases phosphate solubilization in growth medium', *FEMS Microbiology Letters*, 332(1), pp. 84–90. doi: 10.1111/j.1574-6968.2012.02580.x.
- Briard, B. *et al.* (2015) '*Pseudomonas aeruginosa* manipulates redox and iron homeostasis of its microbiota partner *Aspergillus fumigatus* via phenazines', *Scientific Reports*, 5(1), p. 8220. doi: 10.1038/srep08220.
- Briard, B. *et al.* (2019) 'Interactions between *Aspergillus fumigatus* and pulmonary bacteria: current state of the field, new data, and future perspective', *Journal of Fungi*, 5, p. 48. doi: doi:10.3390/jof5020048www.mdpi.com/journal/jof.
- Brillet, K. *et al.* (2012) 'An ABC transporter with two periplasmic binding proteins involved in iron acquisition in *Pseudomonas aeruginosa*', *ACS Chemical Biology*, 7(12), pp. 2036–2045. doi: 10.1021/cb300330v.
- Brown, D. H. *et al.* (1999) 'Filamentous growth of *Candida albicans* in response to physical environmental cues and its regulation by the unique CZF1 gene.', *Molecular microbiology*, 34(4), pp. 651–62. doi: 10.1046/j.1365-2958.1999.01619.x.
- Brown, G. D. *et al.* (2012) 'Hidden killers: Human fungal infections', *Science Translational Medicine*, 4(165), p. 165rv13. doi: 10.1126/scitranslmed.3004404.
- Brugière, O. *et al.* (2005) 'Pulmonary mucormycosis (zygomycosis) in a lung transplant recipient: Recovery after posaconazole therapy.', *Transplantation*, 80(4), pp. 544–545. doi: 10.1097/00007890-200510150-00023.
- Bruni, G. O. *et al.* (2019) 'CRISPR-Cas9 induces point mutation in the mucormycosis fungus *Rhizopus delemar*', *Fungal Genetics and Biology*, 124, pp. 1–7. doi: 10.1016/j.fgb.2018.12.002.
- Buffo, J., Herman, M. a and Soll, D. R. (1984) 'A characterization of pH-regulated dimorphism in *Candida albicans*', *Mycopathologia*, 85(1–2), pp. 21–30. doi: 10.1007/BF00436698.
- Bullen, J. J., Rogers, H. J. and Griffiths, E. (1978) 'Role of iron in bacterial infection.', *Current Topics in Microbiology and Immunology*, 80, pp. 1–35. doi: 10.1007/978-3-642-66956-9\_1.
- van Burik, J. *et al.* (2006) 'Posaconazole is effective as salvage therapy in zygomycosis: a retrospective summary of 91 cases', *Clinical Infectious Diseases*, 42(7), pp. e61-65. doi: 10.1086/500212.
- Bussmann, J. and Raz, E. (2015) 'Chemokine-guided cell migration and motility in zebrafish development', *The EMBO Journal*, 34(10), pp. 1309–1318. doi: 10.15252/embj.201490105.
- Cabral, D. J. *et al.* (2018) 'Microbial competition between *Escherichia coli* and

- Candida albicans* reveals a soluble fungicidal factor', *Microbial Cell*, 5(5), pp. 249–255. doi: 10.15698/mic2018.05.631.
- Cano, V. *et al.* (2014) '*Klebsiella pneumoniae* survives within macrophages by avoiding delivery to lysosomes', *Cell Microbiol*, 17(11), pp. 1537–1560.
- Caramalho, R. *et al.* (2017) 'Intrinsic short-tailed azole resistance in mucormycetes is due to an evolutionary conserved amino acid substitution of the lanosterol 14 $\alpha$ -demethylase', *Scientific Reports*, 7(1), p. 15898. doi: 10.1038/s41598-017-16123-9.
- Carlson, E. (1982) 'Synergistic effect of *Candida albicans* and *Staphylococcus aureus* on mouse mortality.', *Infection and immunity*, 38(3), pp. 921–924.
- Carrano, C. J. and Raymond, K. N. (1979) 'Ferric ion sequestering agents. 2. Kinetics and mechanism of iron removal from transferrin by enterobactin and synthetic tricatechols', *Journal of the American Chemical Society*, 101(18), pp. 5401–5404. doi: 10.1021/ja00512a047.
- Cascales, E. and Cambillau, C. (2012) 'Structural biology of type VI secretion systems', *Philosophical Transactions of the Royal Society B Biological Sciences*, 367(1592), pp. 1102–1111. doi: 10.1098/rstb.2011.0209.
- Castelo-Branco, D. *et al.* (2016) 'Farnesol increases the susceptibility of *Burkholderia pseudomallei* biofilm to antimicrobials used to treat melioidosis', *J Appl Microbiol*, 120(3), pp. 600–6.
- Cézard, C., Farvacques, N. and Sonnet, P. (2015) 'Chemistry and biology of pyoverdines, *Pseudomonas* primary siderophores.', *Current medicinal chemistry*, 22(2), pp. 165–186.
- Chakrabarti, A. and Dhaliwal, M. (2013) 'Epidemiology of mucormycosis in India', *Current Fungal Infection Reports*, 7(4), pp. 287–292. doi: 10.1007/s12281-013-0152-z.
- Chamilos, G. *et al.* (2008) 'Zygomycetes hyphae trigger an early, robust proinflammatory response in human polymorphonuclear neutrophils through toll-like receptor 2 induction but display relative resistance to oxidative damage', *Antimicrobial Agents and Chemotherapy*, 52(2), pp. 722–724. doi: 10.1128/AAC.01136-07.
- Chao, C. C. *et al.* (2010) 'Zebrafish as a model host for *Candida albicans* infection', *Infection and Immunity*, 78(6), pp. 2512–2521. doi: 10.1128/IAI.01293-09.
- Chao, Y. *et al.* (2015) '*Streptococcus pneumoniae* biofilm formation and dispersion during colonization and disease', *Frontiers in Cellular and Infection Microbiology*, 4, p. 194. doi: 10.3389/fcimb.2014.00194.
- Cheng, K. *et al.* (1996) 'Spread of  $\beta$ -lactam-resistant *Pseudomonas aeruginosa* in a cystic fibrosis clinic', *Lancet*, 348(9028), pp. 639–642. doi: 10.1016/S0140-6736(96)05169-0.
- Cheng, S. *et al.* (2013) 'Profiling of *Candida albicans* gene expression during

- intra-abdominal candidiasis identifies biologic processes involved in pathogenesis', *Journal of Infectious Diseases*, 208(9), pp. 1529–1537. doi: 10.1093/infdis/jit335.
- Chibucos, M. C. *et al.* (2016) 'An integrated genomic and transcriptomic survey of mucormycosis-causing fungi', *Nature Communications*, 7, p. 12218. doi: 10.1038/ncomms12218.
- Cho, Y. and Struijk, D. G. (2017) 'Peritoneal dialysis–related peritonitis: Atypical and resistant organisms', *Seminars in Nephrology*, 37(1), pp. 66–76. doi: 10.1016/j.semnephrol.2016.10.008.
- Chougule, A. *et al.* (2015) 'Pulmonary gangrene due to *Rhizopus spp.*, *Staphylococcus aureus*, *Klebsiella pneumoniae* and probable *Sarcina* organisms', *Mycopathologia*. Springer Netherlands, 180(1–2), pp. 131–136. doi: 10.1007/s11046-015-9904-3.
- Christy Hunter, A. *et al.* (2009) 'An unusual ring-A opening and other reactions in steroid transformation by the thermophilic fungus *Myceliophthora thermophila*', *Journal of Steroid Biochemistry and Molecular Biology*, 116(3–5), pp. 171–177. doi: 10.1016/j.jsbmb.2009.05.012.
- Citiulo, F. *et al.* (2012) '*Candida albicans* scavenges host zinc via Pra1 during endothelial invasion', *PLoS Pathogens*, 8(6), p. e1002777. doi: 10.1371/journal.ppat.1002777.
- Clatworthy, A. E. *et al.* (2009) '*Pseudomonas aeruginosa* infection of zebrafish involves both host and pathogen determinants', *Infection and Immunity*, 77(4), pp. 1293–1303. doi: 10.1128/IAI.01181-08.
- Compos-Takaki G.M, Dietrich, S. M. C. and Beakes, G. W. (2014) 'Cytochemistry, ultrastructure and x-ray microanalysis methods applied to cell wall characterization of Mucoralean fungi strains', *Microscopy: advances in scientific research and education*. Edited by A. Mendez-Vilas, pp. 121–127. doi: 10.1016/j.taap.2007.12.028.
- Cordeiro, R. de A. *et al.* (2012) 'Farnesol inhibits in vitro growth of the *Cryptococcus neoformans* species complex with no significant changes in virulence-related exoenzymes', *Veterinary Microbiology*, 159(3–4), pp. 375–380. doi: 10.1016/j.vetmic.2012.04.008.
- Courcol, R. J. *et al.* (1991) 'Effects of iron depletion and sub-inhibitory concentrations of antibodies on siderophore production by *Staphylococcus aureus*', *The Journal of antimicrobial chemotherapy*, 28, pp. 663–668.
- Cox, C. D. and Adams, P. (1985) 'Siderophore activity of pyoverdinin for *Pseudomonas aeruginosa*', *Infection and Immunity*, 48(1), pp. 130–138.
- Cox, C. D. and Graham, R. (1979) 'Isolation of an iron binding compound from *Pseudomonas aeruginosa*', *Journal of Bacteriology*, 137(1), pp. 357–364.
- Crull, M. R. *et al.* (2016) 'Change in *Pseudomonas aeruginosa* prevalence in cystic fibrosis adults over time', *BMC Pulmonary Medicine*, 16(1), p. 176. doi:

10.1186/s12890-016-0333-y.

Cuív, P. Ó. *et al.* (2007) 'FoxB of *Pseudomonas aeruginosa* functions in the utilization of the xenosiderophores ferrichrome, ferrioxamine B, and schizokinen: Evidence for transport redundancy at the inner membrane', *Journal of Bacteriology*, 189(1), pp. 284–287. doi: 10.1128/JB.01142-06.

Cuív, P. Ó., Clarke, P. and O'Connell, M. (2006) 'Identification and characterization of an iron-regulated gene, *chtA*, required for the utilization of the xenosiderophores aerobactin, rhizobactin 1021 and schizokinen by *Pseudomonas aeruginosa*', *Microbiology*, 152(Pt 4), pp. 945–954. doi: 10.1099/mic.0.28552-0.

Dannaoui, E. (2017) 'Antifungal resistance in mucorales', *International Journal of Antimicrobial Agents*. doi: 10.1016/j.ijantimicag.2017.08.010.

Dao, K.-H. T. *et al.* (1990) 'Pyoverdine production by *Pseudomonas aeruginosa* exposed to metals or an oxidative stress agent', *Faculty Publications in the Biological Sciences*, 9(2), p. 274.

Darling, P. *et al.* (1998) 'Siderophore production by cystic fibrosis isolates of *Burkholderia cepacia*', *Infection and Immunity*, 66(2), pp. 874–877.

Datta, S. *et al.* (2012) 'A ten year analysis of multi-drug resistant blood stream infections caused by *Escherichia coli* & *Klebsiella pneumoniae* in a tertiary care hospital', *Indian J Med Res*, 135(6), pp. 907–912.

Davis-Hanna, A. *et al.* (2008) 'Farnesol and dodecanol effects on the *Candida albicans* Ras1-cAMP signalling pathway and the regulation of morphogenesis', *Molecular Microbiology*, 67(1), pp. 47–62. doi: 10.1111/j.1365-2958.2007.06013.x.

Davis, J. M. *et al.* (2002) 'Real-time visualization of *Mycobacterium*-macrophage interactions leading to initiation of granuloma formation in zebrafish embryos', *Immunity*, 17(6), pp. 693–702. doi: 10.1016/S1074-7613(02)00475-2.

Davis, J. M. *et al.* (2016) 'A zebrafish model of cryptococcal infection reveals roles for macrophages, endothelial cells, and neutrophils in the establishment and control of sustained fungemia', *Infection and Immunity*, 84(10), pp. 3047–3062. doi: 10.1128/iai.00506-16.

Deacon, J. (2006) *Fungal Biology: 4th Edition*. Blackwell Publishing. doi: 10.1002/9781118685068.

Delic-Attree, I. *et al.* (1996) 'Isolation of an IHF-deficient mutant of a *Pseudomonas aeruginosa* mucoid isolate and evaluation of the role of IHF in *algD* gene expression', *Microbiology*, 142(Pt 10), pp. 2785–2793. doi: 10.1099/13500872-142-10-2785.

Denning, D. W. (2015) 'The ambitious "95-95 by 2025" roadmap for the diagnosis and management of fungal diseases', *Thorax*. doi: 10.1136/thoraxjnl-2015-207305.

Diamond, R. D. *et al.* (1978) 'Damage to hyphal forms of fungi by human

leukocytes in vitro. A possible host defense mechanism in aspergillosis and mucormycosis', *Am J Pathol*, 91(2), pp. 313–328. Available at: <http://www.ncbi.nlm.nih.gov/pubmed/347942>.

Diamond, R. D. and Clark, R. A. (1982) 'Damage to *Aspergillus fumigatus* and *Rhizopus oryzae* hyphae by oxidative and nonoxidative microbicidal products of human neutrophils *in vitro*', *Infection and Immunity*, 38(2), pp. 487–495.

Dimaka, K. *et al.* (2014) 'Chronic rhinocerebral mucormycosis: A rare case report and review of the literature', *Mycoses*, 57(11), pp. 699–702. doi: 10.1111/myc.12219.

Dogra, V. *et al.* (2015) 'Trilogy of sequential infections in a diabetic male.', *Respirology case reports*, 3(4), pp. 155–8. doi: 10.1002/rcr2.132.

Droby, S. *et al.* (2016) 'The science, development, and commercialization of postharvest biocontrol products', *Postharvest Biology and Technology*, 122, pp. 22–29. doi: 10.1016/j.postharvbio.2016.04.006.

Dunn, M. *et al.* (2006) 'Compendium of soil fungi', *Taxon*, 59(5). doi: 10.2307/1220704.

von Eiff, C. *et al.* (2001) 'Nasal carriage as a source of *Staphylococcus aureus* bacteremia: Study Group.', *The New England journal of medicine*, 344(1), pp. 11–16. doi: 10.1056/NEJM200101043440102.

Endo, A., Kuroda, M. and Tsujita, Y. (1976) 'ML-236A, ML-236B, and ML-236C, new inhibitors of cholesterol synthesis produced by *Penicillium citrinum*.', *The Journal of Antibiotics*, 29(12), pp. 1346–1348.

Etherington, C. *et al.* (2014) 'The role of respiratory viruses in adult patients with cystic fibrosis receiving intravenous antibiotics for a pulmonary exacerbation', *Journal of Cystic Fibrosis*, 13(1), pp. 49–55. doi: 10.1016/j.jcf.2013.06.004.

Falci, D. R., Da Rosa, F. B. and Pasqualotto, A. C. (2015) 'Comparison of nephrotoxicity associated to different lipid formulations of amphotericin B: A real-life study', *Mycoses*. doi: 10.1111/myc.12283.

Fanos, V. and Cataldi, L. (2000) 'Amphotericin B-induced nephrotoxicity: A review', *Journal of Chemotherapy*, 12(6), pp. 463–470. doi: 10.1179/joc.2000.12.6.463.

Fehr, A. G. J. *et al.* (2016) 'A zebrafish model for *Chlamydia* infection with the obligate intracellular pathogen *Waddlia chondrophila*', *Frontiers in Microbiology*, 7, p. 1829. doi: 10.3389/fmicb.2016.01829.

Ferreira, J. A. G. *et al.* (2015) 'Inhibition of *Aspergillus fumigatus* and its biofilm by *Pseudomonas aeruginosa* is dependent on the source, phenotype and growth conditions of the bacterium', *PLoS ONE*, 10(8). doi: 10.1371/journal.pone.0134692.

Filkins, L. M. *et al.* (2015) 'Coculture of *Staphylococcus aureus* with *Pseudomonas aeruginosa* drives *S. aureus* towards fermentative metabolism and reduced viability in a cystic fibrosis model', *Journal of Bacteriology*, 197, pp.

2252–2264. doi: 10.1128/jb.00059-15.

Finkelstein, A. and Holz, R. (1973) 'Aqueous pores created in thin lipid membranes by the antibiotics nystatin and amphotericin B', *Drugs and Transport Processes*, 2, pp. 377–408. doi: 10.1007/978-1-349-02273-1\_14.

Fisher, K. E. and Roberson, R. W. (2016a) 'Fungal hyphal growth – Spitzenkörper versus apical vesicle crescent', *Fungal Genomics and Biology*, 6(1), p. 136. doi: 10.4172/2165-8056.1000136.

Fisher, K. E. and Roberson, R. W. (2016b) 'Hyphal tip cytoplasmic organization in four zygomycetous fungi', *Mycologia*, 108(3), pp. 533–542. doi: 10.3852/15-226.

Fisher, M. C. *et al.* (2012) 'Emerging fungal threats to animal, plant and ecosystem health.', *Nature*. doi: 10.1038/nature10947.

Fontaine, T. *et al.* (2000) 'Molecular organization of the alkali-insoluble fraction of *Aspergillus fumigatus* cell wall', *Journal of Biological Chemistry*, 275(36), pp. 27594–27607. doi: 10.1074/jbc.M909975199.

Forsberg, K. *et al.* (2019) '*Candida auris*: The recent emergence of a multidrug-resistant fungal pathogen.', *Medical mycology*, 57(1), pp. 1–12. doi: 10.1093/mmy/myy054.

Foster, J. and Waksman, S. (1939) 'The specific effect of zinc and other heavy metals on growth and fumaric-acid production by *Rhizopus*'.

Foster, T. J. and Höök, M. (1998) 'Surface protein adhesins of *Staphylococcus aureus*', *Trends in Microbiology*, 6(12), pp. 484–488. doi: 10.1016/S0966-842X(98)01400-0.

Frank, D. N. *et al.* (2009) 'Culture-independent microbiological analysis of Foley urinary catheter biofilms', *PLoS ONE*, 4(11), p. e7811. doi: 10.1371/journal.pone.0007811.

Frater, J. L., Hall, G. S. and Procop, G. W. (2001) 'Histologic features of zygomycosis: Emphasis on perineural invasion and fungal morphology', *Archives of Pathology and Laboratory Medicine*, 125(3), pp. 375–378.

Fu, Y. *et al.* (2004) 'Cloning and functional characterization of the *Rhizopus oryzae* high affinity iron permease (rFTR1) gene', *FEMS Microbiology Letters*, 235(1), pp. 169–176. doi: 10.1016/j.femsle.2004.04.031.

Garcia de la Torre, M. *et al.* (1985) '*Klebsiella* bacteremia: An analysis of 100 episodes', *Reviews of Infectious Diseases*, 7(2), pp. 143–150. doi: 10.1093/clinids/7.2.143.

Gebremariam, T. *et al.* (2014) 'CotH3 mediates fungal invasion of host cells during mucormycosis', *Journal of Clinical Investigation*, 124(1), pp. 237–250. doi: 10.1172/JCI71349.

Gebremariam, T. *et al.* (2019) 'Anti-CotH3 antibodies protect mice from mucormycosis by prevention of invasion and augmenting opsonophagocytosis',

*Science Advances*, 5(6), p. eaaw1327.

Ghysels, B. *et al.* (2004) 'FpvB, an alternative type I ferripyoverdine receptor of *Pseudomonas aeruginosa*', *Microbiology*, 150(6), pp. 1671–1680. doi: 10.1099/mic.0.27035-0.

Ghysels, B. *et al.* (2005) 'The *Pseudomonas aeruginosa* pir A gene encodes a second receptor for ferrienterobactin and synthetic catecholate analogues', *FEMS Microbiology Letters*, 246(2), pp. 167–174. doi: 10.1016/j.femsle.2005.04.010.

Gibson, J., Sood, A. and Hogan, D. A. (2009) '*Pseudomonas aeruginosa*-*Candida albicans* interactions: Localization and fungal toxicity of a phenazine derivative', *Applied and Environmental Microbiology*, 75(2), pp. 504–513. doi: 10.1128/AEM.01037-08.

Gjødsbøl, K. *et al.* (2006) 'Multiple bacterial species reside in chronic wounds: A longitudinal study', *International Wound Journal*, 3(3). doi: 10.1111/j.1742-481X.2006.00159.x.

Gleissner, B. *et al.* (2004) 'Improved outcome of zygomycosis in patients with hematological diseases?', *Leukemia and Lymphoma*. doi: 10.1080/10428190310001653691.

Goetghebeur, M. *et al.* (2007) 'Methicillin-resistant *Staphylococcus aureus*: A public health issue with economic consequences', *Canadian Journal of Infectious Diseases and Medical Microbiology*, 18(1), pp. 27–34. doi: 10.1155/2007/253947.

Gonzalez, M. *et al.* (2016) 'Effect of human burn wound exudate on *Pseudomonas aeruginosa* virulence', *mSphere*, 1(2), pp. e00111-15. doi: 10.1128/msphere.00111-15.

Gonzalez, M. R. *et al.* (2018) 'Transcriptome analysis of *Pseudomonas aeruginosa* cultured in human burn wound exudates', *Article Front. Cell. Infect. Microbiol*, 8(8), pp. 1–14. doi: 10.3389/fcimb.2018.00039.

Gow, N. A. R., Latge, J.-P. and Munro, C. A. (2017) 'The fungal cell wall: Structure, biosynthesis, and function', *Microbiology Spectrum*, 5(3). doi: 10.1128/microbiolspec.funk-0035-2016.

Granillo, A. R. *et al.* (2015) 'Antibiosis interaction of *Staphylococcus aureus* on *Aspergillus fumigatus* assessed *in vitro* by mixed biofilm formation', *BMC Microbiology*, 15, p. 33. doi: 10.1186/s12866-015-0363-2.

Gratacap, R. L., Bergeron, A. C. and Wheeler, R. T. (2014) 'Modeling mucosal candidiasis in larval zebrafish by swimbladder injection', *Journal of Visualized Experiments*, (93), p. e52182. doi: 10.3791/52182.

Gratacap, R. L., Rawls, J. F. and Wheeler, R. T. (2013) 'Mucosal candidiasis elicits NF- $\kappa$ B activation, proinflammatory gene expression and localized neutrophilia in zebrafish', *Disease Models & Mechanisms*, 6(5), pp. 1260–1270. doi: 10.1242/dmm.012039.

- Graves, B. *et al.* (2016) 'Isavuconazole as salvage therapy for mucormycosis', *Medical Mycology Case Reports*, 11, pp. 36–39. doi: 10.1016/j.mmcr.2016.03.002.
- Griffin, A. S., West, S. A. and Buckling, A. (2004) 'Cooperation and competition in pathogenic bacteria', *Nature*, 430, pp. 1024–1027. doi: 10.1038/nature02744.
- Gupta, V. *et al.* (2014) 'Aspergillus and mucormycosis presenting with normal chest X-ray in an immunocompromised host', *BMJ Case Reports*, 2014, p. bcr2014204022. doi: 10.1136/bcr-2014-204022.
- Haas, H. (2014) 'Fungal siderophore metabolism with a focus on *Aspergillus fumigatus*', *Nat. Prod. Rep.*, 31(10), pp. 1266–1276. doi: 10.1039/C4NP00071D.
- Haldi, M. *et al.* (2006) 'Human melanoma cells transplanted into zebrafish proliferate, migrate, produce melanin, form masses and stimulate angiogenesis in zebrafish', *Angiogenesis*, 9(3), pp. 139–151. doi: 10.1007/s10456-006-9040-2.
- Hall, R. A. *et al.* (2011) 'The quorum-sensing molecules farnesol/homoserine lactone and dodecanol operate via distinct modes of action in *Candida albicans*', *Eukaryotic Cell*, 10(8), pp. 1034–1042. doi: 10.1128/EC.05060-11.
- Hall, S. *et al.* (2016) 'Cellular effects of pyocyanin, a secreted virulence factor of *Pseudomonas aeruginosa*', *Toxins*, 8(8), p. 236. doi: 10.3390/toxins8080236.
- Hallen-Adams, H. E. and Suhr, M. J. (2017) 'Fungi in the healthy human gastrointestinal tract', *Virulence*, 8(3), pp. 352–358. doi: 10.1080/21505594.2016.1247140.
- Harriott, M. M. and Noverr, M. C. (2009) '*Candida albicans* and *Staphylococcus aureus* form polymicrobial biofilms: Effects on antimicrobial resistance', *Antimicrobial Agents and Chemotherapy*, 53(9), pp. 3914–3922. doi: 10.1128/AAC.00657-09.
- Harvie, E. A. *et al.* (2013) 'Innate immune response to *Streptococcus iniae* infection in zebrafish larvae', *Infection and Immunity*, 81(1), pp. 110–121. doi: 10.1128/iai.00642-12.
- Hawksworth, D. L. and Lucking, R. (2017) 'Fungal diversity revisited: 2.2 to 3.8 million species', *The Fungal Kingdom*, 5(4). doi: 10.1128/microbiolspec.funk-0052-2016.
- Hawley, C. A. *et al.* (2013) 'A MAM7 peptide-based inhibitor of *Staphylococcus aureus* adhesion does not interfere with *in vitro* host cell function', *PLoS ONE*, 8(11), p. e81216. doi: 10.1371/journal.pone.0081216.
- Van Der Heijden, M. G. A. *et al.* (1998) 'Mycorrhizal fungal diversity determines plant biodiversity, ecosystem variability and productivity', *Nature*, 396, pp. 69–72. doi: 10.1038/23932.
- Heitman, K. L. and Brasher, W. J. (1971) 'Oral infection due to *Klebsiella pneumoniae* microorganism: case report', *J Periodontol*, 42, pp. 552–554.
- Heller, S. F. *et al.* (2017) 'Amphotericin-impregnated polymethylmethacrylate

- beads as treatment for soft tissue mucormycosis', *Surgery*. doi: <https://doi.org/10.1016/j.surg.2017.03.021>.
- Hennigar, S. R. and McClung, J. P. (2016) 'Nutritional immunity: Starving pathogens of trace minerals', *American Journal of Lifestyle Medicine*, 10(3), pp. 170–173. doi: 10.1177/1559827616629117.
- Herbomel, P., Thisse, B. and Thisse, C. (1999) 'Ontogeny and behaviour of early macrophages in the zebrafish embryo.', *Development (Cambridge, England)*, 126(17), pp. 3735–3745.
- Heymann, P. *et al.* (2002) 'The siderophore iron transporter of *Candida albicans* (Sit1p/Arn1p) mediates uptake of ferrichrome-type siderophores and is required for epithelial invasion', *Infection and Immunity*, 70(9), pp. 5246–5255. doi: 10.1128/IAI.70.9.5246-5255.2002.
- Hill, D. *et al.* (2018) 'Embryonic zebrafish xenograft assay of human cancer metastasis', *F1000Research*, 7, p. 1682. doi: 10.12688/f1000research.16659.1.
- Hitchcock, C. A. *et al.* (2015) 'Interaction of azole antifungal antibiotics with cytochrome P -450-dependent 14 $\alpha$ -sterol demethylase purified from *Candida albicans*', *Biochemical Journal*, 266(2), pp. 475–480. doi: 10.1042/bj2660475.
- Hof, H. (2006) 'A new, broad-spectrum azole antifungal: Posaconazole - Mechanisms of action and resistance, spectrum of activity', *Mycoses*, 49(Suppl 1), pp. 2–6. doi: 10.1111/j.1439-0507.2006.01295.x.
- Hoffmann, K. *et al.* (2013) 'The family structure of the Mucorales: A synoptic revision based on comprehensive multigene-genealogies', *Persoonia*, 30, pp. 57–76. doi: 10.3767/003158513X666259.
- Hogan, D. A. and Kolter, R. (2002) '*Pseudomonas-Candida* interactions: An ecological role for virulence factors', *Science*, 296(5576), pp. 2229–2232. doi: 10.1126/science.1070784.
- Hogan, D. A., Vik, Å. and Kolter, R. (2004) 'A *Pseudomonas aeruginosa* quorum-sensing molecule influences *Candida albicans* morphology', *Molecular Microbiology*, 54(5), pp. 1212–1223. doi: 10.1111/j.1365-2958.2004.04349.x.
- Holcombe, L. J. *et al.* (2010) '*Pseudomonas aeruginosa* secreted factors impair biofilm development in *Candida albicans*', *Microbiology*, 156(5), pp. 1476–1485. doi: 10.1099/mic.0.037549-0.
- Holloway, B. W. (1955) 'Genetic recombination in *Pseudomonas aeruginosa*', *J Gen Microbiol*, 13(3), pp. 572–581. doi: 10.1099/00221287-13-3-572.
- Holmes, G. J. and Stange, R. R. (2007) 'Influence of wound type and storage duration on susceptibility of sweet potatoes to *Rhizopus* soft rot', *Plant Disease*, 86(4), pp. 345–348. doi: 10.1094/pdis.2002.86.4.345.
- HomeOffice (2017) 'Annual statistics of scientific procedures on living animals, Great Britain'.
- Hood, M. I. and Skaar, E. P. (2012) 'Nutritional immunity: transition metals at the

pathogen-host interface.', *Nature reviews. Microbiology*. Nature Publishing Group, 10(8), pp. 525–537. doi: 10.1038/nrmicro2836.

Hood, R. D. *et al.* (2010) 'A type VI secretion system of *Pseudomonas aeruginosa* targets a toxin to bacteria', *Cell Host and Microbe*, 7(1), pp. 25–37. doi: 10.1016/j.chom.2009.12.007.

Hope, W. W., Walsh, T. J. and Denning, D. W. (2005) 'Laboratory diagnosis of invasive aspergillosis', *Lancet Infectious Diseases*. doi: 10.1016/S1473-3099(05)70238-3.

Hornby, J. M. *et al.* (2001) 'Quorum sensing in the dimorphic fungus *Candida albicans* is mediated by farnesol', *Applied and environmental microbiology*, 67(7), pp. 2982–2992. doi: 10.1128/AEM.67.7.2982.

Hosseinioust, Z., Tufenkji, N. and van de Ven, T. G. M. (2013) 'Predation in homogeneous and heterogeneous phage environments affects virulence determinants of *Pseudomonas aeruginosa*', *Applied and Environmental Microbiology*, 79(9), pp. 2862–2871. doi: 10.1128/aem.03817-12.

Hover, T. *et al.* (2016) 'Mechanisms of bacterial (*Serratia marcescens*) attachment to, migration along, and killing of fungal hyphae', *Applied and Environmental Microbiology*, 82(9), pp. 2585–2594. doi: 10.1128/AEM.04070-15.

Howard, R. J. and Aist, J. R. (1979) 'Hyphal tip cell ultrastructure of the fungus *Fusarium*: Improved preservation by freeze-substitution', *Journal of Ultrastructure Research*, 66(3), pp. 224–234. doi: 10.1016/S0022-5320(79)90120-5.

Howe, K. *et al.* (2013) 'The zebrafish reference genome sequence and its relationship to the human genome', *Nature*, 496(7446), pp. 498–503. doi: 10.1038/nature12111.

Humber, R. A. (2012) 'Entomophthoromycota: a new phylum and reclassification for entomophthoroid fungi', *Mycotaxon*, 120, pp. 477–492. doi: 10.5248/120.477.

Hunstad, D. A., Cohen, A. H. and St. Geme, J. W. (1999) 'Successful eradication of mucormycosis occurring in a pulmonary allograft', *Journal of Heart and Lung Transplantation*. doi: 10.1016/S1053-2498(99)00033-9.

Hunter, R. C. and Newman, D. K. (2010) 'A putative ABC transporter, hatABCDE, is among molecular determinants of pyomelanin production in *Pseudomonas aeruginosa*', *Journal of Bacteriology*, 192(22), pp. 5962–5971. doi: 10.1128/JB.01021-10.

Hwang, S. Y. *et al.* (2014) 'Spontaneous fungal peritonitis: A severe complication in patients with advanced liver cirrhosis', *European Journal of Clinical Microbiology and Infectious Diseases*, 33(2), pp. 259–264. doi: 10.1007/s10096-013-1953-2.

Ibrahim, A. S., Bowman, J. C., *et al.* (2005) 'Caspofungin inhibits *Rhizopus oryzae* 1,3- $\beta$ -D-glucan synthase, lowers burden in brain measured by quantitative PCR, and improves survival at a low but not a high dose during murine disseminated zygomycosis', *Antimicrobial Agents and Chemotherapy*, 49(2), pp. 721–727. doi:

10.1128/AAC.49.2.721-727.2005.

Ibrahim, A. S., Spellberg, B., *et al.* (2005) '*Rhizopus oryzae* adheres to, is phagocytosed by, and damages endothelial cells in vitro', *Infection and Immunity*, 73(2), pp. 778–783. doi: 10.1128/IAI.73.2.778-783.2005.

Ibrahim, A. S. *et al.* (2007) 'The iron chelator deferasirox protects mice from mucormycosis through iron starvation', *Journal of Clinical Investigation*, 117(9), pp. 2649–2657. doi: 10.1172/JCI32338.

Ibrahim, A. S. *et al.* (2008) 'Bacterial endosymbiosis is widely present among zygomycetes but does not contribute to the pathogenesis of mucormycosis', *The Journal of Infectious Diseases*, 198(7), pp. 1083–1090. doi: 10.1086/591461.

Ibrahim, A. S. *et al.* (2010) 'The high affinity iron permease is a key virulence factor required for *Rhizopus oryzae* pathogenesis', *Molecular Microbiology*, 77(3), pp. 587–604. doi: 10.1111/j.1365-2958.2010.07234.x.

Ibrahim, A. S. *et al.* (2012) 'Pathogenesis of mucormycosis', *Clinical Infectious Diseases*, 54(SUPPL. 1), pp. 1–7. doi: 10.1093/cid/cir865.

Ibrahim, A. S., Spellberg, B. and Edwards, J. (2008) 'Iron acquisition: a novel perspective on mucormycosis pathogenesis and treatment', *Current Opinion in Infectious Diseases*, 21(6), pp. 620–625. doi: 10.1097/QCO.0b013e3283165fd1.

Inglesfield, S. *et al.* (2018) 'Robust phagocyte recruitment controls the opportunistic fungal pathogen *Mucor circinelloides* in innate granulomas in vivo', *mBio*, 9(2), pp. e02010-17. doi: 10.1128/mbio.02010-17.

Isogai, S., Horiguchi, M. and Weinstein, B. M. (2001) 'The vascular anatomy of the developing zebrafish: An atlas of embryonic and early larval development', *Developmental Biology*, 230(2), pp. 278–301. doi: 10.1006/dbio.2000.9995.

Itabangi, H. *et al.* (2019) 'A bacterial endosymbiont enables fungal immune evasion during fatal mucormycete infection', *bioRxiv*. doi: <https://doi.org/10.1101/584607>.

Jabeen, K. *et al.* (2017) 'Serious fungal infections in Pakistan', *European Journal of Clinical Microbiology and Infectious Diseases*, 36(6), pp. 949–956. doi: 10.1007/s10096-017-2919-6.

Jabra-Rizk, M. A. *et al.* (2006) 'Effect of farnesol on *Staphylococcus aureus* biofilm formation and antimicrobial susceptibility.', *Antimicrob Agents Chemother*, 50(4), pp. 1463–1469.

Jault, C., Pichon, L. and Chluba, J. (2004) 'Toll-like receptor gene family and TIR-domain adapters in *Danio rerio*', *Molecular Immunology*, 40(11), pp. 759–771. doi: 10.1016/j.molimm.2003.10.001.

Jawhara, S. *et al.* (2012) 'Modulation of intestinal inflammation by yeasts and cell wall extracts: Strain dependence and unexpected anti-inflammatory role of glucan fractions', *PLoS ONE*, 7(7), p. e40648. doi: 10.1371/journal.pone.0040648.

- Jeong, W. *et al.* (2019) 'The epidemiology and clinical manifestations of mucormycosis: a systematic review and meta-analysis of case reports', *Clinical Microbiology and Infection*, 25(1), pp. 26–34. doi: 10.1016/j.cmi.2018.07.011.
- Jim, K. K. *et al.* (2016) 'Infection of zebrafish embryos with live fluorescent *Streptococcus pneumoniae* as a real-time pneumococcal meningitis model', *Journal of Neuroinflammation*, 13, p. 188. doi: 10.1186/s12974-016-0655-y.
- Johnston, G. C., Prendergast, J. A. and Singer, R. A. (1991) 'The *Saccharomyces cerevisiae* MYO2 gene encodes an essential myosin for vectorial transport of vesicles', *Journal of Cell Biology*, 113(3), pp. 539–551. doi: 10.1083/jcb.113.3.539.
- Jones, A. M. *et al.* (2004) '*Burkholderia cenocepacia* and *Burkholderia multivorans*: Influence on survival in cystic fibrosis', *Thorax*, 59(11), pp. 948–951. doi: 10.1136/thx.2003.017210.
- Kabir, M. A., Hussain, M. A. and Ahmad, Z. (2012) '*Candida albicans*: a model organism for studying fungal pathogens', *International Scholarly Research Network Microbiology*, 2012, pp. 1–15. doi: 10.5402/2012/538694.
- Kabulski, G. M. and MacVane, S. H. (2018) 'Isavuconazole pharmacokinetics in a patient with cystic fibrosis following bilateral orthotopic lung transplantation', *Transplant Infectious Disease*, 20(3), p. e12878. doi: 10.1111/tid.12878.
- Kahl, B. *et al.* (1998) 'Persistent infection with small colony variant strains of *Staphylococcus aureus* in patients with cystic fibrosis', *The Journal of infectious diseases*, 177(4), pp. 1023–1029.
- Kalan, L. *et al.* (2016) 'Redefining the chronic-wound microbiome: Fungal communities are prevalent, dynamic, and associated with delayed healing', *mBio*, 7(5), pp. 1–12. doi: 10.1128/mBio.01058-16.
- Kang, C. *et al.* (2003) '*Pseudomonas aeruginosa* bacteremia: Risk factors for mortality and influence of delayed receipt of effective antimicrobial therapy on clinical outcome', *Clinical Infectious Diseases*, 37(6), pp. 745–751. doi: 10.1086/377200.
- Kaper, J. B., Nataro, J. P. and Mobley, H. L. (2004) 'Pathogenic *Escherichia coli*', *Nature reviews. Microbiology*, 2(2), pp. 123–140. doi: 10.1038/nrmicro818.
- Karageorgopoulos, D. E. *et al.* (2011) 'β-D-glucan assay for the diagnosis of invasive fungal infections: A meta-analysis', *Clinical Infectious Diseases*. doi: 10.1093/cid/ciq206.
- Katragkou, A., Walsh, T. J. and Roilides, E. (2014) 'Why is mucormycosis more difficult to cure than more common mycoses?', *Clinical Microbiology and Infection*, pp. 74–81. doi: 10.1111/1469-0691.12466.
- Kazak, E. *et al.* (2013) 'A mucormycosis case treated with a combination of caspofungin and amphotericin B', *Journal de Mycologie Medicale*, 23(3), pp. 179–184. doi: 10.1016/j.mycmed.2013.06.003.
- Kennedy, K. J. *et al.* (2016) 'Mucormycosis in Australia: contemporary

- epidemiology and outcomes', *Clinical Microbiology and Infection*, 22(9), pp. 775–781. doi: 10.1016/j.cmi.2016.01.005.
- Kerr, J. R. *et al.* (1999) 'Pseudomonas aeruginosa pyocyanin and 1-hydroxyphenazine inhibit fungal growth.', *Journal of clinical pathology*, 52(5), pp. 385–387.
- Kimmel, C. B. *et al.* (1995) 'Stages of embryonic development of the zebrafish', *Developmental Dynamics*, 303(3), pp. 253–310. doi: 10.1002/aja.1002030302.
- Kipnis, E., Sawa, T. and Wiener-Kronish, J. (2006) 'Targeting mechanisms of Pseudomonas aeruginosa pathogenesis', *Medecine et Maladies Infectieuses*, pp. 78–91. doi: 10.1016/j.medmal.2005.10.007.
- Kisser, M., Kubicek, C. P. and Rohr, M. (1980) 'Influence of manganese on morphology and cell wall composition of Aspergillus niger during citric acid fermentation', *Archives of Microbiology*, 128(1), pp. 26–33. doi: 10.3747/pdi.2011.00058.
- Kline, K. A. *et al.* (2012) 'Immune modulation by Group B Streptococcus influences host susceptibility to urinary tract infection by uropathogenic Escherichia coli', *Infection and Immunity*, 80(12), pp. 4186–4194. doi: 10.1128/IAI.00684-12.
- Kluytmans, J., Van Belkum, A. and Verbrugh, H. (1997) 'Nasal carriage of Staphylococcus aureus: Epidemiology, underlying mechanisms, and associated risks', *Clinical Microbiology Reviews*, 10(3), pp. 505–520.
- Knox, B. P. *et al.* (2014) 'Distinct innate immune phagocyte responses to Aspergillus fumigatus conidia and hyphae in zebrafish larvae', *Eukaryotic Cell*, 13(10), pp. 1266–1277. doi: 10.1128/ec.00080-14.
- Kolenbrander, P. E. (2002) 'Oral microbial communities: Biofilms, interactions, and genetic systems', *Annual Review of Microbiology*, 54, pp. 413–437. doi: 10.1146/annurev.micro.54.1.413.
- Kong, E. F. *et al.* (2016) 'Commensal protection of Staphylococcus aureus against antimicrobials by Candida albicans biofilm matrix', *mBio*, 7(5), pp. e01365-16. doi: 10.1128/mbio.01365-16.
- Kontoyiannis, D. P. *et al.* (2016) 'Prevalence, clinical and economic burden of mucormycosis-related hospitalizations in the United States: a retrospective study', *BMC Infectious Diseases*, 16(1), p. 730. doi: 10.1186/s12879-016-2023-z.
- Kontoyiannis, D. P. and Lewis, R. E. (2011) 'How I treat mucormycosis', *Blood*, 118(5), pp. 1216–1224. doi: 10.1182/blood-2011-03-316430.
- Koo, H. *et al.* (2003) 'Inhibition of Streptococcus mutans biofilm accumulation and polysaccharide production by apigenin and tt-farnesol.', *J Antimicrob Chemother*, 52(5), pp. 782–789.
- Kostoulias, X. *et al.* (2015) 'The impact of a cross-kingdom signalling molecule of Candida albicans on Acinetobacter baumannii physiology', *Antimicrobial Agents*

- and Chemotherapy, 60(1), pp. 161–167. doi: 10.1128/AAC.01540-15.
- Kousser, C. *et al.* (2019) 'Pseudomonas aeruginosa inhibits Rhizopus microsporus germination through sequestration of free environmental iron', *Scientific Reports*, 9, p. 5714. doi: 10.1038/s41598-019-42175-0.
- Kousser, C., Alam, F. and Hall, R. A. (2019) 'Fungal interactions in health and disease', *Microbiology Today*, 46(2), pp. 95–97.
- Kozel, T. R. and Wickes, B. (2014) 'Fungal diagnostics', *Cold Spring Harbor Perspectives in Medicine*. doi: 10.1101/cshperspect.a019299.
- Kubak, B. M. (2012) 'Fungal infection in lung transplantation', *Transpl Infect Dis*, 4 Suppl 3, pp. 24–31.
- Kumar, S. *et al.* (2011) 'Fournier's gangrene with testicular infarction caused by mucormycosis', *Indian J Pathol Microbiol*, 54, pp. 847–848.
- Lackner, M., Caramalho, R. and Lass-Flörl, C. (2014) 'Laboratory diagnosis of mucormycosis: Current status and future perspectives', *Future Microbiology*, 9(5), pp. 683–695. doi: 10.2217/fmb.14.23.
- Lam, T. I. *et al.* (2005) 'Bumetanide reduces cerebral edema formation in rats with diabetic ketoacidosis', *Diabetes*, 54(2), pp. 210–216. doi: 10.2337/diabetes.54.2.510.
- Lamont, I. *et al.* (2002) 'Siderophore-mediated signaling regulates virulence factor production in Pseudomonas aeruginosa.', *Proceedings of the National Academy of Sciences of the United States of America*, 99(10), pp. 7072–7. doi: 10.1073/pnas.092016999.
- Lecoite, K. *et al.* (2019) 'Polysaccharides cell wall architecture of Mucorales', *Frontiers in Microbiology*, 10(469), pp. 1–8. doi: 10.3389/fmicb.2019.00469.
- Lee, B. Y. *et al.* (2013) 'The economic burden of community-associated methicillin-resistant Staphylococcus aureus (CA-MRSA)', *Clinical Microbiology and Infection*, 19(6), pp. 528–536. doi: 10.1111/j.1469-0691.2012.03914.x.
- Lee, S. C. and Heitman, J. (2014) 'Sex in the Mucoralean fungi', *Mycoses*, 57(3), pp. 18–24. doi: 10.1111/myc.12244.
- Lelievre, L. *et al.* (2014) 'Posttraumatic mucormycosis', *Medicine*, 93(24), pp. 395–404. doi: 10.1097/MD.0000000000000221.
- Levison, M. E. and Pitsakis, P. G. (1987) 'Susceptibility to experimental Candida albicans urinary tract infection in the rat', *Journal of Infectious Diseases*, 155(5), pp. 841–846. doi: 10.1093/infdis/155.5.841.
- Levitz, S. M. *et al.* (1986) 'In vitro killing of spores and hyphae of Aspergillus fumigatus and Rhizopus oryzae by rabbit neutrophil cationic peptides and bronchoalveolar macrophages', *Journal of Infectious Diseases*, 154(3), pp. 483–489. doi: 10.1093/infdis/154.3.483.
- Lieschke, G. J. *et al.* (2001) 'Morphologic and functional characterization of

- granulocytes and macrophages in embryonic and adult zebrafish', *Blood*, 98(10), pp. 3087–3096. doi: 10.1182/blood.V98.10.3087.
- Lin, Y. T. *et al.* (2012) 'Seroepidemiology of *Klebsiella pneumoniae* colonizing the intestinal tract of healthy chinese and overseas chinese adults in Asian countries', *BMC Microbiology*, 12, p. 13. doi: 10.1186/1471-2180-12-13.
- Liu, M. *et al.* (2010) 'The endothelial cell receptor GRP78 is required for mucormycosis pathogenesis in diabetic mice', *Journal of Clinical Investigation*, 120(6), pp. 1914–1924. doi: 10.1172/JCI42164.
- Liu, M. *et al.* (2015) 'Fob1 and Fob2 proteins are virulence determinants of *Rhizopus oryzae* via facilitating iron uptake from ferrioxamine', *PLoS Pathogens*, 11(5), pp. 1–33. doi: 10.1371/journal.ppat.1004842.
- Liu, P. *et al.* (2010) 'Farnesol induces apoptosis and oxidative stress in the fungal pathogen *Penicillium expansum*', *Mycologia*, 102, pp. 311–318.
- Lockhart, S. R. *et al.* (2017) 'Simultaneous emergence of multidrug-resistant *Candida auris* on 3 continents confirmed by whole-genome sequencing and epidemiological analyses', *Clinical Infectious Diseases*, 64(2), pp. 134–140. doi: 10.1093/cid/ciw691.
- Lopez-Medina, E. *et al.* (2015) '*Candida albicans* inhibits *Pseudomonas aeruginosa* virulence through suppression of pyochelin and pyoverdine biosynthesis', *PLoS Pathogens*, 11(8). doi: 10.1371/journal.ppat.1005129.
- López-Muñoz, A. *et al.* (2018) 'An adult zebrafish model reveals that mucormycosis induces apoptosis of infected macrophages', *Scientific Reports*, 8, p. 12802. doi: 10.1038/s41598-018-30754-6.
- López, L. *et al.* (2015) 'The detection of fungal diseases in the "Golden Smoothie" apple and "Blanquilla" pear based on the volatile profile', *Postharvest Biology and Technology*, 99, pp. 120–130. doi: 10.1016/j.postharvbio.2014.08.005.
- Loutet, S. A. and Valvano, M. A. (2011) 'Extreme antimicrobial peptide and olymyxin B resistance in the genus *Burkholderia*', *Frontiers in Microbiology*, 2, p. 159. doi: 10.3389/fmicb.2011.00159.
- Lulloff, S. J., Hahn, B. L. and Sohnle, P. G. (2004) 'Fungal susceptibility to zinc deprivation', *Journal of Laboratory and Clinical Medicine*, 144(4), pp. 208–214. doi: 10.1016/j.lab.2004.07.007.
- Malavia, D. *et al.* (2017) 'Zinc limitation induces a hyper-adherent Goliath phenotype in *Candida albicans*', *Frontiers in Microbiology*, 8, p. 2238. doi: 10.3389/fmicb.2017.02238.
- Mallick, E. M. and Bennett, R. J. (2013) 'Sensing of the microbial neighborhood by *Candida albicans*', *PLoS Pathogens*, 9(10), pp. 1–4. doi: 10.1371/journal.ppat.1003661.
- Mandal, P. K. *et al.* (2013) 'Primary squamous cell carcinoma with mucormycosis in a diabetic foot ulcer', *Journal of the Indian Medical Association*, 111(2), pp.

125–126.

Martinello, M. *et al.* (2012) “‘We are what we eat!’ Invasive intestinal mucormycosis: A case report and review of the literature’, *Medical Mycology Case Reports*, 1(1), pp. 52–55. doi: 10.1016/j.mmcr.2012.07.003.

Matzanke, B. (1994) ‘Iron storage in fungi’, in Winklemann, G. and Winge, D. (eds) *Metal Ions in Fungi*. New York: Marcel Dekker, Inc., pp. 179–214.

Mayer, F. L., Wilson, D. and Hube, B. (2013) ‘*Candida albicans* pathogenicity mechanisms’, *Virulence*, 4(2), pp. 119–128. doi: 10.4161/viru.22913.

McCarthy, M. *et al.* (2018) ‘Recent advances in the treatment of scedosporiosis and fusariosis’, *Journal of Fungi*, 4(2), p. E73. doi: 10.3390/jof4020073.

McCarthy, R. R. *et al.* (2017) ‘Cyclic-di-GMP regulates lipopolysaccharide modification and contributes to *Pseudomonas aeruginosa* immune evasion’, *Nature Microbiology*, 6(2), p. 17027. doi: 10.1038/nmicrobiol.2017.27.

McCormick, J. K., Yarwood, J. M. and Schlievert, P. M. (2001) ‘Toxic shock syndrome and bacterial superantigens: An update’, *Annual Review of Microbiology*, 55, pp. 77–104. doi: 10.1146/annurev.micro.55.1.77.

Mear, J. B. *et al.* (2014) ‘*Candida albicans* airway exposure primes the lung innate immune response against *Pseudomonas aeruginosa* infection through innate lymphoid cell recruitment and interleukin-22-associated mucosal response’, *Infection and Immunity*, 82(1), pp. 306–315. doi: 10.1128/IAI.01085-13.

Meijer, A. H. and Spaik, H. P. (2011) ‘Host-pathogen interactions made transparent with the zebrafish model.’, *Current drug targets*.

Mélida, H. *et al.* (2015) ‘Deciphering the uniqueness of Mucoromycotina cell walls by combining biochemical and phylogenomic approaches’, *Environmental Microbiology*, 17(5), pp. 1649–1662. doi: 10.1111/1462-2920.12601.

Mendoza, L. *et al.* (2015) ‘Human fungal pathogens of Mucorales and Entomophthorales’, *Cold Spring Harbor Perspectives in Medicine*, 5(4). doi: 10.1101/cshperspect.a019562.

Mesland, D. A. M., Huisman, J. G. and Van Den Ende, H. (1974) ‘Volatile sexual hormones in *Mucor mucedo*’, *Journal of General Microbiology*, 80, pp. 111–117. doi: 10.1099/00221287-80-1-111.

Meyer, J. M. *et al.* (1996) ‘Pyoverdinin is essential for virulence of *Pseudomonas aeruginosa*’, *Infection and Immunity*, 64(2), pp. 518–523.

Meyer, J. M. and Abdallah, M. A. (1978) ‘The fluorescent pigment of *Pseudomonas fluorescens*: biosynthesis, purification and physicochemical properties’, *Journal of General Microbiology*, 107, pp. 319–328.

Meyers, E. *et al.* (1968) ‘Biological characterization of prasinomycin, a phosphorus-containing antibiotic’, *Applied Microbiology*, 16(4), pp. 603–608.

Miethke, M. and Marahiel, M. A. (2007) ‘Siderophore-based iron acquisition and

pathogen control', *Microbiology and Molecular Biology Reviews*, 71(3), pp. 413–451. doi: 10.1128/MMBR.00012-07.

Mobarra, N. *et al.* (2016) 'A review on iron chelators in treatment of iron overload syndromes.', *International journal of hematology-oncology and stem cell research*, 10(4), pp. 239–247.

Mondo, S. J. *et al.* (2017) 'Bacterial endosymbionts influence host sexuality and reveal reproductive genes of early divergent fungi', *Nature Communications*, 8, p. 1843. doi: 10.1038/s41467-017-02052-8.

Monecke, S. *et al.* (2006) 'A case of peritonitis caused by *Rhizopus microsporus*', *Mycoses*, 49(2), pp. 139–142. doi: 10.1111/j.1439-0507.2006.01190.x.

Money, N. P. (2016a) 'Fungal genetics and life cycles', in *Fungi: A very short introduction.*, p. 51. doi: <https://doi.org/10.1093/actrade/9780199688784.003.0003>.

Money, N. P. (2016b) 'What is a fungus?', in *Fungi: A very short introduction*. Oxford University Press. doi: 10.1093/actrade/9780199688784.001.0001.

Monheit, J. E., Cowan, D. F. and Moore, D. G. (1984) 'Rapid detection of fungi in tissues using calcofluor white and fluorescence microscopy', *Archives of Pathology and Laboratory Medicine*, 108(8), pp. 616–618.

Morales, D. K. *et al.* (2013) 'Control of *Candida albicans* metabolism and biofilm formation by *Pseudomonas aeruginosa* phenazines', *mBio*, 4(1). doi: 10.1128/mBio.00526-12.

Moreira, J. *et al.* (2016) 'The burden of mucormycosis in HIV-infected patients: A systematic review', *Journal of Infection*, 73(3), pp. 181–188. doi: 10.1016/j.jinf.2016.06.013.

Mougous, J. D. *et al.* (2006) 'A virulence locus of *Pseudomonas aeruginosa* encodes a protein secretion apparatus', *Science*, 312(5779), pp. 1526–1530. doi: 10.1126/science.1128393.

Mousavi, B. *et al.* (2018) 'Occurrence and species distribution of pathogenic Mucorales in unselected soil samples from France', *Medical Mycology*, 56(3), pp. 315–321. doi: 10.1093/mmy/myx051.

Mowat, E. *et al.* (2010) '*Pseudomonas aeruginosa* and their small diffusible extracellular molecules inhibit *Aspergillus fumigatus* biofilm formation', *FEMS Microbiology Letters*, pp. 96–102. doi: 10.1111/j.1574-6968.2010.02130.x.

Muller, M. (2002) 'Pyocyanin induces oxidative stress in human endothelial cells and modulates the glutathione redox cycle', *Free Radical Biology and Medicine*, 33(11), pp. 1527–1533. doi: 10.1016/S0891-5849(02)01087-0.

Murad, A. M. *et al.* (2001) 'NRG1 represses yeast  $\pm$  hypha morphogenesis and hypha-specific gene expression in *Candida albicans*', *EMBO Journal*, 20(17), pp. 4742–4752.

Nagy, G. *et al.* (2017) 'Development of a plasmid free CRISPR-Cas9 system for

- the genetic modification of *Mucor circinelloides*', *Scientific Reports*, 7(1), p. 16800. doi: 10.1038/s41598-017-17118-2.
- Nain, P. S. *et al.* (2015) 'Post-operative abdominal wall mucormycosis—a case series', *Indian J Surg*, 77(Suppl 2), pp. S253–S256.
- Nash, G. *et al.* (1971) 'Fungal burn wound infection.', *The journal of the American Medical Association*, 215(10), pp. 1664–6. Available at: <http://www.ncbi.nlm.nih.gov/pubmed/5107690>.
- Nazik, H. *et al.* (2017) 'Pseudomonas phage inhibition of *Candida albicans*', *Microbiology (United Kingdom)*, 163(11), pp. 1568–1577. doi: 10.1099/mic.0.000539.
- Nealson, K. H. and Hastings, J. W. (1979) 'Bacterial bioluminescence: Its control and ecological significance', *Microbiol Rev*, 43(4), pp. 496–518.
- Neto, F. M. F. D. *et al.* (2014) 'Fungal infection by mucorales order in lung transplantation: 4 case reports', in *Transplantation Proceedings*, pp. 1849–1851. doi: 10.1016/j.transproceed.2014.05.033.
- Nevitt, T. and Thiele, D. J. (2011) 'Host iron withholding demands siderophore utilization for *Candida glabrata* to survive macrophage killing', *PLoS Pathogens*, 7(3), p. e1001322. doi: 10.1371/journal.ppat.1001322.
- Nguyen, M. H. *et al.* (2012) 'Performance of *Candida* real-time polymerase chain reaction,  $\beta$ -D-glucan assay, and blood cultures in the diagnosis of invasive candidiasis', *Clinical Infectious Diseases*, 54(9), pp. 1240–1248. doi: 10.1093/cid/cis200.
- Northover, J. and Zhou, T. (2002) 'Control of rhizopus rot of peaches with postharvest treatments of tebuconazole, fludioxonil, and *Pseudomonas syringae*', *Canadian Journal of Plant Pathology*, 24(2). doi: 10.1080/07060660309506989.
- Nseir, S. *et al.* (2007) 'Impact of antifungal treatment on *Candida-Pseudomonas* interaction: A preliminary retrospective case-control study', *Intensive Care Medicine*, 33(1), pp. 137–142. doi: 10.1007/s00134-006-0422-0.
- O'Brien, I, G., Cox, G. B. and Gibson, F. (1970) 'Biologically active compounds containing 2,3-dihydroxybenzoic acid and serine formed by *Escherichia coli*', *Biochimica et Biophysica Acta*, 201(3), pp. 453–60. doi: 10.1016/0304-4165(70)90165-0.
- Odabasi, Z. *et al.* (2006) 'Differences in beta-glucan levels in culture supernatants of a variety of fungi', *Medical Mycology*, 44(3), pp. 267–272. doi: 10.1080/13693780500474327.
- De Oliveira, F. P. *et al.* (2017) 'Prevalence, antimicrobial susceptibility, and clonal diversity of *Pseudomonas aeruginosa* in chronic wounds', *Journal of Wound, Ostomy and Continence Nursing*, 44(6), pp. 528–535. doi: 10.1097/WON.0000000000000373.
- Oliver, A. *et al.* (2000) 'High frequency of hypermutable *Pseudomonas*

- aeruginosa* in cystic fibrosis lung infection', *Science*, 288(5469), pp. 1251–1254. doi: 10.1126/science.288.5469.1251.
- Oshero, N. and May, G. (2000) 'Conidial germination in *Aspergillus nidulans* requires RAS signaling and protein synthesis', *Genetics*, 155(2), pp. 647–656.
- Otto, M. (2014) '*Staphylococcus aureus* toxins', *Current Opinion in Microbiology*, 17, pp. 32–37. doi: 10.1016/j.mib.2013.11.004.
- Pammi, M. *et al.* (2013) 'Biofilm extracellular DNA enhances mixed species biofilms of *Staphylococcus epidermidis* and *Candida albicans*', *BMC Microbiology*, 13, p. 257. doi: 10.1186/1471-2180-13-257.
- Parad, R. B. *et al.* (1999) 'Pulmonary outcome in cystic fibrosis is influenced primarily by mucoid *Pseudomonas aeruginosa* infection and immune status and only modestly by genotype', *Infection and Immunity*, 67(9), pp. 4744–4750.
- Parente, A. F. A. *et al.* (2013) 'A proteomic view of the response of *Paracoccidioides* yeast cells to zinc deprivation', *Fungal Biology*, 117(6), pp. 399–410. doi: 10.1016/j.funbio.2013.04.004.
- Paris, S. *et al.* (2003) 'Conidial hydrophobins of *Aspergillus fumigatus*', *Applied and Environmental Microbiology*, 69(3), pp. 1581–1588. doi: 10.1128/AEM.69.3.1581-1588.2003.
- Partida-Martinez, L. P. *et al.* (2007) '*Burkholderia rhizoxinica* sp. nov. and *Burkholderia endofungorum* sp. nov., bacterial endosymbionts of the plant-pathogenic fungus *Rhizopus microsporus*', *International Journal of Systematic and Evolutionary Microbiology*, 57(11), pp. 2583–2590. doi: 10.1099/ijls.0.64660-0.
- Patel, A. *et al.* (2010) 'Elderly diabetic patient with surgical site mucormycosis extending to bowel', *Journal of Global Infectious Diseases*. doi: 10.4103/0974-777x.62877.
- Patel, G. *et al.* (2008) 'Outcomes of carbapenem-resistant infection and the impact of *Klebsiella pneumoniae* antimicrobial and and the impact of antimicrobial and adjunctive therapies', *Source: Infection Control and Hospital Epidemiology*, 29(12), pp. 1099–1106. doi: 10.1086/592412.
- Peixoto, D. *et al.* (2014) 'Green herring syndrome: Bacterial infection in patients with mucormycosis cavitory lung disease', *Open Forum Infectious Diseases*, 1(1), p. ofu014. doi: 10.1093/ofid/ofu014.
- Peleg, A. Y. *et al.* (2008) 'Prokaryote-eukaryote interactions identified by using *Caenorhabditis elegans*.', *Proceedings of the National Academy of Sciences of the United States of America*, 105(38), pp. 14585–14590. doi: 10.1073/pnas.0805048105.
- Peleg, A. Y., Hogan, D. A. and Mylonakis, E. (2010) 'Medically important bacterial–fungal interactions', *Nature Reviews Microbiology*. Nature Publishing Group, 8(5), pp. 340–349. doi: 10.1038/nrmicro2313.
- Penner, J. C. *et al.* (2016) 'Pf4 bacteriophage produced by *Pseudomonas*

- aeruginosa* inhibits *Aspergillus fumigatus* metabolism via iron sequestration', *Microbiology (United Kingdom)*, 162(9), pp. 1583–1594. doi: 10.1099/mic.0.000344.
- Pérez-Arques, C. *et al.* (2019) '*Mucor circinelloides* thrives inside the phagosome through an atf-mediated germination pathway', *mBio*, 10(1), pp. e02765-18. doi: 10.1128/mBio.02765-18.
- Personett, H. A. *et al.* (2019) 'Renal recovery following liposomal amphotericin B-induced nephrotoxicity', *International Journal of Nephrology*, 2019, p. 8629891. doi: 10.1155/2019/8629891.
- Peters, B. M. *et al.* (2012) 'Polymicrobial interactions: Impact on pathogenesis and human disease', *Clinical Microbiology Reviews*, 25(1), pp. 193–213. doi: 10.1128/CMR.00013-11.
- Peters, B. M. and Noverra, M. C. (2013) '*Candida albicans*-*Staphylococcus aureus* polymicrobial peritonitis modulates host innate immunity', *Infection and Immunity*, 81(6), pp. 2178–2189. doi: 10.1128/IAI.00265-13.
- Petrikkos, G. *et al.* (2012) 'Epidemiology and clinical manifestations of mucormycosis', 54(Suppl 1), pp. 23–34. doi: 10.1093/cid/cir866.
- Pidwill, G. R. *et al.* (2018) 'Coassociation between Group B *Streptococcus* and *Candida albicans* promotes interactions with vaginal epithelium', *Infection and Immunity*, 86(4), pp. e00669-17. doi: 10.1128/iai.00669-17.
- Podschun, R. and Ullmann, U. (1998) '*Klebsiella spp.* as nosocomial pathogens: Epidemiology, taxonomy, typing methods, and pathogenicity factors', *Clinical Microbiology Reviews*, 11(4), pp. 589–603. doi: 0893-8512/98/\$04.00?0.
- Poole, K. *et al.* (1993) 'Cloning and nucleotide sequence analysis of the ferripyoverdine receptor gene *fpvA* of *Pseudomonas aeruginosa*', *Journal of Bacteriology*, 175(15), pp. 4597–4604. doi: 10.1128/jb.175.15.4597-4604.1993.
- Pouvaret, A. *et al.* (2019) 'Concurrent cerebral aspergillosis and abdominal mucormycosis during ibrutinib therapy for chronic lymphocytic leukaemia', *Clinical Microbiology and Infection*, 25(6), pp. 771–773. doi: 10.1016/j.cmi.2019.01.016.
- Prakash, H. and Chakrabarti, A. (2019) 'Global epidemiology of mucormycosis', *Journal of Fungi*, 5(1), p. 26. doi: 10.3390/jof5010026.
- Prince, L. R. *et al.* (2013) 'Subversion of a lysosomal pathway regulating neutrophil apoptosis by a major bacterial toxin, pyocyanin', *J Immunol* *References The Journal of Immunology at Osaka University Library on*, 180, pp. 3502–3511. doi: 180/5/3502 [pii].
- Purschke, F. G. *et al.* (2012) 'Flexible survival strategies of *Pseudomonas aeruginosa* in biofilms result in increased fitness compared with *Candida albicans*', *Molecular & Cellular Proteomics*, 11(12), pp. 1652–1669. doi: 10.1074/mcp.m112.017673.
- Quick, J. *et al.* (2014) 'Seeking the source of *Pseudomonas aeruginosa* infections

in a recently opened hospital: An observational study using whole-genome sequencing', *BMJ Open*, 4(11). doi: 10.1136/bmjopen-2014-006278.

Quintin, J. *et al.* (2012) 'Candida albicans infection affords protection against reinfection via functional reprogramming of monocytes', *Cell Host and Microbe*, 12(2), pp. 223–232. doi: 10.1016/j.chom.2012.06.006.

Rabin, H. R. and Surette, M. G. (2012) 'The cystic fibrosis airway microbiome', *Current Opinion in Pulmonary Medicine*. doi: 10.1097/MCP.0b013e328358d49a.

Rada, B. *et al.* (2011) 'Reactive oxygen species mediate inflammatory cytokine release and EGFR-dependent mucin secretion in airway epithelial cells exposed to *Pseudomonas* pyocyanin', *Mucosal Immunology*, 4(2), pp. 158–171. doi: 10.1038/mi.2010.62.

Rahme, L. G. *et al.* (1995) 'Common virulence factors for bacterial pathogenicity in plants and animals.', *Science*, 268(5219), pp. 1899–902. doi: 10.1126/science.7604262.

Ramage, G. *et al.* (2002) 'Inhibition of *Candida albicans* biofilm formation by farnesol, a quorum-sensing molecule.', *Appl Environ Microbiol*, 68, pp. 5459–5463.

Rapisarda, F. *et al.* (2015) 'Candida peritonitis and sepsis due to *Acinetobacter baumannii* in peritoneal dialysis: an association with prognosis not always unfavourable', *G Ital Nefrol*, 32(6), p. pii: gin/32.6.8.

Reece, E. *et al.* (2017) 'Co-colonisation with *Aspergillus fumigatus* and *Pseudomonas aeruginosa* is associated with poorer health in cystic fibrosis patients: An Irish registry analysis', *BMC Pulmonary Medicine*, 17(1), p. 70. doi: 10.1186/s12890-017-0416-4.

Reece, E. *et al.* (2018) 'Aspergillus fumigatus inhibits *Pseudomonas aeruginosa* in co-culture: Implications of a mutually antagonistic relationship on virulence and inflammation in the CF airway', *Frontiers in Microbiology*, 9, p. 1205. doi: 10.3389/fmicb.2018.01205.

Reed, C. *et al.* (2006) 'Deferasirox, an iron-chelating agent, as salvage therapy for rhinocerebral mucormycosis [2]', *Antimicrobial Agents and Chemotherapy*, 50(11), pp. 3968–3969. doi: 10.1128/AAC.01065-06.

Reed, C. *et al.* (2008) 'Combination polyene-caspofungin treatment of rhino-orbital-cerebral mucormycosis', *Clinical Infectious Diseases*, 47(3), pp. 364–371. doi: 10.1086/589857.

Regev-Yochay, G. *et al.* (2004) 'Association between carriage of *Streptococcus pneumoniae* and *Staphylococcus aureus* in children', *Journal of the American Medical Association*, 294(6), pp. 716–720. doi: 10.1001/jama.292.6.716.

Rhodes, K. A. and Schweizer, H. P. (2016) 'Antibiotic resistance in *Burkholderia* species', *Drug Resistance Updates*, 28, pp. 82–90. doi: 10.1016/j.drug.2016.07.003.

Ribes, J. A., Vanover-Sams, C. L. and Baker, D. J. (2000) 'Zygomycetes in

- human disease', *Clinical Microbiology Reviews*, pp. 236–301. doi: 10.1128/CMR.13.2.236-301.2000.
- Richardson, M. (2009) 'The ecology of the zygomycetes and its impact on environmental exposure', *Clinical Microbiology and Infection*, 15(Suppl 5), pp. 2–9. doi: 10.1111/j.1469-0691.2009.02972.x.
- Richardson, M. and Page, I. (2018) 'Role of serological tests in the diagnosis of mold infections', *Current Fungal Infection Reports*, 12(3), pp. 127–136. doi: 10.1007/s12281-018-0321-1.
- Robbins, N., Caplan, T. and Cowen, L. E. (2017) 'Molecular evolution of antifungal drug resistance', *Annual Review of Microbiology*, 8(71), pp. 753–775. doi: 10.1146/annurev-micro-030117-020345.
- Rocker, A. J. *et al.* (2015) 'Visualizing and quantifying *Pseudomonas aeruginosa* infection in the hindbrain ventricle of zebrafish using confocal laser scanning microscopy', *Journal of Microbiological Methods*, 117, pp. 85–94. doi: 10.1016/j.mimet.2015.07.013.
- Roden, M. M. *et al.* (2005) 'Epidemiology and outcome of zygomycosis: A review of 929 reported cases', *Clinical Infectious Diseases*, 41(5), pp. 634–653. doi: 10.1086/432579.
- Rogers, G. B. *et al.* (2003) 'Bacterial diversity in cases of lung infection in cystic fibrosis patients: 16S ribosomal DNA (rDNA) length heterogeneity PCR and 16S rDNA terminal restriction fragment length polymorphism profiling.', *Journal of clinical microbiology*.
- Rosen, D. A. *et al.* (2016) '*Klebsiella pneumoniae* FimK promotes virulence in murine pneumonia', *Journal of Infectious Diseases*, 213(4), pp. 649–658. doi: 10.1093/infdis/jiv440.
- Rosowski, E. *et al.* (2018) 'The zebrafish as a model host for invasive fungal infections', *Journal of Fungi*, 4(4), p. 136. doi: 10.3390/jof4040136.
- Saito, S., Michailides, T. J. and Xiao, C. L. (2016) '*Mucor* rot—An emerging postharvest disease of mandarin fruit caused by *Mucor piriformis* and other *Mucor* spp. in California', *Plant Disease*, 100(6), pp. 1054–1063. doi: 10.1094/pdis-10-15-1173-re.
- Sass, G. *et al.* (2018) 'Studies of *Pseudomonas aeruginosa* mutants indicate pyoverdine as the central factor in inhibition of *Aspergillus fumigatus* biofilm', *Journal of Bacteriology*, 200(1), pp. e00345-17. doi: 10.1128/JB.00345-17.
- Schalk, I. J., Abdallah, M. A. and Pattus, F. (2002) 'Recycling of pyoverdin on the FpvA receptor after ferric pyoverdin uptake and dissociation in *Pseudomonas aeruginosa*', *Biochemistry*, 41(5), pp. 1663–1671. doi: 10.1021/bi0157767.
- Schindelin, J. *et al.* (2012) 'Fiji: an open-source platform for biological-image analysis', *Nature methods*, 9(7), pp. 676–682. doi: 10.1038/nmeth.2019.
- Schlecht, L. M. *et al.* (2015) 'Systemic *Staphylococcus aureus* infection mediated by *Candida albicans* hyphal invasion of mucosal tissue', *Microbiology (Reading)*,

- England), 161, pp. 168–181. doi: 10.1099/mic.0.083485-0.
- Schneider, R. de O. *et al.* (2012) 'Zap1 regulates zinc homeostasis and modulates virulence in *Cryptococcus gattii*', *PLoS ONE*, 7(8), p. e43773. doi: 10.1371/journal.pone.0043773.
- Scott, F. W. and Pitt, T. L. (2004) 'Identification and characterization of transmissible *Pseudomonas aeruginosa* strains in cystic fibrosis patients in England and Wales', *Journal of Medical Microbiology*, 53(Pt 7), pp. 609–615. doi: 10.1099/jmm.0.45620-0.
- Seman, B. G. *et al.* (2018) 'Yeast and filaments have specialized, independent activities in a zebrafish model of *Candida albicans* infection', *Infection and Immunity*, 86(10), pp. e00415-18. doi: 10.1128/iai.00415-18.
- Semighini, C. P. *et al.* (2006) 'Farnesol-induced apoptosis in *Aspergillus nidulans* reveals a possible mechanism for antagonistic interactions between fungi', *Molecular Microbiology*, 59(3), pp. 753–764. doi: 10.1111/j.1365-2958.2005.04976.x.
- Semighini, C. P., Murray, N. and Harris, S. D. (2008) 'Inhibition of *Fusarium graminearum* growth and development by farnesol', *FEMS Microbiology Letters*, 279(2), pp. 259–264. doi: 10.1111/j.1574-6968.2007.01042.x.
- Sephton-Clark, P. C. S. *et al.* (2018) 'Pathways of pathogenicity: Transcriptional stages of germination in the fatal fungal pathogen *Rhizopus delemar*', *mSphere*, 3(5), pp. e00403-18. doi: 10.1128/msphere.00403-18.
- Shekhova, E., Kniemeyer, O. and Brakhage, A. A. (2017) 'Induction of mitochondrial reactive oxygen species production by itraconazole, terbinafine, and amphotericin B as a mode of action against *Aspergillus fumigatus*', *Antimicrobial Agents and Chemotherapy*, 61(11), pp. e00978-17. doi: 10.1128/AAC.00978-17.
- Shibata, N. *et al.* (2007) 'Chemical structure of the cell-wall mannan of *Candida albicans* serotype A and its difference in yeast and hyphal forms', *Biochemical Journal*, 404(Pt 3), pp. 365–372. doi: 10.1042/bj20070081.
- Shirazi, F. *et al.* (2016) 'Biofilm filtrates of *Pseudomonas aeruginosa* strains isolated from cystic fibrosis patients inhibit preformed *Aspergillus fumigatus* biofilms via apoptosis', *PLoS ONE*, 11(3), p. e0150155. doi: 10.1371/journal.pone.0150155.
- Shirazi, F., Kontoyiannis, D. P. and Ibrahim, A. S. (2015) 'Iron starvation induces apoptosis in *Rhizopus oryzae in vitro*', *Virulence*, 6(2), pp. 121–126. doi: 10.1080/21505594.2015.1009732.
- Simionato, A. S. *et al.* (2017) 'The effect of phenazine-1-carboxylic acid on mycelial growth of *Botrytis cinerea* produced by *Pseudomonas aeruginosa* LV strain', *Frontiers in Microbiology*, 8, p. 1102. doi: 10.3389/fmicb.2017.01102.
- Simitsopoulou, M. *et al.* (2010) '*Cunninghamella bertholletiae* exhibits increased resistance to human neutrophils with or without antifungal agents as compared

- to *Rhizopus spp.*', *Medical Mycology*, 48(5), pp. 720–724. doi: 10.3109/13693780903476635.
- Singh, P. *et al.* (2016) 'Stress response in medically important Mucorales', *Mycoses*, 59, pp. 628–635. doi: 10.1111/myc.12512.
- Smith, M. L., Bruhn, J. N. and Anderson, J. B. (1992) 'The fungus *Armillaria bulbosa* is among the largest and oldest living organisms', *Nature*, 356, pp. 428–431. doi: 10.1038/356428a0.
- Snelders, E. *et al.* (2009) 'Possible environmental origin of resistance of *Aspergillus fumigatus* to medical triazoles', *Applied and Environmental Microbiology*, pp. 4053–4057. doi: 10.1128/AEM.00231-09.
- Sokal, R. R. and Rohlf, F. J. (1995) *Biometry: The principles and practice of statistics in biological research, third edition*, Biological Research.
- Spellberg, B. *et al.* (2012) 'The deferasirox-AmBisome therapy for mucormycosis (Defeat Mucor) study: A randomized, double-blinded, placebo-controlled trial', *Journal of Antimicrobial Chemotherapy*, 67(3), pp. 715–722. doi: 10.1093/jac/dkr375.
- Spellberg, B. and Ibrahim, A. S. (2010) 'Recent advances in the treatment of mucormycosis', *Current Infectious Disease Reports*, pp. 423–429. doi: 10.1007/s11908-010-0129-9.
- Stasiak, M. *et al.* (2009) 'Mucormycosis complicating lower limb crash injury in a multiple traumatised patient: An unusual case', *BMJ Case Reports*, 2009, p. bcr10.2008.1170. doi: 10.1136/bcr.10.2008.1170.
- Stearman, R. *et al.* (1996) 'A permease-oxidase complex involved in high-affinity iron uptake in yeast', *Science*, 271(5255), pp. 1552–1557. doi: 10.1126/science.271.5255.1552.
- Stein, C. *et al.* (2007) 'Conservation and divergence of gene families encoding components of innate immune response systems in zebrafish', *Genome Biology*, 8(11), p. R251. doi: 10.1186/gb-2007-8-11-r251.
- Steinberg, G. (2007) 'Hyphal Growth: a tale of motors, lipids, and the Spitzenkörper', *Eukaryotic Cell*, 6(3), pp. 351–360. doi: 10.1128/EC.00381-06.
- Stintzi, A. *et al.* (1996) 'Novel pyoverdine biosynthesis gene(s) of *Pseudomonas aeruginosa* PAO', *Microbiology*, 142(5), pp. 1181–1190. doi: 10.1099/13500872-142-5-1181.
- Stoldt, V. R. *et al.* (1997) 'Efg1p, an essential regulator of morphogenesis of the human pathogen *Candida albicans*, is a member of a conserved class of bHLH proteins regulating morphogenetic processes in fungi', *EMBO Journal*, 16(8), pp. 1982–1991. doi: 10.1093/emboj/16.8.1982.
- Stones, D. H. *et al.* (2017) 'Zebrafish (*Danio rerio*) as a vertebrate model host to study colonization, pathogenesis, and transmission of foodborne *Escherichia coli* O157', *mSphere*, 2(5), pp. e00365-17. doi: 10.1128/mspheredirect.00365-17.

- Strange, H. R., Zola, T. A. and Cornelissen, C. N. (2011) 'The fbpABC operon is required for Ton-independent utilization of xenosiderophores by *Neisseria gonorrhoeae* strain FA19', *Infection and Immunity*, 79(1), pp. 267–278. doi: 10.1128/iai.00807-10.
- Struve, C. and Krogfelt, K. A. (2004) 'Pathogenic potential of environmental *Klebsiella pneumoniae* isolates', *Environmental Microbiology*, 6(6), pp. 584–590. doi: 10.1111/j.1462-2920.2004.00590.x.
- Suhling, H. *et al.* (2013) 'Inhaled colistin following lung transplantation in colonised cystic fibrosis patients', *European Respiratory Journal*, 42, pp. 542–544. doi: 10.1183/09031936.00201012.
- Svahn, K. S. *et al.* (2014) 'Induction of gliotoxin secretion in *Aspergillus fumigatus* by bacteria-associated molecules', *PLoS ONE*, 9(4), p. e93685. doi: 10.1371/journal.pone.0093685.
- Syed, S. A. *et al.* (2016) 'Reemergence of lower-airway microbiota in lung transplant patients with cystic fibrosis', *Annals of the American Thoracic Society*, 13(12), pp. 2132–2142. doi: 10.1513/AnnalsATS.201606-431OC.
- Tajdini, F. *et al.* (2010) 'Production, physicochemical and antimicrobial properties of fungal chitosan from *Rhizomucor miehei* and *Mucor racemosus*', *International Journal of Biological Macromolecules*, 47(2), pp. 180–183. doi: 10.1016/j.ijbiomac.2010.05.002.
- Tangen, K. L. *et al.* (2007) 'The iron- and cAMP-regulated gene SIT1 influences ferrioxamine B utilization, melanization and cell wall structure in *Cryptococcus neoformans*', *Microbiology*, 153(Pt 1), pp. 29–41. doi: 10.1099/mic.0.2006/000927-0.
- Tapping, R. I. *et al.* (2000) 'Toll-like receptor 4, but not toll-like receptor 2, is a signaling receptor for *Escherichia* and *Salmonella* lipopolysaccharides', *The Journal of Immunology*, 165(10), pp. 5780–5787. doi: 10.4049/jimmunol.165.10.5780.
- Taylor, L. H., Latham, S. M. and Woolhouse, M. E. J. (2001) 'Risk factors for human disease emergence', *Philosophical Transactions of the Royal Society B: Biological Sciences*, 356(1411), pp. 983–989. doi: 10.1098/rstb.2001.0888.
- Telford, G. *et al.* (1998) 'The *Pseudomonas aeruginosa* quorum-sensing signal molecule N-(3- Oxododecanoyl)-L-homoserine lactone has immunomodulatory activity', *Infection and Immunity*, 66(1), pp. 36–42.
- Teng, Y. *et al.* (2013) 'Evaluating human cancer cell metastasis in zebrafish', *BMC Cancer*, 13, p. 453. doi: 10.1186/1471-2407-13-453.
- Tenor, J. L. *et al.* (2015) 'Live imaging of host-parasite interactions in a zebrafish infection model reveals cryptococcal determinants of virulence and central nervous system invasion', *mBio*, 6(5), pp. e01425-15. doi: 10.1128/mbio.01425-15.
- Thieken, A. and Winkelmann, G. (1992) 'Rhizoferrin: A complexone type

- siderophore of the mucorales and entomophthorales (Zygomycetes)', *FEMS Microbiology Letters*, 94(1–2), pp. 37–41. doi: 10.1016/0378-1097(92)90579-D.
- Tian, J. *et al.* (2013) 'BDSF inhibits *Candida albicans* adherence to urinary catheters', *Microbial Pathogenesis*, 64, pp. 33–38. doi: 10.1016/j.micpath.2013.07.003.
- Torres-Narbona, M. *et al.* (2007) 'Impact of zygomycosis on microbiology workload: A survey study in Spain', *Journal of Clinical Microbiology*, 45(6), pp. 2051–2053. doi: 10.1128/JCM.02473-06.
- Trieu, T. A. *et al.* (2017) 'RNAi-based functional genomics identifies new virulence determinants in mucormycosis', *PLoS Pathogens*, 13(1). doi: 10.1371/journal.ppat.1006150.
- Trunk, K. *et al.* (2018) 'The type VI secretion system deploys antifungal effectors against microbial competitors', *Nature Microbiology*, 3, pp. 920–931. doi: 10.1038/s41564-018-0191-x.
- Trzaska, W. J. *et al.* (2015) 'pH manipulation as a novel strategy for treating mucormycosis', *Antimicrobial Agents and Chemotherapy*, 59(11), pp. 6968–6974. doi: 10.1128/AAC.01366-15.
- Tsang, C. S. P. and Samaranayake, L. P. (2000) 'Oral yeasts and coliforms in HIV-infected individuals in Hong Kong', *Orale Hefen und Coliforme bei HIV-Infizierten in Hongkong*, 308, pp. 303–308.
- Turgeman, T. *et al.* (2014) 'Induction of *Rhizopus oryzae* germination under starvation using host metabolites increases spore susceptibility to heat stress', *Phytopathology*, 104(3), pp. 240–247. doi: 10.1094/PHYTO-08-13-0245-R.
- Turgeman, T. *et al.* (2016) 'The role of aquaporins in pH-dependent germination of *Rhizopus delemar* spores', *Plos One*, 11(3), p. e0150543. doi: 10.1371/journal.pone.0150543.
- Tuzcu, A. *et al.* (2006) 'Necrotizing (malignant) otitis externa: An unusual localization of mucormycosis', *Indian Journal of Medical Microbiology*.
- Tzianabos, A. O., Wang, J. Y. and Lee, J. C. (2001) 'Structural rationale for the modulation of abscess formation by *Staphylococcus aureus* capsular polysaccharides.', *Proceedings of the National Academy of Sciences of the United States of America*, 98(16), pp. 9365–9370. doi: 10.1073/pnas.161175598.
- Vellanki, S. *et al.* (2018) '*Mucor circinelloides*: growth, maintenance, and genetic manipulation', *Current Protocols in Microbiology*, 49(1). doi: 10.1002/cpmc.53.
- Vermitsky, J. P. *et al.* (2008) 'Survey of vaginal-flora *Candida* species isolates from women of different age groups by use of species-specific PCR detection', *Journal of Clinical Microbiology*, 46(4), pp. 1501–1503. doi: 10.1128/JCM.02485-07.
- Visca, P. *et al.* (1992) 'Metal regulation of siderophore synthesis in *Pseudomonas aeruginosa* and functional effects of siderophore-metal complexes', *Applied and Environmental Microbiology*, 58(9), pp. 2886–2893.

- Vitale, R. G. *et al.* (2012) 'Antifungal susceptibility and phylogeny of opportunistic members of the order Mucorales', *Journal of Clinical Microbiology*, 50(1), pp. 66–75. doi: 10.1128/JCM.06133-11.
- Voelz, K., Gratacap, R. L. and Wheeler, R. T. (2015) 'A zebrafish larval model reveals early tissue-specific innate immune responses to *Mucor circinelloides*.', *Disease models & mechanisms*, 8(11), pp. 1375–88. doi: 10.1242/dmm.019992.
- Wagener, J. *et al.* (2014) 'Fungal chitin dampens inflammation through IL-10 induction mediated by NOD2 and TLR9 activation.', *PLoS pathogens*, 10(4), p. e1004050. doi: 10.1371/journal.ppat.1004050.
- Waldorf, A. R. and Diamond, R. D. (1985) 'Neutrophil chemotactic responses induced by fresh and swollen *Rhizopus oryzae* spores and *Aspergillus fumigatus* conidia', *Infection and Immunity*, 48(2), pp. 458–463.
- Waldorf, A. R., Ruderman, N. and Diamond, R. D. (1984) 'Specific susceptibility to mucormycosis in murine diabetes and bronchoalveolar macrophage defense against *Rhizopus*', *Journal of Clinical Investigation*, 74(1), pp. 150–160. doi: 10.1172/JCI111395.
- Walker, L. A. *et al.* (2008) 'Stimulation of chitin synthesis rescues *Candida albicans* from echinocandins', *PLoS Pathogens*, 4(4), p. e1000040. doi: 10.1371/journal.ppat.1000040.
- Wallace, R. L., Hirkala, D. L. and Nelson, L. M. (2018) 'Efficacy of *Pseudomonas fluorescens* for control of *Mucor* rot of apple during commercial storage and potential modes of action', *Can J Microbiol*, 64(6), pp. 420–431. doi: <https://doi.org/10.1139/cjm-2017-0776>.
- Wang, X. *et al.* (2014) 'Farnesol induces apoptosis-like cell death in the pathogenic fungus *Aspergillus flavus*', *Mycologia*, 106(5), pp. 881–888. doi: 10.3852/13-292.
- Wang, Y., Aisen, P. and Casadevall, A. (1995) '*Cryptococcus neoformans* melanin and virulence: mechanism of action.', *Infection and immunity*, 63, pp. 3131–3136.
- Warkentien, T. E. *et al.* (2015) 'Impact of Mucorales and other invasive molds on clinical outcomes of polymicrobial traumatic wound infections', *Journal of Clinical Microbiology*, 53(7), pp. 2262–2270. doi: 10.1128/JCM.00835-15.
- Wartenberg, D. *et al.* (2012) 'Proteome analysis of the farnesol-induced stress response in *Aspergillus nidulans*-The role of a putative dehydrin', *Journal of Proteomics*, 75(13), pp. 4038–4049. doi: 10.1016/j.jprot.2012.05.023.
- Waters, C. M. and Bassler, B. L. (2005) 'QUORUM SENSING: Cell-to-Cell Communication in Bacteria', *Annual Review of Cell and Developmental Biology*, 21(1), pp. 319–346. doi: 10.1146/annurev.cellbio.21.012704.131001.
- Watkins, T. N. *et al.* (2018) 'Inhibition of EGFR signaling protects from mucormycosis', *mBio*, 9(4), pp. e01384-18. doi: 10.1128/mbio.01384-18.
- Wegener, W. and Romano, A. (1963) 'Zinc stimulation of RNA and protein

- synthesis in *Rhizopus nigricans*', *Science*, 142(3600), pp. 1669–1670. doi: DOI: 10.1126/science.142.3600.1669.
- Weinberg, E. D. (1975) 'Nutritional immunity: Host's attempt to withhold iron from microbial invaders', *JAMA: The Journal of the American Medical Association*, 231(1), pp. 39–41. doi: 10.1001/jama.1975.03240130021018.
- Wessels, J. G. H. (1996) 'Hydrophobins: proteins that change the nature of the fungal surface', *Advances in Microbial Physiology*, 38, pp. 1–45. doi: 10.1016/s0065-2911(08)60154-x.
- Wheeler, R. T. *et al.* (2008) 'Dynamic, morphotype-specific *Candida albicans*  $\beta$ -glucan exposure during infection and drug treatment', *PLoS Pathogens*, 4(12), p. e1000227. doi: 10.1371/journal.ppat.1000227.
- White, R. M. *et al.* (2008) 'Transparent adult zebrafish as a tool for *in vivo* transplantation analysis', *Cell Stem Cell*, 2(2), pp. 183–189. doi: 10.1016/j.stem.2007.11.002.
- WHO (2014) 'Antimicrobial resistance: global report on surveillance'. Available at: <http://go.nature.com/2tTi59N>.
- WHO (2017) 'Global priority list of antibiotic-resistant bacteria to guide research, discovery, and development of new antibiotics'. Available at: [http://www.who.int/medicines/publications/WHO-PPL-Short\\_Summary\\_25Feb-ET\\_NM\\_WHO.pdf?ua=1](http://www.who.int/medicines/publications/WHO-PPL-Short_Summary_25Feb-ET_NM_WHO.pdf?ua=1).
- WHO (2018) *Meeting on global surveillance of antimicrobial resistance invasive Candida infections*. Available at: <https://www.who.int/glass/events/AMR-in-invasive-candida-infections-meeting/en/>.
- Willett, C. E. *et al.* (1999) 'Early hematopoiesis and developing lymphoid organs in the zebrafish', *Developmental Dynamics*. doi: 10.1002/(SICI)1097-0177(199904)214:4<323::AID-AJA5>3.0.CO;2-3.
- Willis, A. R. *et al.* (2016) 'Injections of predatory bacteria work alongside host immune cells to treat *Shigella* infection in zebrafish larvae', *Current Biology*, 26(24), pp. 3343–3351. doi: 10.1016/j.cub.2016.09.067.
- Wilson, C. L., Franklin, J. D. and Pusey, P. L. (1987) 'Biological control of *Rhizopus* rot of peach with *Enterobacter cloacae*', *Phytopathology*, 77, pp. 303–305. doi: 10.1094/phyto-77-303.
- Wilson, R. *et al.* (1988) 'Measurement of *Pseudomonas aeruginosa* phenazine pigments in sputum and assessment of their contribution to sputum sol toxicity for respiratory epithelium', *Infection and Immunity*, 56(9), pp. 2515–2517.
- Windus, D. W. *et al.* (1987) 'Fatal *Rhizopus* infections in hemodialysis patients receiving deferoxamine', *Annals of Internal Medicine*, 107(5), pp. 678–679. doi: 10.7326/0003-4819-107-5-678.
- Wisniewski, M., Wilson, C. and Hershberger, W. (1989) 'Characterization of inhibition of *Rhizopus stolonifer* germination and growth by *Enterobacter cloacae*', *Canadian Journal of Botany*, 67(8), pp. 2317–2323. doi: 10.1139/b89-

296.

Xiao, R. and Kisaalita, W. S. (1997) 'Iron acquisition from transferrin and lactoferrin by *Pseudomonas aeruginosa* pyoverdin', *Microbiology*, 143(Pt 7), pp. 2509–2515. doi: 10.1099/00221287-143-7-2509.

Yadav, V. *et al.* (2005) 'A fraction from *Escherichia coli* with anti-*Aspergillus* properties', *Journal of Medical Microbiology*, 54(Pt 4), pp. 375–379. doi: 10.1099/jmm.0.45748-0.

Yahr, T. L., Goranson, J. and Frank, D. W. (1996) 'Exoenzyme S of *Pseudomonas aeruginosa* is secreted by a type III pathway', *Molecular Microbiology*, 22(5), pp. 991–1003. doi: 10.1046/j.1365-2958.1996.01554.x.

Yamanaka, K. *et al.* (2005) 'Desferrioxamine E produced by *Streptomyces griseus* stimulates growth and development of *Streptomyces tanashiensis*', *Microbiology*, 151(Pt 9), pp. 2899–2905. doi: 10.1099/mic.0.28139-0.

Yin, L. *et al.* (2015) 'Multiplex conditional mutagenesis using transgenic expression of Cas9 and sgRNAs', *Genetics*, 200(2), pp. 431–441. doi: 10.1534/genetics.115.176917.

Zahavi, T. *et al.* (2000) 'Biological control of *Botrytis*, *Aspergillus* and *Rhizopus* rots on table and wine grapes in Israel', *Postharvest Biology and Technology*, 20(2), pp. 115–124. doi: 10.1016/S0925-5214(00)00118-6.

Zhang, H. *et al.* (2007) 'Effect of yeast antagonist in combination with hot water dips on postharvest *Rhizopus* rot of strawberries', *Journal of Food Engineering*. doi: 10.1016/j.jfoodeng.2005.09.027.

Zhang, Y. Q. *et al.* (2011) 'Blocking of *Candida albicans* biofilm formation by cis-2-dodecenoic acid and trans-2-dodecenoic acid', *Journal of Medical Microbiology*, 60(Pt 11), pp. 1643–1650. doi: 10.1099/jmm.0.029058-0.

Zheng, W. *et al.* (2011) 'Comparative transcriptome analyses indicate molecular homology of zebrafish swimbladder and mammalian lung', *PLoS ONE*, 6(8), p. e24019. doi: 10.1371/journal.pone.0024019.

Zhou, T., Northover, J. and Schneider, K. E. (1999) 'Biological control of postharvest diseases of peach with phyllosphere isolates of *Pseudomonas syringae*', *Canadian Journal of Plant Pathology*, 21(4), pp. 375–381. doi: 10.1080/07060669909501174.

# SCIENTIFIC REPORTS

## OPEN *Pseudomonas aeruginosa* inhibits *Rhizopus microsporus* germination through sequestration of free environmental iron

Received: 11 October 2018  
Accepted: 26 March 2019  
Published online: 05 April 2019

Courtney Kousser, Callum Clark, Sarah Sherrington, Kerstin Voelz & Rebecca A. Hall 

*Rhizopus spp* are the most common etiological agents of mucormycosis, causing over 90% mortality in disseminated infection. Key to pathogenesis is the ability of fungal spores to swell, germinate, and penetrate surrounding tissues. Antibiotic treatment in at-risk patients increases the probability of the patient developing mucormycosis, suggesting that bacteria have the potential to control the growth of the fungus. However, research into polymicrobial relationships involving *Rhizopus spp* has not been extensively explored. Here we show that co-culturing *Rhizopus microsporus* and *Pseudomonas aeruginosa* results in the inhibition of spore germination. This inhibition was mediated via the secretion of bacterial siderophores, which induced iron stress on the fungus. Addition of *P. aeruginosa* siderophores to *R. microsporus* spores in the zebrafish larval model of infection resulted in inhibition of fungal germination and reduced host mortality. Therefore, during infection antibacterial treatment may relieve bacterial imposed nutrient restriction resulting in secondary fungal infections.

Mucormycosis is a life threatening, disfiguring infection caused by ubiquitous environmental fungi belonging to the order Mucorales, with *Rhizopus spp.* accounting for approximately 70% of infections<sup>1,2</sup>. In healthy individuals, innate immune cells are capable of controlling spore germination, thus preventing infection<sup>3</sup>. However, patients with uncontrolled diabetes, cancer, neutropenia, burn/traumatic wounds, post-transplantation and those undergoing corticosteroid therapy or renal dialysis are prone to mucormycosis<sup>4,5</sup>. Mucorales are inherently resistant to antifungals, requiring surgical debridement of infected tissue followed by an aggressive antifungal regime. As a result, mucormycosis is associated with high mortality rates (up to 96% in disseminated infections), and significant morbidity<sup>2</sup>.

Mucorales spores enter the body through inhalation or open wounds<sup>6</sup>. As a result mucormycosis is commonly associated with pulmonary, rhinocerebral, or cutaneous infections<sup>7</sup>. Germination is key to the pathogenesis of Mucorales, leading to tissue penetration, endothelial angioinvasion, and vessel thrombosis, ultimately resulting in debilitating necrosis<sup>8</sup>. Traumatic and burn wound infections, including military-associated blast wounds, are known predisposing conditions for mucormycosis in the immunocompetent<sup>2</sup>, with over 70% of these infections being polymicrobial in nature<sup>8,9</sup>. *Pseudomonas aeruginosa*, *Staphylococcus aureus*, and *Escherichia coli* are the most commonly co-isolated bacterial species from chronic wounds<sup>10,11</sup>, and are therefore likely to interact and compete with Mucorales spores. In addition, the emergence of mucormycosis has been associated with broad-spectrum antimicrobial treatment<sup>12–14</sup>, suggesting that the surrounding microbiome plays a role in controlling fungal growth.

Here we show that *P. aeruginosa* inhibits the germination, and therefore virulence, of *Rhizopus microsporus*, a common cause of mucormycosis. This inhibition was mainly caused by bacterial secretion of iron-chelating molecules, which sequester iron from the fungus. Considering the prevalence of opportunistic bacteria and Mucorales in traumatic wounds, antibacterial treatment may reduce the presence of nutrient-restricting molecules like bacterial secreted siderophores in the wound environment rendering the environment more permissive to fungal germination, although we acknowledge that other factors including the immune status of the host also play critical roles in controlling fungal infection.

Institute of Microbiology and Infection, School of Biosciences, University of Birmingham, Birmingham, B15 2TT, UK. Correspondence and requests for materials should be addressed to K.V. (email: K.Voelz@bham.ac.uk) or R.A.H. (email: r.a.hall@bham.ac.uk)

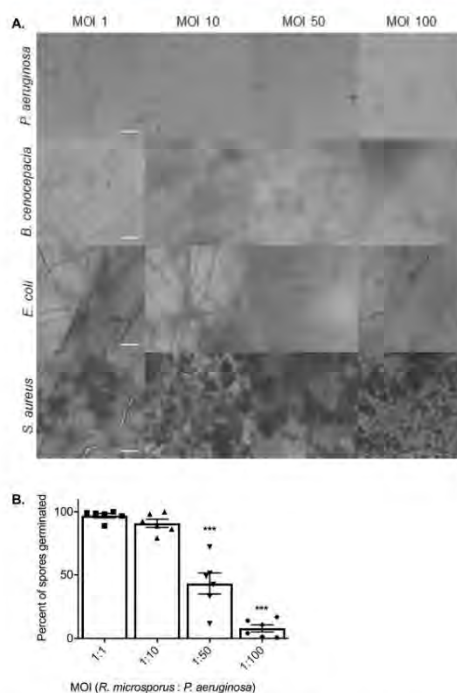


**Figure 1.** *Pseudomonas aeruginosa* strongly inhibits the germination of *Rhizopus microsporus*. *R. microsporus* spores were incubated with live *P. aeruginosa*, *B. cenocepacia*, *S. aureus*, and *E. coli* at increasing multiplicities of infection (MOI) for 24 h (A) Representative images after 24 h exposure (37 °C, static). Scale bars depict 50  $\mu$ m. (B) Percent of spores germinated after 24 h exposure to *P. aeruginosa*. One-way ANOVA performed on arcsine transformed data (n = 6). \*\*\*p < 0.001. Error bars depict SEM.

## Results

***Pseudomonas aeruginosa* inhibits the germination of *Rhizopus microsporus*.** Key to the pathogenesis of mucormycosis is the ability of spores to germinate and penetrate surrounding tissues<sup>4</sup>. To identify whether bacteria can influence fungal germination, *R. microsporus* spores were co-cultured with *Pseudomonas aeruginosa*, *Burkholderia cenocepacia*, *Staphylococcus aureus*, and *Escherichia coli*. Co-culture of *R. microsporus* with *P. aeruginosa* at multiplicities of infection (MOI) of 1:50 and 1:100 resulted in 56.8% (+/-8.269, p = 0.0023) and 92% (+/-2.784, p < 0.001) inhibition of fungal germination, respectively (Fig. 1A,B). Conversely, co-culturing *R. microsporus* spores with *S. aureus*, *E. coli*, and *B. cenocepacia* did not affect fungal growth at any of the MOIs tested (Fig. 1A). Taken together, the results obtained from live co-cultures between *R. microsporus* and *P. aeruginosa* indicate that these two microbes undergo a competitive relationship resulting in reduced fungal germination.

***P. aeruginosa* inhibits spore germination through secreted factors.** Microbes are able to communicate through the secretion of secondary metabolites, quorum sensing molecules, and metabolic by-products<sup>15–20</sup>. Therefore, to deduce whether the observed inhibition of *R. microsporus* germination was a result of direct cell-cell interactions or mediated through secreted products, *R. microsporus* spores were incubated in *P. aeruginosa* spent culture supernatants. Incubation of *R. microsporus* spores with 50% *P. aeruginosa* supernatant resulted in 94.4% (+/-0.01769, p = 0.0022) inhibition of fungal growth (Fig. 2A), confirming that the inhibitory molecule(s) are secreted by *P. aeruginosa*. Time-lapse microscopy confirmed that the presence of the supernatant resulted in a significant reduction in spore germination (Fig. 2B,C, Videos 1 and 2), with only 6.7% (+/-3.8, p < 0.0001) of spores germinating after 18 h. However, the inhibition of germination did not affect spore swelling (Videos 1 and 2). To deduce whether *P. aeruginosa* supernatants are able to inhibit fungal growth after the initiation of germination, spores were pre-germinated, and then subsequently incubated with 50% supernatant. Fungal growth was significantly reduced (by 81.4% +/- 5.252, p = 0.0286) in the presence of the supernatant compared to the media

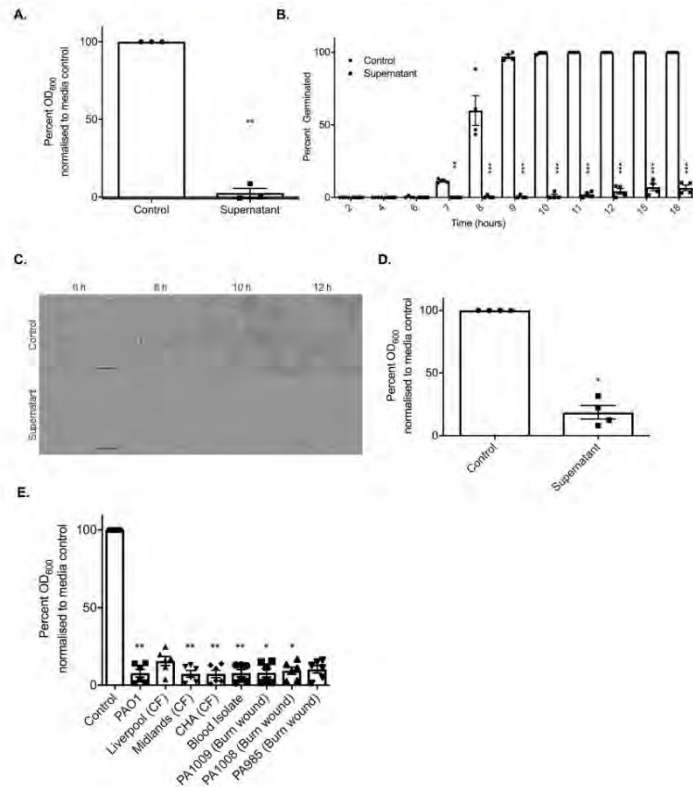


**Figure 2.** *P. aeruginosa* inhibits spore germination through secreted factors. *R. microsporus* spores were exposed to 50% *P. aeruginosa* PAO1 supernatant for 24 h. (A) Fungal growth was measured through absorbance ( $OD_{600}$ ) and normalised to media control ( $n = 3$ ). To determine the point of inhibition, spore germination was observed via live-cell imaging and (B) the per cent of spores germinated over time was quantified ( $n = 4$ , Two-way ANOVA performed on arcsine transformed data). (C) Representative images of spores germinating over time were collected. Scale bar = 50  $\mu\text{m}$ . (D) To determine whether the supernatant also inhibits the continuation of growth after germination is initiated, spores were incubated in SAB for 4–5 h until germlings emerged, and subsequently exposed to 50% PAO1 supernatant for 18 h ( $n = 4$ , Mann-Whitney  $U$  test). (E) To test whether this is a lab strain-specific phenomenon, *R. microsporus* spores were exposed to supernatants from *P. aeruginosa* clinical isolates for 24 h ( $n = 6$ ). Fungal growth was determined through absorbance ( $OD_{600}$ ). All data was analysed by a Kruskal-Wallis test with Dunn's multiple comparisons test unless indicated otherwise. \* $p < 0.05$ , \*\* $p < 0.01$ , \*\*\* $p < 0.001$ . Error bars depict SEM.

control (Fig. 2D). Therefore, *P. aeruginosa* supernatants are able to inhibit both germination and growth of *R. microsporus*.

To determine whether the inhibitory molecule(s) is produced by other *P. aeruginosa* strains, we tested the ability of supernatants from a series of *P. aeruginosa* isolates to inhibit spore germination. *R. microsporus* germination was inhibited in the presence of supernatants from all *P. aeruginosa* clinical isolates (Fig. 2E), suggesting that the production of this inhibitory molecule is a general trait of *P. aeruginosa* and is not limited to laboratory-evolved strains.

As fungal germination is dependent on environmental pH and nutrient availability<sup>21,22</sup>, we assessed whether the addition of the supernatant was inhibiting germination through modulation of these parameters. Addition of the bacterial supernatant to SAB broth resulted in mild alkalinisation of the media (pH 7.33 vs. 6.45). However, adjusting the pH of the control media to pH 7.33, to mimic the conditions in media containing the *P. aeruginosa* supernatant, did not affect *R. microsporus* germination rates (Supplementary Fig. S1). To elucidate the role of

macronutrient restriction, SAB broth was diluted with 50% phosphate buffered solution (PBS) to mimic the nutrient limitation imposed by the addition of 50% supernatant. However, the spores were still able to germinate under these conditions (Supplementary Fig. S1). Therefore, *P. aeruginosa* secretes a molecule(s) that is able to inhibit *R. microsporus* germination independent of pH and macronutrient limitation.

**Inhibition of *R. microsporus* germination is not mediated by quorum sensing molecules or pyocyanin.** Bacteria secrete a diverse range of proteins and secondary metabolites to aid in host colonisation and inter-species competition. To determine whether the secreted factor responsible for inhibiting spore germination is proteinaceous, *P. aeruginosa* supernatants were boiled or treated with Proteinase K to degrade any secreted proteins. Supernatants that were boiled or treated with Proteinase K inhibited *R. microsporus* growth (97.62%,  $+/-1.558$ ,  $p=0.0355$  and 99.03%,  $+/-1.634$ ,  $p=0.0140$ , respectively) (Supplementary Fig. S2A), suggesting that a secreted, heat-stable molecule mediates the observed inhibition of *R. microsporus* germination.

*P. aeruginosa* secretes several heat-stable cell density-dependent signalling molecules into the environment to regulate virulence by sensing population density and inducing the expression or inhibition of population-dependent mechanisms<sup>23</sup>. These quorum sensing molecules (QSMs) are well known to regulate intra- and inter-species interactions including inhibiting the morphological switch of *Candida albicans*<sup>24–27</sup>. Therefore, we tested the ability of the major *P. aeruginosa* QSMs to inhibit *R. microsporus* germination. Exposure of *R. microsporus* spores to N-butanoyl-L-homoserine lactone (C4 HSL), N-hexanoyl-DL-homoserine lactone (C6 HSL), and N-octanoyl-L-homoserine lactone (C8 HSL), did not affect fungal growth (Supplementary Fig. S2B–D). At high concentrations (200  $\mu$ M) N-(3-oxododecanoyl)-L-homoserine lactone (C12 HSL) resulted in 42.1% ( $+/-0.1518$ ,  $p=0.1331$ ) reduction in fungal growth (Supplementary Fig. S2E). Therefore, secreted QSMs appear to not be the major regulators of *R. microsporus* growth.

Pyocyanin is a heat stable, secreted blue-pigmented toxin, which is known to increase the virulence of *P. aeruginosa* by depressing the host immune responses through induction of neutrophil apoptosis<sup>28,29</sup>. Pyocyanin also inhibits the growth and morphogenesis of *C. albicans* and *Aspergillus fumigatus*<sup>30</sup>. Therefore, we determined whether the presence of pyocyanin in the supernatant was inhibiting the germination of *R. microsporus*. Addition of purified pyocyanin resulted in 31.4% ( $+/-0.1434$ ,  $p>0.9999$ ) inhibition of *R. microsporus* growth at concentrations above 100  $\mu$ M (Supplementary Fig. S2F). To deduce whether these pyocyanin concentrations were physiologically relevant the concentration of pyocyanin in the *P. aeruginosa* supernatants was quantified through absorbance measurement (690 nm) and compared to a standard curve of pre-defined pyocyanin concentrations. Growth of *P. aeruginosa* in LB media at 200 rpm, 37 °C did not result in the secretion of detectable levels of pyocyanin (not shown). Therefore, the inhibition of *R. microsporus* growth in the *P. aeruginosa* supernatant was not due to pyocyanin.

To determine whether the secreted factor is a lipophilic molecule, chloroform extractions were performed. The organic phase of the supernatant did not significantly inhibit spore germination (18% inhibition,  $+/-3.058$ ,  $p=0.0926$ ), while the aqueous phase maintained its inhibitory action (95.1% inhibition,  $+/-0.9559$ ,  $p=0.0079$ , Supplementary Fig. S2G). Therefore, a secreted, heat-stable, water-soluble molecule(s) inhibits the growth of *R. microsporus*.

***P. aeruginosa* inhibits *R. microsporus* germination via iron sequestration.** Research has established the importance of metal micronutrients for microbial growth and pathogenicity, and the ability of host metal sequestering proteins to inhibit both fungal and bacterial growth through nutritional immunity<sup>31–33</sup>. Iron, zinc, copper, and manganese are considered the most important trace metals for the growth of fungi and the availability of iron is key to the pathogenesis of Mucorales<sup>34,35</sup>. Therefore, we investigated whether the supernatants were imposing micronutrient restriction on *R. microsporus*. Supplementing the supernatants with iron was able to partially restore fungal growth, resulting in 46.2% *R. microsporus* growth at concentrations above 200  $\mu$ M ( $+/-6.660$ , Fig. 3A,C) and an insignificant difference as compared to the control ( $p>0.9999$ ). However, supplementation with zinc, copper or manganese did not rescue *R. microsporus* growth (Supplementary Fig. S3). Therefore, the majority of growth inhibition appears to result from the *P. aeruginosa* supernatants specifically sequestering iron from the environment. However, we acknowledge that other unidentified factors may play a role as supplementation with iron did not completely restore fungal growth. To confirm that the inhibition of spore germination observed in the co-cultures was also attributed to iron restriction, co-cultures of *R. microsporus* and *P. aeruginosa* were spiked with iron. Germination and therefore growth of *R. microsporus* in the co-culture was recovered at concentrations above 100  $\mu$ M (41.9%  $+/-12.46$ ,  $p=0.1540$ ) to levels comparable to those observed for iron spiked supernatants (Fig. 3B), confirming that in both scenarios the major contributing factor, resulting in the inhibition of fungal growth, appears to be the sequestration of iron by *P. aeruginosa*.

Iron starvation has previously been shown to up-regulate the high affinity iron permease *FTR1* in other *Rhizopus* species<sup>36</sup>. Therefore, to confirm that *R. microsporus* is undergoing iron starvation in the presence of *P. aeruginosa* supernatants, the expression levels of *FTR1* were determined by qRT-PCR. *FTR1* was highly upregulated (10-fold increase,  $p=0.0286$ ) when exposed to 50% *P. aeruginosa* supernatant for 7 h, as compared to the control (Fig. 3D). This confirms that *P. aeruginosa* mediated iron restriction inhibits *R. microsporus* growth and germination.

Iron starvation has been shown to induce apoptosis in *R. oryzae* after prolonged starvation<sup>36</sup>. Therefore, if spores are undergoing iron starvation when exposed to *P. aeruginosa* supernatant, prolonged exposure should decrease survival. To isolate the effects of the supernatant, we used 100% *P. aeruginosa* supernatant to monitor spore survival over time. In this condition, the viability of spores was reduced by 82.40% ( $+/-13.44$ ) after 24 h, and no viable spores were recovered after 120 h ( $p=0.0490$ , Fig. 3E). This indicates that iron is essential for the survival and pathogenicity of *R. microsporus*.

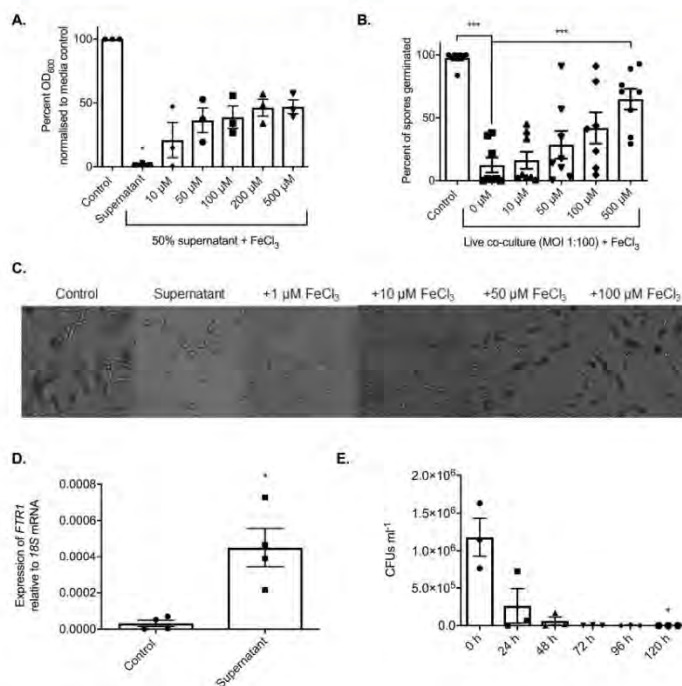


**Figure 3.** *P. aeruginosa* inhibits *R. microsporus* germination via iron sequestration. *R. microsporus* spores were exposed to (A) 50% *P. aeruginosa* supernatant and spiked with increasing concentrations of iron chloride for 24 h statically at 37 °C. Fungal growth was measured through absorbance ( $OD_{600}$ ) and normalised to media control ( $n = 3$ , Kruskal-Wallis test with Dunn's multiple comparisons test). (B) This ability to rescue was confirmed in a live co-culture setting, where the addition of exogenous iron increased the per cent of spores germinated after 24 h in a dose-dependent manner ( $n = 8$ ). As the addition of iron in 50% supernatant increased overall growth, (C) representative images were collected at 9 h to confirm ability to rescue germination. Scale bar depicts 50  $\mu\text{m}$ . (D) Iron starvation of *R. microsporus* spores after 7 h exposure to *P. aeruginosa* supernatant was determined through strong upregulation of the high-affinity iron permease *FTR1* ( $n = 4$ , Mann-Whitney *U* test). (E) As iron starvation is associated with Mucorales apoptosis, the viability of spores exposed to 100% *P. aeruginosa* supernatant over time was quantified by counting colony forming units (CFUs) every 24 h for 120 h ( $n = 3$ , Kruskal-Wallis test with Dunn's multiple comparisons test). \* $p < 0.05$ , \*\*\* $p < 0.001$ .

To delineate whether bacteria-associated iron restriction inhibits the growth of Mucorales in general, we tested the ability of *P. aeruginosa* supernatant to inhibit the growth of *R. microsporus var. microsporus*, *R. microsporus var. chinensis*, *R. delemar*, and *Mucor circinelloides*. The growth of all isolates was significantly reduced in the presence of *P. aeruginosa* supernatant [83.85% ( $\pm 15.23$ ), 98.26% ( $\pm 1.977$ ), 99.01% ( $\pm 0.8695$ ), and 87.54% ( $\pm 10.78$ ), respectively], and was significantly rescued by the addition of 100  $\mu\text{M}$  of iron [64.36% ( $\pm 4.450$ ), 41.30% ( $\pm 10.48$ ), 55.14% ( $\pm 10.01$ ), and 87.54% ( $\pm 6.219$ ), respectively]. This confirms that the bacteria-associated inhibition of growth is a general trait of Mucorales and highlights the potential differences between Mucorales strains in response to bacteria (Fig. 4).

**Siderophore deficient *P. aeruginosa* strains lack the ability to suppress germination.** Iron sequestering is mediated via iron binding proteins and molecules known as siderophores. Pyoverdine and pyochelin are the two predominate siderophores produced by *P. aeruginosa*, with pyoverdine exhibiting the highest affinity for iron<sup>37,38</sup>. To identify the role of these siderophores in this interaction, we quantified fungal growth in the presence of the supernatants from *P. aeruginosa* strains deficient in either siderophore alone, or in combination. Growth of *R. microsporus* was inhibited when incubated with culture supernatants from *P. aeruginosa* strains defective in pyochelin biosynthesis ( $\Delta\text{pchEF}$ ), with growth being rescued by exogenous iron (Fig. 5A), suggesting that this siderophore plays a minor role in sequestering iron in these experiments. However, *R. microsporus*

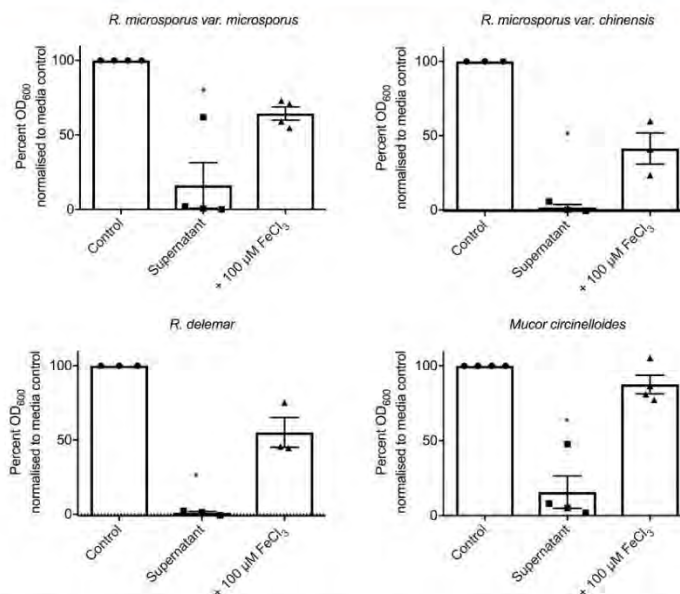


**Figure 4.** Iron-dependent inhibition of Mucorales by *P. aeruginosa* is not *R. microsporus* strain-specific. Most experiments in this study were performed using an *R. microsporus* clinical isolate. To ensure the inhibitory effect of *P. aeruginosa* is not limited to this isolate, *R. microsporus var. microsporus*, *R. microsporus var. chinensis*, *R. delemar*, and *Mucor circinelloides* were exposed to 50% *P. aeruginosa* supernatant with and without the addition of 100 µM FeCl<sub>3</sub>. Fungal growth was determined at 24 h by measuring absorbance (OD<sub>600</sub>) and normalising to control (n = 3), \*p < 0.05. All data was analysed by a Kruskal-Wallis test with Dunn's multiple comparisons test.

germinated in the presence of bacterial supernatants from *P. aeruginosa* mutants defective in pyoverdine biosynthesis ( $\Delta pvdD$ ) or in pyoverdine and pyochelin biosynthesis ( $\Delta pchE\Delta pvdD$ ) (Fig. 5A), confirming that, under the tested conditions, *P. aeruginosa* imposed iron restriction is largely mediated by the secretion of pyoverdine.

To confirm that pyoverdine alone is sufficient to inhibit *R. microsporus* growth, spores were exposed to exogenous pyoverdine. *P. aeruginosa* supernatants contained 58.9 µg ml<sup>-1</sup> (+/-1.194) siderophores, making the concentration of siderophores in our assay 29.45 µg ml<sup>-1</sup>. Therefore, *R. microsporus* spores were grown in the presence of 20 µg ml<sup>-1</sup> purified pyoverdine to resemble siderophore concentrations similar to the culture supernatants. Incubation of fungal spores with pyoverdine significantly reduced fungal growth (73.8%, +/-5.503, p = 0.0022, Fig. 5B). Therefore, pyoverdine alone is sufficient to inhibit *R. microsporus* growth and germination.

***R. microsporus* induces iron stress and promotes bacterial siderophore production.** *C. albicans* can decrease *P. aeruginosa* siderophore production through suppression of the pyoverdine and pyochelin biosynthetic pathways<sup>19</sup>. To determine whether *R. microsporus* is also able to interfere with *P. aeruginosa* siderophore production, the concentration of siderophores after 24 h mono- and co-culture was quantified (Fig. 5C). Surprisingly, the concentration of siderophores in mono-cultures in SAB/LB was lower than in LB (4.99 µg ml<sup>-1</sup>, +/-5.834, vs 58.9 µg ml<sup>-1</sup> (+/-1.194)) suggesting that LB/SAB has a higher iron content, reducing siderophore production. However, in co-cultures, siderophore levels were increased to levels similar to the LB supernatant (53.25 µg ml<sup>-1</sup>, +/-0.4335 compared to 58.9 µg ml<sup>-1</sup> (+/-1.194) indicative of imposed iron stress. This increase in siderophore concentration was not observed in co-cultures containing siderophore deficient *P. aeruginosa* (Fig. 5D), confirming that the increase in siderophore concentration is likely due to increased bacterial rather than fungal siderophore biosynthesis. In agreement with this, key genes involved in pyoverdine and pyochelin biosynthesis were upregulated during co-culture with *R. microsporus*. However, this regulation was lost in the presence of exogenous iron (Fig. 5E). These results confirm that during co-culture, the two organisms compete for iron, resulting in the upregulation of bacterial siderophore biosynthesis and *P. aeruginosa* outcompeting *R. microsporus* for iron and therefore growth.

**The concentration of siderophores produced by bacteria correlates with inhibition of *R. microsporus* growth.** While live *E. coli*, *B. cenocepacia*, and *S. aureus* did not inhibit the growth of *R. microsporus*, these bacteria all produce siderophores<sup>39-41</sup>. To determine the ability of secreted factors to inhibit growth,

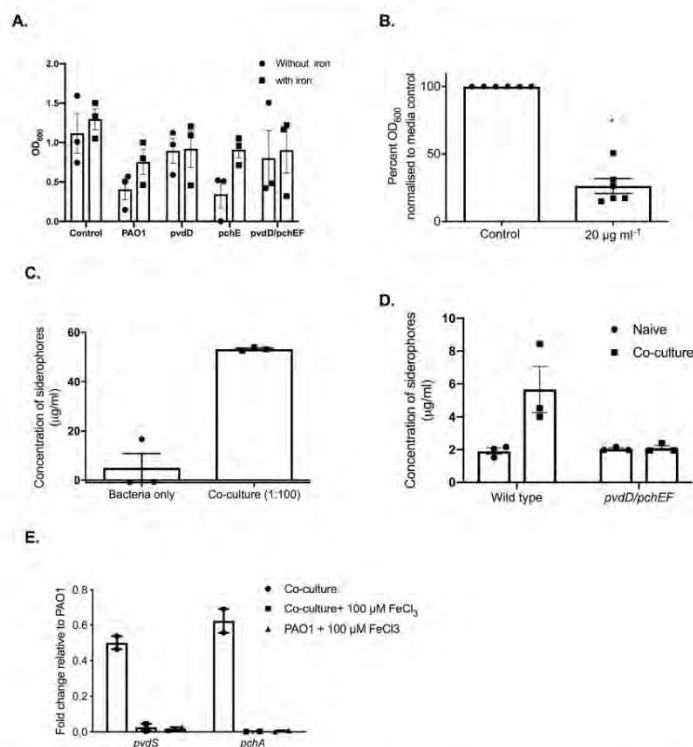


**Figure 5.** *P. aeruginosa*-imposed iron restriction is largely mediated via pyoverdine production. (A) *R. microsporus* was grown in bacterial supernatants from wild type *P. aeruginosa*, strains defective in siderophore biosynthesis, or standard LB mixed 25:75 with SAB, with and without iron. *R. microsporus* spores were exposed to these mixtures for 24 h and fungal growth was determined via absorbance ( $OD_{600}$ ,  $n=3$ ). (B) *R. microsporus* spores were incubated in SAB with  $20\mu\text{g ml}^{-1}$  of exogenous pyoverdine at  $37^\circ\text{C}$  for 24 h. Fungal growth was measured through absorbance ( $OD_{600}$ ) and normalised to media control ( $n=6$ ). (C) *P. aeruginosa* was exposed to *R. microsporus* at an MOI of 1:100 (*R. microsporus*:*P. aeruginosa*) for 24 h ( $37^\circ\text{C}$ ). Siderophore production was measured by using the Siderotec Assay (EmerginBio) ( $n=3$ , Mann-Whitney *U* test). (D) *P. aeruginosa* strains defective in siderophore biosynthesis were exposed to *R. microsporus* at an MOI of 1:100 (*R. microsporus*:*P. aeruginosa*) for 24 h ( $37^\circ\text{C}$ ). Siderophore production was measured by using the Siderotec Assay (EmerginBio) ( $n=3$ , Mann-Whitney *U* test). (E) *P. aeruginosa* was exposed to *R. microsporus* at an MOI of 1:100 (*R. microsporus*:*P. aeruginosa*) for 7 h, snap frozen and total RNA extracted. The expression levels of *PvdS* and *PchA* were quantified by qRT-PCR relative to *RpoD* and normalised to PAO1 grown in isolation.

*R. microsporus* spores were exposed to sterile supernatants from *E. coli*, *B. cenocepacia* and *S. aureus* to determine their ability to inhibit *R. microsporus* growth as compared to *P. aeruginosa* PAO1 and PA14. Consistent with the co-culture experiments, *P. aeruginosa* was the only supernatant able to significantly inhibit growth (Fig. 6A). We further investigated whether this lack of inhibition was associated with insufficient production of iron binding molecules by measuring the amount of siderophores produced after 24 h growth in LB. There was a negative correlation between fungal growth and siderophore production across different bacterial species ( $p=0.0029$ , Fig. 6B), suggesting that siderophore mediated iron restriction may be a common mechanism of bacteria to compete with fungi. However, the presence of supernatants from *E. coli* had no effect on fungal growth. This was surprising, as *E. coli* produces enterobactin, a siderophore with a high affinity ( $10^{22}\text{M}$ ) for iron<sup>42</sup>. In agreement with this data, exogenous enterobactin did not inhibit *R. microsporus* growth (91%,  $+/-6.170$ ,  $p=0.936$ , Fig. 6C), suggesting that *R. microsporus* may utilise enterobactin as a xenosiderophore. Therefore, the addition of enterobactin in the presence of *P. aeruginosa* may provide an advantage to *R. microsporus*. To explore this possibility, we added exogenous enterobactin to *R. microsporus*-*P. aeruginosa* co-cultures. However, the presence of the

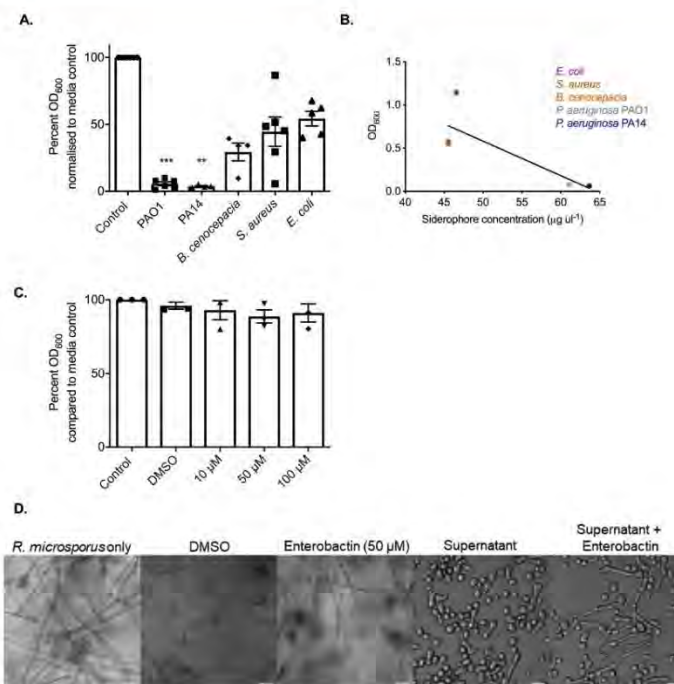


**Figure 6.** *R. microsporus* can utilise enterobactin as a xenosiderophore. (A) *R. microsporus* spores were exposed to 50% supernatants harvested from *P. aeruginosa* PAO1, *P. aeruginosa* PA14, *B. cenocepacia*, *S. aureus*, and *E. coli* for 24 h. Fungal growth was determined by absorbance (OD<sub>600</sub>) and normalised to control. (n = 6). (B) Concentration of siderophores produced by bacteria was determined by using the Siderotec Assay (EmerginBio). Correlation between total siderophore production and fungal growth was determined by performing a linear regression with Pearson correlation (n = 3). (C) *R. microsporus* spores were exposed to varying concentrations of purified enterobactin for 24 h at 37 °C (n = 3). Fungal growth was determined by absorbance (OD<sub>600</sub>) and normalised to control. (D) Enterobactin was added to PAO1 sterile supernatants diluted 50% with SAB to a final concentration of 50 µM and incubated at 37 °C for 24 h. Scale bar represents 20 µm. All data was analysed by a Kruskal-Wallis test with Dunn's multiple comparisons test unless indicated otherwise. \*p < 0.05, \*\*p < 0.01, \*\*\*p < 0.001.

enterobactin appeared to enhance the growth of the *P. aeruginosa*, presumably because *P. aeruginosa* can also utilise enterobactin as a xenosiderophore. Therefore, instead we added enterobactin to sterile bacterial supernatants. *R. microsporus* displayed increased germination in *P. aeruginosa* supernatants supplemented with enterobactin, although fungal growth was not fully restored (Fig. 6D), presumably due to pyoverdine and pyochelin binding the majority of the free iron. Therefore, taken together this data indicates that *R. microsporus* can use enterobactin as a xenosiderophore.

**The bacterial siderophore, pyoverdine, reduces the virulence of *R. microspores*.** To determine whether the effects of the bacterial siderophores have a role in controlling fungal infection in the host, we utilised the zebrafish larval model (Fig. 7A). Co-injection of *R. microsporus* with pyoverdine (80 µg ml<sup>-1</sup>) resulted in a mild but significant increase in fish survival when compared to spores alone (Fig. 7B) with 89% (+/-6.377) of fish surviving across a 96-h time course. As a control to rule out any impact of the siderophore on innate immune cell function, fish were also infected with *R. microsporus* in the presence of enterobactin, which should induce iron restriction on the host, but not on the pathogen due to its ability to use enterobactin as a xenosiderophore. Unlike pyoverdine, the addition of enterobactin did not increase the survival of the larvae compared to larvae infected with *R. microsporus* alone (Fig. 7C). Together these data confirm that the presence of pyoverdine is sufficient to reduce host damage caused by *R. microsporus* infection.

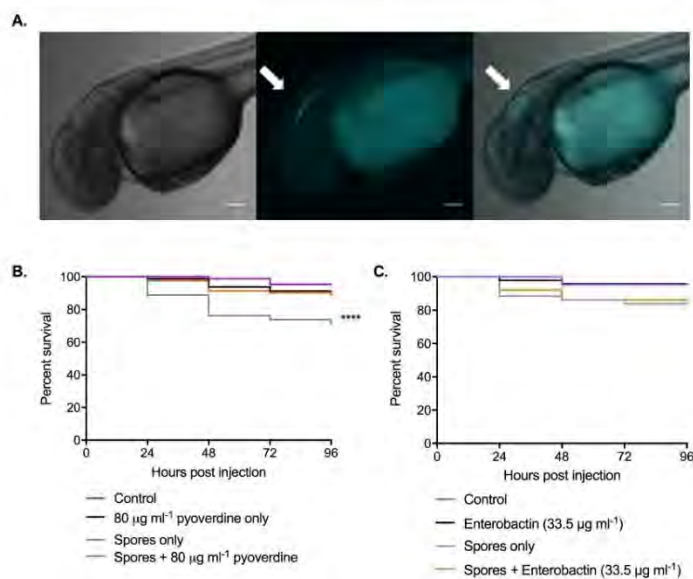


**Figure 7.** The bacterial siderophore, pyoverdine, reduces *R. microsporus* virulence in a zebrafish model of infection. To determine the impact of pyoverdine on fungal virulence within a host, zebrafish larvae were injected in the hindbrain with 50 spores  $\pm$  80  $\mu\text{g ml}^{-1}$  pyoverdine. (A) Representative images of zebrafish larvae at 0 hpi. White arrows indicate *R. microsporus* spores (Calcofluor White stain, cyan pseudo-coloured) located within hindbrain compartment. Scale bars depict 100  $\mu\text{m}$ . (B) Survival of larvae was quantified over time. Shown are data pooled from four separate experiments with a total of 87, 80, 80, and 81 fish for control, pyoverdine only, spores only, and spores + pyoverdine, respectively. Data analysed with Mantel-Cox log-rank test. (C) Survival of larvae was quantified over time. Data shown is pooled from two independent experiments with a total of 42, 44, 46, 43, and 50 fish for control, enterobactin only, spores only, and spores + enterobactin, respectively. Data analysed with Mantel-Cox log-rank test.

## Discussion

Mucormycosis is a lethal infection with high mortality rates and lack of treatment options due to intrinsic anti-fungal resistance<sup>43</sup>. Our current understanding of the pathogenesis is incomplete, especially when compared to other opportunistic fungal pathogens such as *C. albicans* and *A. fumigatus*. Because of this, it is important to understand the pressures Mucorales encounter within the human body. This not only includes pressures from the host, but also from the microbiota. Here we identify that *P. aeruginosa* is able to inhibit the germination of *R. microsporus* through the secretion of siderophores.

*Pseudomonas* species interact with and control the growth of a variety of fungal species including important plant and animal pathogens<sup>26,44,45</sup>. These interactions have been linked to a variety of contact dependent<sup>46</sup> and bacterial secreted factors<sup>26,44,45</sup>. The most characterised secreted molecules known to affect fungal growth and morphology are the phenazines<sup>47,48</sup> and the homoserine lactones<sup>26,44</sup>. For example, in *C. albicans* low levels of phenazines inhibit filamentation and biofilm formation, and are fungicidal at high concentrations<sup>49</sup>. Furthermore, the quorum sensing molecule, 3-oxo-C12-homoserine lactone (C12 HSL) induces apoptosis in *C. albicans*<sup>26</sup> and *A. fumigatus*<sup>44</sup>. Despite this, these molecules had negligible impact on the growth of *R. microsporus*, confirming that other bacterial secreted factors control the growth of *R. microsporus*. However, high concentrations of C12 HSL (200  $\mu\text{M}$ ) had a marginal effect on *R. microsporus* growth, indicating that intra-species QS may play a role in polymicrobial biofilms.

Instead we identified that this antagonistic relationship between *P. aeruginosa* and *R. microsporus* to be the result of competition for iron. Iron acquisition is key to Mucorales pathogenesis<sup>50</sup>. For example, medical conditions (i.e. diabetic ketoacidosis) that result in increased serum levels of iron predispose individuals to mucormycosis<sup>51</sup>, whereas iron chelation therapy, or reduction in fungal iron acquisition mechanisms reduce mortality in murine models of mucormycosis<sup>50,52</sup>. *P. aeruginosa* secretes several iron binding molecules, with pyoverdine being the major siderophore with a high affinity for iron. In agreement with this, we found that exogenous pyoverdine, at concentrations equal to those secreted by *P. aeruginosa* in our culture conditions, was sufficient to inhibit the growth of *R. microsporus* to levels comparable to the bacterial supernatant. In addition, deletion of key

enzymes in the biosynthesis pathways of the major *P. aeruginosa* siderophores was sufficient to reduce the effect of the bacterial supernatant, confirming a role for these siderophores in controlling fungal growth.

The presence of fungi has been shown to modulate the expression of siderophore biosynthetic genes in *P. aeruginosa*. For instance, *C. albicans* was described as down-regulating the production of pyoverdine and pyochelin through secreted proteins<sup>39</sup>. Conversely, this study has found the production of pyoverdine to be increased in response to *P. aeruginosa* co-cultured with *R. microsporus*. This is clinically important, as pyoverdine production is directly linked to virulence of *P. aeruginosa* and is shown to modulate the production of other toxins<sup>53,54</sup>.

The addition of exogenous iron or the inhibition of bacterial siderophore production only resulted in the restoration of approximately 50% fungal growth compared to media only controls, suggesting that other factors also contribute to this inhibition. However, in *Rhizopus oryzae*, iron starvation induces apoptosis<sup>36</sup>, suggesting that spore viability may also be affected. In agreement with this, growth of *R. microsporus* in 100% *P. aeruginosa* supernatant decreased spore viability. As such, it is possible that reduced viability may account for the inability to completely rescue fungal growth. Interestingly though, exogenous iron was able to fully restore the growth of *Mucor circinelloides*, suggesting that *M. circinelloides* is less susceptible to apoptosis induced by iron starvation. Differences in the ability of iron to rescue growth between Mucorales strains also suggests the presence of other potential interactions beyond iron starvation.

*R. microsporus* can utilise some bacterial siderophores as sources of iron within the host, such as deferoxamine (a siderophore produced by some actinomycetes) to promote its growth and virulence<sup>55</sup>. However, unlike deferoxamine, and potentially enterobactin, *R. microsporus* cannot scavenge iron from pyoverdine, which suggests that molecules with similar structure may have the potential to be used to control mucormycosis. While utilising pyoverdine itself would be problematic due to its ability to enhance *P. aeruginosa* virulence<sup>54</sup>, this siderophore could provide a starting point for the development of novel iron chelators. Given that pyoverdine has also been shown to limit the growth of other invasive fungi, such as *A. fumigatus*<sup>18,56</sup>, molecules based on pyoverdine may have wide implications for the treatment of a range of invasive fungal diseases. This is further enforced by the fact that the presence of pyoverdine in our zebrafish larval model of infection was able to reduce mortality. Similar effects have also been observed in mouse models of infection where deferasirox protects against mucormycosis<sup>57</sup>. Therefore, iron chelation therapy could be an important preventative treatment for mucormycosis. However, it should be noted that iron is not only important for microbial growth, but also plays essential roles in immunity<sup>57</sup>. Consequently, iron chelation therapy may have unexpected effects on host immunity. For example, in *C. elegans*, pyoverdine has been shown to induce mitochondrial damage triggering autophagy and an altered host immune response<sup>58</sup>. Therefore, it is important to understand the consequences these iron scavenging molecules have on the host before such therapies are applied.

Taken together, our results agree with the current understanding of Mucorales pathogenesis where iron availability is considered essential for pathogenesis. However, here we present this in a different scenario where iron availability is controlled by surrounding bacteria. Given that a high percentage of invasive mucormycosis results from burn and blast wound infections, where iron availability will be high due to tissue damage, we propose that opportunistic bacteria like *P. aeruginosa* will sequester iron away from the fungus restricting fungal growth. In agreement with this, burn wound exudate enhances *P. aeruginosa* siderophore production<sup>59</sup> resulting in high concentrations of pyoverdine in the wound. However, antibiotic treatment would reduce this competition for iron, and promote fungal germination. This, coupled with natural immunosuppression following trauma could lead to aggressive secondary mucormycosis<sup>60</sup>. Therefore, patients that have potentially been exposed to fungal spores (i.e. soldiers with blast wounds where significant environmental contamination of the wound has occurred) should be closely monitored for secondary fungal infections. The discovery of suitable iron chelators that do not promote bacterial virulence would be advantageous in this setting to help prevent fungal infection.

## Methods

**Ethics.** Zebrafish care and experiments were performed under Home Office project license P51AB7F76 and personal license I5B923969 in accordance with the Animal Scientific Procedures Act 1986.

**Strains and culture conditions.** All media and chemicals were purchased from Sigma-Aldrich unless stated otherwise. For details of fungal and bacterial strains used, please see (Table 1). *R. microsporus* was routinely sub-cultured and maintained on Sabouraud 4% dextrose agar (SAB, Merck Millipore, Germany) and incubated for 10–14 days before use (25 °C). Bacteria were maintained on Lysogeny broth (LB) with 2% agar.

**Live co-cultures.** LB broth was inoculated with *P. aeruginosa*, *B. cenocepacia*, *E. coli*, or *S. aureus* and incubated for 24 h (37 °C, 200 rpm). Bacteria were washed three times with phosphate buffered solution (PBS). *R. microsporus* sporangiospores were harvested through flooding with PBS, washed once, and counted via haemocytometer. Spores ( $1 \times 10^8$  spores/ml) were added to 50% SAB, 50% LB in a 96-well plate. Bacteria were added to each well at a multiplicity of infection (MOI) ratio of 1:1, 1:10, 1:50, and 1:100 and incubated for 24 h (static, 37 °C). Wells were imaged using an inverted Zeiss AxioObserver microscope (20x magnification) and the number of germinated spores per field of view quantified. Germination was defined as the point in which the germ tube reached the same size as the spore diameter.

**Spore germination when exposed to bacterial supernatants.** Bacterial cultures were prepared as previously detailed and grown to at least stationary phase ( $OD_{600} > 3.0$ ). Cultures were centrifuged ( $3220 \times g$ , 10 min) and the resulting supernatant filter sterilised. Sterile supernatants were stored at  $-80$  °C until required. Spores ( $1 \times 10^8$ /ml) were added to a 96-well plate containing either 50% SAB and 50% LB broth, or 50% SAB and 50% supernatant. Fungal growth was determined by endpoint analysis using  $OD_{600}$  as a quantifier of growth (FLUOstar Omega plate reader).

Strain	Characteristics	Source
<i>Rhizopus microsporus</i> 12.6652333	Clinical isolate	Queen Elizabeth Hospital Birmingham
<i>R. microsporus</i> var. <i>microsporus</i> CBS 699.68	Clinical isolate	Westerdijk Fungal Biodiversity Institute
<i>R. microsporus</i> var. <i>chinensis</i> CBS 631.82	Clinical isolate	Westerdijk Fungal Biodiversity Institute
<i>R. delemar</i> RA 99–880	Clinical isolate	Fungal Genetics Stock Centre
<i>Mucor circinelloides</i> NRRL3631	Clinical isolate	ARS Culture Collection (NRRL)
<i>Burkholderia cenocepacia</i> K56–2	Clinical isolate from cystic fibrosis	Amy Dumigan, Queen's University Belfast
<i>Staphylococcus aureus</i> MRSA	Wild type	Anne-Marie Krachler, University of Texas
<i>Escherichia coli</i> MG1655	Wild type	Anne-Marie Krachler, University of Texas
<i>Pseudomonas aeruginosa</i> PAO1 ATCC15692	Wild type	ATCC
<i>P. aeruginosa</i> PAO1	Wild type	<sup>62,63</sup>
<i>P. aeruginosa</i> $\Delta$ pchEF	PAO1, deleted pyochelin	<sup>64</sup>
<i>P. aeruginosa</i> $\Delta$ pvdD	PAO1, deleted pyoverdine	<sup>65</sup>
<i>P. aeruginosa</i> $\Delta$ pchEF $\Delta$ pvdD	PAO1, deleted pyochelin and pyoverdine	<sup>66</sup>

**Table 1.** Strains used in this study.

To investigate the role of iron restriction, ferric chloride (100 mM) was diluted to 1, 10, 50, 100, 200, and 500  $\mu$ M in supernatants. The iron was allowed to associate with any chelating molecules for 15 min before the addition of an equal volume of SAB. Wells containing the SAB/supernatant mixture without iron were included as controls.

**Live cell imaging.** Live-cell imaging was performed for 12–18 h at 37 °C with humidity using a Zeiss AxioObserver microscope (20x magnification). Images were taken every 10 min to create a time-lapse movie, and the percentage of germinated spores in each field of view was determined.

**Exposure of pre-germinated spores to *P. aeruginosa* supernatant.** Spores were harvested and added to 500  $\mu$ l of SAB broth at a concentration of  $1 \times 10^6$  spores/ml in triplicate in a 24 well plate. Spores were incubated statically for 4–5 h at 37 °C until germlings emerged and then either 500  $\mu$ l of *P. aeruginosa* supernatant or 500  $\mu$ l LB was added. The plate was incubated for 18 h at 37 °C, and the endpoint absorbance (OD<sub>600</sub>) of each well measured.

**Viability of spores exposed to *P. aeruginosa* supernatant.** *R. microsporus* spores ( $1 \times 10^6$  spores/ml) were exposed to 100% *P. aeruginosa* supernatant for 96 h (statically, 37 °C). Every 24 h, 100 spores were plated on SAB agar and incubated at 25 °C for 24 h. Following incubation, the number of viable spores were counted and compared to 0 h control plates.

**Pyocyanin secretion.** *P. aeruginosa* supernatants were prepared as described previously. Absorbance (690 nm) was measured using a FLUOstar Omega plate reader and compared to a pyocyanin standard curve.

**RNA extraction of fungi.** *R. microsporus* spores ( $2.5 \times 10^6$  spores/ml) were exposed to SAB/LB (50:50) (media only control) or 50% PAO1 supernatant. Flasks were incubated statically at 37 °C for 7 h. Spores were centrifuged (1,811  $\times$  g, 3 min), snap frozen in liquid nitrogen, and stored at –80 °C. When ready to extract RNA, 1 ml of TRIzol (Invitrogen) was added to each sample and thawed on ice. These samples were homogenised as before. Chloroform (200  $\mu$ l) was added to each sample, vortexed thoroughly, and centrifuged at 4 °C, 9,400  $\times$  g for 15 min. The aqueous layer was collected, and an equal volume of 100% ethanol was added. 700  $\mu$ l of this was transferred to RNeasy columns, and the RNeasy Mini Plus Kit (Qiagen) protocol followed according to manufacturer guidelines. The RNA concentration and quality were measured using a spectrophotometer.

**RNA extraction of bacteria.** *P. aeruginosa* ( $1 \times 10^8$  CFUs/ml) were exposed to 50:50 SAB/LB (+/–100  $\mu$ M FeCl<sub>3</sub>) or *R. microsporus* spores ( $1 \times 10^6$  spores/ml, +/–100  $\mu$ M FeCl<sub>3</sub>). Flasks were incubated at 37 °C and 50 rpm for 7 h. Cultures were centrifuged (6,000  $\times$  g for 3 min), snap frozen in liquid nitrogen, and stored at –80 °C. The RNeasy Mini Plus Kit (Qiagen) protocol for purification of total RNA from bacteria was followed according to manufacturer guidelines. The RNA concentration and quality were measured using a spectrophotometer.

**Quantitative Reverse Transcriptase PCR.** qRT-PCR was performed using an iTaq Universal SYBR Green One-Step Kit (Bio Rad) using 50 ng RNA with a total reaction volume of 20  $\mu$ l. Protocol was followed according to manufacturer's recommendations. *FTR1* was amplified using the forward primer (5'-GTGGTGCTCCTTGG GTGTT-3') and reverse primer (5'-CCACCACGGTAGATGAGGA-3'). This was normalised to 18 s rRNA using the forward primer (5'-GGCGACGGTCCACTCGATT-3') and reverse primer (5'-TCACTACCTCCCGT GTCGG-3').

*PvdS* was amplified using the forward primer (5'-ACCGTACGATCCTGGTGAAG-3') and reverse primer (5'-TGAACGACGAAGTGATCTGC-3'). *PchA* was amplified using the forward primer (5'-CTGCCTGTACTGG GAACAGC-3') and reverse primer (5'-GCAGAGCAATGCCCAGTTT-3'). These were normalised to *rpoD* using the forward primer (5'-GGGCGAAGAAGGAAATGGTC-3') and the reverse primer (5'-CAGGTGGCGTA GGTGGAGAA-3').

**Quantification of overall siderophore production.** Siderophore concentrations in bacterial supernatants were quantified by using the SideroTec Assay Kit (Emergen Bio) according to the manufacturer recommendations.

**Zebrafish infections.** Adult wild type (AB) *Danio rerio* zebrafish were maintained at the University of Birmingham Aquatic Facility in recirculating tanks with 14 h light/10 h dark cycles at 28 °C. Adult zebrafish naturally spawned overnight in groups of 11 fish (six female, five males). Embryos were transferred to E3 medium (5 mM NaCl, 0.17 mM KCl, 0.33 mM CaCl<sub>2</sub>, 0.33 mM MgSO<sub>4</sub>, pH 7) with 0.3 µg ml<sup>-1</sup> methylene blue and 0.003% 1-phenyl-2-thiourea (PTU) for the first 24 hours post fertilisation (hpf) and maintained at 32 °C.

Hindbrain injections were performed as previously described<sup>61</sup>. Sample sizes were calculated via power analysis using an alpha value of 0.05, power of 80%, mean effect size of 4.2%, and standard deviation of 8%, based on preliminary data and standards accepted by the zebrafish infection community. At 24 hpf larvae were manually dechlorinated and anaesthetised (160 µg ml<sup>-1</sup> Ethyl 3-aminobenzoate methanesulfonate salt [Tricaine]). *R. microsporus* spores were suspended in either polyvinylpyrrolidone (PVP, 10% in PBS + 0.05% phenol red), PVP + 80 µg ml<sup>-1</sup> pyoverdine, dimethyl sulfoxide (DMSO, solvent for enterobactin) or 33.5 µg ml<sup>-1</sup> enterobactin at a concentration of 5 × 10<sup>8</sup> spores/ml. Suspended spores (2 nl) were injected into the hindbrain via the otic vesicle to achieve a dose of 50 spores/larva. Control larvae were injected with either PVP only or PVP + 80 µg ml<sup>-1</sup> pyoverdine. Any fish that did not survive the injection process were removed. Survival was recorded every 24 h until larvae were sacrificed at 5 dpf (96 hours post infection) through 10x overdose of Tricaine. For the pyoverdine experiment, data were pooled from four separate experiments with a total of 87, 80, 80, and 81 fish for control, pyoverdine only, spores only, and spores + pyoverdine, respectively. For the enterobactin experiment, data were pooled from two separate experiments with a total of 42, 44, 46, 43, and 50 fish for control, DMSO, enterobactin only, spores only, and spores + enterobactin, respectively.

**Statistical analysis.** Each experiment was performed with at least two technical and two biological replicates. Microsoft Excel 2016 and GraphPad Prism 6 were used to record and analyse data. Statistical tests used are indicated in figure legends. All analysis was performed on non-normalised raw data or arcsine transformed data where appropriate. A p-value of p < 0.05 was considered to indicate statistical significance. Statistical significance is indicated by \*p < 0.05, \*\*p < 0.01, and \*\*\*p < 0.001.

#### Data Availability

The datasets generated during this study are available from the corresponding author upon reasonable request.

#### References

- Alvarez, E. *et al.* Spectrum of zygomycete species identified in clinically significant specimens in the United States. *J. Clin. Microbiol.* **47**, 1650–1656 (2009).
- Roden, M. M. *et al.* Epidemiology and outcome of zygomycosis: A Review of 929 reported cases. *Clin. Infect. Dis.* **41**, 634–653 (2005).
- Waldorf, A. R., Levitz, S. M. & Diamond, R. D. *In vivo* bronchoalveolar macrophage defense against *Rhizopus oryzae* and *Aspergillus fumigatus*. *J. Infect. Dis.* **150**, 752–760 (1984).
- Ibrahim, A. S., Spellberg, B., Walsh, T. J. & Kontoyiannis, D. P. Pathogenesis of mucormycosis. *Clin. Infect. Dis.* **54**, 1–7 (2012).
- Spellberg, B., Edwards, J. & Ibrahim, A. Novel perspectives on mucormycosis: Pathophysiology, presentation, and management. *Clinical Microbiology Reviews* **18**, 556–569 (2005).
- Rammaert, B. *et al.* Healthcare-associated mucormycosis. *Clin. Infect. Dis.* **54** (2012).
- Torres-Narbona, M. *et al.* Impact of zygomycosis on microbiology workload: A survey study in Spain. *J. Clin. Microbiol.* **45**, 2051–2053 (2007).
- Warkentien, T. E. *et al.* Impact of Mucorales and other invasive molds on clinical outcomes of polymicrobial traumatic wound infections. *J. Clin. Microbiol.* **53**, 2262–2270 (2015).
- Akers, K. S. *et al.* Biofilms and persistent wound infections in United States military trauma patients: A case-control analysis. *BMC Infect. Dis.* **14** (2014).
- Gjodsbøl, K. *et al.* Multiple bacterial species reside in chronic wounds: A longitudinal study. *Int. Wound J.* **3** (2006).
- Kalan, I. *et al.* Redefining the chronic-wound microbiome: Fungal communities are prevalent, dynamic, and associated with delayed healing. *MBio* **7**, 1–12 (2016).
- Struck, M. F. & Gille, J. Fungal infections in burns: A comprehensive review. *Ann. Burns Fire Disasters* **26**, 147–153 (2013).
- Baker, R. Mucormycosis; a new disease? *J. Am. Med. Assoc.* **163**, 805–808 (1957).
- Nash, G. *et al.* Fungal burn wound infection. *J. Am. Med. Assoc.* **215**, 1664–6 (1971).
- Jabra-Rizk, M. A., Meiller, T. F., James, C. E. & Shirtliff, M. E. Effect of farnesol on *Staphylococcus aureus* biofilm formation and antimicrobial susceptibility. *Antimicrob. Agents Chemother.* **50**, 1463–9 (2006).
- Peleg, A. Y. *et al.* Prokaryote-eukaryote interactions identified by using *Caenorhabditis elegans*. *Proc. Natl. Acad. Sci. USA* **105**, 14585–14590 (2008).
- Boon, C. *et al.* A novel DSF-like signal from *Burkholderia cenocepacia* interferes with *Candida albicans* morphological transition. *ISME J* **2**, 27–36 (2008).
- Penner, J. C. *et al.* Pf4 bacteriophage produced by *Pseudomonas aeruginosa* inhibits *Aspergillus fumigatus* metabolism via iron sequestration. *Microbiol. (United Kingdom)* **162**, 1583–1594 (2016).
- Lopez-Medina, E. *et al.* *Candida albicans* inhibits *Pseudomonas aeruginosa* virulence through suppression of pyochelin and pyoverdine biosynthesis. *PLoS Pathog.* **11** (2015).
- Hogan, D. A. *Pseudomonas-Candida* Interactions: An ecological role for virulence factors. *Science (80-)*. **296**, 2229–2232 (2002).
- Buflo, J., Herman, M. A. & Soll, D. R. A characterization of pH-regulated dimorphism in *Candida albicans*. *Mycopathologia* **85**, 21–30 (1984).
- Singh, P., Paul, S., Shivaprakash, M. R., Chakrabarti, A. & Ghosh, A. K. Stress response in medically important Mucorales. *Mycoses* **59**, 628–635 (2016).
- Waters, C. M. & Bassler, B. L. QUORUM SENSING: Cell-to-cell communication in bacteria. *Annu. Rev. Cell Dev. Biol.* **21**, 319–346 (2005).
- Enjalbert, B. & Whiteway, M. Release from quorum-sensing molecules triggers hyphal formation during *Candida albicans* resumption of growth. *Eukaryot. Cell* **4**, 1203–1210 (2005).
- Davies, D. G. The Involvement of cell-to-cell Signals in the development of a bacterial biofilm. *Science (80-)*. **280**, 295–298 (1998).

26. Hogan, D. A., Vik, Å. & Kolter, R. A. *Pseudomonas aeruginosa* quorum-sensing molecule influences *Candida albicans* morphology. *Mol. Microbiol.* **54**, 1212–1223 (2004).
27. Cruz, M. R., Graham, C. E., Gagliano, B. C., Lorenz, M. C. & Garsin, D. A. *Enterococcus faecalis* inhibits hyphal morphogenesis and virulence of *Candida albicans*. *Infect. Immun.* **81**, 189–200 (2013).
28. Allen, L. *et al.* Pyocyanin production by *Pseudomonas aeruginosa* induces neutrophil apoptosis and impairs neutrophil-mediated host defenses *in vivo*. *J. Immunol.* **174**, 3643–3649 (2005).
29. Prince, L. R. *et al.* Subversion of a lysosomal pathway regulating neutrophil apoptosis by a major bacterial toxin, pyocyanin. *J. Immunol. Res. J. Immunol. Osaka Univ. Libr.* **180**, 3502–3511 (2013).
30. Iau, G. W., Hassett, D. J., Ran, H. & Kong, F. The role of pyocyanin in *Pseudomonas aeruginosa* infection. *Trends in Molecular Medicine* **10**, 599–606 (2004).
31. Weinberg, E. D. Nutritional immunity: Host's attempt to withhold iron from microbial invaders. *JAMA J. Am. Med. Assoc.* **231**, 39–41 (1975).
32. Corbin, B. D. *et al.* Metal chelation and inhibition of bacterial growth in tissue abscesses. *Science* (80). **319**, 962–965 (2008).
33. Foster, J. The heavy metal nutrition of fungi. *Bot Rev* **5**, 207–239 (1939).
34. Ballou, E. R. & Wilson, D. The roles of zinc and copper sensing in fungal pathogenesis. *Curr. Opin. Microbiol.* **32**, 128–134 (2016).
35. Ibrahim, A. S., Spellberg, B. & Edwards, J. Iron acquisition: a novel perspective on mucormycosis pathogenesis and treatment. *Curr. Opin. Infect. Dis.* **21**, 620–625 (2008).
36. Shirazi, F., Kontoyiannis, D. P. & Ibrahim, A. S. Iron starvation induces apoptosis in *Rhizopus oryzae* *in vitro*. *Virulence* **6**, 121–126 (2015).
37. Braud, A., Hannauer, M., Mislin, G. L. A. & Schalk, I. J. The *Pseudomonas aeruginosa* pyochelin-iron uptake pathway and its metal specificity. *J. Bacteriol.* **191**, 3517–3525 (2009).
38. Braud, A., Hoegy, F., Jezequel, K., Lebeau, T. & Schalk, I. J. New insights into the metal specificity of the *Pseudomonas aeruginosa* pyoverdine-iron uptake pathway. *Environ. Microbiol.* **11**, 1079–1091 (2009).
39. Courcol, R. J., Lambert, P., Fournier, P., Martin, G. R. & Brown, M. R. Effects of iron depletion and sub-inhibitory concentrations of antibodies on siderophore production by *Staphylococcus aureus*. *J. Antimicrob. Chemother.* **28**, 663–668 (1991).
40. O'Brien, I. G., Cox, G. B. & Gibson, F. Biologically active compounds containing 2,3-dihydroxybenzoic acid and serine formed by *Escherichia coli*. *Biochim. Biophys. Acta* **201**, 453–60 (1970).
41. Darling, P., Chan, M., Cox, A. D. & Sokol, P. A. Siderophore production by cystic fibrosis isolates of *Burkholderia cepacia*. *Infect. Immun.* **66**, 874–877 (1998).
42. Carrano, C. J. & Raymond, K. N. Kinetics and mechanism of iron removal from transferrin by enterobactin and synthetic trisacchols. *J. Am. Chem. Soc.* **101**, 5401–5404 (1979).
43. Sun, Q. N., Fothergill, A. W., McCarthy, D. I., Rinaldi, M. G. & Graybill, J. R. *In vitro* activities of posaconazole, itraconazole, voriconazole, amphotericin B, and fluconazole against 37 clinical isolates of zygomycetes. *Antimicrob. Agents Chemother.* **46**, 1581–1582 (2002).
44. Mowat, E. *et al.* *Pseudomonas aeruginosa* and their small diffusible extracellular molecules inhibit *Aspergillus fumigatus* biofilm formation. *FEMS Microbiology Letters* **313**, 96–102 (2010).
45. Wallace, R. L., Hirkala, D. L. & Nelson, L. M. Efficacy of *Pseudomonas fluorescens* for control of *Mucor* rot of apple during commercial storage and potential modes of action. *Can J Microbiol e-First ar*, 1–12 (2018).
46. Hogan, D. A. & Kolter, R. *Pseudomonas-Candida* interactions: an ecological role for virulence factors. *Science* **296**, 2229–32 (2002).
47. Morales, D. K. *et al.* Control of *Candida albicans* metabolism and biofilm formation by *Pseudomonas aeruginosa* phenazines. *MBio* **4** (2013).
48. Briard, B. *et al.* *Pseudomonas aeruginosa* manipulates redox and iron homeostasis of its microbiota partner *Aspergillus fumigatus* via phenazines. *Sci. Rep.* **5** (2015).
49. Gibson, J., Sood, A. & Hogan, D. A. *Pseudomonas aeruginosa-Candida albicans* interactions: Localization and fungal toxicity of a phenazine derivative. *Appl. Environ. Microbiol.* **75**, 504–513 (2009).
50. Ibrahim, A. S. *et al.* The high affinity iron permease is a key virulence factor required for *Rhizopus oryzae* pathogenesis. *Mol. Microbiol.* **77**, 587–604 (2010).
51. Artis, W. M., Fountain, J. A., Delcher, H. K. & Jones, H. E. A mechanism of susceptibility to mucormycosis in diabetic ketoacidosis: Transferrin and iron availability. *Diabetes* **31**, 1109–1114 (1982).
52. Ibrahim, A. S. *et al.* The iron chelator deferasirox protects mice from mucormycosis through iron starvation. *J. Clin. Invest.* **117**, 2649–2657 (2007).
53. Meyer, J. M., Neely, A., Stintzi, A., Georges, C. & Holder, I. A. Pyoverdinin is essential for virulence of *Pseudomonas aeruginosa*. *Infect. Immun.* **64**, 518–523 (1996).
54. Lamont, I. L., Beare, P. A., Ochsner, U., Vasil, A. I. & Vasil, M. L. Siderophore-mediated signaling regulates virulence factor production in *Pseudomonas aeruginosa*. *Proc. Natl. Acad. Sci. USA* **99**, 7072–7 (2002).
55. Boelaert, J. R. *et al.* Mucormycosis during deferoxamine therapy is a siderophore-mediated infection: *In vitro* and *in vivo* animal studies. *J. Clin. Invest.* **91**, 1979–1986 (1993).
56. Sass, G. *et al.* Studies of *Pseudomonas aeruginosa* mutants indicate pyoverdinin as the central factor in inhibition of *Aspergillus fumigatus* biofilm. *J. Bacteriol.* **200** (2018).
57. Hood, M. I. & Skaar, E. P. Nutritional immunity: transition metals at the pathogen-host interface. *Nature Rev. Microbiol.* **10**, 525–537 (2012).
58. Kang, D., Kirienko, D. R., Webster, P., Fisher, A. I. & Kirienko, N. V. Pyoverdinin, a siderophore from *Pseudomonas aeruginosa*, translocates into *C. elegans*, removes iron, and activates a distinct host response. *Virulence*, <https://doi.org/10.1080/21505594.2018.1449508> (2018).
59. Gonzalez, M. R. *et al.* Effect of human burn wound exudate on *Pseudomonas aeruginosa* virulence. *mSphere* **1**, 1–14 (2016).
60. Kimura, E., Shimizu, H., Yoshidome, H., Ohtsuka, M. & Miyazaki, M. Immunosuppression following surgical and traumatic injury. *Surgery Today* **40**, 793–808 (2010).
61. Voelz, K., Gratacap, R. L. & Wheeler, R. T. A zebrafish larval model reveals early tissue-specific innate immune responses to *Mucor circinelloides*. *Dis. Model. Mech.* **8**, 1375–88 (2015).
62. Holloway, B. W. Genetic recombination in *Pseudomonas aeruginosa*. *J. Gen. Microbiol.* **13**, 572–581 (1955).
63. Ghysels, B. *et al.* FpvB, an alternative type I ferripyoverdinin receptor of *Pseudomonas aeruginosa*. *Microbiology* **150**, 1671–1680 (2004).

### Acknowledgements

We would like to acknowledge Steve Diggle, Anne-Marie Krachler, Amy Dumigan, and Mark Webber for the generous gifts of bacterial strains; Francisco Fernandez-Trillo, and Oliver Creese for assistance with the organic extractions; Kevin Waldron and Daniel Stones for valuable consultation regarding experimental design with metals; Fabien Cottier for critical input while preparing the manuscript; Elizabeth Ballou for help with power calculations for animal studies; and the Host and Pathogen Interaction laboratory at the University of Birmingham for helpful discussion and valuable support. C.K is funded by the Darwin Trust of Edinburgh. R.A.H, C.C and S.S are funded by the Medical Research Council (MR/L00903X/1).

#### Author Contributions

C.K., C.C. and S.S. acquired and analysed the data. C.K. and R.H. wrote the manuscript. R.H. and K.V. conceptualised and designed the study.

#### Additional Information

**Supplementary information** accompanies this paper at <https://doi.org/10.1038/s41598-019-42175-0>.

**Competing Interests:** The authors declare no competing interests.

**Publisher's note:** Springer Nature remains neutral with regard to jurisdictional claims in published maps and institutional affiliations.



**Open Access** This article is licensed under a Creative Commons Attribution 4.0 International License, which permits use, sharing, adaptation, distribution and reproduction in any medium or format, as long as you give appropriate credit to the original author(s) and the source, provide a link to the Creative Commons license, and indicate if changes were made. The images or other third party material in this article are included in the article's Creative Commons license, unless indicated otherwise in a credit line to the material. If material is not included in the article's Creative Commons license and your intended use is not permitted by statutory regulation or exceeds the permitted use, you will need to obtain permission directly from the copyright holder. To view a copy of this license, visit <http://creativecommons.org/licenses/by/4.0/>.

© The Author(s) 2019